Title

Sealed and Insulated Attic Hygrothermal Performance in New California Homes Using Vapor and Air Permeable Insulation—Field Study and Simulation

Authors

Less, Brennan
Walker, Iain
Slack, Jonathan
et al.

Publication Date

2019-04-01

DOI

10.2172/1526610

Peer reviewed

LBNL - 2001213

Lawrence Berkeley National Laboratory

Sealed and Insulated Attic Hygrothermal Performance in New California Homes Using Vapor and Air Permeable Insulation—Field Study and Simulations

Brennan Less
Iain Walker
Jonathan Slack
Leo Rainer
Ronnen Levinson

Lawrence Berkeley National Laboratory

Energy Technologies Area
April 2019

This work was supported by the Assistant Secretary for Energy Efficiency and Renewable Energy, Building Technologies Office of the U.S. Department of Energy under Contract No. DE-AC02-05CH11231, and by the California Energy Commission under contract EPC-14-012.

Disclaimer

Copyright notice

ACKNOWLEDGEMENTS

This work was supported by the California Energy Commission EPIC Program Contract EPC-14-012 and the Assistant Secretary for Energy Efficiency and Renewable Energy, Building Technologies Program, of the U.S. Department of Energy under Contract No. DE-AC02-05CH11231. The authors would like to acknowledge the contributions of Francis Babineau, Elam Leed, and Todd Bridgeford of Johns Manville for supplying insulation and information to insulation contractors, Dave Hegarty of Duct Testers, Broken Drum Insulation, and Anna Liao, Stephen Czarnecki, Woody Delp and Darryl Dickerhoff of LBNL.

PREFACE

The California Energy Commission's Energy Research and Development Division supports energy research and development programs to spur innovation in energy efficiency, renewable energy and advanced clean generation, energy-related environmental protection, energy transmission and distribution and transportation.

In 2012, the Electric Program Investment Charge (EPIC) was established by the California Public Utilities Commission to fund public investments in research to create and advance new energy solution, foster regional innovation and bring ideas from the lab to the marketplace. The California Energy Commission and the state's three largest investor-owned utilities – Pacific Gas and Electric Company, San Diego Gas & Electric Company and Southern California Edison Company – were selected to administer the EPIC funds and advance novel technologies, tools, and strategies that provide benefits to their electric ratepayers.

The Energy Commission is committed to ensuring public participation in its research and development programs that promote greater reliability, lower costs, and increase safety for the California electric ratepayer and include:

- Providing societal benefits.
- Reducing greenhouse gas emission in the electricity sector at the lowest possible cost.
- Supporting California's loading order to meet energy needs first with energy efficiency and demand response, next with renewable energy (distributed generation and utility scale), and finally with clean, conventional electricity supply.
- Supporting low-emission vehicles and transportation.
- Providing economic development.
- Using ratepayer funds efficiently.

Sealed and Insulated Attic Hygrothermal Performance in New California Homes Using Vapor and Air Permeable Insulation—Field Study and Simulations is the final report for the Comparing Attic Approaches for ZNE Homes project (Contract Number EPC-14-012) conducted by Lawrence Berkeley National Laboratory. The information from this project contributes to Energy Research and Development Division's EPIC Program.

All figures and tables are the work of the author(s) for this project unless otherwise cited or credited.

For more information about the Energy Research and Development Division, please visit the Energy Commission's website at www.energy.ca.gov/research/ or contact the Energy Commission at 916-327-1551.

ABSTRACT

This project investigated the thermal and moisture performance of a low-cost approach to sealing and insulating attics using glass fiber insulation. The work included a combination of: (1) field measurements of attic and HVAC system performance in two new, high performance homes in California's Central Valley (Fresno), and (2) hygrothermal simulations of attic performance. Each field study attic was continuously monitored at multiple locations for over a year for wood moisture content, air humidity, condensation, temperature, and heat flux, together with on-site weather and solar conditions. The Fresno test home showed periodic condensation and high surface wood moisture content, but no surface mold or degradation upon visual inspection at the end of the test period. The Clovis test home showed less indication of high moisture levels—either from surface condensation or wood moisture content—but did have visible suspected mold growth on the inside of the North sheathing at the end of the field testing. These results show the limitations of current moisture measurement techniques focused on wood moisture content, rather than potential for mold growth. From a thermal/energy perspective the attics were close to indoor conditions thereby realizing the design intent for reducing duct system losses. Simulated site HVAC energy savings for sealed vs. vented attics averaged 18% across California climate regions (8% TDV energy savings). Savings were dominated by heating energy reductions; cooling savings were substantially lower. The moisture issues are investigated in greater detail in the simulations. First, we identified the climate regions and house characteristics that are associated with increased risk of mold growth or wood rot in new CA homes. Climate region was very important in determining risk, as were house features that reduced outside air exchange (e.g., 1-story homes, very tight envelopes, very tight attics, no IAQ fan), along with those that increased flow of moist air from the living space to the attic (e.g., supply ventilation fans, larger ceiling leaks, duct leakage). Second, we investigated several approaches to reduce moisture risks, and the best approach was to use a vapor retarder on the inner face of the fiberglass insulation. Both the field and simulation results indicate that the use of air and vapor permeable insulation can be acceptable from a thermal/energy point of view, but additional measures need to be taken to reduce moisture risks, primarily from mold growth.

Keywords: Attic, Moisture, Heat, HVAC, Ventilation, Air Leakage, Insulation, Fiberglass, Mold, Wood Moisture Content, Condensation

Please use the following citation for this report:

Less, Brennan; Iain Walker, Jonathan Slack, Leo Rainer, Ronnen Levinson. 2018. *Sealed and Insulated Attic Hygrothermal Performance in New California Homes Using Vapor and Air Permeable Insulation—Field Study and Simulations*. California Energy Commission. Publication Number: CEC-XXX-201X-XXX.

TABLE OF CONTENTS

LIST OF FIGURES

Page

LIST OF TABLES

Page

EXECUTIVE SUMMARY

1.1.1 Introduction

In California, Heating and Cooling (HVAC) equipment and ductwork are commonly installed in the attic of new homes, particularly in slab-on-grade construction. Because traditional vented attics remain very hot in the summer and cold in the winter, they are one of the worst locations in the home to place HVAC equipment. Inefficiencies in the HVAC equipment and ducts can increase a home's heating and cooling energy use by 10 to 50%.

Starting in the mid-1990s, high performance builders in hot-dry climates in the U.S. began to experiment with air sealing attics and placing insulation at the sloped roof surface, rather than on the flat ceiling. This was intended to make the attic a semi-conditioned space and to recover the thermal losses from HVAC equipment in attic spaces. Short-term testing showed that the attic temperatures were very similar to the living space. This led to measurable short-term cooling and heating energy savings of 5-20% relative to similar homes with vented attics. Subsequent fieldwork and simulations demonstrated that HVAC energy savings for sealed and insulated attics were strongly dependent on duct leakage, with greater savings in homes with leaky ducts. This construction method became popular amongst high performance builders, and thousands have been built using this approach across many U.S. climates, including more than 10,000 new homes in California.

Almost as soon as sealed and insulated attics gained popularity, their potential to lead to moisture and mold problems became evident. Two types of moisture issues have been demonstrated: (1) cold weather condensation on cold roof sheathing, and (2) warm weather issues where the attic air itself is at high humidity levels, even approaching 100% RH, leading to condensation on supply air ducts, ceiling penetrations, etc. Most moisture that accumulates in sealed attics comes from the living space of the home (outside moisture plus water vapor from cooking, bathing and breathing), and in some rare cases, from water leaks in the roofing material. These moisture issues can have cosmetic (visible mold), health (mold exposure to occupants) and major structural implications (rotting of structural framing and roof sheathing).

Addressing these moisture issues in sealed and insulated attics has been the subject of much development in the model building codes (e.g., International Energy Conservation Code) and in the California Residential Code. With variability by climate region, the model codes require some amount of insulation that does not allow air movement through it (e.g., foam board or spray foam) either above or below the roof sheathing. The remainder of the insulation at the roof deck can be lower-cost fibrous insulation (e.g., fiberglass or cellulose). This limits condensation potential by warming up the first surface that moist inside air comes into contact with. If the moist air does not contact a cold surface, then there is no condensation or mold risk. In select climate regions, the codes also require a vapor retarder be used to further protect the wood from moist

inside air. This moisture risk is commonly thought to worsen as climate regions become colder or more humid. Recent model codes have added a requirement to supply air directly to the attic from the HVAC system. They have also included an option to use only fibrous insulation in mild climates, while also requiring a vapor diffusion vent at the roof ridge, which is similar to a traditional attic vent, but it allows water vapor to escape and not air. Finally, the California Residential Code recently added the ability for homes in select climates with tile roofing to use only fibrous insulation with no venting or moisture barriers of any kind.

Traditionally, these code requirements have been managed by using spray polyurethane foam (SPF) insulation on the underside of the roof deck. SPF does not allow air movement through it, and it can be specified as a vapor retarder, allowing it to meet all code requirements in a single product. It was common for many builders to insulate sealed attics to roughly R20 using this approach (approximately half what would be required for a vented attic by modern prescriptive codes). In fact, this has been done in roughly 10,000 homes by a California production builder. But SPF is expensive insulation, particularly when targeting higher R-values between R30 and R49. SPF costs can be a factor of four or more than those for lower-cost insulation materials, like fiberglass or cellulose. In addition, concerns have been raised about indoor air quality issues related to spray foam products, which have been shown to emit flame retardants (e.g., TCPP) and numerous aldehyde compounds over periods greater than one year. The builder partner for this project estimates the additional cost to be about $1600 compared to a traditional attic. This is about $1000 less than current sealed attic approaches. Despite its flame retardant components, SPF is also considered a human health hazard in structure or wildfire scenarios, as well as during application and when disturbed (e.g., drilled, sanded, cut). Finally, the propellants used to create some foam insulations (namely extruded polystyrene and closed cell spray foam) have high global warming potentials (700 to 900 times worse than CO_2) that are roughly 90 times greater than those associated with fiberglass insulation. This may limit the ability of SPF insulation to provide a net-carbon benefit over its useful service life.

1.1.2 Project Purpose

Throughout the many mild and dry climates of California, a dramatically lower-cost insulated roof deck assembly consisting only of fiberglass or cellulose (batts or blown) may be possible without undue moisture risk. This could potentially eliminate the costly model code requirements and avoid the potential chemical exposures and global warming impacts from SPF products. On behalf of the California Energy Commission's (CEC) Title 24 Building Energy Code (T24), we investigated the thermal, moisture and energy performance of sealed and insulated attics in new homes, using only fibrous insulations, such as fiberglass or cellulose.

There are two key questions to be answered by this study:

- Do fibrous insulation approaches result in an attic that can be considered thermally within conditioned space with consummate energy savings?

- Does moisture permeable insulation used in new California homes lead to increased moisture risk or definite moisture problems in the state's climate regions?

Answering these two questions will enable California builders and homeowners to reduce energy use with lower costs, and it will facilitate a construction strategy that strongly contributes to making the state's new homes zero-net energy.

1.1.3 Project Process

The project goals were to:

- Assess the thermal conditions in the attic to determine if a sealed and insulated attic can be counted as "conditioned space". If yes, then predict HVAC energy savings across new California homes.
- Evaluate moisture performance for sealed attics using vapor permeable insulation to identify:
    - Moisture risks,
    - Parameters associated with increased and decreased risk,
    - Potential solutions to moisture issues.

To address these goals the study had two main components: (1) a field study to directly measure the performance of sealed attics with vapor permeable insulation, and (2) simulations to assess sealed attic performance in other climates and house conditions. These efforts will be used to systematically identify parameters of interest that could inform future California building standards and to evaluate factors that could reduce or increase moisture risk for these building assemblies.

For the field study, two newly built homes were instrumented and measured for at least one-year in the Fresno, CA region (CEC CZ 13; U.S. DOE CZ 3B). Sensors were installed throughout the sealed and insulated attics in the attic air and embedded in the insulated roof deck assembly, in varying locations (e.g., eave vs. roof ridge) and cardinal exposures (e.g. North vs. South). Measured values included temperature, relative humidity, surface condensation, wood moisture content, outside weather, heat flux and HVAC energy use. These attics were manually air sealed using canned foam sealant, and they were insulated solely with R38 fiberglass batts from Johns Manville held against the roof sheathing by support wires.

For the simulations, we used the validated heat, air and moisture REGCAP tool to predict energy use and moisture performance in two prototype homes located in all California CEC climate regions with varying features believed to effect moisture risk, including attic type, envelope leakage, attic leakage, duct leakage, ceiling leakage, internal moisture generation, roof finish, IAQ fan sizing and type, and house size. All cases were run for four consecutive years to assess long-term moisture risks. We also implemented a number of mitigation measures intended to safeguard against any possible moisture risks.

Our moisture performance metrics included the ASHRAE 160 mold index, which estimates the risk of mold growth on a building surface under dynamic temperature and

relative humidity conditions, including the effects of the substrate and cyclic wetting/drying periods. An assembly meets the criteria if the mold index remains less than 3, indicating <10% visible mold growth on the surface. We also assessed if the assemblies exceeded wood fiber saturation (28-30% moisture content), which is the minimum level required for rot and decay organisms to become established. Condensation was taken as an indicator of potentially problematic moisture performance, but no strict criteria was used to pass or fail an assembly. Mold index is the most conservative of these moisture metrics, because it only requires high humidity levels in the attic (>80%RH).

1.1.4 Project Results

1.1.4.1 Field Testing

In the Fresno test home (2-story, 3,605 ft^2), two attic spaces were monitored continuously from September 2016 to the end of April 2018, while in the Clovis test home (1-story, 2,019 ft^2), monitoring occurred from June 2017 through mid-May 2018.

1.1.4.1.1 Temperature Patterns

Temperature measurements in the field study homes suggested that the living space and attic air temperatures were similar, with annual average differences of 0.1˚C to 0.7˚C for the two Fresno attic spaces and 1.7˚C for the Clovis home. The attics were, on average, slightly warmer than the living space below. Daytime solar gains increased the attic air temperatures relative to the living space temperature by up to 4.5˚C (in Fresno) and 10˚C (in Clovis). These solar gains also drove vertical temperature stratification in the attic air, where the temperature at the ridge averaged 2.5˚C hotter than at the attic floor (and reached maximum values of 11.5˚C and 14˚C hotter in Fresno and Clovis homes). Overall, the Clovis attic air temperature was much more variable relative to the living space temperature, varying roughly between -10 and 10˚C, depending on season (compared with -2 and 4.5˚C in the Fresno home). We believe the Clovis attic's thermal performance was more varied because of its unique characteristics. The Clovis test home had an unusual geometry—a square shaped home with a central courtyard—resulting in four minimally connected attic volumes, and the monitored attic volume did not have HVAC equipment/ducts inside. The monitored attic was also situated partially over an unconditioned garage, rather than being fully over conditioned living space. We measured high levels of leakage to outside in the Clovis attic. This type of geometry and set-up may not be ideal in sealed attic homes. Also of note, one of the two attic volumes in the Fresno test home had solar PV panels shaded one roof orientation, and this roof experienced less stratification and smaller overall temperature differences between the attic and living space (0.1 vs. 0.7˚C).

1.1.4.1.2 Moisture Risk

Moisture measurements in the two test homes showed the potential for elevated humidity conditions to occur at the North roof deck surfaces near the roof ridge. Surface relative humidity was much higher at the North vs. South ridge, with numerous

periods of condensation recorded and times above the critical mold growth threshold (>80%). All mold index values in both field test homes remained below the failure threshold of 3 established by ASHRAE Standard 160 for moisture control analysis of building assemblies. The Fresno home North ridge sheathing reached a maximum value of 2 (two winters), while the Clovis home only reached 0.25 (one winter). Wood moisture content was elevated at the North ridge sheathing of the Fresno test home in the first winter of 2016/17, which was an unusually wet winter. It reached a one-hour maximum value of 26% in December 2016, and spent roughly 2-weeks at this high level (>24%). The North sheathing at the eave had much lower peak moisture content of 14%, similar to all other measured wood locations, which remained safely dry (<10%). During the second winter of 2017/18, maximum wood moisture content at the North ridge was 21% but did not remain elevated, while other locations were dry. The Clovis test home maximum wood moisture at the North ridge was 16.4% in the winter of 2017/18 and it rapidly decreased to around 12%. Condensation was recorded only at the North ridge sheathing location in the Fresno test attic. No other locations in either test home had any recorded condensation.

The ridge was often the warmest location, despite being the location where moisture was found to accumulate. This indicates that controlling moisture is more than simply a condensation issue. Complex moisture dynamics in the attic lead to daytime periods of higher moisture content in attic air at the ridge, but this difference completely disappeared during non-daylight hours, which is when high surface RH and condensation occurs due to cold outside conditions and night sky heat losses. This suggests that higher moisture content in the attic air at the ridge might not explain moisture accumulation at the ridge during cold nighttime hours. Our measurements are not sufficient for us to clearly identify other mechanisms that explain the high moisture at the ridge. This remains an item for further research.

The measurements indicated that the Fresno home has the highest moisture risk. However, visual inspections of the roof deck surfaces at the end of monitoring revealed visible spotty mold growth on the North-oriented OSB sheathing in the Clovis test home, along with other signs of moisture, such as rusted roofing nails and raised grain on the OSB surface. The Fresno home had no such moisture issues. At least one other study has found similar results in sealed and insulated attics, with contradicting visual mold findings and calculated mold index predictions (Ueno & Lstiburek (2018)). This implies that our field measurement capability may be insufficient to predict mold growth, and/or it suggests a lack of precision in the ASHRAE 160 mold index metric, particularly when applied to insulated roof decks in sealed attics.

1.1.4.1.3 Field Study Conclusions

- The sealed and insulated attics are the same temperature on average as the living space, such that they can be considered to be inside conditioned space from a modeling and T24 compliance perspective. But particularities of attic and house geometry, attic leakage, presence of HVAC equipment, and other factors can contribute to some sealed attics having widely varying thermal performance.

- Moisture risk at the North ridge sheathing is evident, and while mold index calculations predict safe assemblies, visual inspection revealed spotty mold growth in the Clovis home. This was particularly surprising, as the measured moisture parameters all appeared to be lower in the Clovis home. Measured wood moisture contents were in the safe range below fiber saturation at all measured locations. Current methods for predicting safe moisture performance in sealed attic assemblies may be inadequate to the complexities inherent in these assemblies, particularly when they are completely vapor and air permeable, as they were in this research.
- Design, implementation and inspection issues were observed in the sealed attics of field study homes, including large areas of missing insulation above an unconditioned garage and substantial disruption to the roof deck insulation by other subcontractors. Careful design review and planning are critical, as are experienced energy raters and building inspectors. Also, all sealed attics should be designed to be accessible for inspection or remedial work if ever needed. Finally, sealed attic eave locations should be treated with raised heal trusses or the like, similar to vented attics.

1.1.4.2 Simulations

1.1.4.2.1 HVAC Energy Savings

The simulations were used to estimate potential HVAC energy savings for new homes in California climate regions. We found median total HVAC energy savings of 18% (from 4 to 25% by climate region) across all homes and climate regions, comprised of 27% heating energy savings, 5% cooling savings and 10% air handler savings. Insulated roof decks are strongly coupled to the sky, including solar heat gains and nighttime heat losses. Sealed attics benefit from eliminating duct system energy losses, but they face cooling penalties due to this sky-coupling. These effects reduced and sometimes eliminated cooling energy savings. Similarly, peak cooling power demand reductions were minimal (though positive), and time-dependent valuation energy savings were roughly half the site energy savings (median of 8%), because electricity is heavily weighted in TDV assessments and the simulated homes used electric cooling and gas heating. Energy performance of sealed attics was robust across the varied simulation parameters, such that savings were not drastically different when varying envelope leakage, duct leakage, fan type, etc. Climate region was the primary driver of varying energy performance.

1.1.4.2.2 Moisture Risk

Most simulated sealed and insulated attic assemblies met moisture performance criteria, such that we classify them as safe. However, a substantial minority of the simulated cases had elevated risks for surface mold growth (mold index >3) and high wood surface moisture content (>28% for 7-days or more) sufficient to potentially lead to structural damage over time. Mold index failures were most common in the North sheathing location (18% failure rate) and the general attic framing nodes (19% failure rate), and were lower at the South sheathing (4% failure rate). The 28% wood moisture content metric was exceeded in 10% of cases at the North sheathing, while failures at the attic framing and South sheathing were much lower, at 1% and 0%, respectively. The highest

risk location was the North-oriented roof deck. The roof deck risks were associated with cold periods in the heating season, particularly on clear nights when the roof deck surface temperature were substantially below the outside air temperature. The attic framing and attic air humidity were at their highest in the late-winter and spring seasons, which we hypothesize to be the result of moisture storage in the roof deck during winter, which is then emitted into the attic air with increasing outside temperatures and greater solar gains.

The most important house features in determining simulated moisture risk at the North roof deck in sealed and insulated attics using solely fibrous, vapor permeable insulation were:

- **CEC climate region**, estimated highest to lowest risk were: 1, 13, 2, 5, 6, 3, 12, 7, 4, 8, 11, 16, 9, 14, 10, 15.
- **IAQ fan sizing** (larger fans reduced mold and WMC risk)
- **House prototype** (1-story 2,100 ft^2 prototype had substantially higher risk than the 2-story 2,700 ft^2 prototype)
- **Envelope leakage** (more leakage led to less risk)
- **Attic leakage** (more leakage led to less risk)
- **Internal moisture generation rate** (higher internal generation led to greater risk)
- **IAQ fan type** (exhaust IAQ fans had lower risk than supply fans)

Our observations about moisture risk in sealed attics lead us to the following more general principles or design guidance:

- Sealed attics have much higher moisture risks than vented or HPA attics.
- Climate zone is one of the strongest drivers of moisture risk. The ordering of climate zones by risk is not intuitive, and it differs for North sheathing risk vs. attic framing risk (attic framing risk was highest in CZ 2, 3, 5-8 and 13). The coldest locations do not necessarily have the highest risk; instead coastal climates and select central valley locations seem most at risk.
- Increased outside air exchange reduced mold and wood moisture risks, whether through larger IAQ fans, greater envelope or attic leakage areas, greater natural infiltration in 2-story vs. 1-story homes, or mechanical supply of outside air into the attic.
- Increased mixing of the attic and living space air volumes tended to marginally increase mold risk, whether this resulted from increased duct leakage or ceiling leakage, or by intentional supply of HVAC air into the attic (as required by the 2018 IECC). This finding assumes that the living space has moisture content elevated above the attic, which may not be a consistent assumption. Mixing may help to avoid elevated attic air moisture during spring, when moisture that accumulates in the roof deck during winter is re-emitted.
- Roof deck moisture risk was driven by cold roof sheathing temperatures, so parameters that increased roof deck temperatures during cold nights reduced moisture risks. This included the placement of air impermeable insulation above the roof deck per the CRC (2018), and the use of tile roofing vs. asphalt shingles.
- The living space is the source of moisture for sealed and insulated attics, and outside air is generally a source of potential drying in California climates. This explains why supply IAQ fans worsened moisture performance, because they drove living space moist air into the attic and reduced the amount of air coming

into the attic from outside, and exhaust fans improved moisture performance by drawing outdoor air into the attic.

1.1.4.2.3 Moisture Interventions

The most effective interventions were the use of a 1-perm vapor retarder on the surface of the fibrous insulation at the roof deck, and the provision of mechanically supplied outside air directly into the attic air volume. The use of the vapor retarder had nearly no impact on energy use, whereas the outside air ventilation increased energy consumption in all cases (and reduced savings), by an average of 428 or 871 kWh, depending on the outside airflow target. The use of insulation above the roof deck at levels required by the California Residential Code drastically reduced condensation at the roof deck, but it was much less effective at reducing the risk of mold growth. This strategy warmed the roof deck surface, which reduced the surface relative humidity. Condensation was nearly eliminated, but the surface RH at the roof deck remained high enough (>80%) to support mold growth in some instances. Finally, the addition of HVAC supply air into the attic volume, which is required by the IECC (2018) model code, actually marginally increased the mold risk, wood moisture content and condensation levels in our simulations. It also increased energy use on average by 161 kWh/year. This strategy did reduce springtime elevated attic air moisture and it supplied dehumidified air to the attic in the cooling season. This strategy was developed for use in humid climate regions, and we expect it may be effective in those locations, but it does not appear beneficial in California new homes.

1.1.4.2.4 Simulation Study Conclusions

- Statewide, total HVAC energy savings are predicted be 18% in terms of site energy and 8% for TDV energy. Thermal penalties of insulated roof decks partly counteract the benefits of ducts inside the conditioned space, which reduces cooling energy savings, limits peak cooling demand reductions, and provides lower TDV than site energy savings.
- Mold index failures occurred in roughly 15% of sealed attics at the North roof deck. Failure rates were lower for wood moisture content rot and decay thresholds. Failures were largely concentrated in homes with any of the following features: 1-story geometry, higher internal moisture generation rates, no IAQ fan operating, or very airtight envelopes. Any one of these elements represents a risk for a sealed attic home, though in combination they dramatically increased likelihood of moisture failure. Climate zone variability was the other primary driver of moisture risk, with the worst locations being Pacific coastal and select Central Valley locations. Attic air relative humidity was sometimes at unacceptable levels (>80%) leading to potential mold growth on attic framing, as moisture that accumulated in the roof deck during winter was driven into the attic air by solar radiation during sunny late-winter and spring days.
- Primary moisture interventions should be either: (1) a vapor retarder on the attic air side of the fibrous insulation, or (2) outside air supplied mechanically to the attic volume at either 20 or 50 cfm per 1,000 ft^2 of ceiling area, depending on climate region. The latter substantially increases energy use. If the air impermeable insulation requirements are to be kept in the CRC (Table R806.5), the insulation values should be increased to improve their effectiveness in controlling mold risk. This strategy may work better when air and vapor

impermeable insulation is installed below the roof deck, rather than above the roof deck.

1.1.5 Benefits to California

This research provides California policymakers and builders with detailed knowledge on the moisture risks and mitigation strategies for sealed and insulated attics. It has combined the benefits of field study and simulation methods to increase the value and insights beyond what is possible with either approach in isolation. Energy savings of 18% are available on average in new California homes that meet the 2016 Title 24 prescriptive energy code requirements. These savings can safely be achieved without undue moisture risks using lower-cost fibrous insulation approaches, while avoiding the potential human health and environmental implications of spray foam insulation using straightforward moisture mitigation measures. The California building code will require changes to accommodate this assembly type.

1.1.5.1 California Building Code and Building Energy Code Concerns and Suggested Requirements

- The 2019 Residential Compliance Manual Section 3.6.1 describes requirements for unvented attics in energy code compliance. It references the requirements contained in the 2016 California Building code Section R806.5. The compliance manual then goes on to specify two conditions under which unvented attics are acceptable, and both conditions in part contradict Section R806.5 of the CBC.
    - Item 1 in Section 3.6.1 of the compliance manual states that unvented assemblies can use air permeable insulation below and in direct contact with the underside of the roof sheathing, if they also provide at least R5 insulation above the sheathing. This contradicts the referenced Section R806.5 in the CBC. The CBC explicitly allows use of air permeable insulation without insulation above the sheathing in homes with tile roofing in CZ 6-15 (Table R806.5). It also requires air impermeable insulation at R10 and R15 in select climates. Our work shows this may be inadequate to control mold risk in some situations.
    - Item 2 in Section 3.6.1 states that all assemblies using air impermeable insulation below the roof deck (e.g., spray foam or board foam) must also provide a layer of air permeable insulation (e.g., fiberglass or cellulose) below the air impermeable insulation. In contrast, the CBC explicitly allows assemblies composed entirely of air impermeable insulation (R806.5.5.1.1).
- The California Building Code Section R806.5.4 requires that in CZ 14 and 16, any air impermeable insulation must be a class II vapor retarder (or be covered by one). Our simulation work has shown that these are not the most risk-prone climate regions in the state. In fact, CZ 14 and 16 were among the safest locations assessed. We recommend that this requirement be revised.
- The California Building Code Section R806.5.4.1 is unclear in what climate regions it applies to. It appears to apply only in CZ14 and 16. It requires that any air permeable insulation (e.g., fiberglass) in an unvented attic be covered with a class I or II vapor retarder on the indirectly conditioned space side. The following clarifications are required:
    - In what climate zones is this applicable?

- Does this apply only to assemblies composed entirely of air permeable insulation? Or does it also apply to assemblies with other vapor/air control mechanisms, such as air impermeable insulation (e.g., closed cell SPF) installed below and in direct contact with the roof sheathing, which is then covered from below with air permeable insulation? Or when air permeable insulation is used below the roof sheathing, but additional insulation is placed above the roof sheathing?

There is a need for improved guidance and requirements for the design, construction and inspection of unvented attic assemblies in the California building codes and reference compliance manuals. In order to protect the health and safety of California residents and durability of their homes, we suggest that all sealed and insulated roof deck assemblies should provide a vapor control layer between the attic air and the roof sheathing/attic framing. The following are example roof assemblies that would be acceptable:

- Roof insulation composed entirely of vapor impermeable insulation (class II vapor retarder or less) below the roof deck (e.g., closed cell SPF or foam board).
- Roof assembly composed entirely of vapor permeable insulation below the roof deck (e.g., fiberglass, cellulose, open cell SPF) with a class II vapor retarder installed on the inside surface of the insulation.
- Hybrid roof assemblies composed of a layer of vapor impermeable insulation (class II vapor retarder) below and in direct contact with the roof sheathing, with vapor permeable on the inside of this impermeable layer. The vapor impermeable insulation must enclose the top chord of the roof framing.
- Hybrid roof assemblies composed of insulation above the roof sheathing, along with vapor permeable insulation below and in direct contact with the roof sheathing, with a class II vapor retarder on the inside surface of the vapor permeable insulation.
- Roof assembly with all insulation (either vapor permeable or impermeable, rock wool board, foam board, SPF, etc.) placed above the sheathing with no vapor retarder in the unvented attic.

2 Introduction

Attics have a long tradition in construction as a way to shelter the building below from environmental conditions. The venting of attics has been used to control both the thermal and moisture conditions in the attics space. Model building codes have long-required attic ventilation where the opening area scales with the plan area of the attic in ratios of 1:150 or 1:300, depending on the installed vent locations. Past research has shown that the thermal and moisture control are imperfectly managed in residential attics with these intentional ventilation openings (TenWolde & Rose, 1999), however, they are a well-proven and effective approach in the vast majority of cases.

In North America, changing construction practices have led to Heating and Cooling (HVAC) systems being installed in attics, particularly in new slab-on-grade homes. Because traditional vented attics remain very hot in the summer and cold in the winter, they are the worst location in the home to place HVAC equipment and ducted distribution systems. Thermal losses from HVAC equipment due to conduction and duct leakage can increase a home's heating and cooling loads by 10-50% (Less, Walker, & Levinson, 2016). Starting in the mid-1990s, high performance builders in hot-dry climates in the U.S. began to experiment with air sealing attics and placing insulation at the sloped roof surface, rather than on the flat ceiling (Rudd & Lstiburek, 1996). Short-term testing showed that the attic was a semi-conditioned space, with temperatures overall very similar to the occupied volume (Rudd, 2005). This led to measurable short-term cooling and heating energy savings of 5-20% relative to similarly situated homes with vented attics (Parker, Sonne, & Sherwin, 2002; Rudd, Ueno, & Lstiburek, 1999). Subsequent fieldwork and simulations demonstrated that HVAC energy savings for sealed and insulated attics were strongly dependent on duct leakage, with greater savings relative to vented attic homes for systems with more leakage (Hendron, Anderson, Reeves, & Hancock, 2002; Rudd & Lstiburek, 1998). Past work has shown that very little energy savings are available for homes with airtight (<5% leakage) and insulated duct systems. Yet, this construction method became popular amongst high performance builders, and thousands have been built using this approach across many U.S. climates.

Almost as soon as sealed and insulated attics gained popularity, their potential to lead to moisture and mold problems became evident (Rudd, 2005; Ueno & Lstiburek, 2015). Two types of moisture issues have been demonstrated: (1) cold weather condensation on roof deck sheathing, and (2) warmer weather issues where the attic air volume itself is at high humidity levels, even approaching saturation, leading to condensation on supply air ducts, ceiling penetrations, etc. Most moisture research and model building code requirements have been directed towards reducing the risk of condensation on cold sheathing surfaces. These problems have most often been shown to manifest at the

ridge of the roof on sheathing surfaces with a Northern orientation. The risk of condensation tends to increase as the climate becomes colder.

Moisture risk is managed in sealed and insulated attics in a number of ways: (1) controlling the temperature of the condensing surface, (2) directly conditioning the attic volume, (3) reducing moisture levels in the occupied volume (through dehumidification and use of local exhaust fans), and (4) vapor diffusion venting at the roof peak. Condensing surface temperatures are controlled to be above the dew point temperature of the attic air by using air impermeable insulation applied either above the roof deck or in direct contact with the underside of the roof sheathing, as required in Section R806.5 of the International Residential Code (IRC) since 2009 (see Table 1) (ICC 2012). Schumacher and Lepage (2012) describe how these air impermeable insulation requirements are established, namely that the roof sheathing is designed to be 7.2°C (45°F) or greater when the indoor temperature is 20°C (68°F) and the outdoor temperature is the mean of the coldest three months in that location. This requirement is echoed exactly in item R806.5.1.4 of the 2016 California Residential Code. This calculation uses the total ceiling R-value required for that location (R30 to R49), and then assesses what fraction of the thermal resistance is required to maintain the sheathing temperature as desired. If the total ceiling R-value were less or more than specified in Table 1, then the air impermeable insulation required to maintain sheathing above 7.2°C would change, though the requirement does not change in the building codes. The model code also requires a Class II vapor retarder (or coating) on any air impermeable insulation in zone 5-8. The most recent IRC in 2018 has added a requirement to supply conditioned air to sealed attics at 50 cfm per 1,000 ft^2 of ceiling area. In climate zones 1-3, an optional path was added to use solely air permeable insulation, provided that vapor diffusion vents are installed with more than 20 perms at the roof peak (1:600) (BASC, 2018).

Table 1 Air impermeable insulation requirements for sealed and insulated attics

U.S. DOE Climate Zone	CEC Climate Zone	Minimum Air Impermeable Insulation R-Value	2012 IECC Required Total R-Value of Ceiling	CEC Required Total R-value of Ceiling
2B and 3B tile roof only	6-15 tile roof only	0	30	32 - 40
1, 2A, 2B, 3A-C	3-15	5	38	32 - 40
4C	1-2	10	38	40
4A-B	16	15	49	40
5		20	49	
6		25	49	
7		30	49	
8		35	49	

Source: Table 806.5 2012 IRC and the 2016 California Residential Code Section R806.5.

Spray polyurethane foam (SPF) insulation has traditionally been used to seal and insulate attics, because it manages air leakage and can be used to meet the model code requirements detailed above. It was common for many builders to insulate sealed attics

to roughly R20 using this approach (note that this insulation level is roughly half what would be required for a vented attic and this raises questions regarding overall thermal envelope performance for the home). In fact, this has been done in roughly 10,000 homes by a California production builder (Hoeschele, Weitzel, German, & Chitwood, 2015). But SPF is expensive insulation, particularly when targeting higher resistances between R30 and R49. SPF costs can be a factor of four or more than those for lower-cost insulation materials, like fiberglass or cellulose. In addition, concerns have been raised about indoor air quality issues related to spray foam products, which have been shown to emit flame retardants (e.g., TCPP) and numerous aldehyde compounds over periods greater than one year (Poppendieck, Nabinger, Schlegel, & Persily, 2014; Poppendieck, Persily, & Nabinger, 2014). The builder partner for this project estimates the additional cost to be about $1600 compared to a traditional attic. This is about $1000 less than current sealed attic approaches. Despite its flame retardant components, SPF is also considered a human health hazard in structure or wildfire scenarios, as well as during application and when disturbed (CalEPA DTSC, 2014). Finally, the propellants used to create some foam insulations (namely extruded polystyrene and closed cell spray foam) have high global warming potentials (700 to 900 times worse than CO_2) that are roughly 90 times those associated with fiberglass insulation (Wilson, 2010). This may limit the ability of SPF insulation to provide a net-carbon benefit over its useful service life in building applications (Johnas & Terrinoni, 2011). Notably, fourth generation blowing agents are currently emerging on the market for closed cell SPF with nearly no global warming impacts (e.g., DuPont Formacel (FEA-1100) and Honeywell Solstice (HBA1)), which are used in some market-ready products and could change the net-carbon impacts of this approach to sealed attics if adopted more widely.

Throughout the many mild and dry climates of California, a dramatically lower-cost assembly consisting only of fiberglass or cellulose (batts or blown) may be possible without undue moisture risk, potentially eliminating the costly air impermeable insulation requirements of the IRC and avoiding chemical exposures from SPF products.

On behalf of the California Energy Commission's (CEC) Title 24 Building Energy Code (T24), we have monitored the thermal and moisture performance of two new sealed and insulated attics in the Fresno, CA region (CEC CZ 13; U.S. DOE CZ 3B) for more than a year. These attics were manually air sealed using canned foam sealant, and they were insulated solely with R38 fiberglass batts from Johns Manville held against the roof sheathing by support wires. A partner CEC project is doing similar monitoring of the thermal and moisture performance of attics insulated with the Owens Corning netted and blown EcoTouch fiberglass insulation solution, which includes low-perm netting to control vapor diffusion (Owens Corning, 2015). This monitoring work will be paired with detailed hygrothermal simulations to extend our findings across California's climate zones and new housing types.

2.1 Study Goals

This study is comprised of two main components: 1. A field study to directly measure sealed attic with vapor permeable insulation performance, and 2. Simulations to examine performance in other climates in order to systematically identify parameters of interest that could inform future building standards and to evaluate factors that could reduce moisture risk.

There are two key questions to be answered by this study:

1. Do alternative insulation approaches result in an attic that can be considered thermally within conditioned space with consummate energy savings?
2. Does moisture permeable insulation used in new California homes lead to increased moisture risk or definite moisture problems in the state's climate regions?

For the field study the goals were to:

- Assess the thermal conditions in the attic to determine if a sealed and insulated attic can be counted as "conditioned space".
- Assess the moisture risk of this low-cost method to bring ducts in conditioned space.
- Identify appropriate mitigation measures for reducing moisture risk based on measured field data.

For the simulations, the goals were to:

- Assess attic thermal conditions and potential for energy saving for sealed and insulated attics.
- Evaluate moisture performance for sealed attics using vapor permeable insulation to identify:
    - Moisture risks,
    - Parameters that associated with increased and decreased risk,
    - Potential solutions to moisture issues.

2.2 California Attics

The vast majority of new homes built in California have HVAC systems located in traditional vented attics. These vented spaces experience the most extreme thermal conditions of any location in the home, with winter temperatures similar to outside and summer temperatures often over 120˚F. This challenging environment exacerbates any energy losses from the HVAC system and its ducts, and can have a disproportionate impact on system performance. As new California homes move towards being zero net-energy by 2020, advanced roof constructions, including unvented attics, are key strategies to be used in further reducing building loads—bringing renewable generation closer to satisfying all household demand.

As is currently proposed for the new reference home[1] in California's 2016 Title 24 Building Energy Code (California Energy Commission, 2015), 'advanced roofs' will:

- Be vented,
- Have R-13 below deck in rafters (or R-6 above roof deck)[2],
- Have a radiant barrier and cool roof requirements varying by climate zone

In addition, the HVAC system in the attic will have:

- 5% or less duct leakage, and
- R-8 duct insulation (or R-6 in some climate zones).

Alternatives to this baseline 'advanced roof' include high performance attics that bring ducts inside conditioned space. Strategies to achieve this include unvented attics, plenum truss systems, built-up duct chases and dropped ceiling chases. An alternative option is to bury the ducts in insulation. Others have provided detailed reviews with cost and energy assessments of these approaches in the context of new California homes (GARD Analytics, Inc., 2003a, 2003b; Hoeschele et al., 2015; Wei, Pande, Chappell, Christie, & Dawe, 2014). These advanced roof approaches are being pursued in parallel with other efforts to optimize HVAC performance in new California homes, namely through design and construction of compact duct systems, and improvements to insulation and airtightness of ducts. Unvented residential attics have received the greatest degree of study and assessment in the research literature, with documented use and proven performance for at least two decades in high performance homes throughout the U.S.

While select production builders have years of experience with unvented attics in California[3], most building professionals in the state are unfamiliar with unvented attic

[1] Component Package A, Options A and B.

[2] This assumes an air space beneath the roof cladding (e.g., vented roof tiles). With no air space, below deck requires R18 and above deck R8.

construction. The building trades, namely framing, HVAC and insulation subcontractors are not accustomed to the methods and requirements of unvented attic construction. This approach is not a trivial departure from standard practice. The most common implementation of unvented attics has been through use of spray polyurethane foam (SPF) insulation, which is much more expensive than other insulation solutions, such as fiberglass and cellulose. There are also concerns about the health impacts of off gassing from spray foam insulation. Furthermore, accumulation of moisture and building assembly degradation have been predicted and occasionally reported in the field and in the research literature.

2.2.1 Mandatory and Prescriptive Roof/Attic Options in 2016 California Building Energy Standards (Title 24)

The attic simulations are designed to represent new California construction, so we use the requirements in Title 24 to create the homes and attics to be simulated. Title 24 includes mandatory requirements, as well as prescriptive and performance paths to compliance. Items relevant to sealed and insulated attics are described below.

2.2.1.1 Mandatory Requirements in Title 24

The most directly relevant envelope mandatory requirement is that wood-framed roof/ceiling construction assemblies must have at least R-22 insulation, or a maximum U-factor of 0.043 based on 16 inch on center wood-framed rafter roofs. This forms the minimum installed insulation value for unvented attics. Other mandatory envelope features include radiant barrier and cool roof requirements, but these simply require that products be rated and labeled, or they define acceptable performance criteria, such as emittance of a radiant barrier.

For HVAC systems, heating and cooling equipment minimum efficiencies are specified, and system capacity must be calculated using ACCA Manual J or equivalent methods. Duct sealing and insulation are required in all locations. For ducts inside conditioned space, a minimum of R-4.2 is required. Ducts must be confirmed as inside conditioned space by visual inspection and testing of leakage to outside (See Reference Appendix RA 3.1.4.3.8) by a HERS rater. In all other cases the minimum duct insulation is R-6. All ducts must be measured for air leakage and have no more than 5% leakage, where the total system air flow is based on the nominal heating and cooling equipment capacity. HVAC distribution fans must provide at least 350 CFM per ton of nominal capacity, and they must do this using less than 0.58 watts per CFM. Minimum MERV 6 filtration is required in all air-handling units. All homes are also required to meet the provisions of ASHRAE Standard 62.2-2010 (plus several addenda), which specifies requirements for mechanical ventilation and other related measures.

---

[3] Hoeschele et al. (2015) suggest that one production builder—Meritage homes—has built over 10,000 units using unvented attics insulated with low-density spray polyurethane foam.

2.2.1.2 Prescriptive Compliance Paths for Roofs/Attics

The 2016 version of Title 24 includes numerous provisions for high performance attics and roof systems, and the code offers flexibility to designers and builders in order to achieve energy performance goals.

For ***vented attics***, three approaches are available for prescriptive compliance:

- *High Performance Ventilated Attic (HPVA) Option A*, requires continuous insulation on the exterior of the roof sheathing, as well as insulation on the flat ceiling. *Note: this option has been removed as a prescriptive path to compliance in the proposed 2019 building energy code.*
- *HPVA Option B* requires insulation installed below the roof sheathing, as well as on the flat ceiling. *Note: this is the only HPVA prescriptive option in the proposed 2019 code.*
- *Ducts in Conditioned Space (DCS) Option C* requires that the air handler and ducts be located inside the conditioned volume of the home, with field verification required for prescriptive compliance, namely duct leakage to outside shall be measured to be less than 25 cfm (form CF2R-MCH-20b).

A flow chart describing these three options is reproduced from the Residential Compliance Manual in Figure 1, and a simple checklist is reproduced in Figure 2. In the 2016 Residential Compliance Manual Chapter 3 (*Building Envelope Requirements, Section 3.6.2.1*), compliance options and best practices are detailed for meeting the High Performance Vented Attic (HPVA) requirements. Duct placement and HVAC requirements for HPVA are detailed in Chapter 4 (*Building HVAC Requirements, Section 4.4.2.1*). Specific requirements for each of these options depend on whether or not the roof cladding has a vent space behind it, as is typical with tile roof materials. Insulation and cool roof requirements for each California climate zone are provided for these options in Table 3. Wei et al (2014) outline development of these packages and provide detailed energy savings estimates. As noted above, the proposed 2019 building energy code has eliminated the HPVA Option A prescriptive compliance path, and it has increased the below roof deck insulation to R19 in the Option B path.

Figure 1 Title 24 2016 Ventilated attic prescriptive compliance choices (from Figure 3-15 in Section 3.6.2 of the 2016 Residential Compliance Manual).

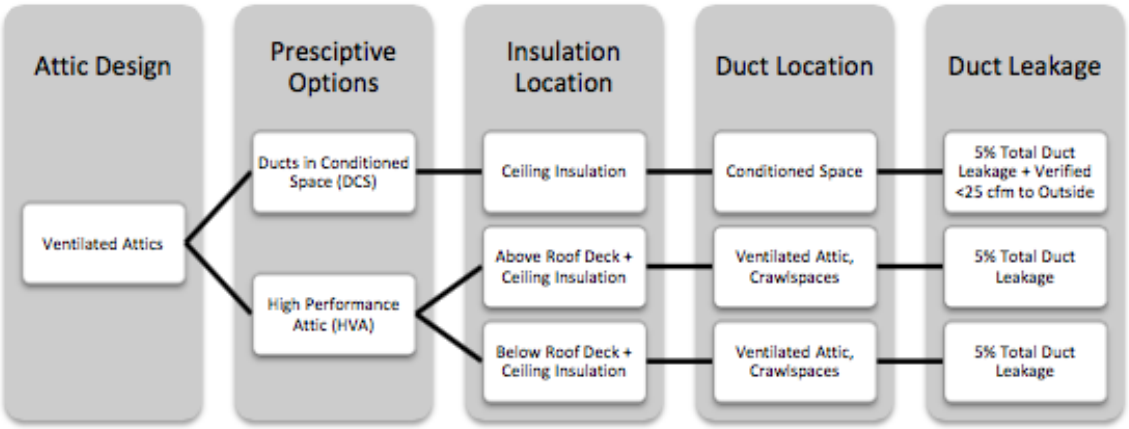

Figure 2 Title 24 2016 checklist for prescriptive requirements for HPVA/DCS for the related climate zones (from Figure 3-17 in Section 3.6.2.1 of the 2016 Residential Compliance Manual).

Option A (CZ 4, 8-16)	Option B[1] (CZ 4, 8-16)	Option C (CZ 4, 8-16)
☐ Vented attic ☐ R6 (air space) or R8 (no air space) continuous above deck rigid foam board insulation ☐ R38 ceiling insulation ☐ Radiant Barrier ☐ R8 duct insulation ☐ 5% total duct leakage	☐ Vented attic ☐ R13 (air space) or R15 (no air space) batt, spray in cellulose/fiberglass below roof deck secured with netting, or SPF ☐ R38 ceiling insulation ☐ R8 duct insulation ☐ 5% total duct leakage	☐ Vented attic ☐ R30 or R38 ceiling insulation (climate zone specific) ☐ R6 or R8 ducts (climate zone specific) ☐ Radiant Barrier ☐ Verified ducts in conditioned space
[1] Standard Design used to set the energy budget for the Performance Approach.		

Table 3 Reproduction of Roof/Attic requirements from Appendix B Table 150.1-A for prescriptive compliance with the Title 24 2016 Building Energy Code.

Attic/Roof Option	Element or Criteria	CEC Climate Zones															
		1	2	3	4	5	6	7	8	9	10	11	12	13	14	15	16
A	*Air Gap, NO – Insulation (R)*	NR	NR	NR	8	NR	NR	NR	8	8	8	8	8	8	8	8	8
	Air Gap, YES – Insulation (R)	NR	NR	NR	6	NR	NR	NR	6	6	6	6	6	6	6	6	6
	Ceiling Insulation (R)	38	38	30	38	30	30	30	38	38	38	38	38	38	38	38	38
	Radiant Barrier (Y/N)	N	Y	Y	Y	Y	Y	Y	Y	Y	Y	Y	Y	Y	Y	Y	N
	Duct Insulation (R)[4]	8	8	6	8	6	6	6	8	8	8	8	8	8	8	8	8
B	*Air Gap, NO – Insulation (R)*	NR	NR	NR	15[5]	NR	NR	NR	15	15	15	15	15	15	15	15	15
	Air Gap, YES – Insulation (R)	NR	NR	NR	13	NR	NR	NR	13	13	13	13	13	13	13	13	13
	Ceiling Insulation (R)	38	38	30	38	30	30	30	38	38	38	38	38	38	38	38	38
	Radiant Barrier (Y/N)	N	Y	Y	N	Y	Y	Y	N	N	N	N	N	N	N	N	N
	Duct Insulation (R)	8	8	6	8	6	6	6	8	8	8	8	8	8	8	8	8
C	*Ceiling Insulation (R)*	38	30	30	30	30	30	30	30	30	30	38	38	38	38	38	38
	Radiant Barrier (Y/N)	N	Y	Y	Y	Y	Y	Y	Y	Y	Y	Y	Y	Y	Y	Y	N
	Duct Insulation (R)	6	6	6	6	6	6	6	6	6	6	8	6	6	6	6	6
Low-Slope	*Aged Solar Reflectance*	NR	NR	NR	NR	NR	NR	NR	NR	NR	NR	NR	NR	0.63	NR	0.63	NR
	Thermal Emittance	NR	NR	NR	NR	NR	NR	NR	NR	NR	NR	NR	NR	0.75	NR	0.75	NR
Steep-Slope	*Aged Solar Reflectance*	NR	NR	NR	NR	NR	NR	NR	NR	NR	0.2	0.2	0.2	0.2	0.2	0.2	NR
	Thermal Emittance	NR	NR	NR	NR	NR	NR	NR	NR	NR	0.75	0.75	0.75	0.75	0.75	0.75	NR

2.2.2 Unvented Attics and the Performance Path to Compliance

Homes that use unvented attics must comply using the code's performance path requirements. The CEC estimates that 95% of permit applications for new home construction use the performance path for compliance, which is described in Chapter 8 of the 2016 Residential Compliance Manual. The performance path requires that the time-dependent valuation (TDV) energy use of the proposed design be equal to or less

[4] Ducts in conditioned space can have a minimum R-value of 4.2, which is only allowed when using the performance path to compliance.

than that for a similar home (i.e., same floor area, volume and surface area) meeting the Prescriptive Package A Option B, whose roof/attic requirements were detailed above.

Performance path projects must still meet the Mandatory elements of Title 24. For example, an unvented attic using the performance method would still need to follow the mandatory requirement of sealed and insulated HVAC ducts, with maximum tested air leakage of 5% of nominal system airflow and a minimum of R-4.2 insulation (even in conditioned space). Unvented attic roofs would also need to be insulated to an average level of R-22. Performance path homes must also meet any pertinent provisions in the California Residential Code.

3 Moisture Performance Metrics

We assess moisture risk in the field measurements and simulation results using a variety of metrics, including wood moisture content, mold index, surface condensation and others as detailed below.

- Mold index calculated per ASHRAE Standard 160P, assembly fails if mold index exceeds 3.
- Maximum 7-day mean wood moisture content at the wood surface nodes, assembly fails is running mean exceeds 28%. (Center of wood nodes remained dry in all cases and are not reported)
- Prior ASHRAE 160, assembly fails if 30-day running mean surface RH exceeds 80% when 30-day running mean surface temperature is between 5-40°C.
- Total condensed mass, no failure criteria.

3.1.1 ASHRAE Standard 160 Mold Index

The mold index model calculation in ASHRAE Standard 160 is the current consensus standard method used for determining the acceptable moisture performance of construction assemblies in the United States (ASHRAE, 2016). The mold index uses surface temperature, relative humidity and material risk class to assess the potential for mold growth on building surfaces. It includes effects of cyclic wetting and drying, temperature dependency, etc. The ability of this model to predict mold growth behavior on building materials in laboratory settings has been demonstrated in the research literature (Ojanen et al., 2010; H. Viitanen et al., 2010; Hannu Viitanen & Ojanen, 2007). The mold index also has a demonstrated track record of capturing truly risky assemblies in actual buildings, while being less likely to identify assemblies that are considered “safe” as problematic (Glass, Gatland, Ueno, & Schumacher, 2017). It is used as a post-processing tool for the suite of hygrothermal simulation tools under the name of WUFI (Fraunhofer IBP, 2018). It represents a much more sophisticated assessment of mold growth potential than the prior Standard 160 method, which required that 30-day running average surface RH be below 80% when the surface is between 5 and 40˚C.

Mold index is assessed on a scale from 0 to 6, as summarized in Table 4 in terms of visible surface mold and mold observed under microscope. To comply with the ASHARE 160 standard, an assembly must maintain a mold index maximum value that is equal to or less than three. Notably, meeting this performance criteria means an assembly can have visual findings of mold on the surface with <10% coverage, or <50% coverage of mold under microscope.

The mold index is the most conservative moisture performance metric, because thresholds for mold growth are commonly reached before structural degradation and rot can occur. The mold index is calculated at the interface of the insulation assembly and the sloped roof sheathing for the two primary roof orientations (typically North and South, in this work). These locations represent the first condensing surfaces in the sloped roof assembly, where we might expect moisture to condense and accumulate. In

addition, we calculate the mold index at the node representing the general attic framing. This node should capture the effects of potentially high moisture levels in the general attic air volume. The model assumptions used for each of the three moisture nodes are summarized in Table 5. In this work, we report failure rates (fraction of cases with mold index > 3), as well as maximum mold index values, where appropriate.

Table 4 Mold index values and their associated growth descriptions, microscope and visual assessments. Reproduced from Glass et al. (2017).

Index	Description of Growth Rate	Microscopic Observation	Visual Observation
0	No growth; spores not activated	None	None
1	Initial stages of growth	Small amounts of mold on surface	None
2	---	Several local colonies	None
3	New spores produced	<50% coverage	<10% coverage
4	Moderate growth	>50% coverage	10-50% coverage
5	Plenty of growth	---	>50% coverage
6	Heavy and tight growth	---	~100% coverage

Table 5 Mold index model assumptions used in sealed and insulated attic assessment.

Material/Moisture Node	Sensitivity Class	Decline Coefficient (k3)
North sheathing OSB	1 (Sensitive)	0.25
South sheathing OSB	1 (Sensitive)	0.25
Attic bulk framing	0 (Very Sensitive)	0.25

As with all metrics used to assess moisture issues, the mold index is not a precise measure of the probability of mold occurring. Although we use it in this study because it has been adopted by the relevant standard (ASHRAE 160) and represents our best effort to assess mold, it is worthwhile to investigate some of its short comings so as to create some context for the project conclusions.

Vereecken, Vanoirbeek, & Roels (2015) compared mold index predictions against experimental studies of mold growth on wood, and they highlight a number of scenarios where the VTT mold index dramatically under-predicts the risk of mold growth. For example, a wood sample held at a constant RH of 78% and 25°C was shown to have 25% mold coverage after 30 weeks (mold index of 3), while the VTT model and WUFI bio models predicted near-zero risk (mold index < 0.1), likely because 78% is just below the critical RH threshold used in the VTT model. Also, another comparison of a wood sample cycled on 12-hour intervals between 90% and 60% RH and 22°C showed similarly low mold index predictions (<1), while the experimental study showed an equivalent mold index of around 5. Vereecken et al. suggest that the critical RH should be revised to below 80% (as low as 75%). They also note that the experimental results have large

variance, while the mold index is deterministic, and they suggest a stochastic approach to modeling might better represent risk. Overall, they suggest that mold growth is a complex microbiologic process that is very challenging to study experimentally and is similarly difficult to predict using deterministic models. In particular, mold growth under transient conditions is identified as requiring further research.

Evy Vereecken & Roels (2012) present a comprehensive summary of different proposed methods to predict mold growth, and they discuss limitations of the VTT mold index model in this context. These limitations include: (1) mold declination during dry conditions is based on limited experiments, with no temperatures below 0°C and no test periods longer than 14-days; (2) the decrease in mold index during dry periods will not be associated with a change in the visual appearance of mold on a surface; (3) a lack of mold index declination during dry periods ranging between 6- and 24-hours appears physically unrealistic; and finally (4) a lack of verification of model predictions under real fluctuating conditions found in building assemblies. In general, they highlight the potential for different models to lead to different conclusions about risk of mold growth, both in terms of time-to-germination and growth intensity. For example, a comparison of the time to germination using different models showed an under prediction of risk for the VTT mold index compared with other available mold models (e.g., isopleths). In general, a large spread was found in the prediction of mold germination times between models, with the VTT mold index (and WUFI bio) models having the longest predicted germination times. For example, predictions under transient moisture conditions were particularly unstable, with VTT mold index suggesting germination after roughly 2,000 hours compared with <200 hours for several other models. The VTT model also showed lower mold growth intensity, compared with WUFI Bio, after 1-year of cycling RH conditions.

A further issue with using the mold index with monitored data is that proper hygrothermal assessments require multiple years, providing ongoing cycles of wetting/drying. The goal is to adequately control the net-effects of elevated surface RH or condensation over-time. It is common for the mold index to increase with time, but with substantial damping of the signal, such that it reaches some rough equilibrium after a handful of years. With less than two years of monitored moisture performance in our test homes, our ability to use this metric is somewhat compromised. However, if we see mold index levels above three during monitoring, that indicates potential problems.

3.1.2 Wood Moisture Content

Wood moisture content is a critical measure of the moisture performance of a building envelope assembly. Past moisture design efforts (Straube, Smegal, & Smith, 2010) have attempted to keep the equilibrium moisture content of wood building materials below 16%, which is approximately the level that is maintained while ambient humidity is fixed at or below 80% (see Figure 2). This was intended to align with the old ASHRAE 160 requirement that 30-day surface RH be less than 80% when temperatures are between 5 and 40°C. Yet, mold index research has suggested that this approach fails many safe

assemblies (Glass et al., 2017), because it is very conservative. Wood fiber saturation—at an average of 28-30% WMC (Richard et al., 2010) —is a more legitimate design threshold for wood moisture content, above which wood risks fungal and structural degradation. But even a transient wood WMC of 28-30% does not mean an assembly must fail. Other critical moisture content levels are often referred to. For example, by manufacturers of wood moisture meters[6], a 15% is usually used where we start to have concerns about corrosion of metal fasteners, near 20% we start to see physical weakening and mold growth and 20% is the usual number targeted for construction lumber prior to construction. "Kiln dried" wood is usually in the range of 15-19% (Richard et al., 2010).

An additional complication is that the surface of the wood interacts strongly with the surrounding air and its moisture content fluctuates on small time scales, which may be of interest and closely coupled to surface condensation and possible mold growth. However the bulk of the wood changes moisture content very slowly by diffusion from the wood surface. Therefore our simulation analysis will focus on the surface wood moisture contents by looking at 7-day running averages. A 7-day running period is used to filter out temporally variable high values that are not representative of long-term conditions. We label an assembly as a failure case if the 7-day running average WMC exceeds 28%, which is the critical threshold for structural wood rot organisms. In the field data, we simply report the time-series of hourly wood moisture contents, and do not calculate a running mean or maximum.

After selecting the maximum of the 7-day running average as our WMC metric, we wanted to ensure that we were still not getting transient high values that did not endure for longer periods of time. To assess this, in a subset of cases (n=384), we also calculated the 14-day and 30-day running averages and calculated their maximum values for comparison to the 7-day metric. As expected, the 7-day maximum WMC values were always higher than the 14-day, which were always higher than the 30-day maximum values. The median reduction in the calculated maximum WMC was a reduction of 0.6% WMC for the 14-day period (e.g., from 30% to 29.4%) and 1.2% for the 30-day period (e.g., from 30% to 28.8%). The greatest differences for any individual cases were 1.7% WMC and 4.3% WMC for 14- and 30-day periods, respectively. While any metric is imperfect, these marginal changes based on 7-, 14- and 30-day periods suggest that our 7-day metric is a reasonably good indication of elevated WMC for even periods up to 30-days, and that the 7-day period is necessarily more conservative and likely to fail an assembly.

[6] For example: https://www.wagnermeters.com/moisture-meters/wood-info/acceptable-moisture-levels-wood/

Figure 2 Illustration of equilibrium wood moisture content at varying ambient relative humidity at 10°C.

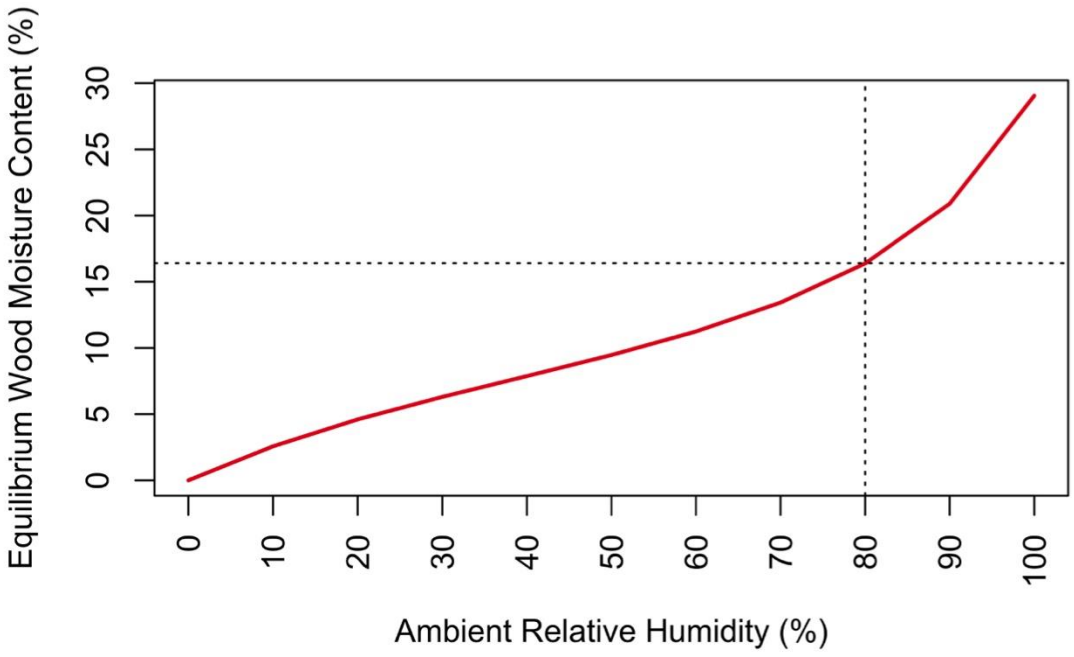

3.1.3 Other moisture parameters

The presence of condensation is a warning sign for moisture problems in a building assembly, but we also expect some condensation in nearly all assemblies at some point in their useful life. There is no hard and fast criterion for assessing risk from condensation, other than less is better. In fact, many assemblies can and do experience condensation events and provide perfectly adequate performance. Overall, we consider that brief periods of condensation are not problematic, as long as they dry fairly rapidly. Longer term, continuous periods of condensation are clearly undesirable and are potentially problematic from both mold growth and structural perspectives. In the field measurements, we have an indicator of condensation (i.e., yes/no), but cannot assess the condensed mass of water. In the simulations, we assess the total mass of condensed moisture that is recorded on a moisture node during the simulation period, and we compare these total masses across simulation parameters and moisture mitigations. This is the sum of cyclic patterns of condensation and re-evaporation; it is not a cumulative sum. In other words, the condensed mass values we report are not the amount of moisture in the wood at the end of the simulation. Instead, most of the condensed mass is either absorbed into the bulk of the wood or re-evaporated into the attic air.

Relative humidity is a related and similarly difficult to interpret value. Many safe assemblies will experience brief periods where the air at a wood surface is at or near

saturation. Prior ASHRAE 160 design criteria were based on simple RH and temperature relationships and have been deemed overly conservative. So, while RH is a critical input to our mold index calculations, we do not feel that it warrants independent reporting, outside of illustrative plots and descriptions related to mold index results and the like.

As a check on the continuous moisture monitoring (and for peace of mind for the builder) we also performed a visual inspection of selected areas of the roof deck where the measurements indicated the potential for condensation and/or high wood moisture content. To do this we carefully moved aside the roof deck insulation at the measurement locations and replaced the insulation after inspection. Visual inspection results are detailed in Section 5.3.1.

4 Field Study Methods

4.1 Test Home Descriptions

Two new slab-on-grade test homes with HVAC equipment located inside sealed and insulated attics were instrumented in Fresno and Clovis California in collaboration with a regional homebuilder who focuses on high-performance homes, for whom this is a new construction strategy. The Fresno test home was monitored continuously from September 2016 to the end of April 2018, while the Clovis test home monitoring occurred from June 2017 through mid-May 2018. The Fresno home exceeds California Title 24 energy performance requirements by 30%, while the Clovis home is designed as a net zero-energy home.

The Fresno home is a two-story residence with conditioned floor area (CFA) of 3,605 ft^2, while the Clovis home is a smaller single-story residence with CFA of 2,019 ft^2. Basic geometry features for each home are tabulated in Table 6, and annotated floor plans are provided for the Fresno and Clovis homes in Figure 4 and Figure 5, respectively. The installed HVAC systems are described in Table 7.

Figure 6 and Figure 7 show images of the Fresno home while under construction. Both test homes have non-traditional geometries that complicate sealed and insulated attic construction, as well as monitoring and performance assessment. The single-story Clovis home is roughly a square that surrounds a small interior courtyard and has four attic volumes connected by modest pathways of 1-2 ft^2. Some of these attic volumes are quite small (estimated at 472 and 296 ft^3 respectively for the EW26N and EW26S attic volumes), with large surface-area-to-volume ratios. The Fresno home is somewhat more traditional, with a basic L-shape and two main conditioned attic volumes—one with East-West orientation named EW52 (and North/South oriented sloped roof surface) and another with North-South orientation NS33 (and East/West sloped roof orientations). Our results focus on the attic volumes with North-South orientations, because North-oriented roof ridge locations have been previously identified as the most likely to experience moisture accumulation and mold growth. Both homes have roofs sloped at 4:12 or 5:12 and are clad with medium-grey colored concrete roof tiles supported by horizontal battens (1.5” depth) with initial laboratory measured albedo of 0.12. The attic volumes were sealed and insulated to bring them inside conditioned space in each home using R38 unfaced fiberglass batt insulation held in place using wire supports. The insulated attic volume of the Fresno home is pictured with fiberglass batts installed in Figure 3.

Construction and inspection challenges were noted in both homes. Visual inspections revealed that insulation was generally held tightly against the underside of the roof deck, though some isolated locations were found with the insulation sagging away from the OSB by ½-1” in the Fresno home. Coordination between HERS inspection, insulation

contractor and builder were required to address these issues. In the Clovis home, visual inspection revealed a number of locations where subsequent trades had disrupted the insulation around plumbing and HVAC roof vent penetrations, which were fixed. Vigilance was required by all trades working on the projects, even the building performance inspectors. For example, in the Clovis home, one of the conditioned attic volumes included a garage ceiling area of several hundred square feet, which was initially missed by the insulation crew and performance inspectors. Insulation was later installed on the garage ceiling to separate the conditioned attic from the unconditioned garage volume below. Similar issues were noted at covered porch overhangs. These issues highlight the critical need for a design review of this attic construction method with all trades involved, including framing, insulation and mechanicals (i.e., electrical, plumbing, HVAC). Even the building performance provider assessing the work needed to ensure that their best-trained inspectors were treating these homes as “different” from standard code and program inspections. Design considerations also surfaced, for example in the Clovis home, once interior sheetrock was installed, the two of the four attic volumes were completely inaccessible for inspection or remedial work, and the other two were only accessible from outside of conditioned space.

Finally, we note that when using batt insulation to insulate the triangular shape where the sloped roof surface meets the roof ridge blocking, there is an obvious mismatch in geometry. Visual inspection of the ridge blocking showed that the batt does not entirely fill the triangular area. A small void is left there: a triangle of roughly 2-3” along the sloped roof.

Table 6 Summary of test home geometries.

Element	Fresno	Clovis
Conditioned floor area (ft^2)	3,605	2,019
Ceiling area (ft^2)	1,985	2,768*
Conditioned volume (ft^3)	39,634	25,437
Living space volume (ft^3)	34,079	20,190
Attic volume (ft^3)	5,554	5,247
Roof slope	5:12	4:12
Roof finish	Cement Tile on battens	Cement Tile on battens
Number of stories	2	1

* Ceiling area is greater than conditioned floor area, because attic includes garage and rear porch ceiling areas.

Table 7 Test home installed HVAC equipment specifications.

Test Home	Compressor			Furnace		
	Make/Model	Capacity	SEER/ EER	Make/Model	Capacity	AFUE
Fresno	Lennox: 14ACX-047-230	47 kBtu/hr	15 / 12.5	Lennox: EL296UH090 XV48C	85 kBtu/hr	0.96
Clovis	Lennox: 14ACX-036-230	34 kBtu/hr	15 / 12.5	Lennox: EL296UH070 XV36B	62 kBtu/hr	0.96

Figure 3 Image of R38 unfaced fiberglass batts installed with wire supports in the Fresno test home main attic.

Figure 4 Fresno home roof framing plan. Primary monitoring locations were both the EW52 and NS33 attic volumes.

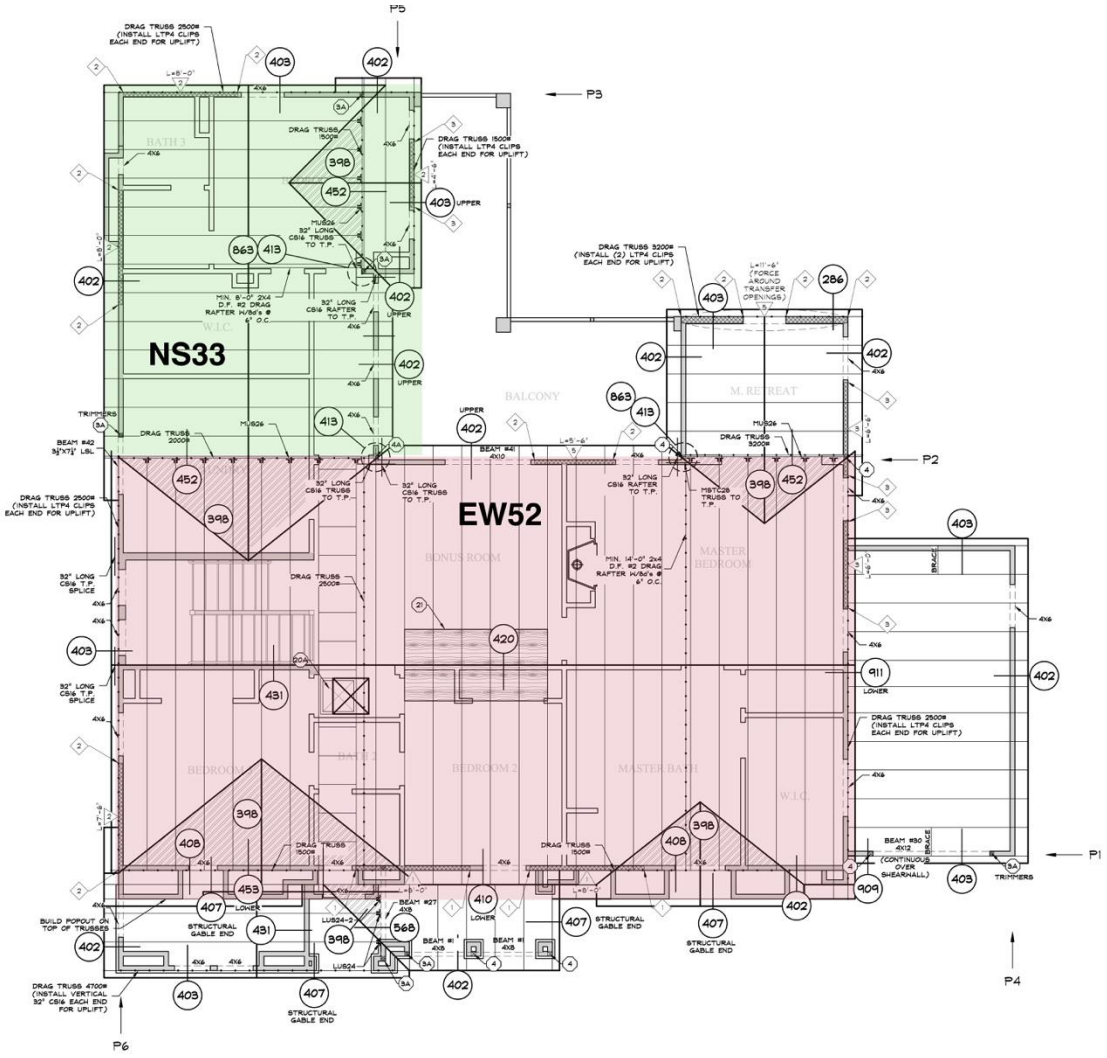

Figure 5 Clovis home roof framing plan. Primary monitoring location was the EW26N volume.

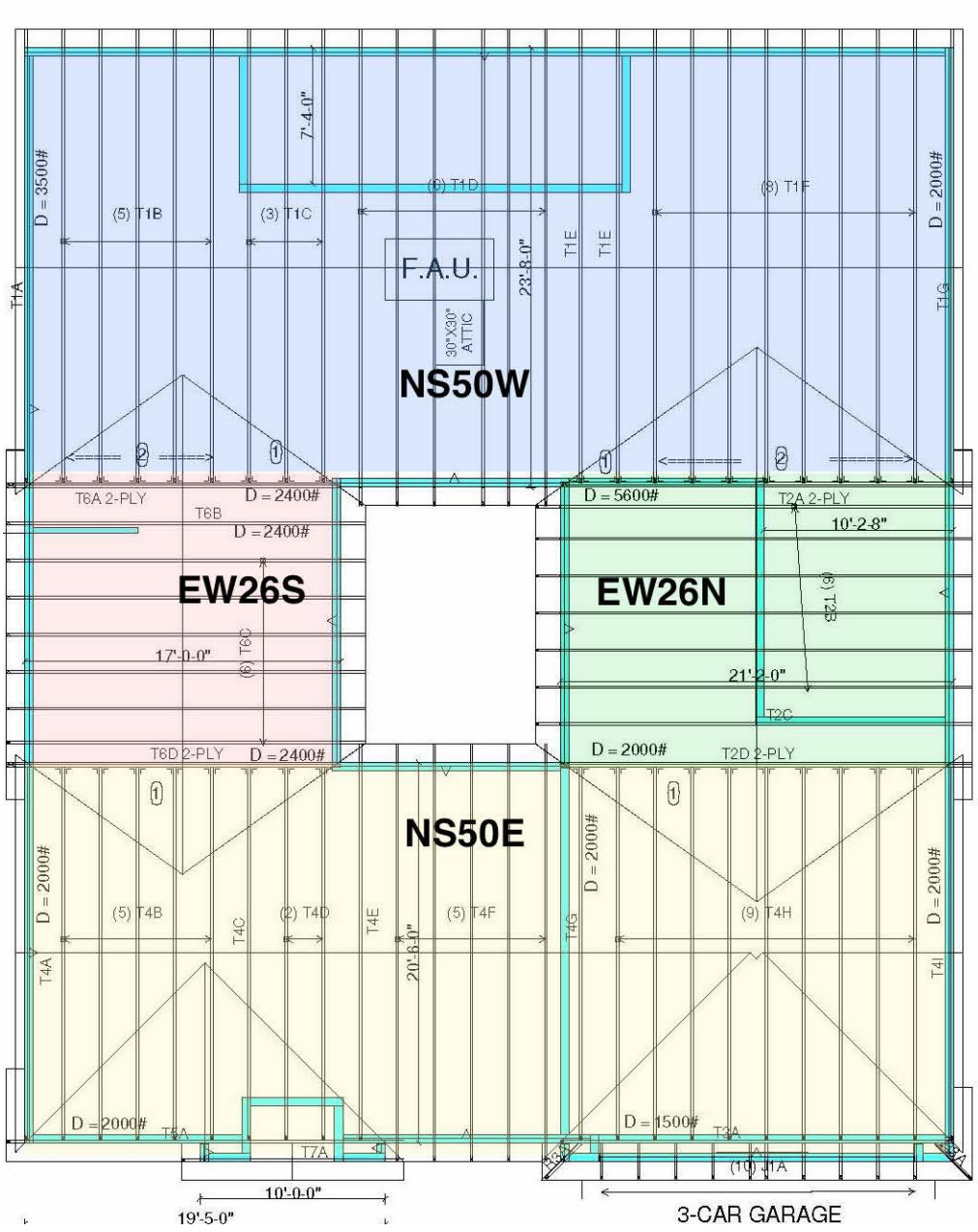

Figure 6 Fresno. Aerial photo of slab being poured in development.

Figure 7 Fresno. Rough framing stage photo.

4.2 Monitoring Hardware

Measurements in the sealed and insulated attic test homes included temperature, relative humidity, condensation, wood moisture content, heat flux, weather, solar irradiance and HVAC energy consumption (see Table 8).

Table 8 Description of measurement parameters, sensors used and accuracy estimates.

Parameter	Method	Accuracy/Calibration
Temperature	NTC Thermistor 10K OHM Bead	Salt bath lab calibration, +/- 0.1°C
Relative Humidity	Vaisala HMP110	Factory calibration, +/- 1.5% RH
Condensation	SMT Condensation Sensor COND-002-006 (dielectric capacitance sensing)	Exact factory calibration unknown.
Wood Moisture Content	Insulated moisture pins, resistance measurement by SMT-A2	Moisture content estimated from temperature and resistance using Equation 2 from Boardman, Glass and Leblow (2017), model coefficients from full data set.
Heat Flux	Hukseflux HPF01	Factory. ± 3 % (k = 2)
Outdoor Conditions	MetPak Weather Station; data acquisition by RaspberryPi	Factory. Wind Speed: ±2% @12m/s; Wind Direction: ±3° @12m/s; Temperature: ±0.1°C; RH: ±0.8% @ 23°C; Barometric Pressure: ±0.5hPa; DewPoint: ±0.15°C
Solar Irradiance	Eppley Precision Spectral Pyranometer (PSP) (Global Horizontal Irradiance)	±3-4%
HVAC Energy	WattNode (WNB-3D-240-P with Option HZ = 10); pulse counting by RaspberryPi	+/- 0.5%

Figure 8 Data acquisition network diagram.

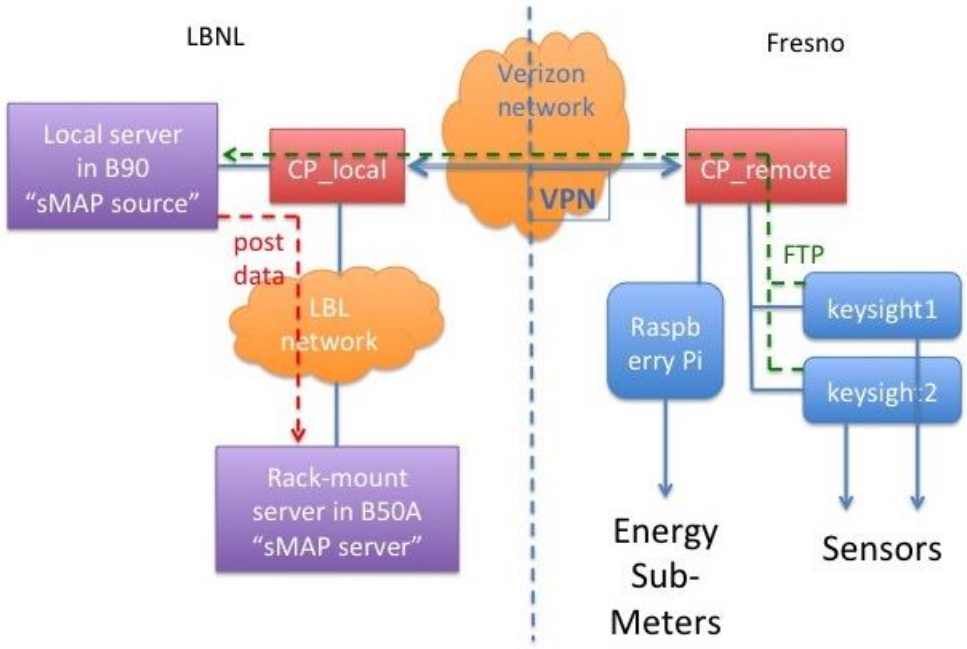

An overview of the data acquisition system is illustrated in Figure 8. The networked system includes:

- Monitoring equipment at remote sites
    - Keysight/Agilent 34972A Data Acquisition/Switch Unit, 60-measurements each, 60-second multiplexer sweep
        - Thermistors
        - Thermocouples
        - Relative Humidity
        - Surface condensation
        - Heat flux
        - Solar irradiance
    - Raspberry Pi 3 Linux computers
        - Pulse counting for air handler, compressor and gas furnace energy sub-meters
        - Weather station
    - SMT Research Building Intelligence Gateway (BiG)
        - A2 Data Logger Wood Moisture Pin resistance
- Local ethernet/WiFi networks at each remote site hosted on Cradlepoint MBR1200b router
- Cellular VPN connecting the remote site Cradlepoints to an LBNL Cradlepoint MBR1400v2
- Two servers at LBNL used for driving data acquisition (sMAP Source) and hosting the sMAP database (sMAP Server).

Data acquisition was driven primarily by Agilent 34972A LXI Data Acquisition/Data Logger Switch Units, and secondarily by custom-programmed RaspberryPi computers used for pulse counting and for weather data acquisition. Each Agilent multiplexer was

capable of 60 independent measurement points. All inputs to the multiplexer were swept once every minute for the duration of the logging period. All date time stamped data were captured by the Agilent's on-board logging system, and a time-stamped .csv file was written to an external USB drive once every hour.

The LBNL server retrieved the Agilent data files once every hour using FTP protocols, with appropriate methods in place to capture any data missed by network interruptions or the like. This data was then immediately posted to a networked sMAP database for efficient storage, retrieval and online visualization. RaspberryPi computers were programmed to push data to the sMAP database once per hour from their remote locations. All data was retrieved as hourly averages from the sMAP database and were analyzed and plotted using R.

Figure 9 Fresno. Keysight DAQ multiplexer.

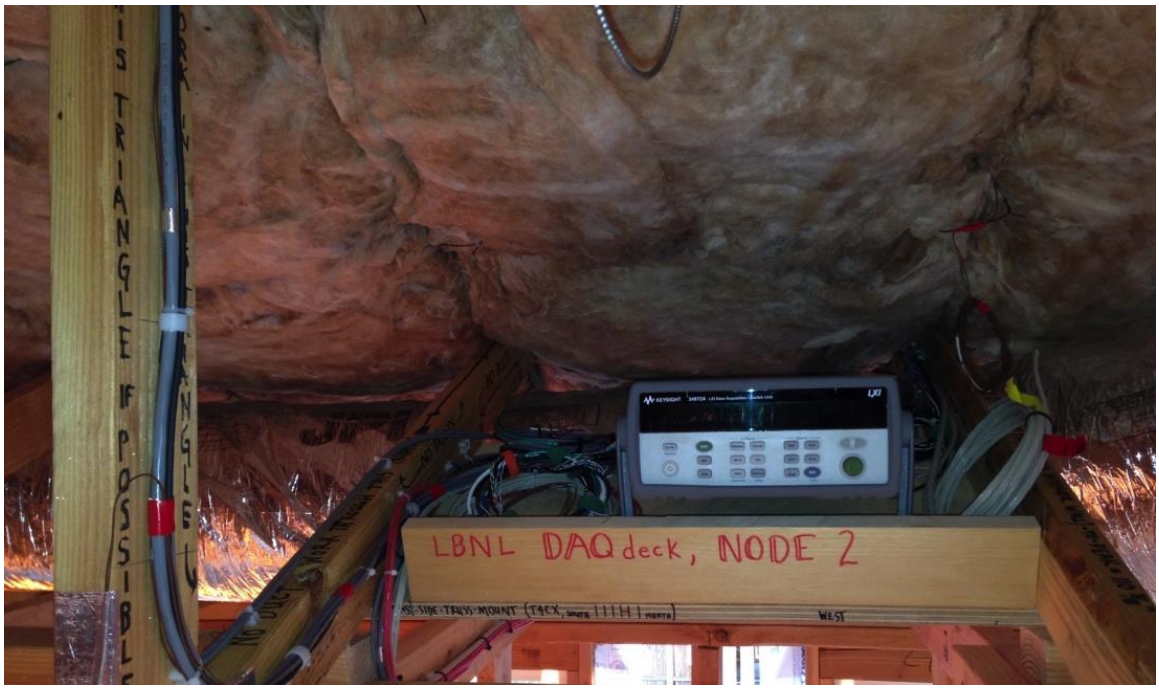

4.2.1 Sensor Placement

The Fresno test home had more extensive monitoring than the Clovis test home and the two attics are described separately.

4.2.1.1 Fresno Test Home

In the Fresno home, the primary monitored attic volume was the EW52 volume, and the secondary attic was the NS33 volume. The NS33 attic is notable, as it has a solar PV array installed on its Western slope, as shown in Figure 10. The HVAC equipment was located primarily in the main EW52 attic volume, with some duct runs extending into the NS33 attic. In Figure 11, the sensor layout is overlaid on the Fresno home floor plan, along with a solar path diagram. Each main attic volume used a separate Keysight data acquisition unit.

Sloped roof measurements were made in the center rafter bay at one of three locations for each orientation:

(1) Eave,
(2) Mid-span
(3) Ridge

At a given location along the sloped roof surface, measurements were made at different depths through the insulated roof deck assembly, including the:

(1) Interface of the insulation and the attic air
(2) Insulation middle
(3) Interface of the insulation and the roof deck

At the mid-span location for each orientation, additional measurements were made:

(1) Temperature measurements were made on the underside of the roof tiles and on the sky-facing top of the roof tiles.
(2) Heat flux was measured at the interface of the insulation and the OSB roof deck.

Temperatures were measured with thermistors for each of the locations described above. Backup thermocouples were also installed at the interface of the insulation and roof deck, due to their higher tolerance for extreme temperatures.

While temperature measurements were spread broadly across the attic surfaces, moisture measurements were concentrated at the roof ridge locations. Wood moisture content of the OSB roof decking was measured within 6 inches of the ridge for each orientation. The North roof slope in the EW52 attic had an additional OSB wood moisture pin measurement at the eave. Surface condensation sensors were co-located with the WMC probes near the roof ridge for each orientation. Surface relative humidity was measured at the roof ridge for each attic volume. The RH sensors were installed on the ridge blocking material (2x4) within 1.5” of the OSB roof deck, and the humidity ratio at that location was paired with the roof deck temperatures for each orientation and translated into a surface RH for each slope.

Measurements in the general attic volume included the following:

(1) Temperature stratification tree arrayed from attic floor to the ridge.
(2) Attic air volume relative humidity at mid-height, attached to the stratification tree.
(3) A separate stratification tree of HOBO T/RH data loggers was also installed to assess moisture gradients in the attic air (solely in the EW52 Fresno attic space).
(4) Heat flux across the sheetrock ceiling (interface between living and attic volumes).
(5) Wood moisture content of the general attic framing, roughly co-located with stratification tree.

Living space measurements included the air temperature and relative humidity for each HVAC thermal zone. Sensors were co-located with the wall thermostats used for HVAC control.

Figure 10 NS33 Fresno. Solar panel installation.

Figure 11 Fresno. DAQ layout, site orientation, sun path.

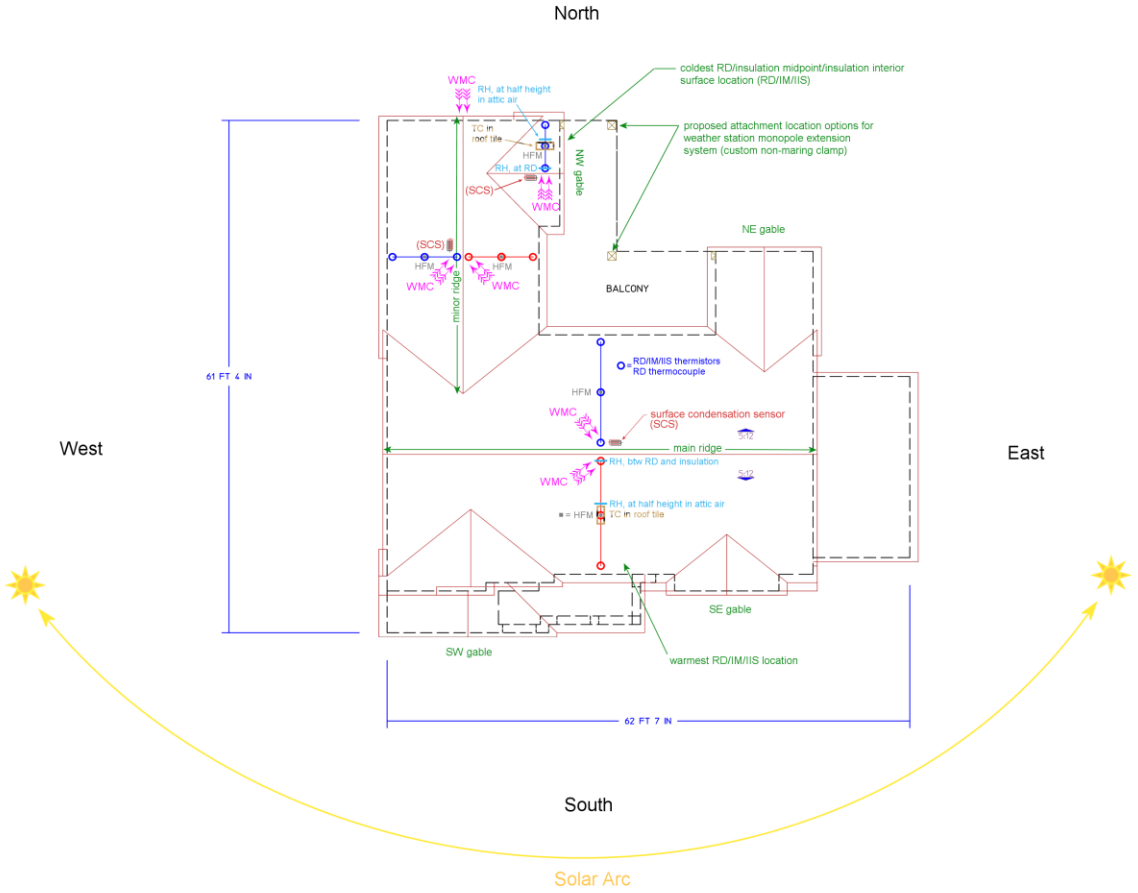

4.2.1.2 Clovis Test Home

Overall, less instrumentation was installed in the Clovis home, with only a single Keysight multiplexer unit serving the entire home. In the Clovis home, nearly all monitoring occurred in the EW26N attic volume, which is situated partially over the unconditioned garage, as well as over the master bathroom and master closet areas. The only measurements made in the other attic volumes were in order to capture wood moisture content near the roof ridge for the East and West oriented roof slopes. Notably, the HVAC system and most of the ducting was located in the NS50W attic volume, which was not monitored, except for roof ridge wood moisture content, as noted. The conditions in the monitored attic may have differed substantially from the conditions in the attic containing the HVAC equipment. First, thermal gains and losses from the HVAC system would have affected the conditions in the NS50W attic, and also the geometries and orientations are different. The monitored EW26N attic volume was quite small and compact, with lots of roof deck surface area facing a small air volume.

4.2.2 Water Bath Thermistor Calibration

All thermistors use the Steinhart-Hart equations built into the Keysight instrument to calculate temperature based on measured voltage for 10 kilo-ohm thermistors. In addition, we used a calibration derived from a water bath cross-calibration, using the following linear equation:

$$Temp_{calibrated} = 0.926884\, Temp_{S-H} + 1.931424$$

$Temp_{calibrated}$ = calibrated temperature, reported to sMAP database, °C

$Temp_{S\text{-}H}$ = temperature reported by Keysight using Steinhart-Hart equations, °C

The water bath calibration process (pictured in Figure 12 and Figure 13) could have facilitated custom calibration coefficients for each thermistor used in the field, but this would have only increased accuracy from the ±0.1°C to ±0.05°C.

Figure 12 Thermistor calibration grid.

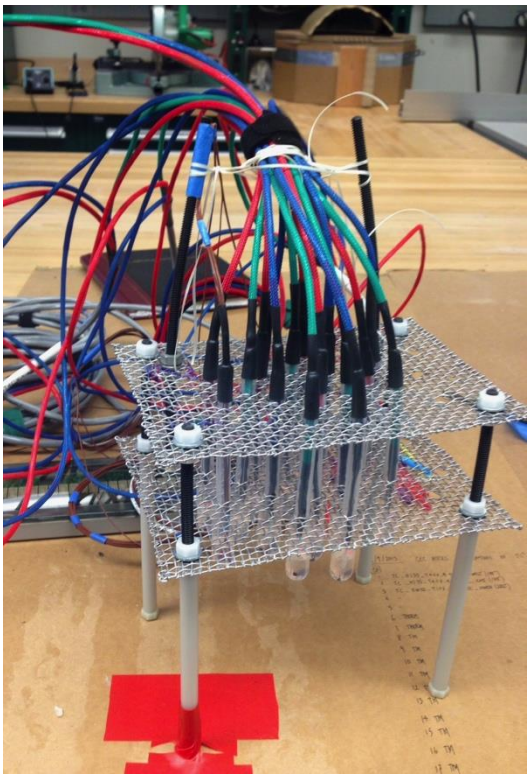

Figure 13 Thermistor water bath calibration.

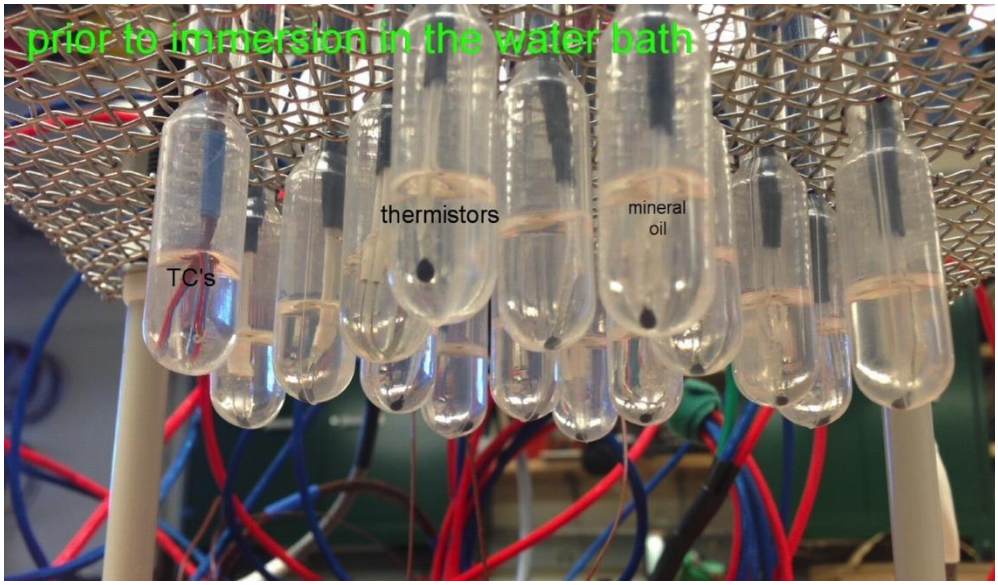

4.2.3 HOBO Moisture Stratification Tree

Past research in sealed and insulated attics has noted that the roof ridge, in particular with a Northern orientation, is the location most sensitive to moisture issues. It is possible that is due to thermal and moisture stratification. To assess this, we assembled a stratification tree comprised of six temperature and relative humidity HOBO U12 data loggers in the EW52 attic volume of the Fresno home (shown in Figure 14). These measurements were an add-on and were not integrated with the Keysight data acquisition system. The HOBOs reported on 10-minute increments from late June of 2016 to early June of 2017.

A cross-calibration was used with these sensors prior to installing them in the Fresno home attic. The intention was to improve the precision between the six sensors, relative to one another, rather than achieving accuracy relative to actual moist air conditions. They were all sealed in an airtight plastic bag and exercised over a wide range of temperatures, for a period of 30-hours. A linear calibration model was then developed for each sensor, with the peak location sensor used as the calibration reference. The resulting calibration coefficients and R-squared values are reported in Table 9. These were applied to all monitored results from the HOBO dataloggers.

Table 9 EW52 Fresno. Linear model calibration coefficients used to correct each HOBO temperature/RH sensor for use in assessing vertical moisture gradient in attic air volume.

Stratification Tree Node, Down From Peak	Temperature			Relative Humidity		
	Intercept	Slope	R^2	Intercept	Slope	R^2
1	-0.475	1.010	0.997	0.574	0.959	0.974
2	-0.806	1.015	0.998	-0.029	0.977	0.986
3	-1.376	1.022	0.994	3.396	0.873	0.935
4	-0.137	1.010	0.993	0.009	0.974	0.956
5	-0.551	1.016	0.994	0.191	0.935	0.981

Figure 14 HOBO Stratification tree in EW52 Fresno Attic.

4.2.4 Weather Station

A Gill MetPak weather station was installed above the roofline at each monitoring site and connected to a local Raspberry Pi unit, which logged data and posted hourly data files to the sMAP database. MetPak measurements included outdoor dry-bulb temperature, relative humidity, dew point temperature, wind speed, wind direction and atmospheric pressure. We relied upon factory calibrations for all outputs associated with the Gill MetPak weather tower. The installed weather tower at the Fresno home is pictured in Figure 15 and Figure 16.

Figure 15 Clovis. Weather tower data station and solar pyranometers.

Figure 16 Fresno. Weather tower and pyranometers.

4.2.5 Wood Moisture Content

Wood moisture content was measured in several locations using calibrated wood moisture pins. The resistance was measured between two nail probes, and the results were reported hourly. We custom-built the nail probe sets, and used the SMT Research A2 Datalogger to measure resistance, because of its off-the-shelf ability to resolve very high resistance numbers (from 100 kilo-ohms to 1 gigaohm), which requires substantial

custom circuitry. This allowed us to have improved resolution at lower wood moisture content (higher resistance).

Moisture pins are spaced 10mm apart, with an uninsulated nail shank depth into the OSB of 10mm. Exposed nail shanks sticking out of the wood were insulated with nail polish, which was tested and confirmed to be non-conductive. The nail polish was spread around the nail shank on onto the surface of the OSB. A split jig was used to maintain precise separation and nail penetration depth for each set of pins (see the sequence in Figure 17). An example of a finished, installed set of WMC probes is provided in Figure 18.

Moisture pin resistance is translated to wood moisture content using the co-located temperature measurement with the equation provided by (Boardman, Glass, & Lebow, 2017), using coefficients derived from the full data set (Equation 2 in Boardman et al), as follows:

$$\boldsymbol{WMC = b_0 + b_1 T^{b_4} + b_3 T^{b_4} log_{10}(log_{10}(R_w) - b_2)}$$

WMC = wood moisture content, %

b_0 = -8.6810

b_1 = 3.7172

b_2 = 3.8974

b_3 = -2.9129

b_4 = 1.9000

T = 1000./(273.15 + t)

t = co-located surface temperature, °C

We further tested this calculation method and our measurements using a mass-based calibration in the lab. OSB samples were taken from the material installed in the Fresno and Clovis attics, and they were bone dried in an oven. The OSB samples were then wetted to target moisture contents of 10 and 20%. We used the Boardman equation above to calculate the WMC from the moisture pin resistance, and we also estimated the actual moisture content using scale mass measurements relative to the mass of the oven dry samples. For the OSB samples, we found a mean absolute error of 6% for these moisture contents, relative to the actual mass-based moisture content. RMS error was 9%. So, for an example sample at 20% WMC, we expect our results to be +/- 1.8% (18.2 to 21.8%).

In the EW52 Fresno attic north peak sheathing location, we added some additional wood moisture probes, with insulation penetrating through the surface of the OSB. This additional insulation cut off the conductive path at the surface of the OSB, with the goal of solely measuring the moisture content in the center of the OSB. Two sets were installed, one with exposed nail shank from 0.25-0.35” below the OSB surface and

another with exposed nail shank from 0.35-0.45”. The installation of these additional moisture pins is pictured in Figure 19.

Figure 17 Installing WMC pin resistance measurements, using insulated nail probes and a precision mounting jig.

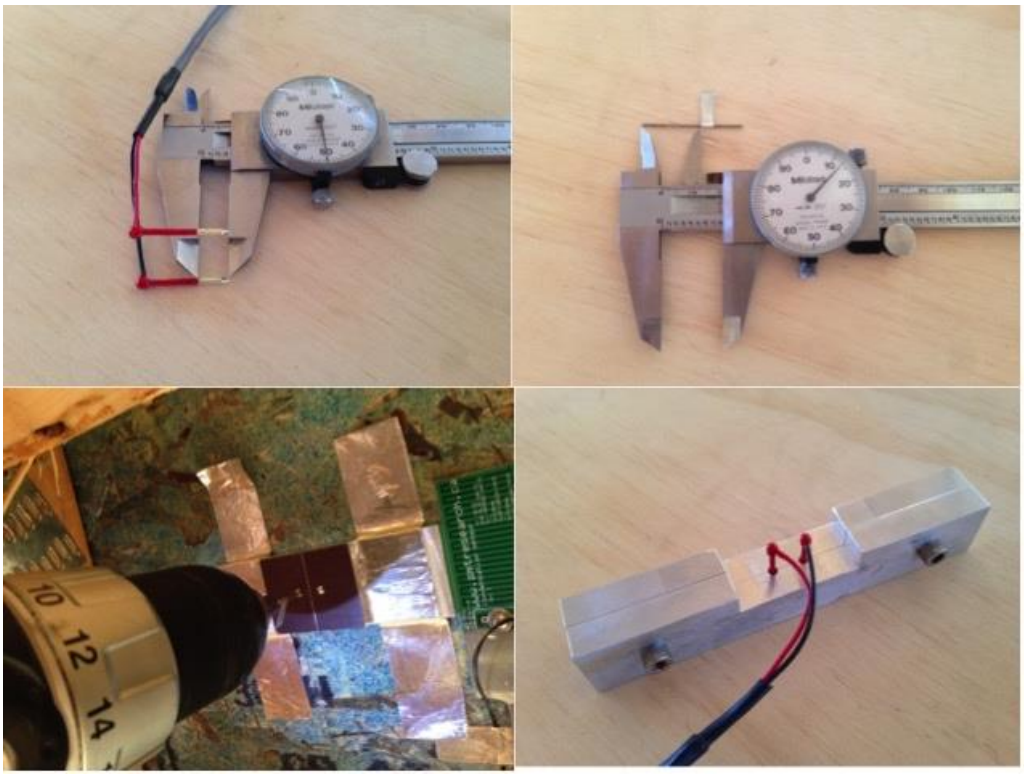

Figure 18 Complete installation of a WMC nail probe set.

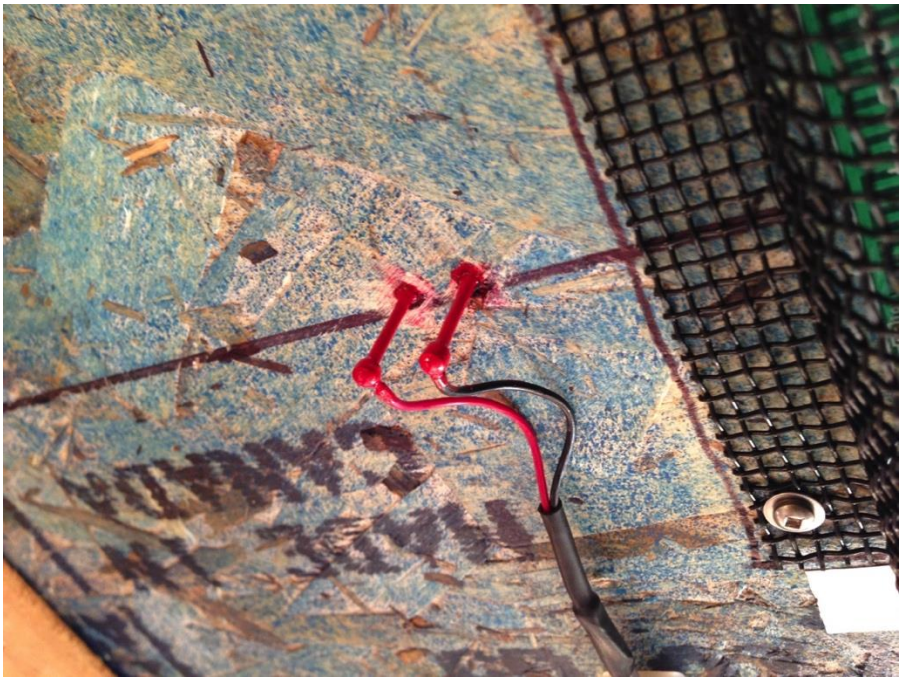

Figure 19 EW52 Fresno. WMC moisture pins, plus center-of-wood moisture pins, installed 2017-04-04.

4.2.6 Surface Condensation Indicator

Surface condensation was indicated using dielectric-based capacitance sensing with the SMT Research Condensation Sensor (COND-002-006) (see an installed example in Figure 20 with mesh screening to keep fiberglass fibers off the face of the sensor). This sensor outputs a voltage signal that is proportional to the mass of liquid water (or snow, ice, etc.) present in its dielectric field. According to the sensor data sheet, output voltage values between 160 and 300 mV indicate that condensation is present, while larger liquid water droplets are indicated in the 400-800 mV range. We created an arbitrary linear equation that is forced through 0 at 160 mV and gives a linear response from roughly -0.1 to 0.8 over the expected range of measured voltages (0-800 mV). The output voltage is scaled as follows.

$$\boldsymbol{Condensation = 0.60606\,V - 0.0969697}$$

Condensation = variable indicating presence of liquid water at the sensor, values >0 indicate that water is present. Negative values are dry.

V = measured voltage

It must be stressed that this is an imperfect indicator of condensation, rather than a precise measure of moisture mass. When we present condensation results, we corroborate them with measured wood moisture contents and surface relative humidities. Furthermore, we rely minimally on the proportional output of the sensor, and rather report any values >0 in a binary fashion, as hours with some condensation present.

Figure 20 EW52 Fresno. Mesh shielding protecting the condensation and relative humidity sensors from direct contact with fiberglass fibers.

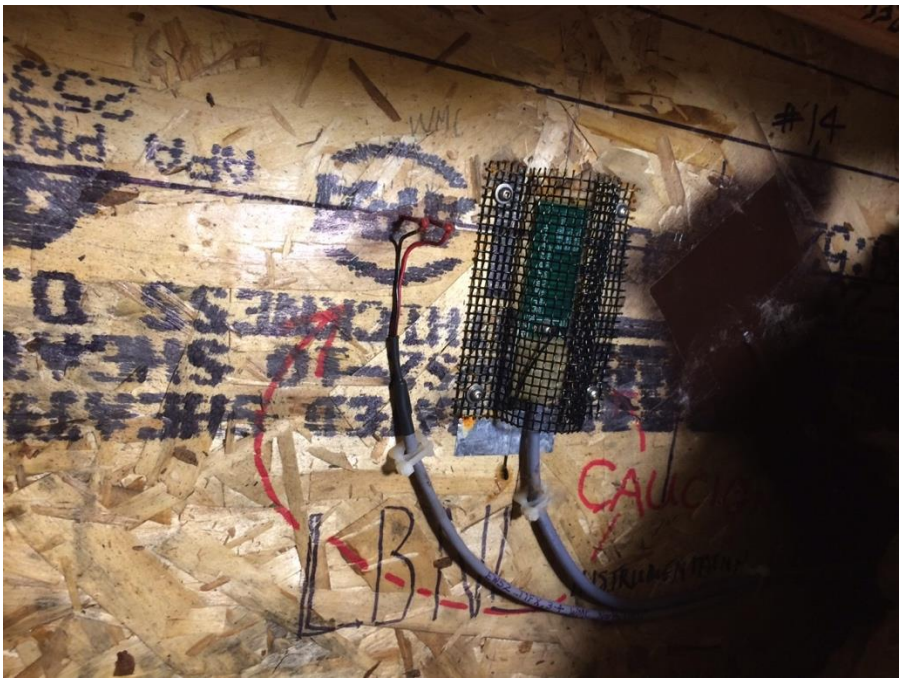

4.2.7 Relative Humidity

Relative humidity was measured using Vaisala HUMICAP Humidity and Temperature Probes (HMP110; 1.5% accuracy from 0-90% RH; ±2.5% from 90-100%; accuracy worsens <0°C and >40°C). These were placed in the air volume in the living space and the attic, as well as surface RH measurements at the roof peak. All sensors were newly purchased prior to installation and factory calibrations were relied upon. An example installation is shown for general attic air volume RH in Figure 21 and for attic peak RH in Figure 22 (note shielding to keep glass fibers off the sensor).

The RH measurements and their co-located temperature measurements are used to calculate the mold index, as well as other moist air properties (i.e., partial vapor pressure and humidity ratio). Moist air relations from the ASHRAE Handbook of Fundamentals were used for all such calculations.

The attic air peak RH measurement in the main EW52 Fresno attic was mounted on the Southern face of the roof deck, which is consistently warmer and dryer than the North roof deck. Given the critical nature of the North-oriented sheathing, we used this sensor to calculate the surface RH at the North sheathing as follows: the South sheathing measured RH and surface temperature were used to calculate a humidity ratio for air at the peak. This humidity ratio was then translated to a Northern surface relative humidity using the measured North sheathing surface temperature.

The same type of corrections were used in the Clovis home, where roof ridge RH was measured as in Figure 22, with the RH sensor mounted on the North-facing ridge blocking, within roughly 1.5” of the OSB roof deck. The temperature at the OSB surface

did not match the temperature at the RH sensor, so the absolute humidity ratio was calculated at the sensor location, and was then translated to a surface RH at the relevant OSB roof deck temperature.

Aside from sensor accuracy as reported by the manufacturer, there are some potential inaccuracies in the RH measurement data. First, as described in the prior two paragraphs, the surface RH was derived from a humidity ratio at the ridge, and was then translated to a surface RH using the relevant surface temperatures. This assumption can introduce errors, to the extent that the actual humidity ratio may be different at the different surfaces. Second, and potentially related to the surface RH translations, are the different time constants for the temperature and humidity sensors within the Vaisala instrument. The temperature time constant is very short (much shorter than the 1-minute measurement time step), such that changes in temperature are very rapidly resolved in the data stream. The time constant for the moisture sensor is typically much longer (longer than the measurement time step), which means that a change in the air moisture level can take several measurement time steps to be resolved in the data. Yet, the data stream demands that an RH estimate be made each minute. This is not a problem when temperature and moisture are changing slowly relative to the time constants of the two sensors. But this may not be the case at the insulated roof deck of a sealed attic, where the temperature changes rapidly, as may the moisture in the air at the OSB surface. For example, with a time constant of 10 minutes for the moisture probe, the RH is derived each minute by the sensor assuming that fixed moisture content while the temperature changes at each time step. This results in erroneous RH estimates. The direction of the error due to this misalignment in time constants can depend on whether a surface is heating up or cooling down. As the sensor heats up, the RH (and calculated vapor pressure) is biased low, and while it cools down, the RH is biased high. The net-effect depends on non-linearities and different time constants in the sensors and was beyond the scope of this study to evaluate.

Figure 21 EW52 Fresno. Attic air volume relative humidity sensor (Vaisala HMP110).

Figure 22 EW26N Clovis. Relative humidity and condensation sensors installed prior to placement of insulation.

4.2.8 Solar Irradiance

Solar irradiance was measured by pyranometers at the weather tower site on each test home. Global horizontal irradiance (GHI) was measured with a level, sky-facing Licor pyranometer sensor connected to the Keysight multiplexer. The GHI is used to estimate clear vs. cloudy days, and to provide overall estimates of incoming irradiance. For use in the REGCAP simulation model, we needed to discern between direct normal (DNI) and diffuse horizontal irradiance (DHI). To do this, we used the DIRINT Direct Normal Irradiance model, as implemented in the Python package *pvlib-python (pvlib-python, n.d.),* which estimates the DNI using measured GHI and outdoor air dew point temperature. This python method is an implementation of the model described in (Ineichen, Perez, Seal, Maxwell, & Zalenka, 1992), which is a revision to the quasi-physical DISC model originally developed by (Maxwell, 1987).

Pyranometers deployed in the test homes were cross-calibrated at LBNL over a number of days (see Figure 23). The Eppley pyranometer used for GHI was corrected using a linear regression equation, which adjusted the outputs of the deployed Eppley to best match the average outputs of two brand new Eppley units. A slope coefficient of 121717.7 with an intercept value of 5.323 were applied to the raw mV output of the Eppley instrument. This correction resulted in an average error, relative to the new Eppley units of 12.7 W/m^2. A handful of minutes showed misreading with large errors (~500 W/m^2), yet the 99th percentile error was 38.2 W/m^2.

Figure 23 Cross-calibration of Eppley PSP and Licor pyranometers at LBNL prior to deployment.

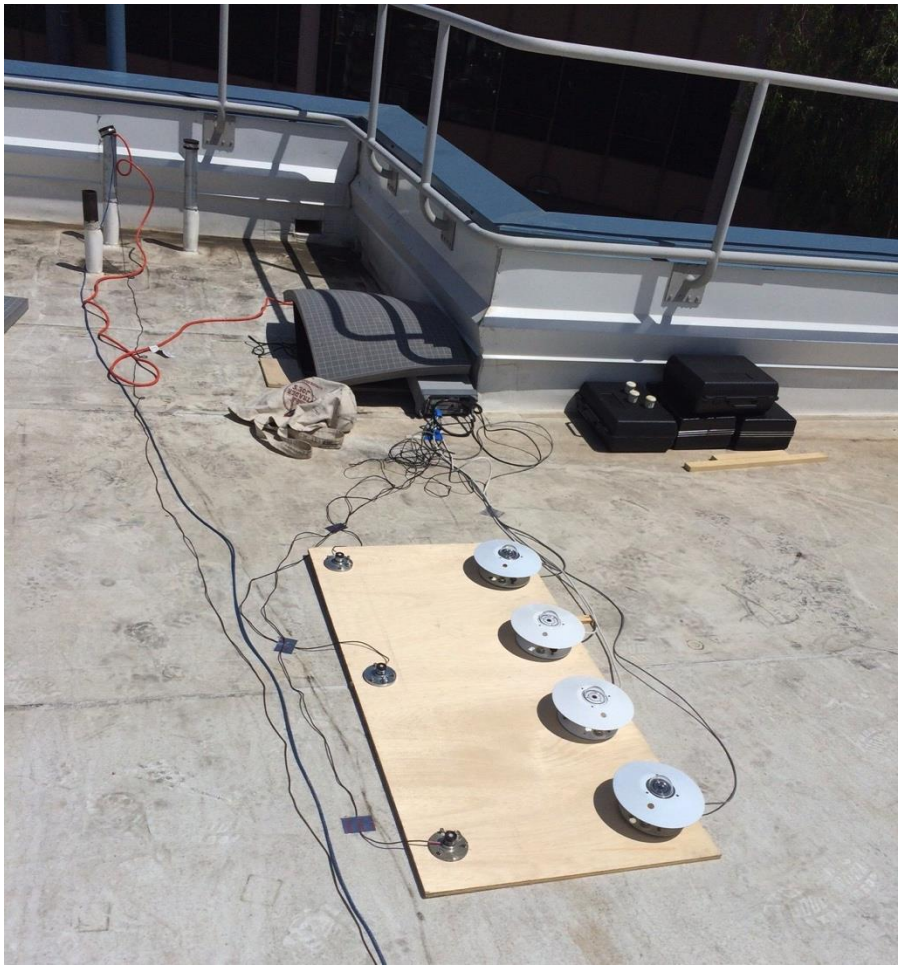

4.2.9 Heat Flux

Huskeflux HFP01-10 heat flux meters were adhered to the underside of the roof deck at the mid-span location for each orientation, as well as in the sheetrock ceiling at the interface of the living space and attic for each primary attic volume (EW52, NS33, and Clovis home EW26N). Factory calibrations were used to adjust raw sensor voltage outputs.

4.2.10 HVAC Energy Sub-Metering

The energy use of the HVAC system components were individually sub-metered. Pulse output Watt-Node electricity meters to monitor the cooling compressor and air handler fan energy uses. An in-line natural gas sub-meter with pulse output was used to measured furnace heating gas consumption. All pulse outputs were read, recorded/time stamped and posted to the sMAP database using Raspberry Pi computer modules. In each home, one raspberry pi was dedicated to the compressor energy, as it was wired at

the main electrical panel. Another raspberry pi was used to count pulses from the air handler and from the gas sub-meter, located in the main attic volumes. The energy consumption per recorded pulse and the recording intervals are summarized for each end-use in Table 10.

The gas sub-meter, an Elster Amco BK-G4, is capable of metering natural gas flow rates from 0 to 199,999 Btu/hr (see an installed example in Figure 24). The meter outputs a single pulse for each cubic foot of natural gas that is consumed. We calculate an energy usage based on the volumetric gas consumption assuming that each cubic foot of natural gas contains 1,023 Btu and that each kilowatt-hour of energy contains 3,412 Btu, such that each pulse is assigned 0.29984 kWh (1023/3412). The gas pulses are counted once every 30-seconds, with a limit of 1 pulse allowed in each 30-second period, in order to overcome jitter on the pulse signal. This limitation simply avoids the accidental recording of multiple pulses, when in fact only one pulse was sent. This limitation does not affect our results, because it is physically impossible for the furnace to consume even 1 entire cubic of gas in a 30-second period. The gas furnace consumes at most 60 kBtu/hr, which means that at most 0.48 cubic feet of gas can be consumed in each 30-second interval (60,000 [Btu/hr] / 1,023 [Btu/ft3] / 60 [min/hour] / 2 [intervals/min]). The limitation was added, because early in the monitoring campaign at the Fresno home, we recorded high furnace gas consumption, which was higher than physically possible for the installed equipment. The issue was addressed on November 17th, 2016; data prior to November 18th is thrown out for that reason.

Table 10 HVAC energy sub-metering. Energy consumption per pulse and reporting intervals, by end-use.

Device	***Energy Consumption per Pulse (kWh)***	***Reporting Interval (seconds)***
Compressor Electricity	0.00050	60
Air Handler Electricity	0.00015	30
Furnace Natural Gas	0.29982	30

Figure 24 Gas sub meter with pulse output plumbed at natural gas furnace in Fresno attic.

System runtimes were estimated using measured supply and return air temperatures. We could not simply use the metered energy data, because they do not sufficiently align with runtimes and related elements (e.g., supply air temperature or AHU blower power). For example, natural gas consumption was recorded every 30-seconds on a unit basis of one cubic foot, which is equivalent to 1,023 Btu. So, even with continuous burner operation, one pulse would not be registered each consecutive 30-second time step. One pulse every 30-seconds would require a heating system capacity of 123 kBtu/hr (2*60*1,023), which is substantially more than the installed system capacities (see Table 7). Instead, one pulse would register at most once every other time step when the burner operates continuously. So, counting time steps with gas consumption is not accurate. Similarly, the compressor operation often precedes the actual delivery of cooling to the space and coincident AHU operation, so simply using the compressor power signal misaligns the cooling runtime index with things like the supply air temperature or AHU blower power. Another runtime method is required. So, we calculated the difference between the measured supply and return duct temperatures for each minute. When in heating mode, the supply air heats up relative to the return air temperature and vice versa in cooling mode. The vast majority of differences were 0˚C. To avoid assigning system operation to random noise or variability in the data, we established positive 2˚C as the heating indicator and negative 2˚C as the cooling indicator. Runtimes reported in Section 5.4 are based on this calculation method.

5 Field Study Results

5.1 Diagnostic Testing

We performed detailed diagnostic testing of the building envelope in the Fresno and Clovis homes using multiple calibrated fans, which allowed us to disaggregate occupied zone leakage to outside, attic exterior leakage to outside, ceiling leakage, total attic leakage and total house+attic leakages with the attic access open and closed.

5.1.1 Fresno Test Home

The results are summarized in Table 11 and in Figure 25. Overall, the total envelope leakage was 1,780 cfm_{50} (3.4 ACH_{50}) with the attic access open and 1,668 cfm_{50} with the access closed (3.2 ACH_{50}). This corresponds to about 0.3 cfm50/ft^2 of exterior envelope. The attic exterior leakage (569 cfm_{50}) was about 0.2 cfm50/ft^2 – slightly less than house envelope on area unit area basis. Having the attic be tighter to outside than the homes can be thought of as qualitatively achieving the goal of being a "sealed" attic (or, at least sealed as well as the house). The ceiling was much leakier per unit area than the exterior surfaces at almost 0.6 cfm50/ft^2 – as is expected for this construction type where no effort is made to seal the ceiling because the aim is to bring the attic inside the conditioned space. The ratio of house exterior to ceiling was very similar to that measured in new California homes with vented attics (Proctor et al. 2011).

Total duct leakage from a pressurization test at 25pa was 84 cfm, while DeltaQ testing of duct leakage indicated a total leakage of 81 cfm under operational conditions (44 cfm supply and 37 cfm return leakage). The HERS rater for the home reported values of 69 cfm_{25}, which is 4.2% of HVAC airflow (5.75 nominal flow). Air handler flow was measured at 1,628 cfm at 788 watts. For comparison, the home's HERS rater also tested depressurization envelope leakage in this home and recorded 1,514 cfm_{50} (2.9 ACH_{50}). We believe this compares most directly with our Total Leakage, attic access closed testing, which was 1,668 cfm_{50}. Differing test set-ups and equipment likely explain this 9% difference.

Table 11 Fresno test home envelope leakage estimates.

Configuration	Airflow (CFM_{50})	Airflow (ACH_{50})	Effective Leakage Area at 4 pa (in^2)
Total Attic Leakage (Qattic+ceil)	1581	17.1	104.5
Total Leakage, Attic Access Closed (Qhouse+ceil)	1668	2.9	100.8
Total Leakage, Attic Access Open (Qhouse+attic)	1780	3.1	105.4
Combined Attic exterior and Occupied Zone Leakage to Outside (Qhouse+attic)	1793	3.2	109.2
Attic exterior Leakage (Qattic)	569	6.1	40.3
Ceiling Leakage (Qceil)	1012		64.2
Occupied Zone Leakage to Outside (Qhouse)	1224	2.2	68.9

Figure 25 Summary of leakage areas derived from fan pressurization testing in the Fresno home.

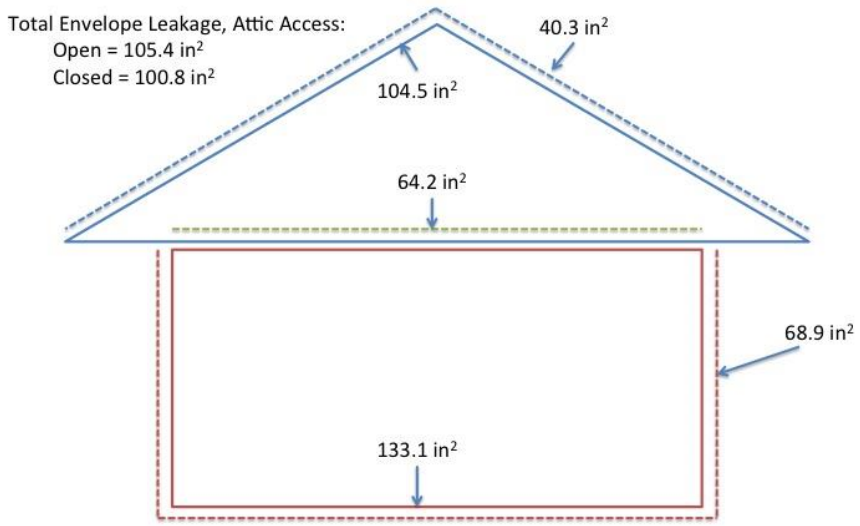

5.1.2 Clovis Test Home

Clovis home diagnostic testing does not allow the same level of leakage area disaggregation, because valving occurred at the ceiling leakage sites. Valving means that depending on whether pressurizing or depressurizing, certain leakage areas either are forced open or closed, which leads to substantially different leakage estimates depending on direction of airflow. For example, when the Clovis home's living space was pressurized with the attic access doors closed, airflow at 50pa was 1,600 cfm, whereas depressurization testing gave a flow roughly 20% lower (1,300 cfm).

Due to this valving, we were not able to discern ceiling leakage area, but we were able to estimate living space and attic leakage to outside, along with total envelope leakage area to outside (see Table 12). Attic and living space leakages to outside were estimated using a two-fan test, where we pressurized the living space using a blower door, while also pressurizing the attic volume using a duct blaster (see Figure 26). As the blower door fan flow was increased, the duct blaster flow was adjusted so that the pressure between the living space and attic (across the ceiling) was 0 pa. When this is achieved, the flow through the blower door represents living space leakage to outside (with no ceiling leaks), and the duct blaster flow represents attic leakage to outside (with no ceiling leaks).

This testing shows that the sealed attic in this home was much more leaky than the living space it was attached to. Attic leakage area to outside was 3.4 times more than that in the living space leakage to outside (103 vs. 30 cm^2). This equates to ACH_{50} values of 19.4 in the attic and 3.1 in the living space (i.e., attic airflow to outside normalized to the attic volume, and living space airflow to outside normalized to the living space volume). For comparison, a vented attic on the same Clovis test home with 1/300 venting area, would have a leakage area of about 8500 cm^2. So, while leaky relative to the living space, this is by no means a "vented" attic in the traditional sense of the word. When the two leakages to outside are combined, the whole envelope leakage estimate is obtained, and when the conditioned volume is used (i.e., combined living space and attic volumes), the airtightness is estimated at 6.5 ACH_{50}.

Values were lower when solely the living space was pressurized with the attic access doors closed (note that the access doors are to outside not to the living space), and only the volume of the living space was used, resulting in a value of 4.8 ACH_{50} . We retested the home when monitoring equipment was removed in September of 2018 and the measured leakage had increased to 5.1 ACH_{50}. There is considerable valving action of leaks in this home: the depressurization result for the living space leakage is only 3.9 ACH_{50}. If total conditioned volume (combined living space and attic) were used, the pressurization results are reduced from initial values of 4.8 to 3.8 ACH_{50} and from 5.1 to 4.0 ACH_{50} during equipment removal. The depressurization test result is 3.1 ACH_{50} when normalized to the entire conditioned volume. This range of results makes it vitally important that measurements used to establish air leakage for code compliance and/or

energy ratings are very specific about test conditions (are interior access panels open or closed) and which volumes are included when calculating ACH_{50}.

The homes were also tested by a HERS rater who reported measured envelope leakage for this home at 917 cfm_{50}, or 2.8 ACH_{50}, which is much lower than either our pressurization or depressurization measurements. This could be the result of differing test set-ups. For example, when performing our testing, we did not tape over exhaust fan inlets in the living space. They may also have tested prior to construction being completed, such that later trades made new unsealed penetrations in the envelope. The HERS rater reported total duct leakage as 44 cfm_{25} (which is 3.6% of measured air handler air flow (1,220 cfm)) and measured fan wattage of 382 Watts at that airflow.

Table 12 Clovis test home envelope leakage estimates.

Envelope Element	**Airflow (CFM_{50})**	**Airflow (ACH_{50}) (reference volume)**	**Effective Leakage Area at 4 pa (in^2)**
Attic Exterior (no ceiling)	1,696	19.4 (attic)	103.4 ± 3.9
Living Space Exterior (no ceiling)	1,050	3.1 (living space)	30.2 ± 6.5
Conditioned Exterior Envelope	2,746	6.5 (attic + living space)	133.6
Living Space attic access closed	1,600 – 1,700	4.8 – 5.1 (living space)	

Figure 26 Two-fan test setup with blower door mounted in living space entrance and duct blaster fan mounted in attic access door.

5.2 Thermal Performance

5.2.1 House Zone Air Temperatures

The Fresno home HVAC system serves four independently controlled thermal zones, with systems of dampers and bypasses, as is common in many new homes. We measured zone air temperatures in each of the four zones, co-located with the zone thermostat wall controllers. One zone was on the first floor serving the main area, and three zones were on the second floor—main, master bedroom and guest bedroom. Monthly diurnal patterns for these four zone air temperatures are shown for June (Figure 27), August (Figure 28) and December (Figure 29), representing typical cooling and heating season conditions.

The zoned system maintained substantially different diurnal air temperatures throughout the house, which is consistent with the intended system design. During August, for example, it was common for the 1st floor main zone to be 3 - 4°C (5.4 - 7.2°F) cooler than the bedroom zones on the second floor. The main zone temperature on the second floor was between the others. It appears that during the cooling season, zone cooling set points varied widely between 23 and 30°C. Heating season set points were more similar, varying between roughly 20 and 23°C. It is not clear that any of the zones were heated preferentially relative to the others, as relationships varied by month.

This variability between zones in the home complicates our assessment of temperature differences between the attic and living spaces, presented in Section 5.2.4. For the Fresno home, when we report temperature differences for the EW52 attic, it is calculated

relative to the Main 2nd Floor location, while the NS33 temperature differences are relative to the Master Bed 2nd floor zone. Neither are calculated relative to the 1st floor temperature, which would give larger differences overall.

The temperature controls in the Fresno home roughly aligned with the assumptions used in Title 24 energy modeling for cooling, but were substantially warmer in the heating season. In cooling, the T24 assumes a minimum set point of 25.5°C and a daytime setback to 28.3. The Fresno home zones were sometimes a little cooler than these assumptions (~23°C) and were other times warmer (up to 30°C). While in heating season, T24 assumes an 18.3°C nighttime setback and daytime setting of 20°C. The Fresno home was consistently heated to higher temperatures, almost always exceeding 20°C.

Figure 27 Fresno. Characteristic indoor zone air temperatures during the cooling season (June).

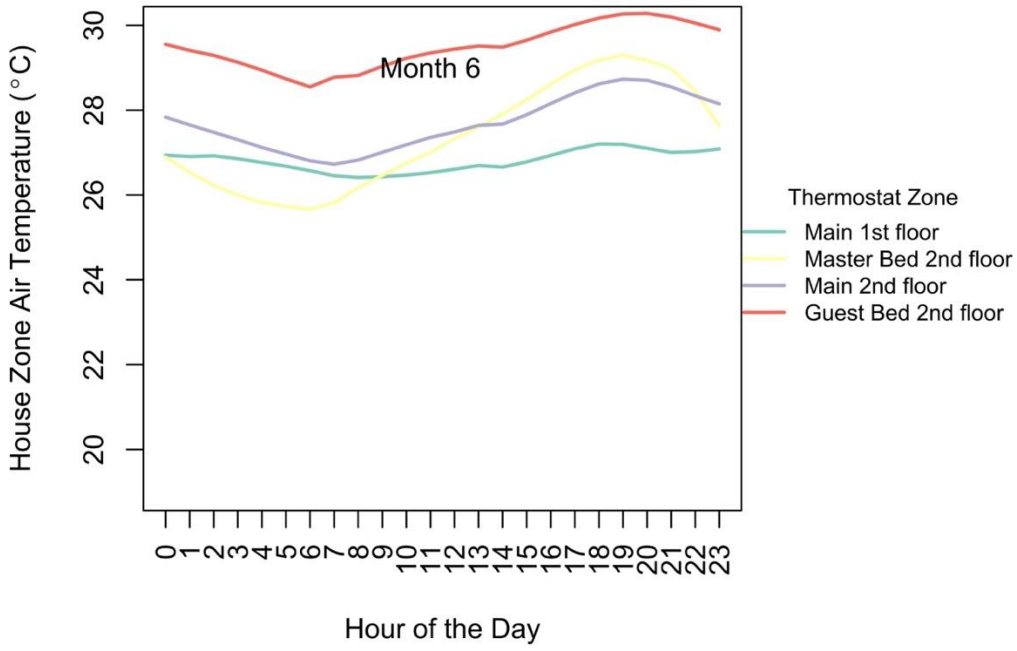

Figure 28 Fresno. Characteristic indoor zone air temperatures during the cooling season (August).

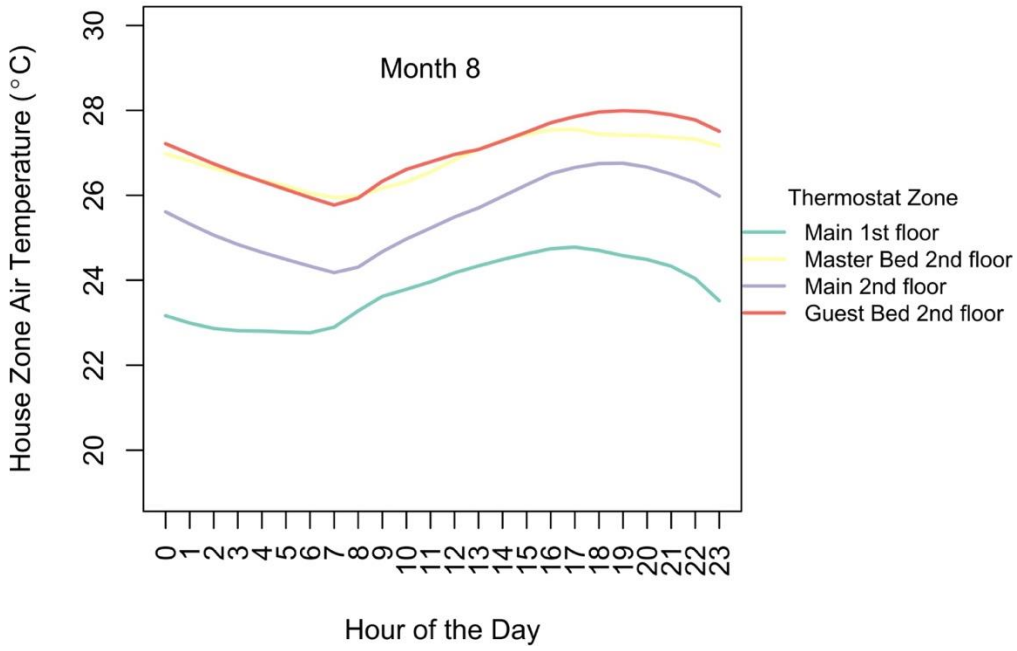

Figure 29 Fresno. Characteristic indoor zone air temperatures during the heating season (January).

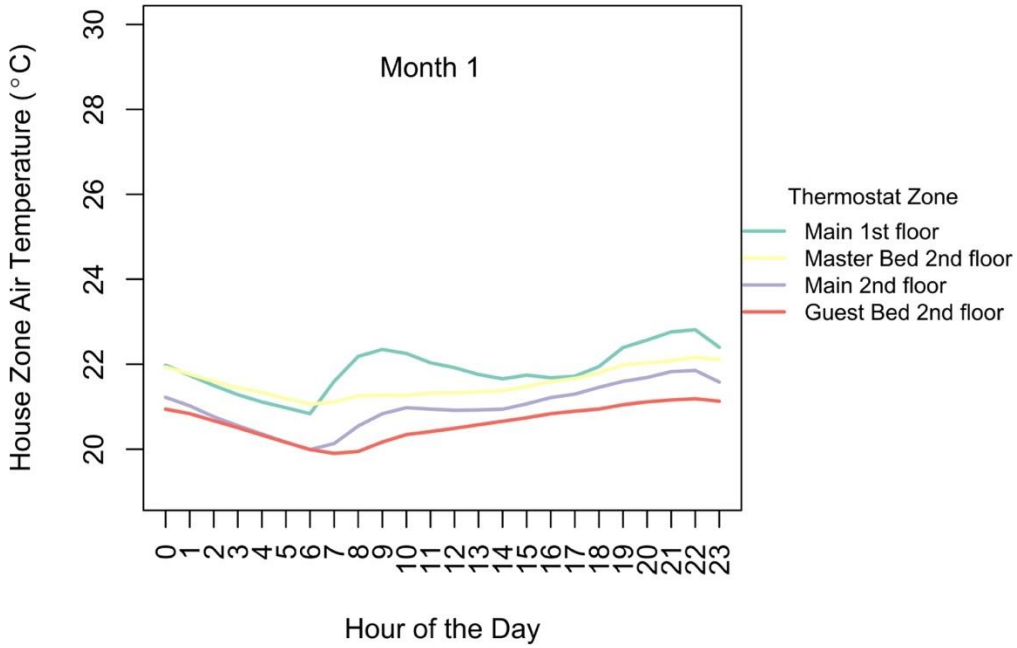

The Clovis test home also used a zone HVAC system, with three independent thermal zones. We monitored the living space temperature in one location (co-located with wall controller thermostat). We did not assess the distribution of temperatures throughout the zones of the living space. In Figure 30, we provide the monthly mean diurnal living

space air temperatures. As expected, we see that the cooling months of June-September have the highest average temperatures, ranging between 23 and 26°C, with the warmest temperatures occurring late in the afternoon and early evening. Heating season months have the lowest indoor temperatures, ranging between 20 and 23°C. These ranges are similar to those measured in the Fresno test home, though in general heating temperatures were marginally warmer and cooling temperatures were cooler. It is unclear if the variation in living space temperature by hour of the day results from programmed thermostat settings, or environmental conditions.

Figure 30 Clovis test home living space diurnal zone air temperatures for each month of the year.

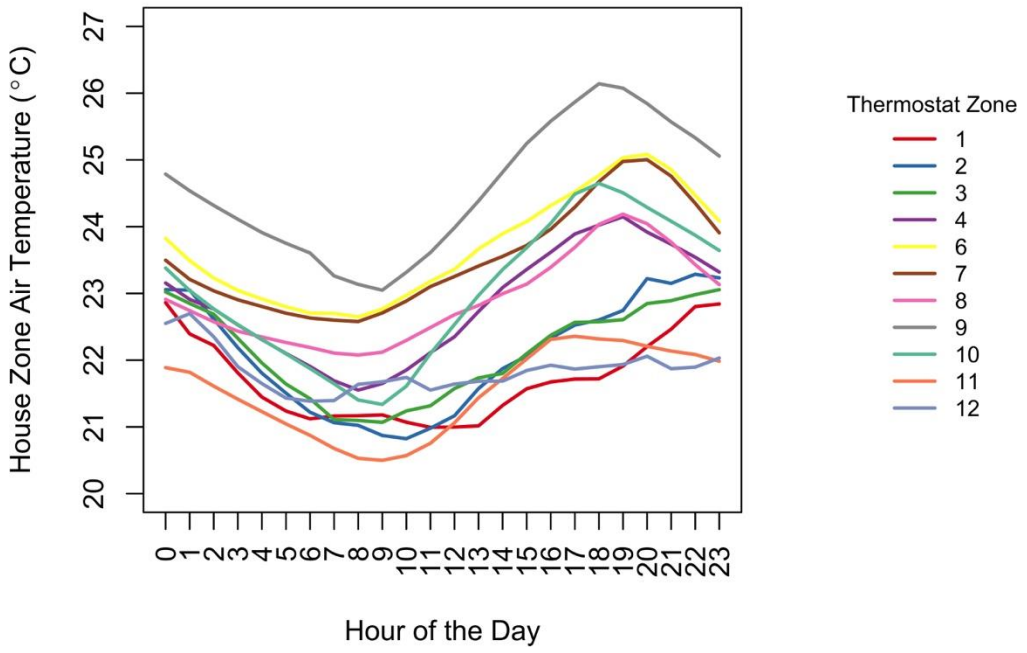

5.2.2 Attic Air Stratification

Attic air stratification occurs when there is minimal mixing of the attic air volume and stable layers of air form due to temperature and density differences. During times of high solar gain (summer days) it was common for attic air to be vertically stratified.

Our measurements included stratification trees of radiation-shielded thermistors arrayed from floor to peak of the two Fresno attic volumes—EW52 and NS33. We show monthly diurnal patterns for the temperature difference between the attic air ridge and floor locations for the EW52 attic in Figure 31 and the NS33 attic in Figure 32. Boxplots in Figure 33 show the distribution of all ridge-to-floor temperature differences by month of the year (top pane) and hour of the day (lower pane). In both attic volumes, the ridge air location is consistently warmer than the floor location. During nighttime periods, the ridge is 1-2°C warmer than the floor, but during the daytime solar gain periods, stratification increases substantially. In the EW52 Fresno attic, maximum one-hour stratification was 11.5°C and average was 2.4°C. The NS33 attic volume experienced

much less thermal stratification, averaging 1.1°C and peaking at 3.9°C. We see that solar gains drive variability in the ridge-to-floor stratification, as values become much more widely distributed in the sunnier cooling months of the year, as well as during the daytime hours of the day.

This stratification could be good from an energy perspective, if the HVAC distribution system is aligned with the floor of the attic, the stratification will ensure that relatively cooler attic air is adjacent to the ducts and air handler. The opposite effect could occur in winter.

The Clovis EW26N attic volume had greater levels of thermal stratification (Figure 34), with peak monthly mean values just shy of 12°C (compared to 9°C in EW52 Fresno). It also experienced inversion of the stratification, where the peak was on average colder than the floor during nighttime hours in Fall and Winter. This inverse stratification could be due to lower effective insulation levels resulting from geometry effects at the peak, compared to the flat roof surfaces.

Figure 31 Diurnal profiles of attic air stratification for each month of the year in the EW52 attic volume of the Fresno test home. Stratification was calculated as the difference between peak and floor thermistor locations.

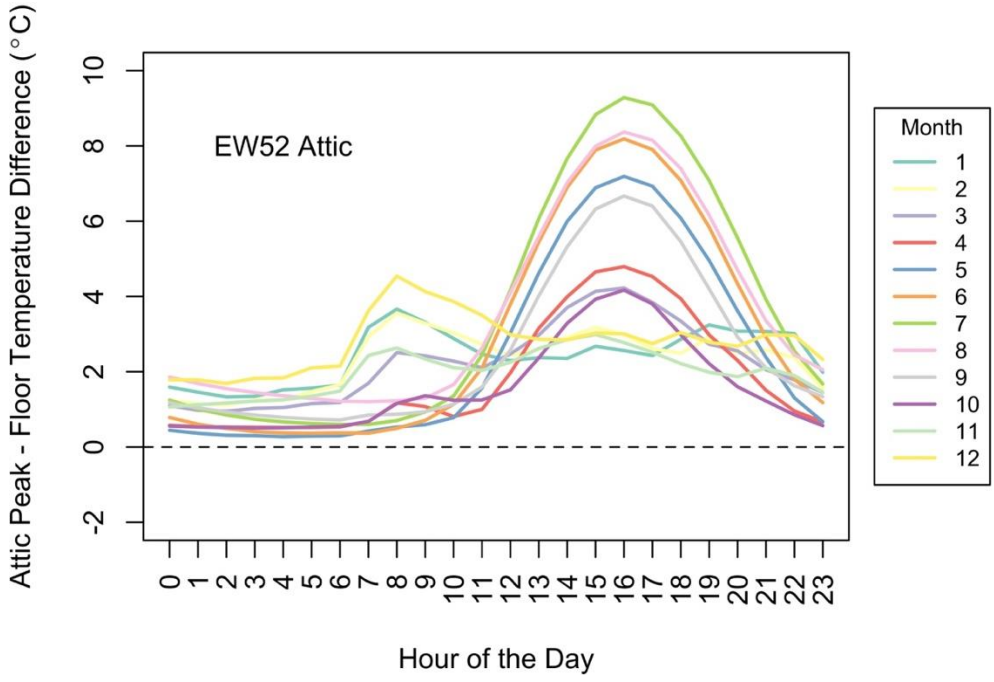

Figure 32 Diurnal profiles of attic air stratification for each month of the year in the NS33 attic volume of the Fresno test home. Stratification was calculated as the difference between peak and floor thermistor locations.

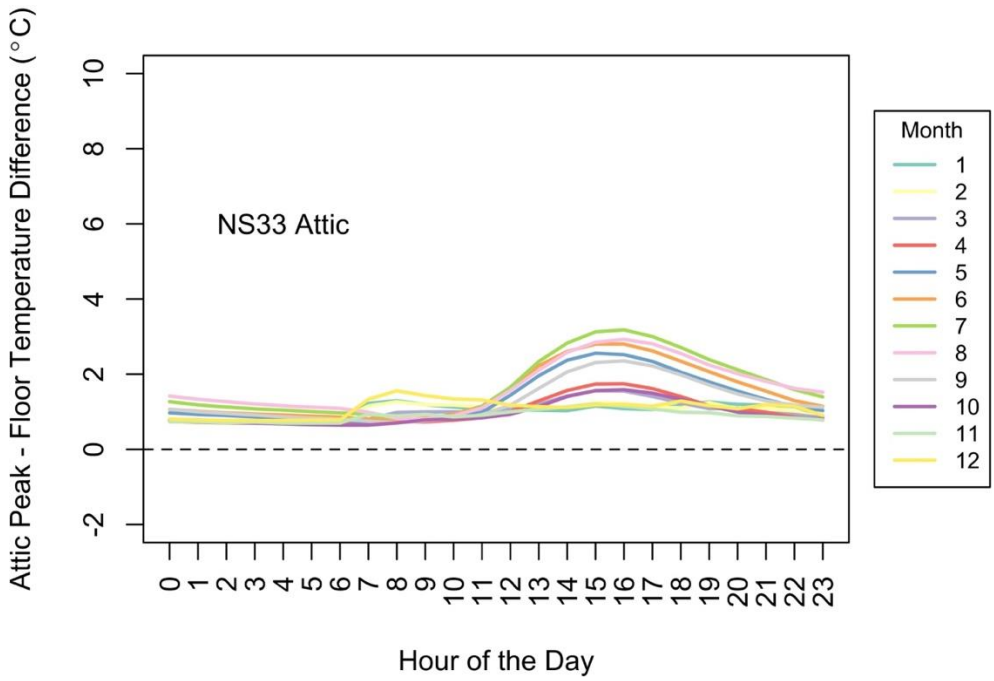

Figure 33 EW52 Fresno. Boxplot distributions of attic air stratification, aggregated by hour of the day (bottom) and by month of the year (top).

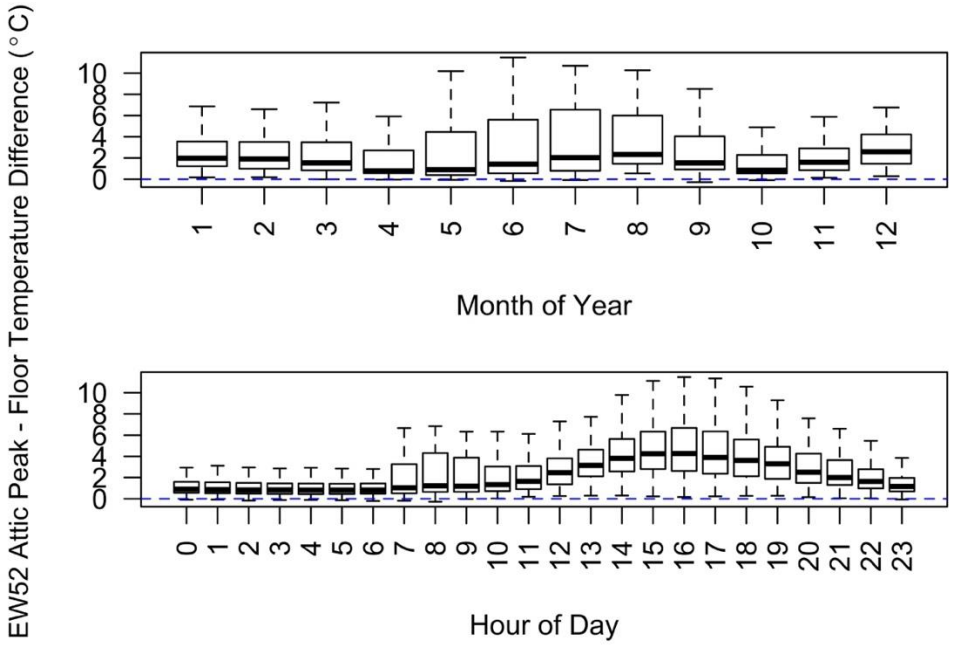

Figure 34 EW26N Clovis. Diurnal profiles of attic air stratification for each month of the year. Stratification was calculated as the difference between peak and floor thermistor locations.

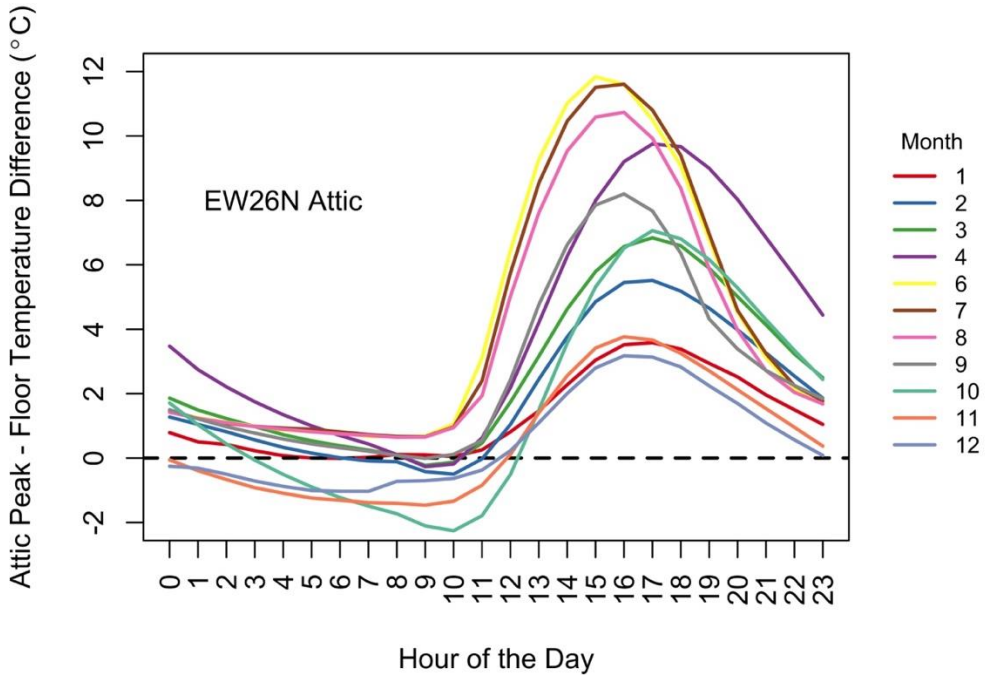

Figure 35 EW26N Clovis. Boxplot distributions of attic air stratification, aggregated by hour of the day (bottom) and by month of the year (top).

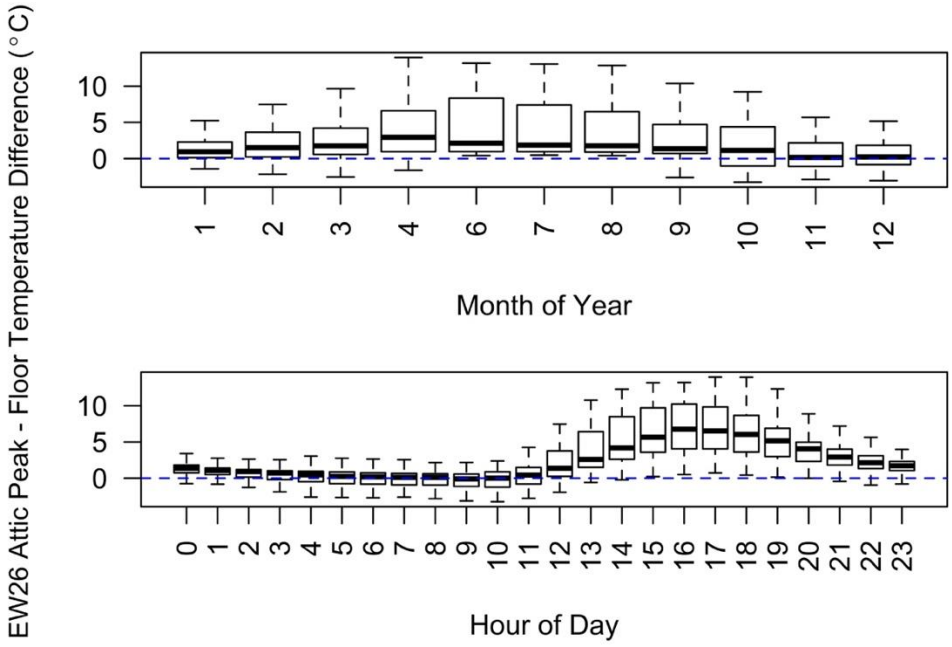

5.2.3 Volume Weighted Attic Air Temperatures

As discussed in Section 5.2.2, there is significant vertical stratification in the attic air, which makes it difficult to say what the attic air temperature is. This is particularly an issue when using attic air temperature as a metric for assessing if the attic is inside conditioned space for HVAC energy assessments, or for comparing attic air temperatures against predicted values from a simulation that treats the attic as one well-mixed thermal zone. In order to express a single attic temperature, we used a volume-weighted approach. This method weights the measured temperatures by our estimate of the fraction of the attic air volume represented by the temperature measurement site. As in Figure 36, it is fairly straightforward to see that as you go up in height in the attic (from h1 to h4), the volume represented by the change in height is reduced. For example, if you split a 60" height attic with a 4:12 roof slope into four 15" height segments, then the fraction of total volume represented by each height increment would be 44, 31, 19 and 6% from floor to peak locations. We see that in terms of attic air mass, the lower half of the attic would represent 75% of the mass in this idealized scenario. From this point on, whenever we refer to the attic air temperature generically, we are referring to the volume-weighted values; other locations will be specified, as necessary. In our test attics, the stratification tree thermistors were not equally spaced in height (e.g., in the Fresno house, the actual weights in the EW52 attic were 35, 40, 22 and 3% for floor to peak locations).

In Figure 37, we show the annual diurnal temperature patterns for the living zone (2nd floor main zone), volume-weighted attic, and stratification tree sensor locations in the Fresno test home. In this home, the volume-weighted average temperature (black) aligns almost perfectly with the thermistor located at the height of the bottom chord of the truss (yellow) (labeled as "Framing" in figure). Relative to the volume-weighted temperature, use of the half height measurement adds roughly 1°C to the daily average peak temperature on an annual basis. In the hottest months, use of the half-height sensor adds roughly 2°C to the daily average peak temperature. The Clovis home annual diurnal temperature patterns are shown in Figure 38, following a similar pattern to the Fresno home, but with a hotter attic volume relative to the living space (4°C hotter in Clovis compared with 2°C hotter in Fresno).

Figure 36 Illustration of attic geometry along vertical path from floor to peak.

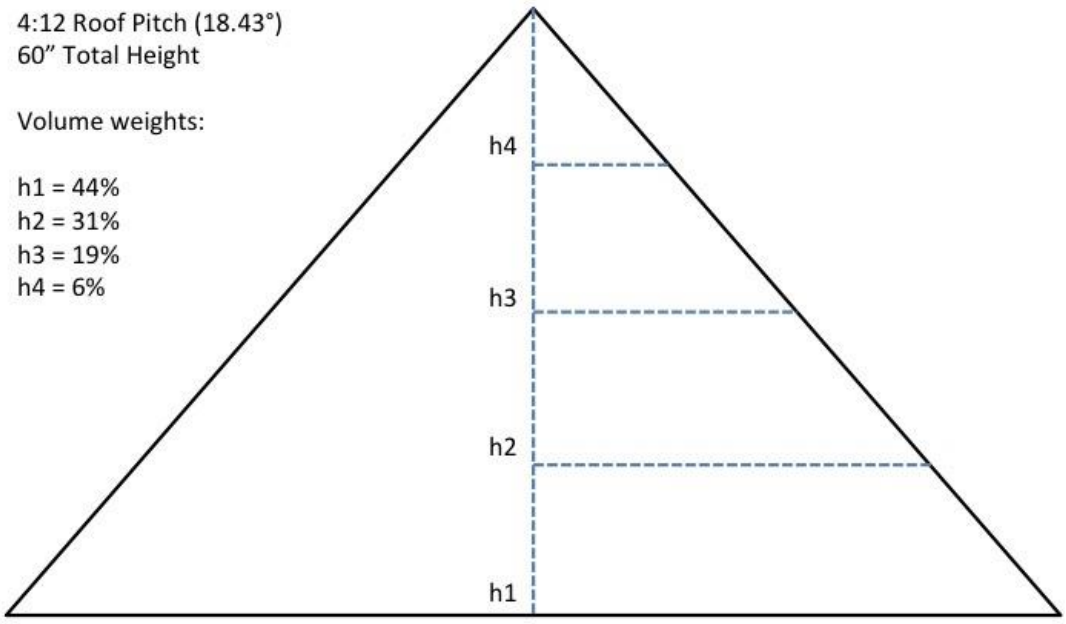

Figure 37 EW52 Fresno. Annual diurnal house, volume-weighted attic and stratification tree temperatures.

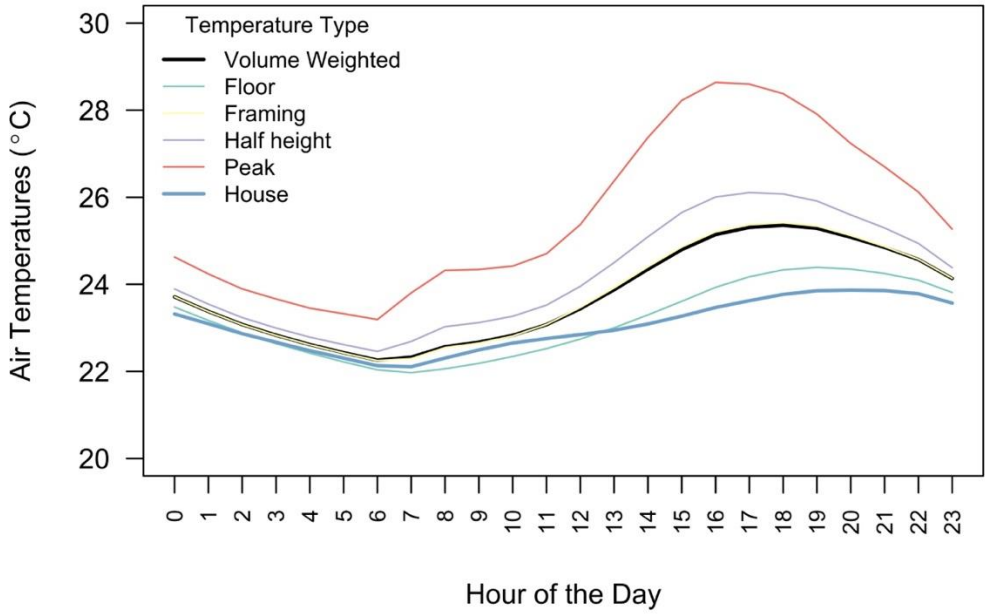

Figure 38 EW26N Clovis. Annual diurnal house, volume-weighted attic and stratification tree temperatures.

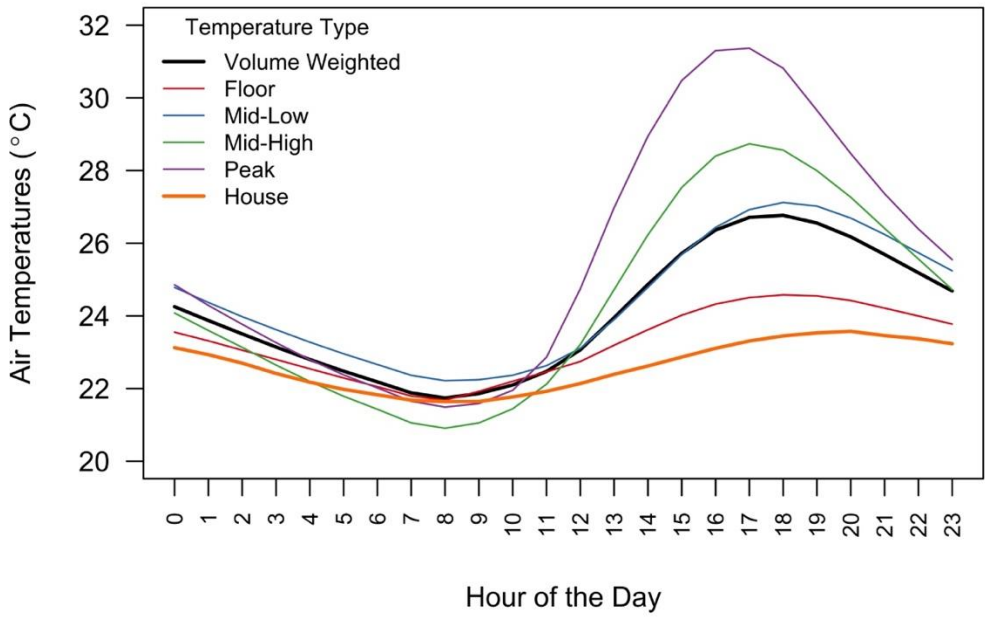

5.2.4 Attic-to-House Air Temperature Differences

A critical goal of this study was to confirm whether or not sealed and insulated attics using solely fiberglass insulation could be considered as “conditioned space” for the purposes of HVAC system thermal calculations. The key metric used is the temperature difference between the volume weighted attic air temperature and the house zone temperature directly below the attic in question. We show the calculated attic vs. living zone temperature differences aggregated by month of the year and hour of the day for the EW52 Fresno attic in Figure 39 and Figure 40, for the NS33 Fresno attic in Figure 41 and Figure 42, and for the EW26N Clovis attic in Figure 43 and Figure 44.

Overall, the attic air volume temperatures are very tightly coupled to the living zone of the house. Mean temperature differences over the entire monitoring period were 0.14°C (NS33) and 0.74°C (EW52) in the Fresno test home, whereas the Clovis test home mean difference was 1.7°C (EW26N). By month of the year, there are no strong patterns in temperature difference, except that the cooling season clearly experiences more variation around the median and slightly higher averages, due to solar gains incident on the roof. This is the case for both the EW52 and the NS33 attic volumes. The primary pattern is diurnal, with small levels of cooling at night and consistently elevated attic temperatures during daytime periods of intense solar gain. The result is that on an average summer day, the attic air temperature is roughly 2-3°C above the living zone temperature. The maximum hourly difference during the entire measurement period in the Fresno home was 4.5°C (8°F). These elevated attic air temperatures occur during the peak cooling demand period, which we expect will slightly increase cooling energy demand relative to an attic zone at exactly the same temperature as the living zone.

Nighttime cooling of the attic air volume during the heating season is less severe than the daytime over-heating experienced during cooling season, because the temperature differences across the roof deck assembly are much larger in cooling than in heating season (see Section 5.2.5, Figure 45 and Figure 46) We expect the heating energy penalty of these temperature differences to be negligible.

Figure 39 EW52 Fresno. Boxplot distributions of temperature difference between the volume-weighted attic temperature and the living space temperature, by month of the year (upper) and hour of the day (lower).

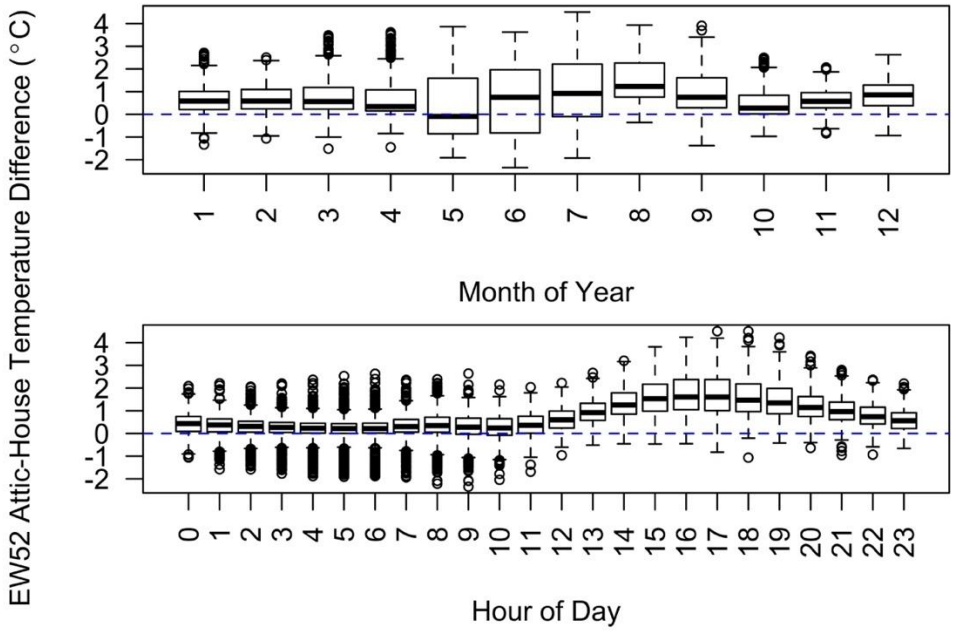

Figure 40 EW52 Fresno. Monthly average diurnal profiles for the temperature difference between the volume-weighted attic temperature and the living space temperature.

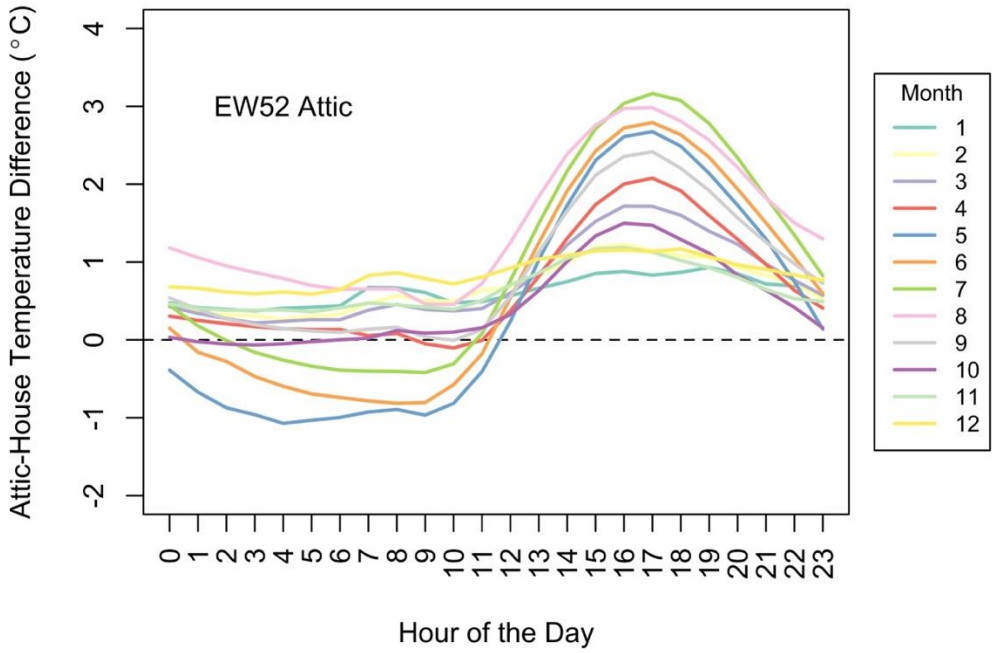

Figure 41 NS33 Fresno. Boxplot distributions of temperature difference between the volume-weighted attic temperature and the living space temperature, by month of the year and hour of the day.

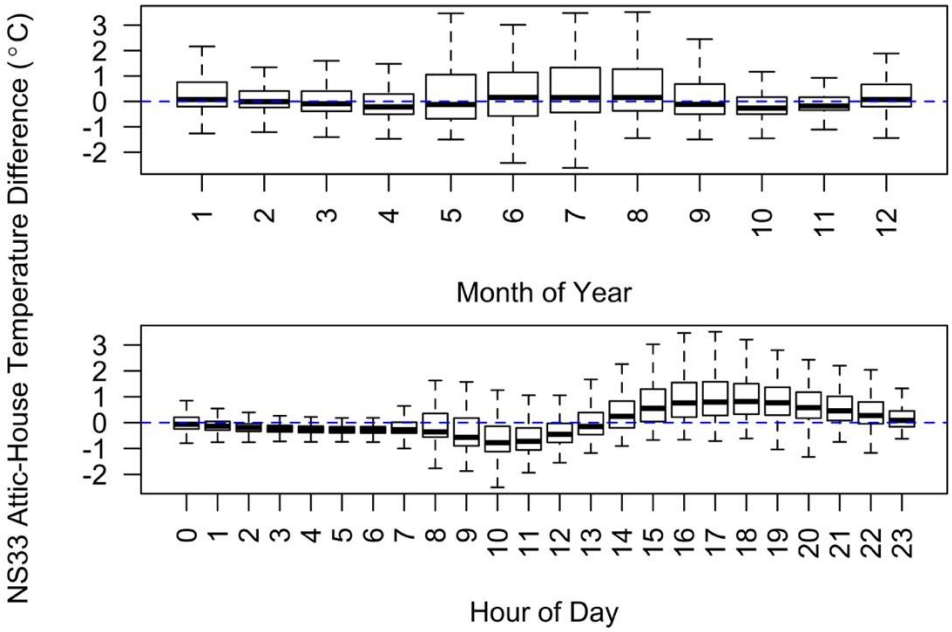

Figure 42 NS33 Fresno. Monthly average diurnal profiles for the temperature difference between the volume-weighted attic temperature and the living space temperature.

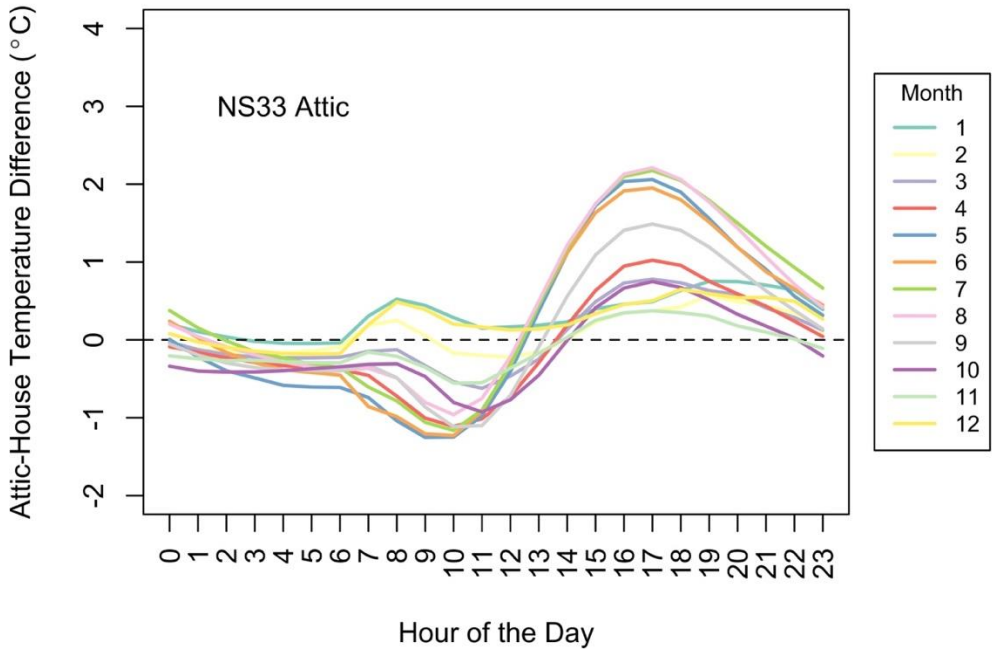

The Clovis results (monthly boxplots in Figure 43 and hourly values in Figure 44) show much more variability than the Fresno results. The Fresno home attics were similar in temperature to the living space across most months of the year, with slightly overall warming during summer. The Clovis home shows much more overall variation, as well as variation between months of the year, with a colder attic in the heating season and a hotter attic in the cooling season. The differences are such that the attic is on average over 5°C hotter than the living space in cooling season, and 2°C colder than the house in heating season. The Fresno attic was warmer than the living space in all seasons.

This pattern suggests that the Clovis attic is less like conditioned space than the Fresno attic, which could be the result of attic air leakage (see Section 5.1), house/attic geometry (see Section 4.1), and/or the lack of HVAC equipment in the EW26N attic volume. The Clovis test home attic was much better connected to outside than the Fresno home, which could contribute to more air leakage from outside thus making the attic hotter or cooler than the main living space. The Clovis home geometry ensures that the attic air volumes are quite small, with a greater surface area to volume ratio; a rough calculation estimates the surface area-to-volume is approximately 40% greater in the Clovis vs. the Fresno attic. This could lead to proportionally less effective thermal mass (e.g., air mass and framing/building materials) in the attic space leading to greater temperature swings. The Clovis attic also has a substantial fraction of the attic floor above the unconditioned garage. This surface was originally uninsulated, but the builder added insulation at the beginning of the monitoring period (in September 2017). In essence, very little heat transfer surface area existed directly between the EW26N attic and the living space below, which limited the thermal connection between living space

and EW26N attic. Being adjacent to the unconditioned garage could be a significant contributor to these more extreme temperatures. Finally, the HVAC equipment is located in the NS50W attic volume, which is connected to the EW26N attic only by a roughly 24”x24” opening. So, thermal losses from duct air leakage and conduction contributed little to the indirect conditioning of air in the EW26N attic.

Figure 43 EW26N Clovis. Boxplot distributions of temperature difference between the volume-weighted attic temperature and the living space temperature, by month of the year.

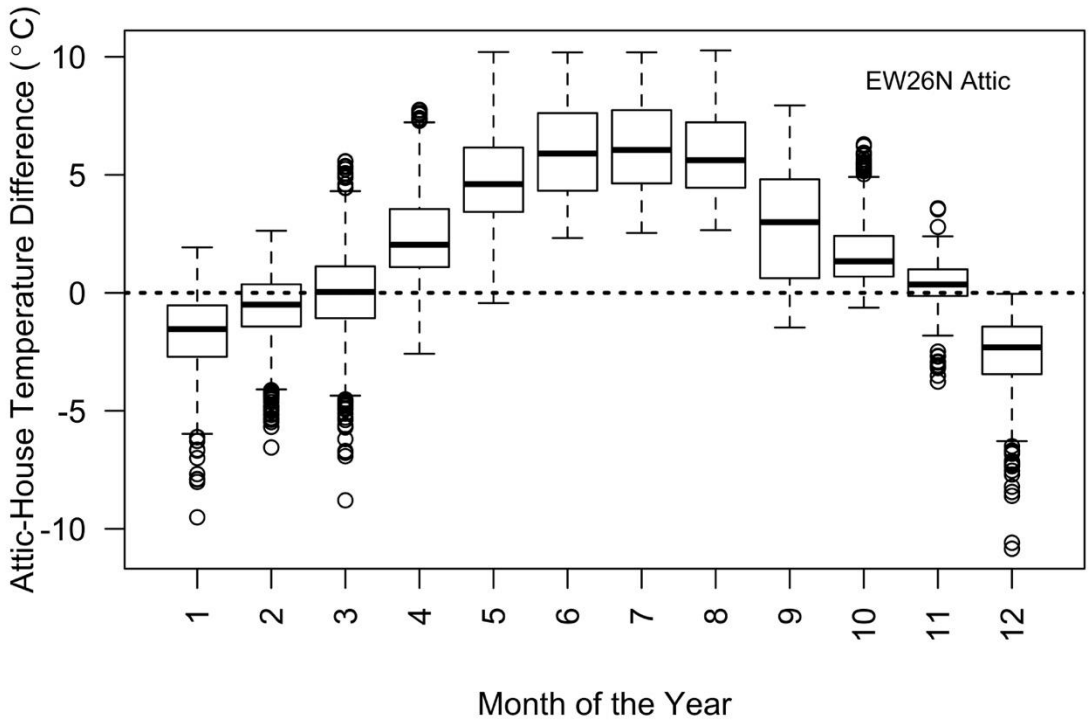

Figure 44 EW26N Clovis. Monthly average diurnal profiles for the temperature difference between the volume-weighted attic temperature and the living space temperature.

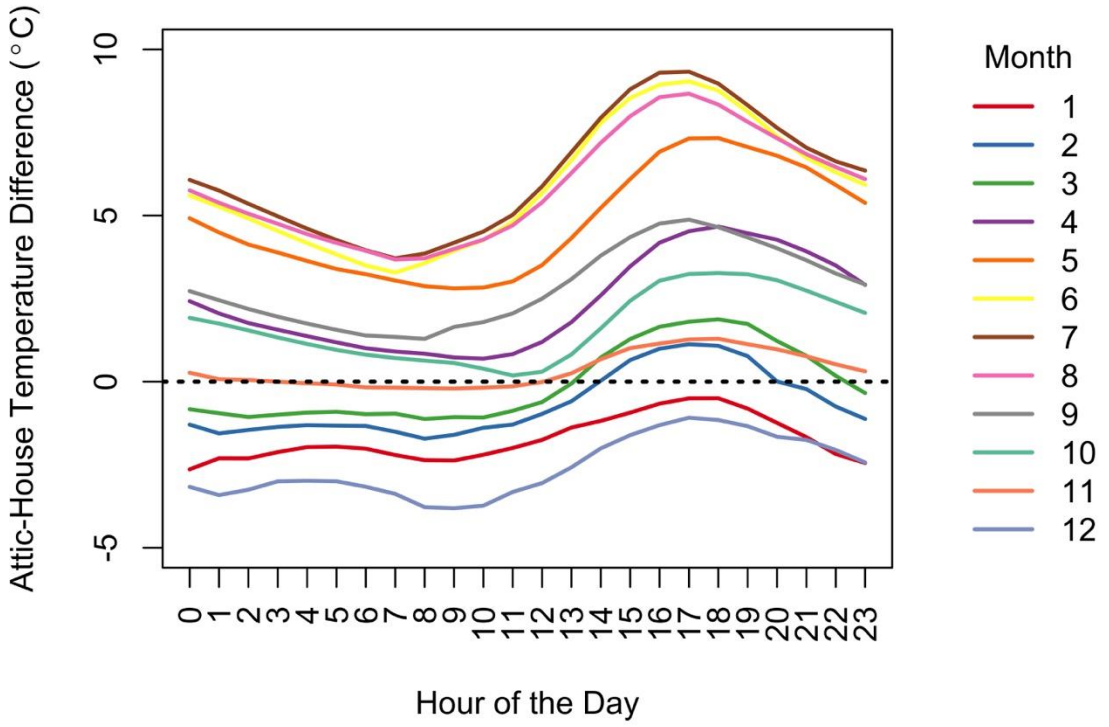

5.2.5 Assembly Temperature Patterns

We show the measured temperature difference across the fiberglass batt insulation for the North- and South-oriented roof slopes in Figure 45 and Figure 46, respectively. Overall, the daytime temperature differences are greater than those at night time—an effect that is particularly acute when comparing peak cooling and heating months. During peak cooling months of June and July, the daytime assembly temperature difference reaches an average of roughly 20 to 25°C on the North slope (i.e., undesired heat gain), while the peak heating season months of December through February have nighttime temperature differences averaging only -10 to 15°C on the North slope (i.e., undesired heat loss). At the South slope, nighttime temperature differences are similar, but daytime differences are even higher, with peak cooling months reaching on average 25 to 30°C across the fiberglass insulation.

Figure 45 EW52 Fresno North-oriented roof slope, diurnal temperature differences across fiberglass insulation for each month of the year. Roof deck temperature vs. insulation surface temperature.

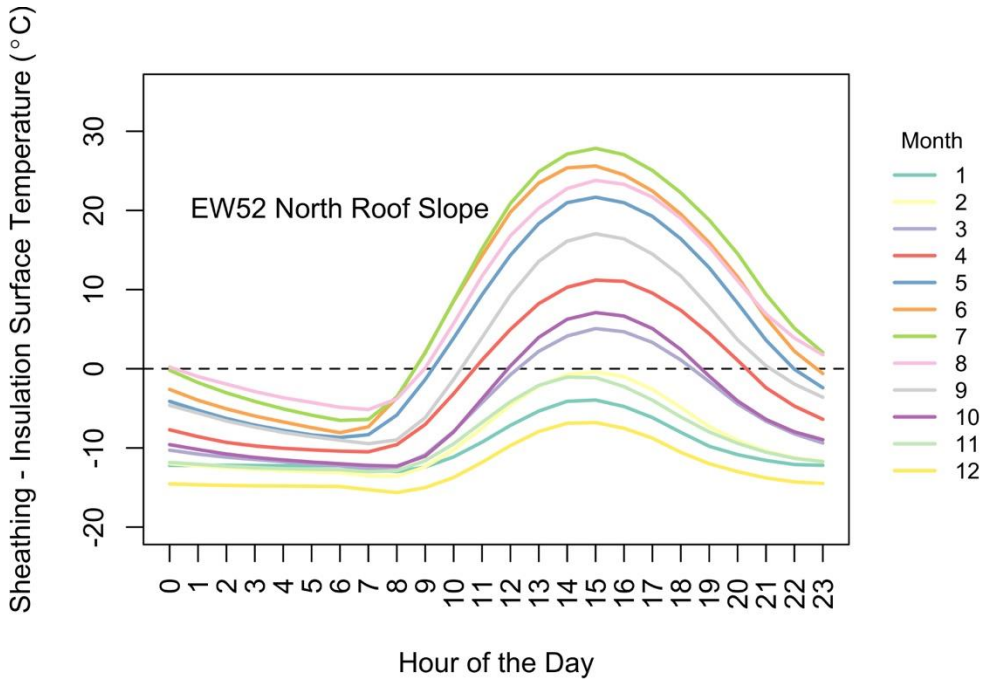

Figure 46 EW52 Fresno South-oriented roof slope, diurnal temperature differences across fiberglass insulation for each month of the year. Roof deck temperature vs. insulation surface temperature.

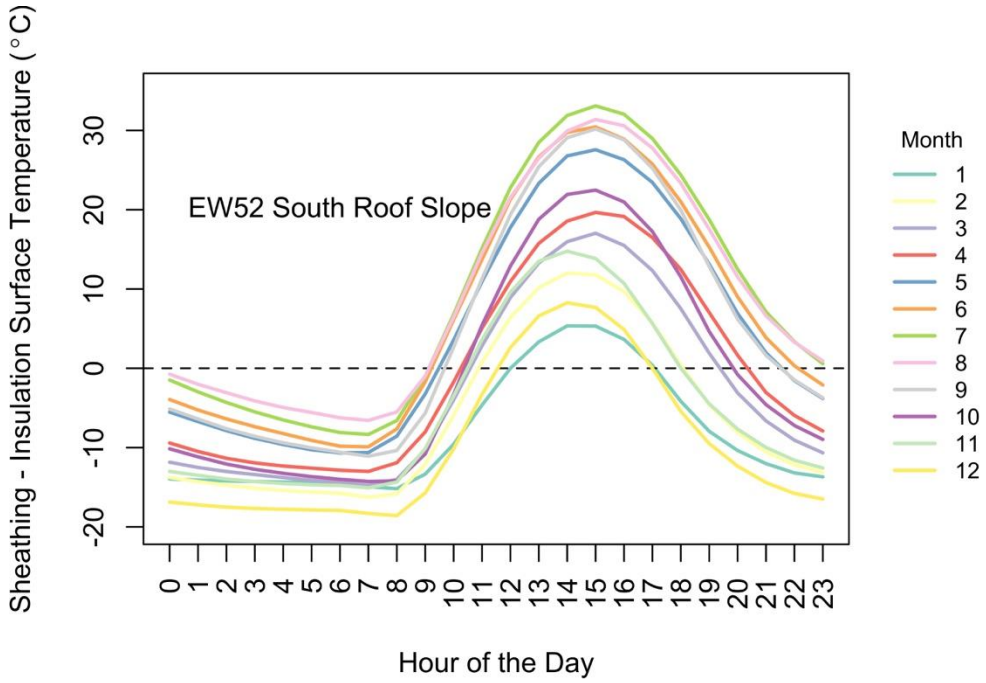

5.2.6 Roof Span from Eave to Midpoint and Peak

We see moisture accumulation at the peak of the roof, and one possible explanation would be that the roof sheathing is colder at that location, possibly due to geometry effects reducing effective R-value or increasing radiation heat loss to the night sky. Yet, we consistently measure the opposite, which is that the peak is on average the warmest of the three interior roof deck measurement locations along the North span of the Fresno EW52 attic. The coldest location is at the eave roof deck, followed by the mid-span location. This is consistent with the attic air stratification measurements presented in Section 5.2.2, which showed that the peak was always warmer than the floor location. Following from this, it makes sense that the roof deck temperature would also be colder at the eaves.

In Figure 47, we show the measured interior roof deck temperatures along the North span of the EW52 attic during a week in January 2017, and we see that during nighttime cold periods, the eave location drops 2-5°C below the temperature at the peak. Notably, the period from January 5-7 in this plot has clear skies, which drives both more stratification and colder eave temperatures. During daytime hours, increased solar gains drive the ridge roof deck temperature 10°C above the mid-span, and at nighttime, radiation losses to then night sky drop the eave roof deck temperature to roughly 7°C below the ridge temperature. The South roof deck in the EW52 attic showed similar behavior, with the South and North eave locations being similarly cold on clear nights. The South exposure, on the other hand, had much more daytime solar heating. We summarize this pattern for the North roof deck using the hourly averages for the entire measurement period in Figure 48 and the monthly averages in Figure 49.

These results show that, on average, the eave location is 2-3°C colder than the other locations at nighttime, and also that this depression only affects the average temperatures at the roof deck occurs during the heating season, roughly October to March.

Why are the eaves consistently colder than the peak? One possibility is that substantial amounts of air leakage occur at the eave, where the sloped roof deck meets the above grade wall assembly. This is a difficult air barrier location to specify and seal appropriately. It is also possible that daytime heating of the peak location, driven largely by attic air stratification, simply leaves the peak roof sheathing location consistently warmer than the eave location when they face roughly similar nighttime heat loss conditions. It could also be that the temperature stratification that exists in the attic air mass simply translates to correspondingly lower and higher temperatures along the OSB roof deck surfaces.

Figure 50 shows the monthly diurnal temperature differences between the eave and peak interior roof deck locations. These results show that during the cold, nighttime periods when condensation typically occurs, the eave is 2-4°C colder than the peak location on average. During the cooling season, the eave roof deck gets hotter than the peak location on average. As we show in Figure 51, the South-sloped roof shows this

behavior during all months of the year, with the eave location getting both coldest at night and hottest during the day.

The Eastern roof slope in NS33 Fresno attic does not display this behavior. The ridge is hottest in the cooling season by roughly 10°C on clear, sunny days. The midpoint and eave are colder at night, as with the EW52 North slope roof deck. The Western sloped roof ridge OSB is hottest in daytime, while the mid-span location is the coldest in both summer and winter seasons. Notably, this Western roof slope is continuously shaded by solar PV panels, which provides cooling throughout the year (though they also shelter the surface from night sky radiative cooling).

These different results for both average and stratified air temperatures show that predicting attic thermal performance is not straightforward or simple to generalize and depends on factors such as solar orientation, presence of HVAC equipment, surface area to volume ratios (thermal mass effects) and shelter by solar panels. The disparities in the results shown here between different attic spaces are indicative of the range of potential performance. Therefore we temper our conclusions to say that in general over all the attic spaces they are a good place to put the HVAC system and overall the HVAC system is close enough to being in conditioned space, but that temperatures will not always match exactly between the house and the attic. One more consideration is that the smaller more sensitive attic volumes rarely contain much HVAC equipment (as we saw in these test homes) so the extra temperature variability in these spaces is acceptable so long as larger attic spaces containing the HVAC system performs well.

Figure 47 EW52 Fresno. Interior roof deck temperatures measured in January 2017 at the eave, midspan and peak of the North-oriented roof slope. Note: roughly January 5-7 are clear skies, while other days are overcast.

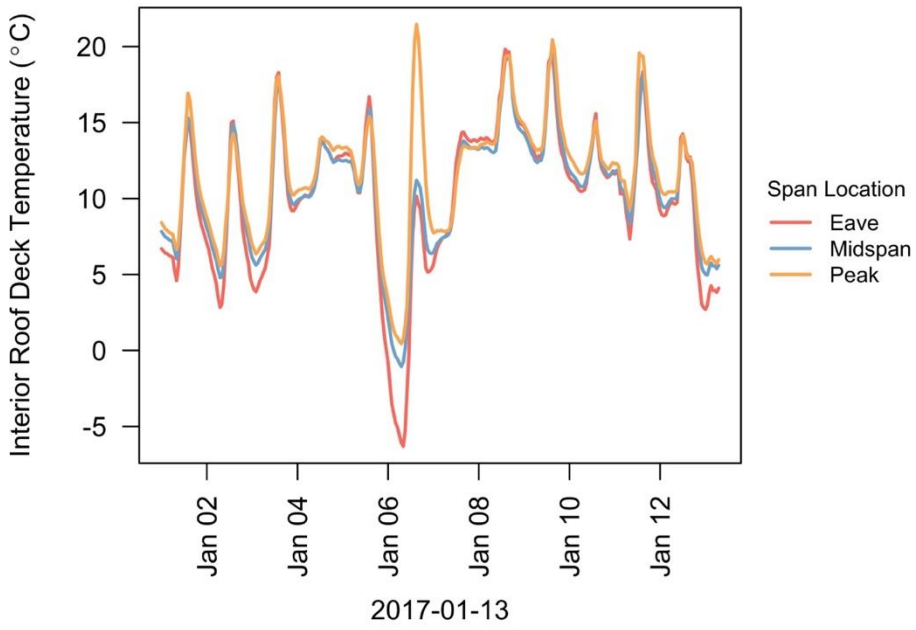

Figure 48 EW52 Fresno. Annual diurnal profiles of the interior roof deck temperatures measured at the eave, midspan and peak of the North-oriented roof slope.

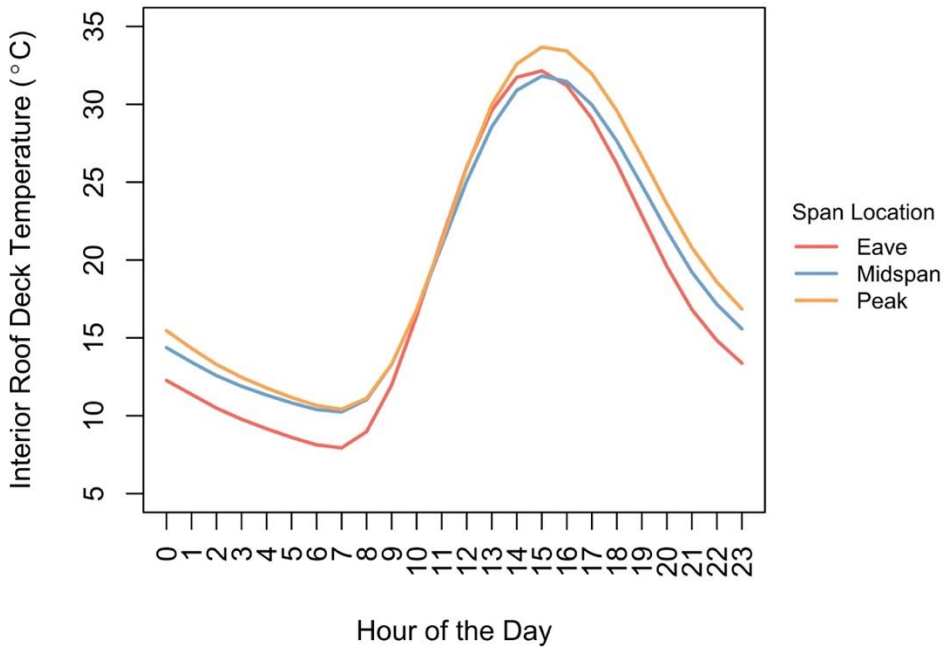

Figure 49 EW52 Fresno. Monthly profiles of the interior roof deck temperatures measured at the eave, midspan and peak of the North-oriented roof slope.

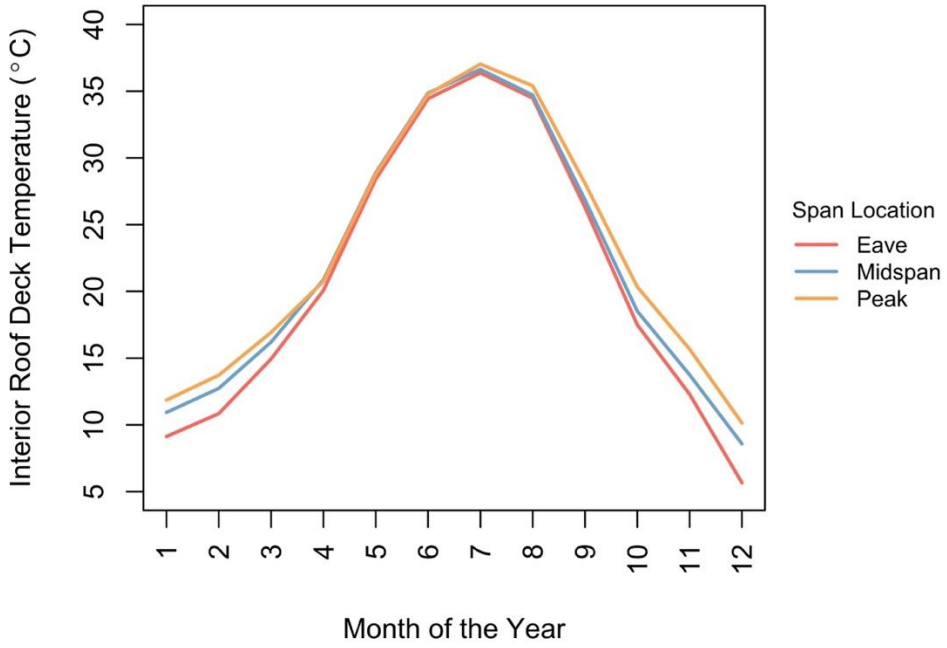

Figure 50 EW52 Fresno. Monthly diurnal profiles of the temperature difference at the interior roof deck eave and peak locations, North-facing slope.

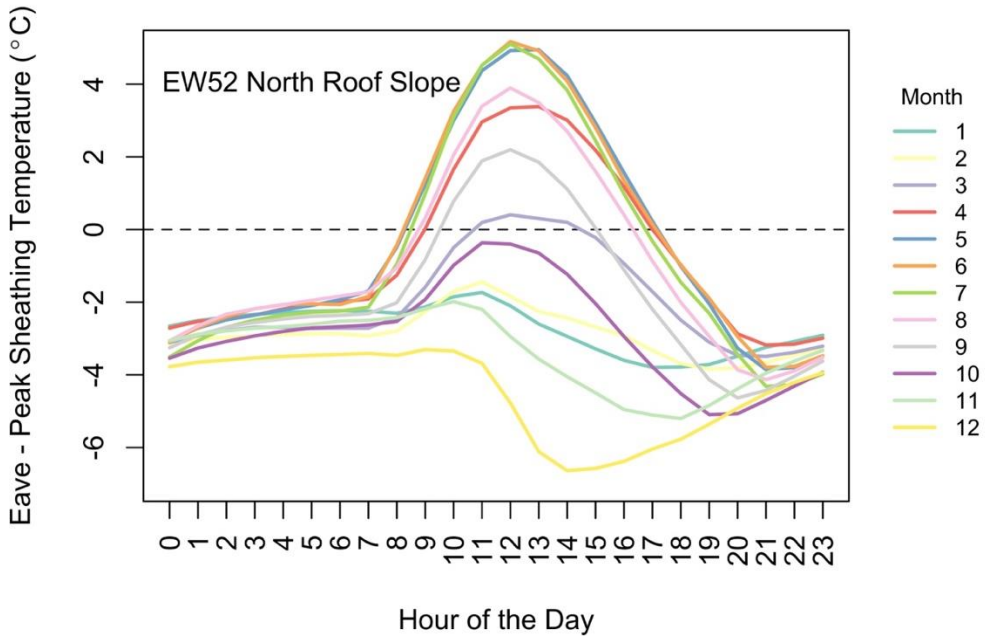

Figure 51 EW52 Fresno. Monthly diurnal profiles of the temperature difference at the interior roof deck eave and peak locations, South-facing slope.

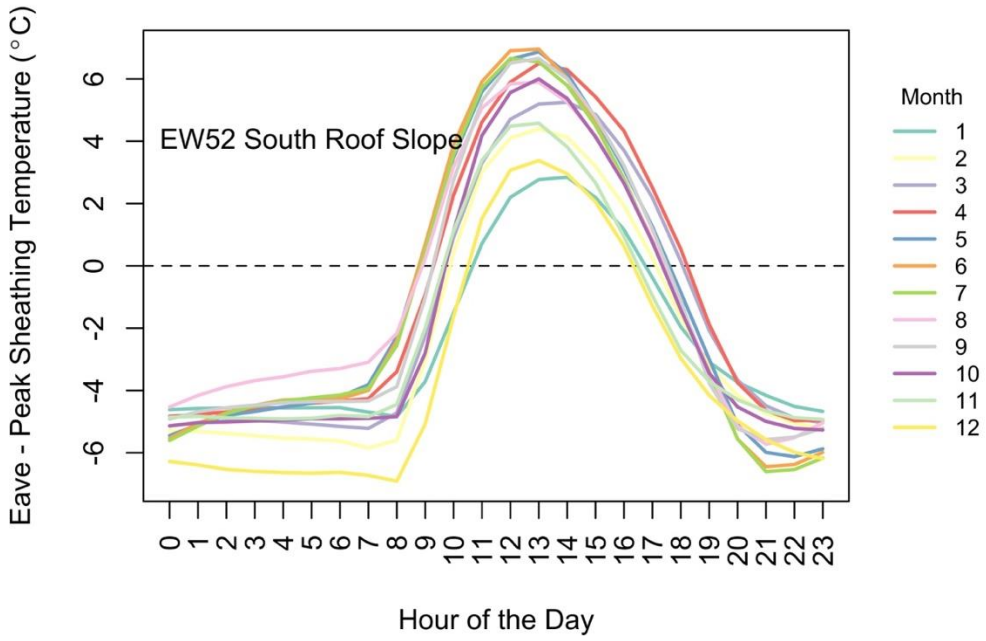

In the Clovis test home, we see somewhat different patterns, as illustrated by a time-series plot for two weeks in December 2017 in Figure 52. Unlike the Fresno test home time-series plotted in Figure 47, most days shown here have clear skies. So, we observe the characteristic hotter temperatures at the peak roof deck (roughly 7°C greater than mid-span and eave), and much lower nighttime temperatures at the eave and mid-span

locations (again, roughly 7°C below the ridge temperature). In the Clovis home, the mid-span location was recorded as the coldest during winter nights, followed by the eave and then the ridge roof deck. This relationship is shown as an annual diurnal roof deck temperature pattern for each location in Figure 53 and as monthly mean values in Figure 54. On average, the mid-span roof deck temperature is between 4 and 5°C below the ridge temperature at nighttime, and during peak daytime periods, the ridge is 4 to 5°C warmer than the eave.

This unexpected temperature pattern in the Clovis test home led us to look at the temperatures measured at the eave, mid-span and ridge locations, but instead of looking at roof deck temperatures, we assessed the temperatures in the insulation middle and insulation surface. These additional measurements confirmed that the mid-span location remains the coldest, which increases our confidence that the sensors were connected and are registering correctly. Notably, the insulation surface temperatures were much lower at the mid-span location, especially when compared to the matching stratification tree attic air temperatures. We expect the insulation surface at a given height to be quite similar to the attic air at that same height. This is the case at the ridge and eave locations (roughly 0 to 1°C colder at insulation surface vs. air), but the mid-span location has an insulation surface that can be 4°C colder than the air at that same height. It is clear that even in these relatively simple geometries there are complex and poorly understood heat transfer mechanisms or issues such as localized air leaks creating temperature differences that vary with location.

Figure 52 EW26N Clovis. Interior roof deck temperatures measured in December 2017 at the eave, midspan and peak of the North-oriented roof slope.

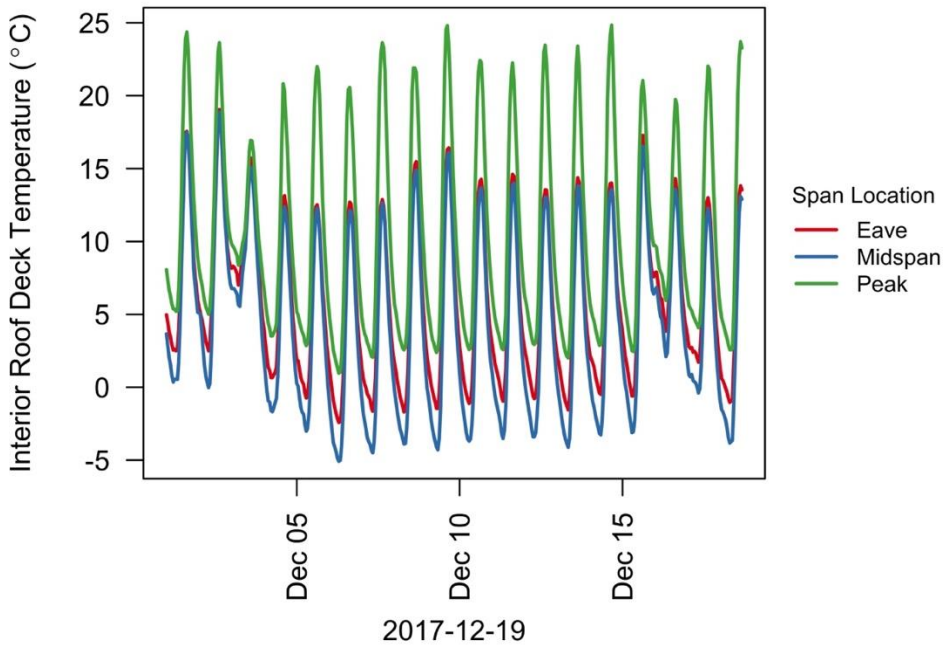

Figure 53 EW26N Clovis. Annual diurnal profiles of the interior roof deck temperatures measured at the eave, midspan and peak of the North-oriented roof slope.

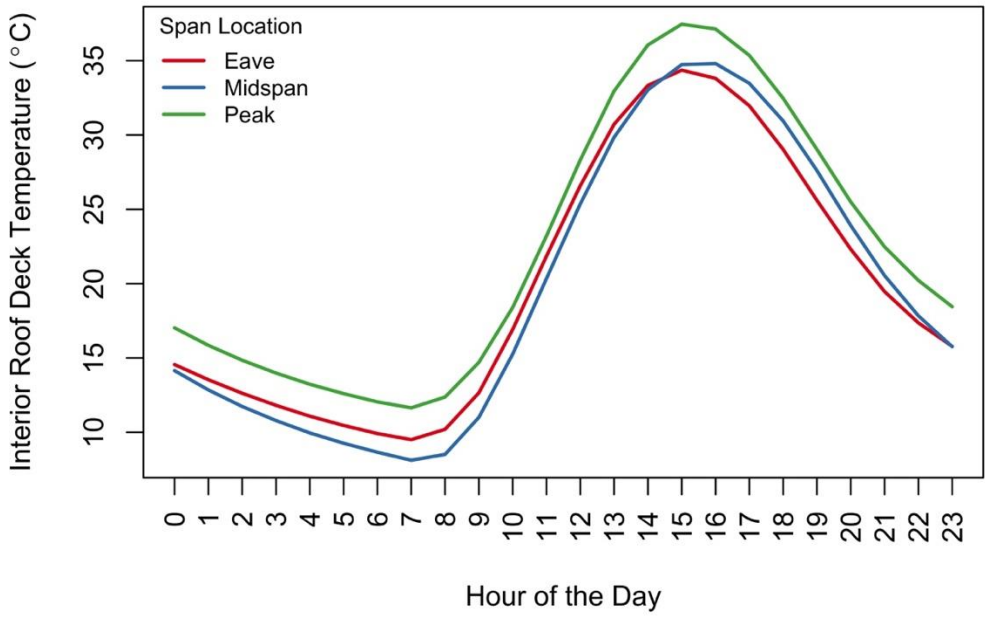

Figure 54 EW26N Clovis. Monthly profiles of the interior roof deck temperatures measured at the eave, midspan and peak of the North-oriented roof slope.

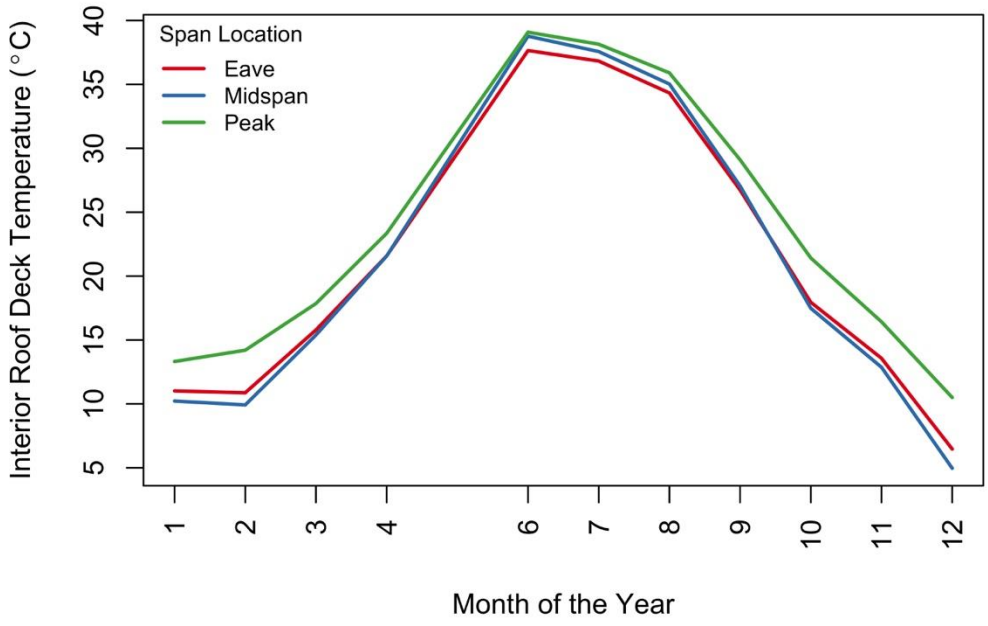

5.3 Moisture Performance

5.3.1 Visual Inspections at End of Monitoring

The final moisture assessment was a visual inspection of the monitored areas during removal of monitoring equipment. This was a simple matter of peeling back the fiberglass batts, starting at the ridge and progressing roughly 36-48" down the roof slope. This easy access for inspection is a benefit of batt insulation that does not exist for other insulation types.

In the Fresno test home, no evidence of mold growth was observed during visual inspection (see Figure 55), though we did observe evidence of prior condensation near the ridge on the North-sloped roof deck in the EW52 attic volume, including rusted roof fasteners, rusted wire mesh netting over some sensors (Figure 56), and raised grain on the OSB roof deck surface.

Figure 55 Fresno test home, picture of the North ridge roof deck area in EW52 attic during sensor removal in May 2018.

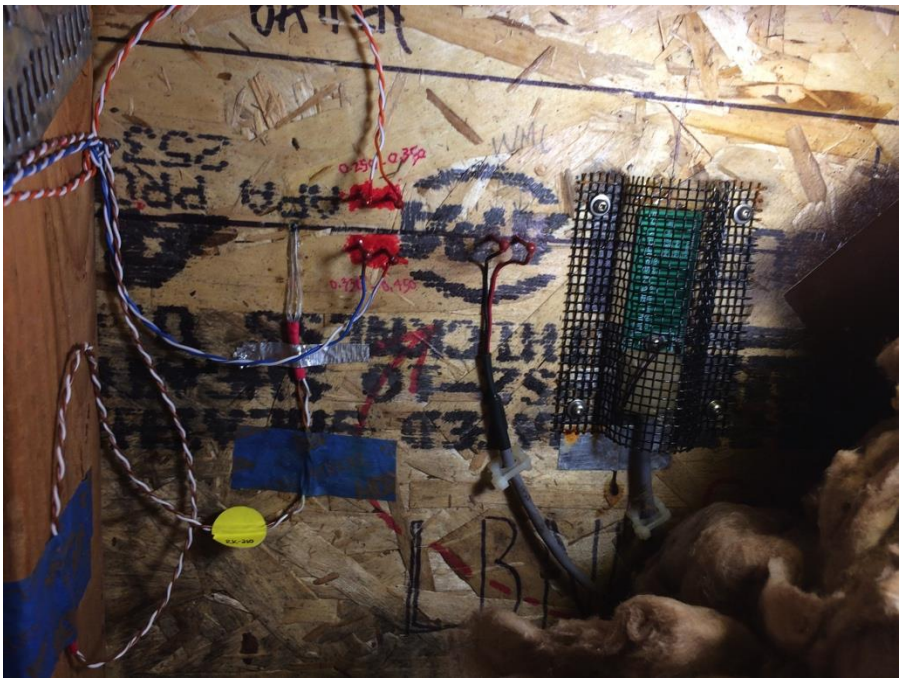

Figure 56 Fresno test home, rusted metal mesh at the North ridge location in the EW52 attic during interim inspection in April 2017.

In the Clovis test home, we inspected the sloped roof surfaces for each orientation at the ridge, and we found visual suspected mold growth on only the North-sloped roof deck, along with evidence of moisture, such as rusted fasteners and raised grain on the OSB. The suspected mold is pictured in Figure 57, and an example rusted roof fastener is shown in Figure 60. The East, West and South orientations were completely free of visual mold (see Figure 58 for comparison of South and North roof deck surfaces), though we did observe some very limited rust formation on roof fasteners in the East and West sloped roof ridges. The suspected mold growth on the North roof deck was spotty and evenly distributed across the surfaces that we exposed. We observed similar suspected mold growth on the top chord of the roof truss, where it intersected with the OSB roof deck (see Figure 59). Areas where we had taped the sensor wiring to the OSB remained unaffected, while all surrounding surfaces showed evidence of suspected mold growth and raised grain on the OSB. No odor was discernable in the attic, nor was any odor detectable when the batt insulation was removed for inspection.

Figure 57 Clovis test home, photo of suspected mold growth on North-sloped OSB roof deck revealed during removal of monitoring equipment in September 2018.

Figure 58 Clovis test home, photo of suspected mold growth on North-sloped OSB roof deck. Image shows location of monitoring equipment at the North slope ridge (right side), as well as the South sloped roof deck (left side) showing clean, unaffected OSB.

Figure 59 Clovis test home, photo of suspected mold growth on the top chord of the roof truss adjacent to the OSB roff deck.

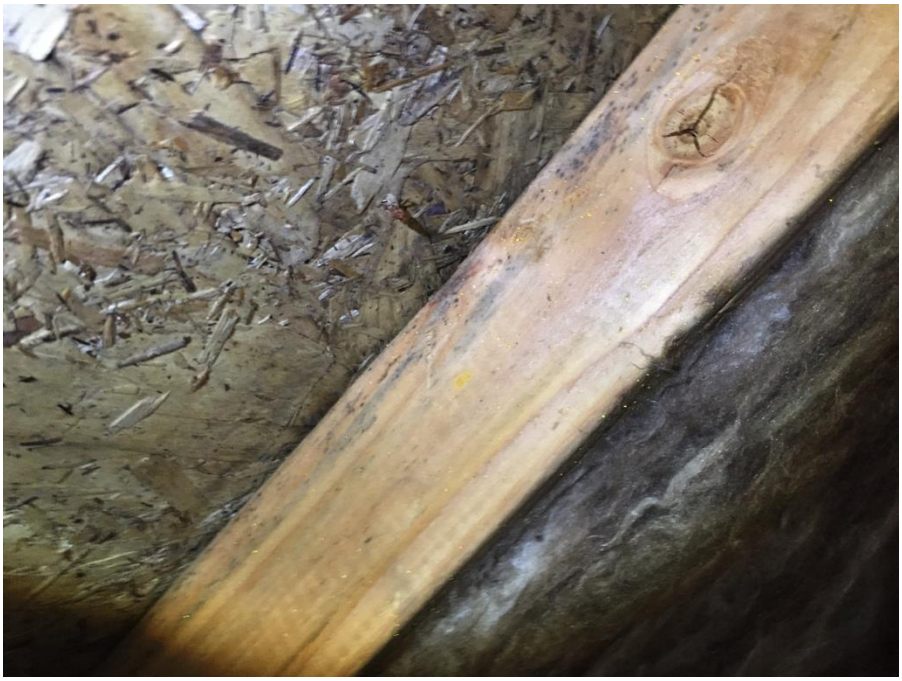

Figure 60 Clovis test home, photo of rusted roofing nail on North sloped roof deck.

5.3.2 Relative Humidity

We show the measured relative humidity in the living zones, attic air zones and at the sloped roof surfaces for the EW52 (Figure 61) and the NS33 (Figure 62) attics (see the Clovis EW26N attic locations in Figure 63). The RH is measured at the ridge blocking on the South (EW52 Fresno), East (NS33 Fresno) and North (EW26N Clovis) exposures, and

all other surface RH values are derived using the measured absolute air humidity ratio and the relevant surface temperatures.

The attic and living space air relative humidities are well aligned with one another in the Fresno test home, though there are some periods where the living space RH exceeds the attic by 5-8% (and vice versa). The Clovis test home was occupied in late September of 2017, and subsequently the attic and living space RH align very well. The living space RH varied roughly between 30 and 60% RH in the Fresno test home, and between 30 and 50% in the Clovis home. The Clovis test home air RH values were quite similar despite the limited connection of the EW26N attic to the living space, due to being largely over an unconditioned garage (see Section 4.1). In the Fresno home, the summer of 2017 shows a prolonged period with a spread of roughly 10% between locations that scales with temperature—the 1st floor was coolest and has the highest RH, and the attic zones were warmest with the lowest RH.

These measurements are consistent with the notion that the living and attic volumes are well mixed and within the same pressure and thermal boundaries (i.e., the air has similar moisture contents, but RH varies somewhat by temperature). The ideal range for indoor relative humidity is commonly referenced to be between 40-60% (Arundel, Sterling, Biggin, & Sterling, 1986; Baughman & Arens, 1996), and this home is within this range throughout the monitoring period. The home is neither particularly dry nor humid.

The peak sheathing locations have much more variable relative humidity, due to their fluctuations in temperature (i.e., cold in winter and hot in summer and due to diurnal solar gains and nighttime re-radiation). As expected, the surface RH rises during the winter in all test attics as the sheathing gets cold. At the ridge sheathing locations, the daily average surface RH is in the 60-80% range for East and West orientations, 70-85% range for South, and 80-100% for the North orientations. Due to lower solar exposure, the North ridge sheathing location gets colder in winter and has a higher surface RH than the South orientation. This divide is not as evident in summer, when the South orientation gets hotter than the North, and the RH is quite similar. In the Clovis test home, we estimated the North sheathing surface RH values at ridge, mid-span and at the eaves. The North sheathing mid-span and eave locations were markedly colder than the ridge location (see Section 5.2.6), and they used the same absolute humidity to estimate surface RH, so the calculated RH values are highest at mid-span and then eave. We are most confident of the measured RH at the North ridge blocking and estimated values at the North ridge sheathing, and these surface RH values remained lower, in the range between 60 and 90%.

Figure 61 Fresno EW52. Daily average relative humidity in the living space, attic air volumes and attic ridge sheathing surfaces.

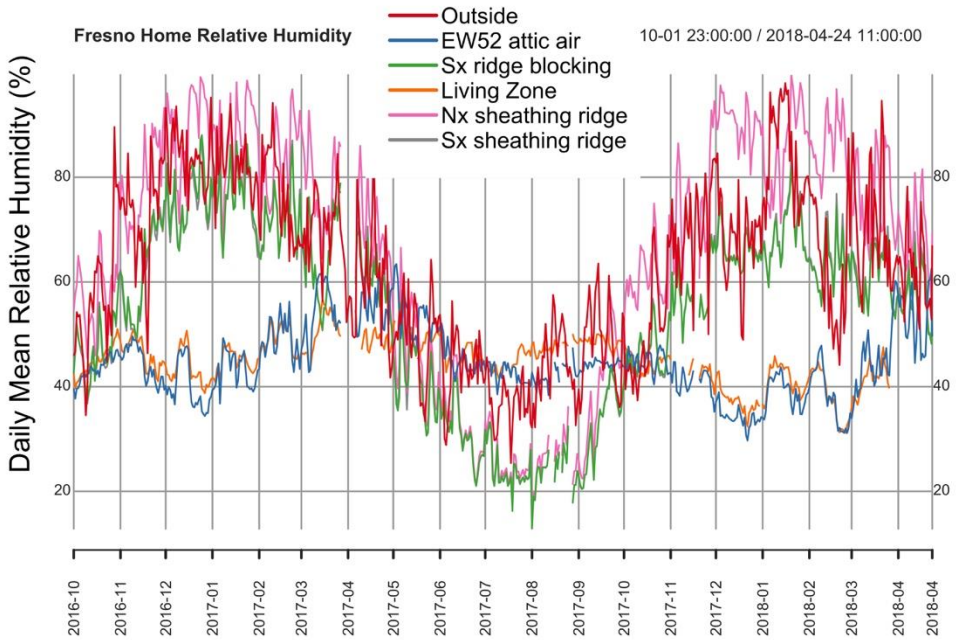

Figure 62 Fresno NS33. Daily average relative humidity in the living space, attic air volumes and attic ridge sheathing surfaces.

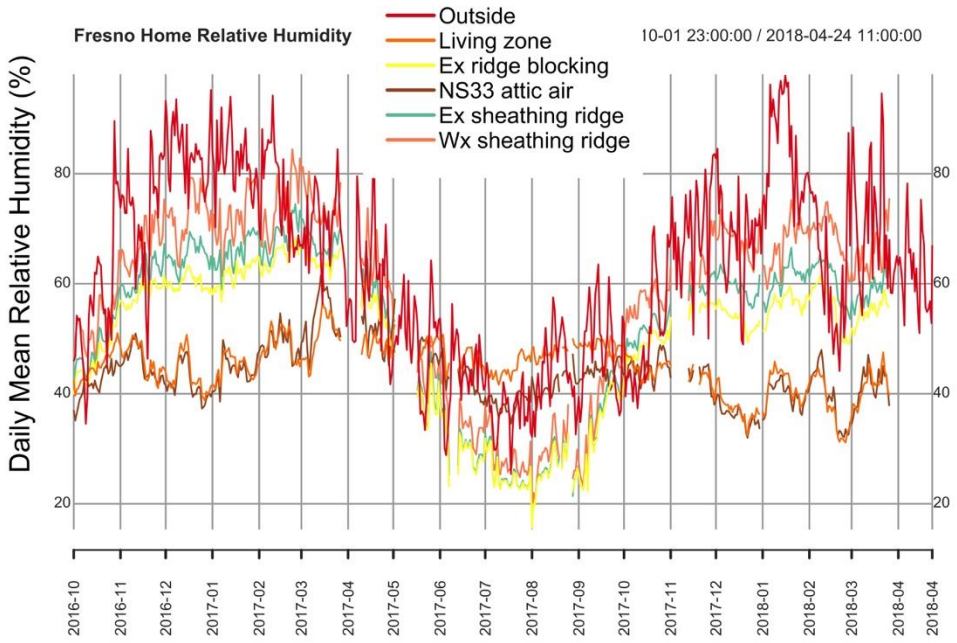

Figure 63 EW26N Clovis. Measured and Estimated daily average relative humidity outside, in the living space, attic air volumes and attic OSB roof deck locations.

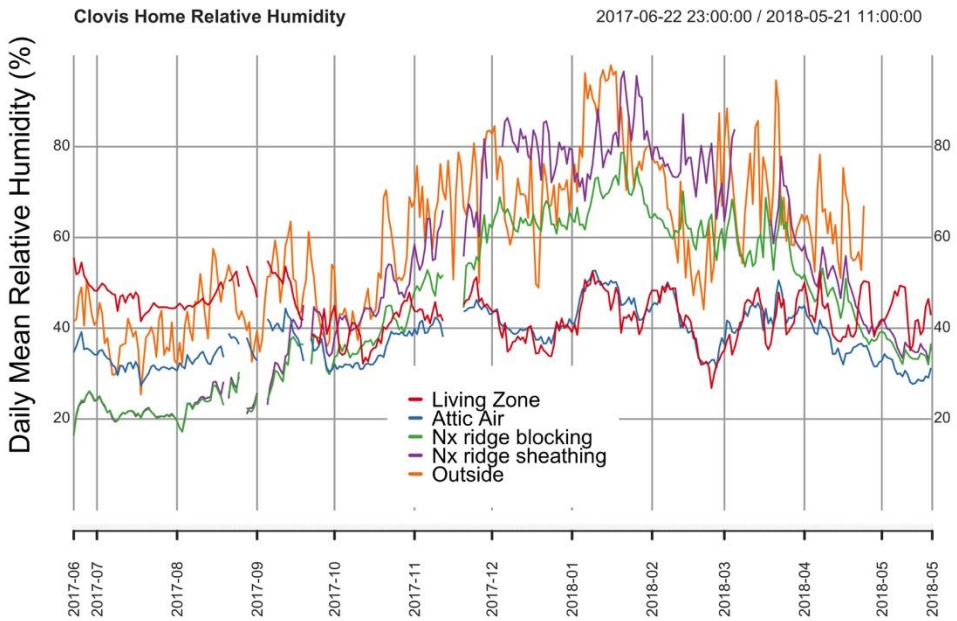

5.3.3 Former ASHRAE 160 Surface RH Criteria

Prior to introduction of the mold index as the moisture performance criteria used in ASHRAE 160, the requirement was that a surface must have 30-day running average RH below 80% while the 30-day running average surface temperature was between 5 and 40°C. We show the 30-day running average surface RH for the peak sheathing locations, along with their hourly values for the EW52 Fresno attic (Figure 64), the NS33 Fresno attic (Figure 65) and the EW26N Clovis attic (Figure 66). In the Fresno home, only the North ridge sheathing in the EW52 attic fails the former ASHRAE 160 criteria. It exceeded the former ASHRAE 160 criteria continuously for 4 months each winter. In the Clovis home, all North sheathing locations (ridge, mid-span or eave) fail the former ASHRAE 160 criteria. The North ridge location exceeds the 80% RH threshold continuously for roughly one month, while the mid-span and eave locations do so for roughly 3 months.

Figure 64 EW52, Fresno. Surface relative humidity measured at the South ridge blocking and calculated at the North and South ridge sheathing surfaces, along with air RH outside, in the attic air and living zone. Hourly and 30-day running mean values. Note that Sx sheathing ridge is essentially identical to Sx ridge blocking.

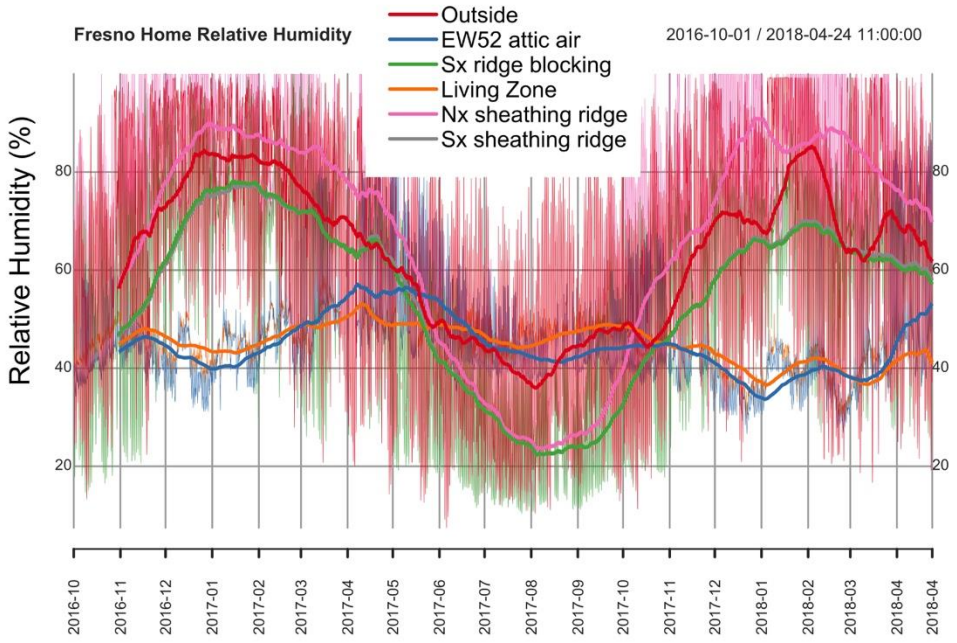

Figure 65 NS33, Fresno. Surface relative humidity measured at the East ridge blocking and calculated at the East and West ridge sheathing surfaces, along with air RH outside, in the attic air and living zone. Hourly and 30-day running mean values.

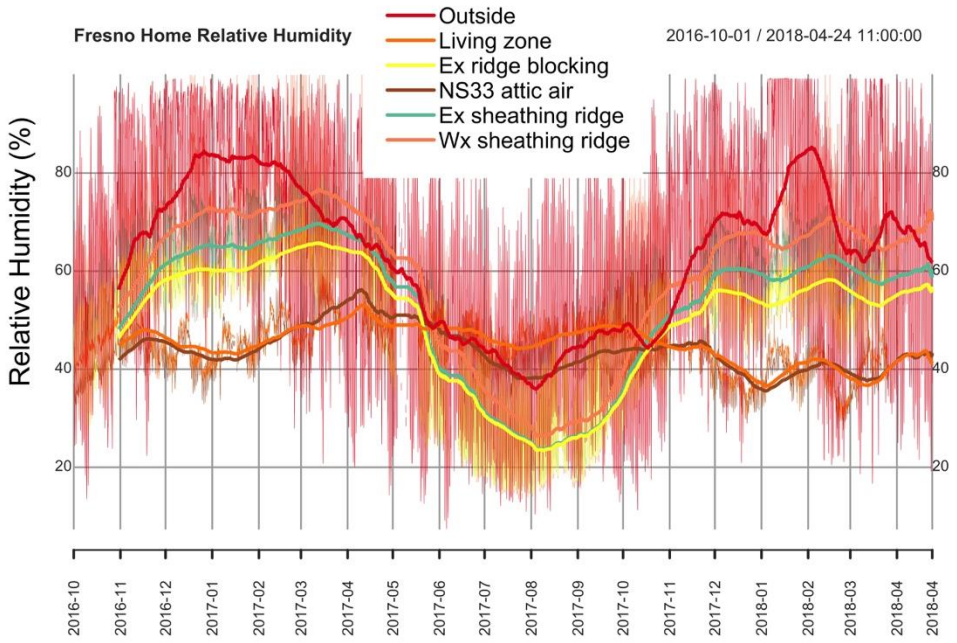

Figure 66 EW26N Clovis. Surface relative humidity measured outside and at attic framing and North sloped roof deck locations, hourly and 30-day running mean values.

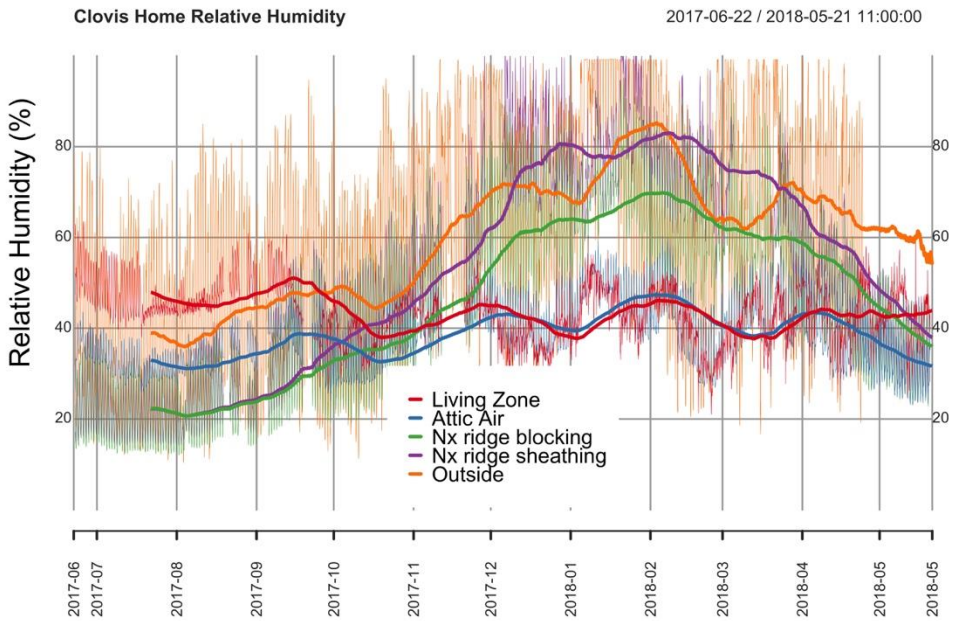

5.3.4 Mold Index (Current ASHRAE 160)

The time-series for the mold index calculated for the EW52 Fresno attic is shown in Figure 67. The maximum for this 565-day period was 1.97 in the North-oriented peak sheathing location, which indicates several local mold growth colonies on the surface visible only under microscope. All other locations peaked below 0.1, including those in the NS33 attic of the same home. This result corresponds to those reported elsewhere (summarized in Less et al. (2016)), that when present, moisture issues occurred at the North, ridge sheathing.

Figure 67 clearly shows the seasonal cyclic wetting and drying that occurs in sealed and insulated attics. The periods from November through April (winter) represented incrementally increasing mold index values, while consistent dry conditions in the attic in May through October (summer) led to reductions in mold index. Notably, the mold index appears to be on the rise, a trend which we expect will continue past this measurement period—peaking at ~1.5 in the winter of 2016/17, falling to ~0.9 the following spring/summer, and then growing again in the winter of 2017/18 to the current new maximum value of 1.97. Additional calculations in the companion simulation report (see Section 7.2.2.2), which cover 4-year performance periods, show that this pattern will dampen out at a stable level, but we cannot say if that level will be above or below the ASHRAE Standard 160 failure threshold of 3.

The Clovis house shows lower Mold Index values, yet, as discussed in Section 5.3.1, evidence of suspected mold growth was found on the North sloped roof OSB surfaces and immediately adjacent truss framing members, from roughly mid-span up to the ridge (eave locations were not visually inspected). This visual finding stands in sharp

contrast to the maximum mold index values calculated from the surface RH and temperature measurements, which was much less than one, indicating no germination of mold spores or growth visible under microscope.

Figure 67 Fresno test home, mold index time-series plot for roof ridge sheathing locations, as well as general attic framing.

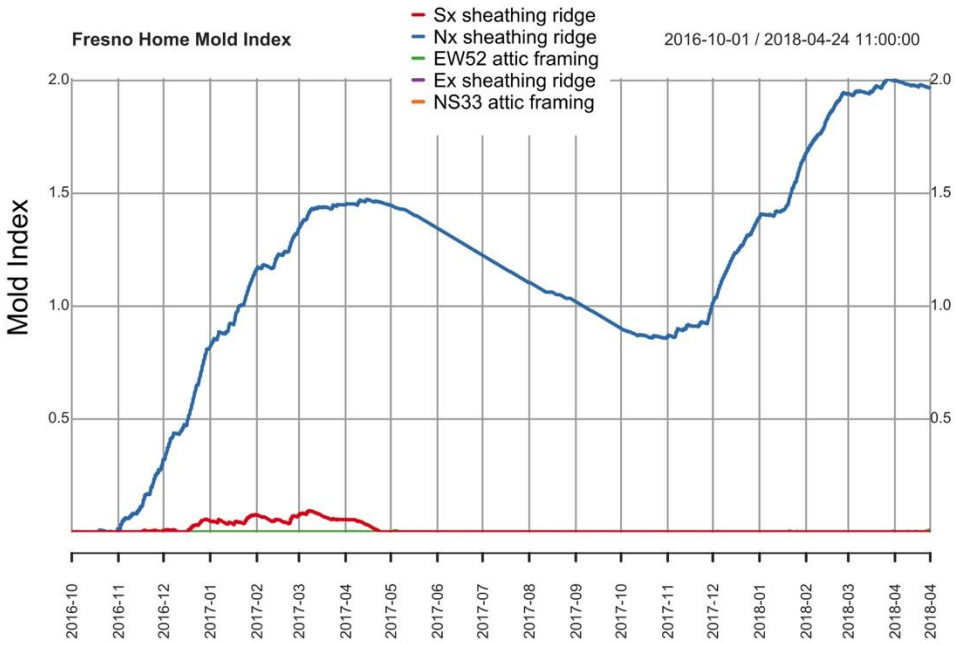

Figure 68 EW26N Clovis. Mold index time-series plot for attic framing and North sloped roof deck locations.

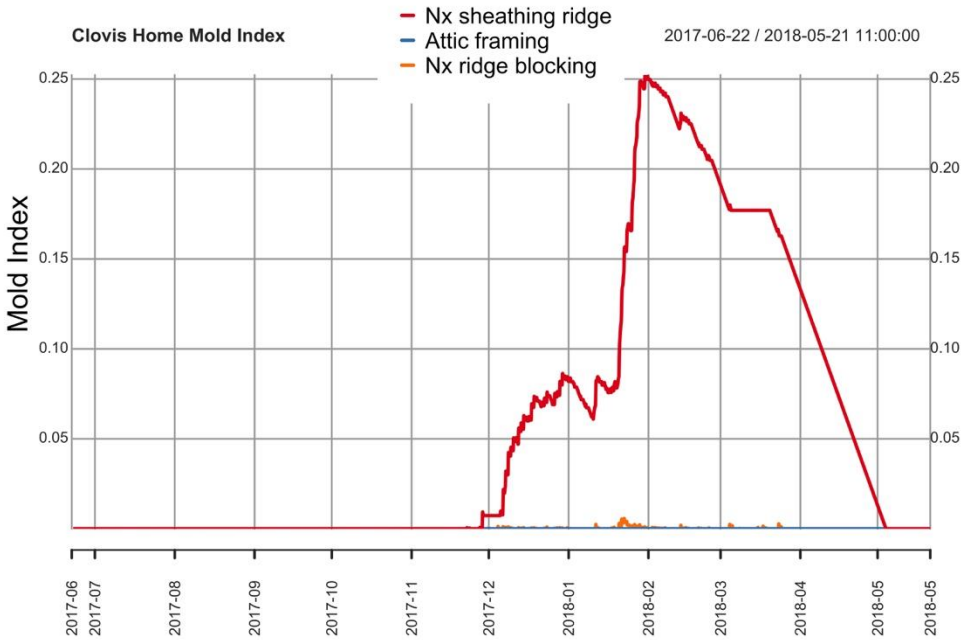

There are several possibilities why the mold index is low, but we observed suspected mold growth. First, it is possible that the OSB sheathing was installed with some prior mold contamination that was not visually evident during installation or placement of monitoring equipment. The moisture conditions were then sufficient at the North sheathing to further produce visible suspected mold growth, while other surfaces were dry enough that further colonization and growth did not occur.

A second potential explanation is that the VTT mold index used in ASHRAE 160 may not be good at predicting risk of mold growth under highly dynamic hygrothermal conditions, such as are experienced at the sheathing-OSB interface in an insulated roof deck assembly. For example, the mold index model was developed and tested initially under fixed RH and temperature conditions, with later assessment using variable conditions. Yet, even the variable conditions were on the order of days. For example, Hannu Viitanen & Ojanen (2007) tested cycles between 97% and 65% RH for varied periods of 3-days vs. 1-day (i.e., 3-1, 3-3, 1-3, 1-1). They found that colder conditions and longer low-RH periods retarded mold growth, while higher temperatures and longer high-RH periods enhanced growth. Yet, none of these conditions approaches the dynamics of temperature and moisture that exist in the boundary layer between glass fiber insulation and the OSB roof deck in a sealed attic roof deck assembly. The mold index model uses solely surface RH and temperature, yet the OSB in an insulated roof assembly can also experience condensation of liquid water, and it has moisture stored in the OSB and framing materials. The presence of liquid condensation could accelerate mold growth in a way not strictly captured by surface RH. Similarly, the storage of moisture in wood could mean that mold growth conditions are not adequately

represented by surface RH, which could appear to decrease below a critical mold growth level when the surface heats up, yet the wood moisture content remains high and potentially serves as a source for local mold growth or generates a localized condition hospitable to growth. For more discussion of the limitations of the VTT mold index, see Methods Section 3.1.1.

We note that similar results were reported by Ueno & Lstiburek (2018) at the 2018 Annual North America Passive House Conference. In their monitoring of moisture risk in sealed attic assemblies in a cold climate test hut, they found visible mold growth while calculated mold indices were below levels of concern. This occurred in assemblies that were dense packed with cellulose insulation, covered with a variable permeable vapor retarders and had varying vapor diffusion vents. Very limited mold growth was similarly observed in fiberglass assemblies that also had mold indices below 3.

Third, it is also possible that measurement errors are leading to arbitrarily low mold index values. As noted throughout this work, air RH was measured at the ridge locations in the test attics, and the humidity ratio was then used to estimate surface RH at the corresponding surface temperatures on the OSB surfaces. Possibly the absolute humidity was higher at the roof sheathing than at the nearby ridge blocking. Other measurement errors could include misalignment in the time constants of the moisture and temperature sensors in the Vaisala RH instruments as discussed earlier.

Finally, it could be that unique aspects of attic geometry and air leakage pathways contributed to the suspected mold growth, but was not captured by the measurement locations. For example, the mid-span location was the coldest location on the North sloped roof in the EW26N attic, yet our RH measurement was at the ridge blocking. Localized air leakage at an unsealed joint between two courses of OSB roof sheathing could lead to localized moisture transport, condensation and accumulation that were missed by condensation and wood moisture sensors at the ridge. The mid-span location may be the source of suspected mold and moisture in this attic, and our measurements were not set-up to capture these unanticipated effects.

5.3.5 Surface Condensation

We show time-series surface condensation measurements for all locations in the Fresno test attic in Figure 69, with varying orientations at sheathing ridge locations, as well as on the NW gable. Liquid water was present at the surface of the sheathing whenever the value exceeded 0, and the values are proportional, with larger y-axis values meaning greater moisture mass at the material surface. The Clovis home experienced no surface condensation during the monitoring period (see Figure 70).

Consistent with mold index results for the Fresno attic, surface condensation occurred exclusively at the North-oriented roof peak sheathing location (orange line) during winter months with significant weather-related variability. The large condensation accumulation events occur during the coldest periods, with daily average sheathing surface temperatures around 6.5 to 8.5°C, and hourly minimum temperatures around

0°C. These surface temperatures correlate with daily average surface RH values very near saturation, from 96 to 99.5%. Surface moisture was present at the North peak sheathing location for 5,487 out of 13,026 monitored hours, which when annualized over a rolling period, averaged 30% of annual hours (from 23 to 43% of annual hours). A marked pattern occurs in the data, where the fraction of annual hours with condensation present increases continuously over the monitoring period from 23 to 43%. This apparent increase in condensation runs contrary to our other moisture measurements, which showed that relative to the wet winter of 2016/2017, the drier winter of 2017/2018 had much lower roof deck wood moisture contents, less increase in the mold index and dryer ambient outdoor conditions.

These results lead us to question whether the condensation sensor in the Fresno North ridge location drifted over the measurement period. The 2016/17 winter was one of the wettest in decades in CA, while the 2017/18 winter rainfall was roughly half of average. Consistent with this, our other measurements do not support the doubling of condensation. Wood moisture measurements at the Northern ridge sheathing location suggest much lower WMC during winter 2017/18, peaking around 18% vs. 25% WMC. In fact, the 2017/18 winter conditions were drier overall, with lower average outdoor vapor pressure (942 vs. 1,061 pa), lower outdoor RH (68% vs. 74%), and lower living space RH (41% vs. 47%). Mean RH at the Northern ridge sheathing was 79% each winter, but the 2017/18 winter spent 6% fewer hours above 98% RH. These measurements suggest that condensation was likely similar or less in the winter of 2017/18 vs. 2016/17 (i.e., ≤ 23% of hours).

As an additional check on the condensation sensor, we calculated the dew point temperature at each roof deck ridge location and assessed when the corresponding dry bulb temperature was below the dew point. Again, the North ridge roof deck was the only location that showed substantial time below the dew point temperature, and when annualized, the fraction of hours with condensation potential ranged between 7.5 and 9%, with no marked trend with time (i.e., it did not increase from the first to the second winter). If anything, condensation assessed by this method was reduced in the second winter, with 26% vs. 24% of hours in December and January having potential condensation in the winter of 2016/2017 vs. 2017/2018. This corresponds with the overall trend towards greater dryness in the second winter, and it heightens our concern over the validity of the condensation sensor accuracy.

It is also possible that the dielectric capacitance sensors that we used to detect surface condensation are very sensitive to moisture mass even at the molecular level, much more so than standard leaf-wetness condensation sensors or the dew point temperature method. It may be that while moisture mass was present for a substantial fraction of the monitoring period, it was at very low levels.

Figure 69 EW52 and NS33 Fresno. Condensation indication in attic peak and gable locations with varying orientations. Values > 1 indicate presence of surface moisture, values are proportional (larger value = more moisture mass).

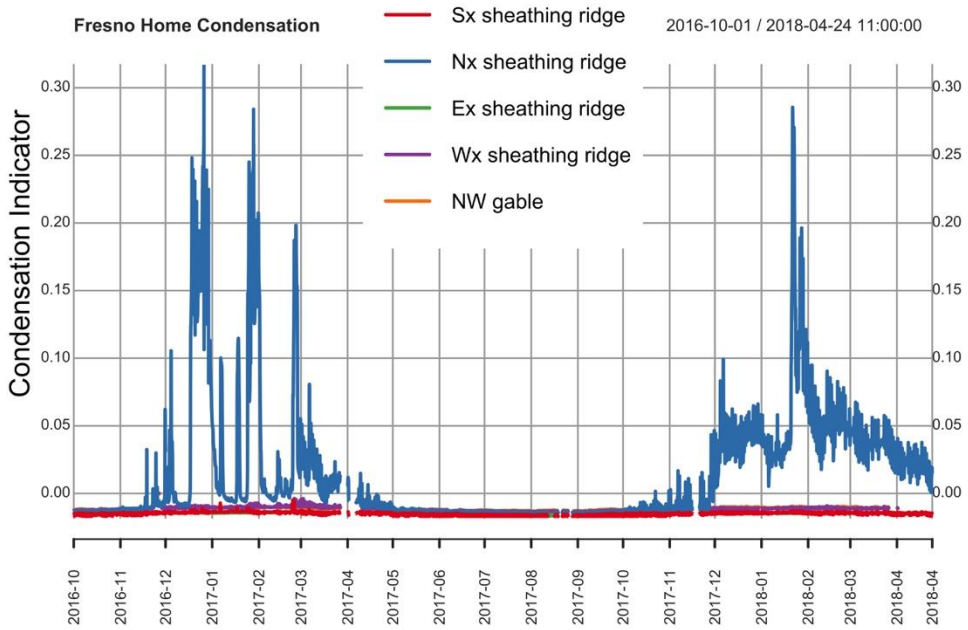

Contrary to the findings in the Fresno home, in the Clovis home no condensation was measured during the entire monitoring period. As shown in Figure 70, the condensation indicator remained below 0 for all monitored minutes. Yet, as described in Section 5.3.1, there was visible suspected mold and evidence of the presence of liquid water, such as rusted roof fasteners. Given this misalignment of our visual and condensation sensor results, we also performed a dew point assessment, looking at when the dry bulb temperature at the OSB roof deck dropped below the co-located dew point temperature, which should also provide an indication of condensation events. We did this assessment at each of the four temperature measurement points along the North roof slope in the EW26N attic—North ridge blocking, ridge, mid-span and eave roof deck. As noted in the Methods Section 4.2.7, we did not measure RH at each of these locations along the roof slope, instead we estimated the absolute humidity at the ridge blocking, and translated that to surface RH using the measured surface temperatures.

At the North ridge blocking (where the RH sensor was located), the dew point assessment suggests 0 hours of condensation potential, while at the adjacent North roof deck OSB location, we estimated 0.6% of monitored hours (41 out of 6,982 hours) with condensation potential. This location is where the condensation sensor was located, and indicates agreement between the dew point assessment and surface condensation measurements. When we examine the mid-span and eave locations, we find potential condensation in 11.1 and 6.8% of monitored hours (773 and 471 hours out of 6,982 hours), respectively. These are substantial periods of time that could clearly lead to rusted fasteners, raised surface grain on the OSB and other observed effects. That being said, we are also less confident of our surface RH estimates, as we apply the absolute

humidity measured at the ridge blocking to surface temperatures as far away as mid-span and the eave. As noted in other sections, the Clovis home is unlike results from other studies because the ridge was not necessarily the most humid or had the greatest moisture risk.

Figure 70 Clovis test home EW26N, condensation indicator at the North roof ridge. Values > 0 indicate presence of liquid water on the surface.

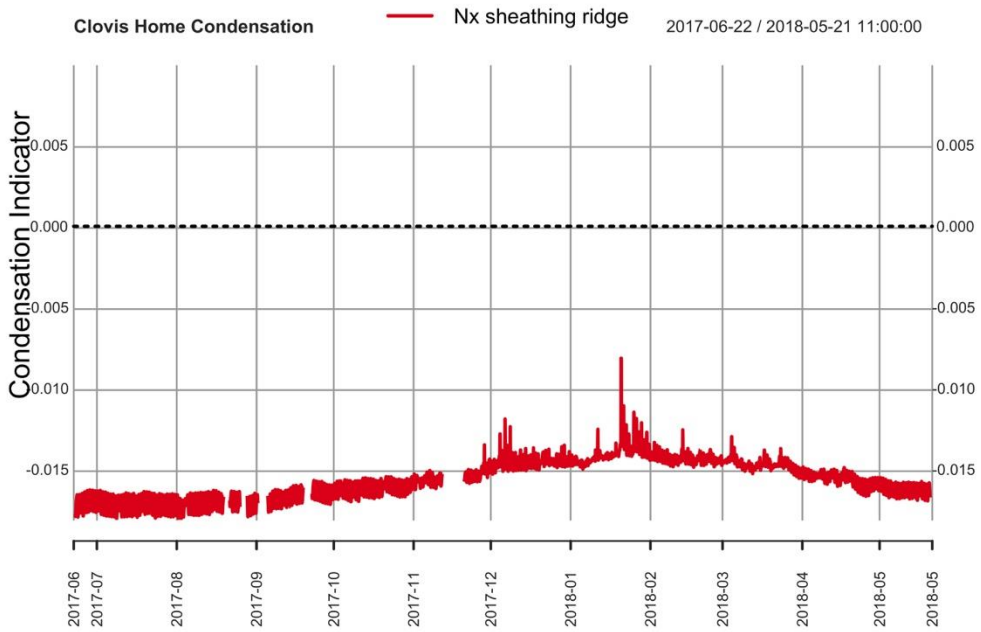

5.3.6 Wood Moisture Content

Measured daily mean wood moisture contents at the wood and OSB surfaces are shown in Figure 71 for the Fresno test home and in Figure 72 for the Clovis test home. Both homes show the expected pattern of increased surface WMC during the heating season, with very dry conditions during the summer season. The intensity of the winter of 2016/2017 is evident in looking at the North ridge sheathing location in the Fresno EW52 attic, which peaks at 25% MC. In comparison, the eave location on the North-sloped roof deck peaked at 12.5%. The other orientated ridge locations in the Fresno test home attic peaked between 9 and 12%. All attic framing locations in both the EW52 and NS33 attics peaked at 8.5% MC.

After relatively high surface moisture levels were observed at the North ridge sheathing location in the winter of 2016/2017, we decided to install two additional North ridge WMC pin sets, but with insulation guarding them from the surface moisture, to depths between 35 and 45mm into the OSB sheathing. These values are indicated as “Nx Ridge Depth2” and “Nx Ridge Depth1” in Figure 71. These were installed too late in the 2016/2017 winter to capture the peak moisture levels, but in the 2017/2018 winter, the depth WMC pins measured peaked at 10.2%, while the North ridge surface reached 16%.

The North sheathing at the eave registered a maximum value of 12.5%, while all other locations remained below 10% in the second winter.

Figure 71 Fresno test home, measured surface wood moisture content at the roof ridge for each sloped roof orientation, at the eave of the North sloped roof deck, and attic framing locations, along with core wood moisture at the North ridge ("Depth1" and "Depth2").

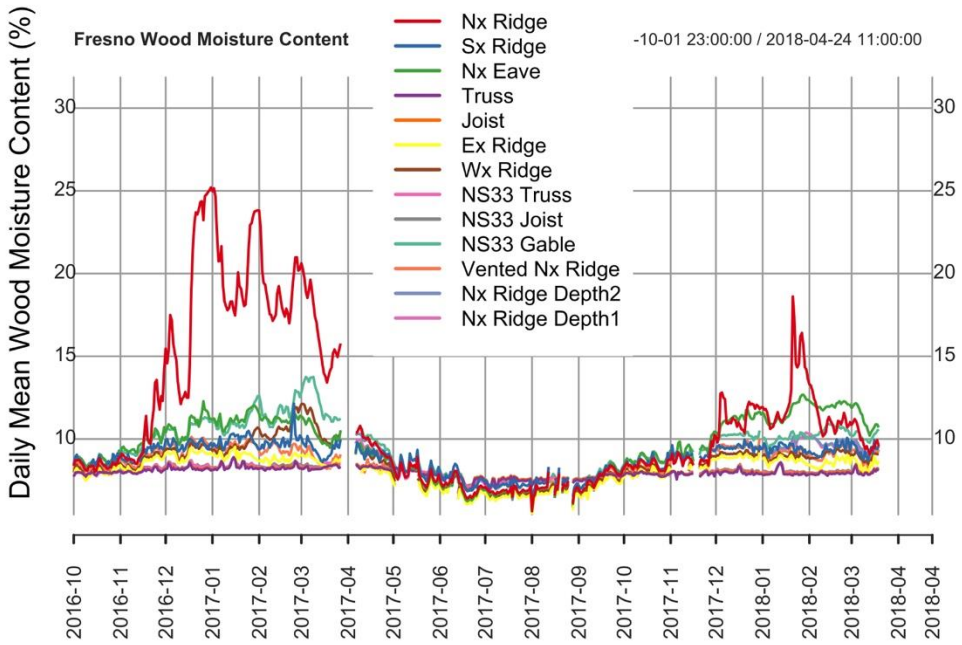

The Clovis test home had North-oriented roof slopes in both the EW26N and EW26S attic volumes, and both ridge sheathing locations were instrumented with moisture pins, along with East and West ridge sheathing locations and general attic framing. Both North-oriented ridge locations experienced the highest moisture contents, with the greater moisture levels registered in the EW26S attic, which was not otherwise monitored (primary monitoring location was EW26N). Again, the bulk framing in the attics remained below 9%, while the non-North oriented ridge locations experienced maximum moisture contents of roughly 10%.

We note that in the winter of 2017/2018, both homes experienced sharp increases in moisture content at the North ridge during the same two-week period at the end of January, which suggests that these jumps in WMC are largely related to ambient conditions, rather than events within the homes.

Overall, the wood moisture measurements in both test homes are mostly within safe conditions. 28% is the common threshold for wood rot and decay organisms, and neither home ever reached this level. 16% is the typical threshold for commencement of mold growth, but it needs to be at 16% over long periods of time (weeks and months, rather than days). The first winter in 2016/2017 did reach levels of concern from a mold growth perspective, but as noted in Section 5.3.4, its mold growth predictions remain in safe territory and no visible growth was observed during decommissioning.

Nevertheless, it is desirable to not reach levels as high as 25%, nor to remain over 16% for months at a time, even during very wet winter seasons. The Clovis home North ridge locations reached short-term maximum values that barely exceeded the minimum requirements for mold growth to begin, yet visible suspected mold was found at the end of monitoring.

Figure 72 Clovis test home, measured surface wood moisture content at the roof ridge for each sloped roof orientation, along with attic framing locations. WMC sensor data was corrupted beginning in February 2018.

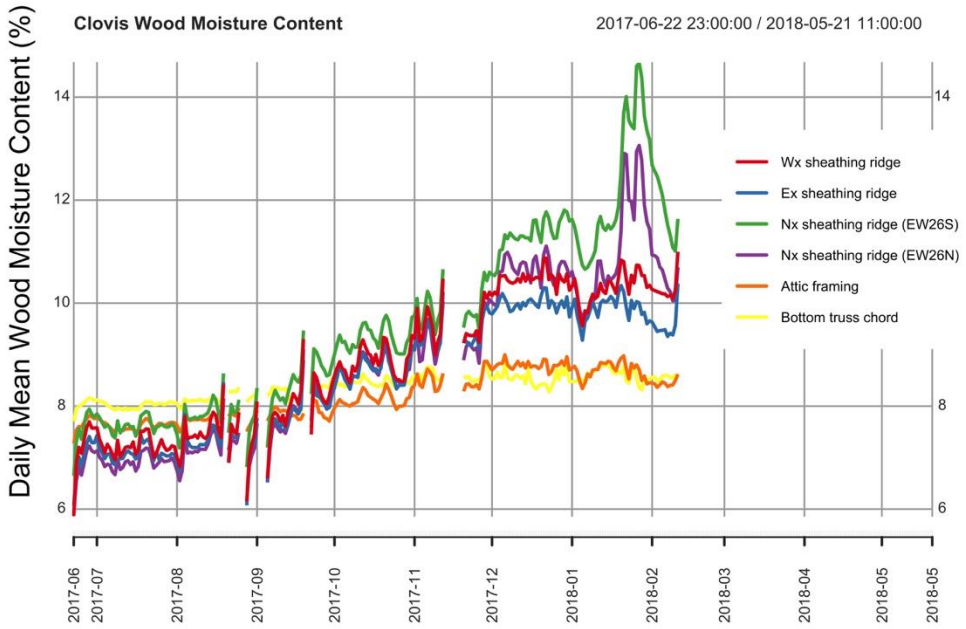

5.3.7 Vapor Pressure and Moisture Transfer

5.3.7.1 Moisture Stratification in Attic Air Volume

Past research has established that the greatest moisture risks are commonly found at the roof ridge in sealed and insulated attics, specifically near the ridge with a North orientation. To better understand vertical moisture gradients in sealed and insulated attic air volumes, we installed a separate vertical stratification tree in the EW52 attic of the Fresno test home made up of HOBO data loggers, with both temperature and RH sensors. These sensors were cross-calibrated as described in Section 4.2.3.

We show the mean diurnal pattern in vapor pressure vertically through the Fresno EW52 test attic for each month of the year in Figure 73. These same data are shown as boxplots for each hour of the day for the month of December Figure 74 and in the month of June in Figure 75. A substantial vertical moisture gradient is established from the attic floor to the ridge during the peak solar gain daytime hours, which is similar to the thermal stratification shown in Section 5.2.2. But moisture stratification in the attic air volume disappears during nighttime hours, when the gradient is nearly zero, and the attic air appears well-mixed from a moisture standpoint. The patterns of stratification

vary substantially by season, depending on solar gains and length of day. During the heating season, vertical moisture stratification is evident, but only from roughly from 2pm to 5pm. Whereas during the cooling season, substantial moisture stratification is evident from roughly 10am to 6pm.

Figure 73 EW52 Fresno test home, diurnal vapor pressure gradient by month of the year, in attic air volume from the attic ridge to the floor.

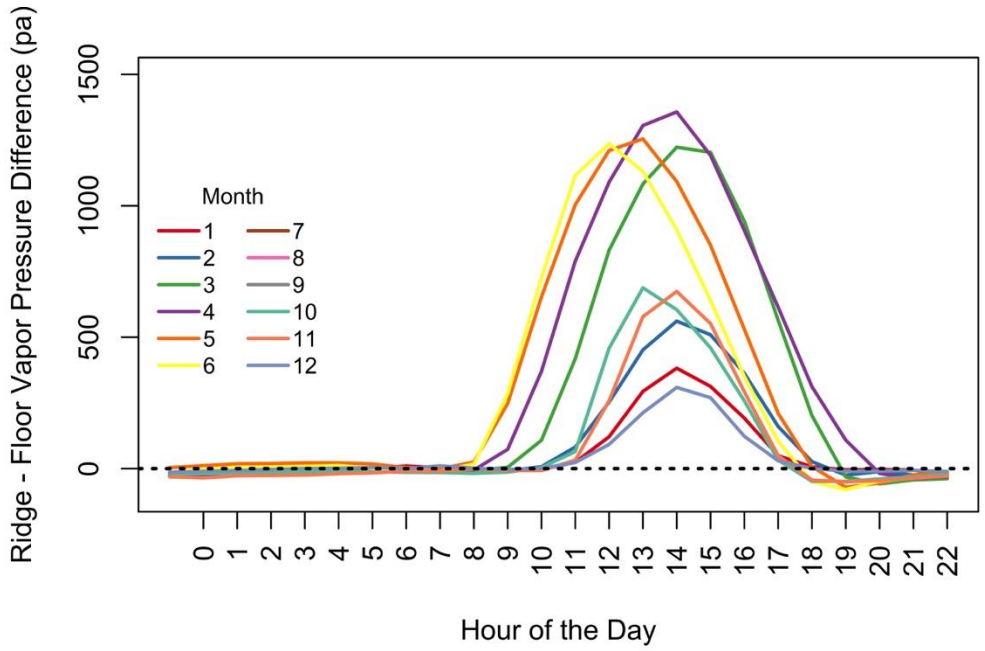

Figure 74 EW52 Fresno test home, diurnal vapor pressure gradient by hour of the day (December).

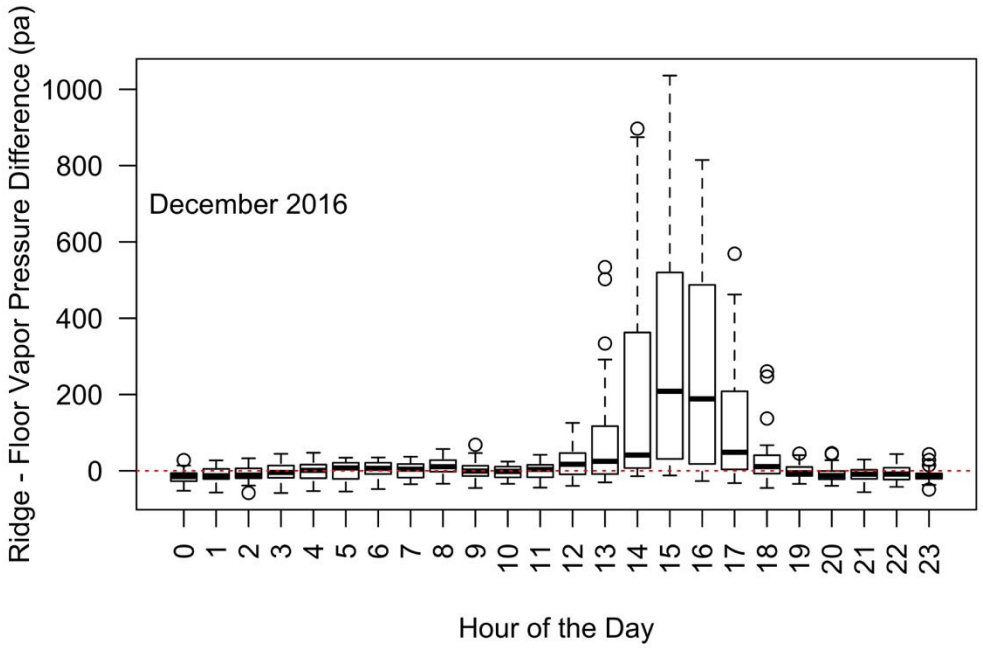

Figure 75 EW52 Fresno test home, diurnal vapor pressure gradient by hour of the day (June).

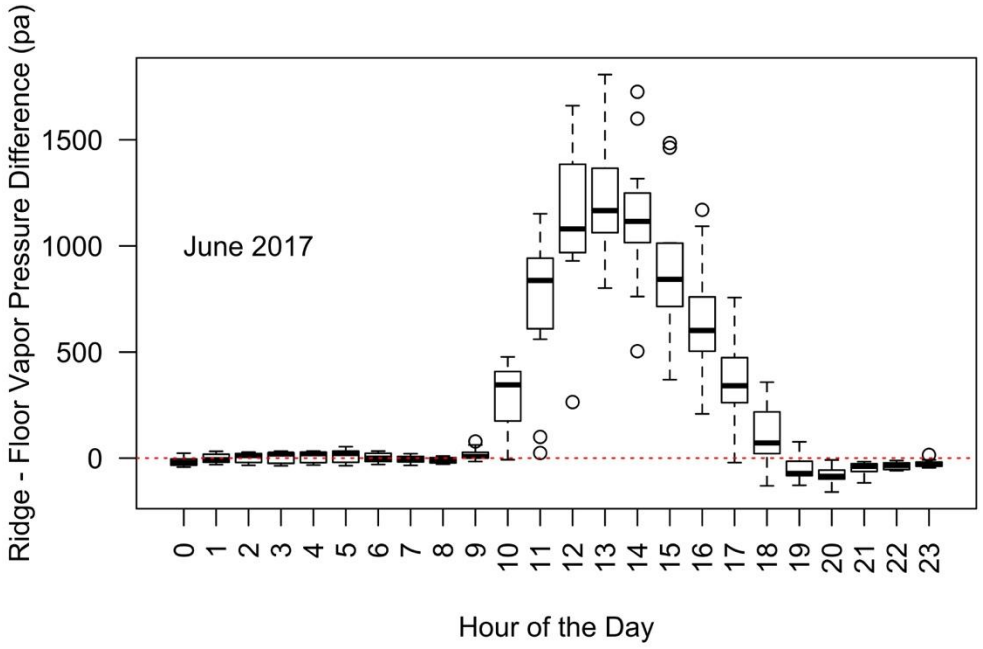

The attic air mass does become stratified with increasing moisture content in the air going from floor to roof ridge, but this only occurs during daytime hours. This is notable, because moisture problems in sealed and insulated attics are largely driven by cold outside temperatures and re-radiation of heat to the night sky during non-daylight

hours. Also, moisture problems tend to occur during the heating season, yet these data show that the daytime moisture gradient in the heating season averages at most 200-300 pa from ridge to attic floor, and it last for only a few hours. The large vapor pressure gradients occur during the summer peak cooling periods, with average maximum gradients around 500-600 pa. From this data, it appears unlikely that vertical moisture stratification in the attic air volume causes moisture accumulation at the roof ridge.

The vertical moisture gradient could be the result of attic geometry. As one rises vertically through the attic, the surface area of OSB sheathing remains constant (same moisture source), but the adjacent air volume gets much smaller (see Figure 36). If the sheathing is roughly similar in temperature, we expect moisture mass emission rates to be consistent along the roof slope, and the increasingly smaller adjacent attic air volume leads to higher moisture contents in the air. The elevated vapor pressure at the ridge could just be moisture emitted at the ridge and re-absorbed at the ridge, with no (or little) net-transport to or from other locations in the attic. This vertical moisture gradient would lead to a corresponding gradient in equilibrium wood moisture content – with high wood moisture at the ridge. However, this explanation may be insufficient because the higher ridge wood moisture content tends to be observed in cold winter months and/or at night time when the vertical moisture gradient is small or non-existent. It may be the case that the daytime gradients in the winter are sufficient to sustain a higher average wood moisture content.

Another possibility is that a vertical moisture gradient exists at times when higher wood moisture contents are observed which is not reflected in the attic air volume. A boundary layer of moisture-laden air may be trapped near the OSB surface, which is allowed to travel vertically up the roof slope, due to small gaps between the insulation and OSB or through the batt itself. Note that we have no measurements or evidence for this boundary-layer explanation.

Unfortunately, we do not have a good explanation for why wood moisture content is higher at the ridge based on our stratification measurements, and this remains an area for further research.

5.3.7.2 Vapor Pressure in Attic and Living Spaces, at the Roof Deck and Outside

Time-series of the outside, living zone, attic peak and attic air vapor pressures in the EW52 Fresno attic are shown for summer in Figure 76 and for winter in Figure 77. The vapor pressure patterns are strongly diurnal, driven by solar radiation during daytime hours, which increases the vapor pressure at the roof deck, as well as in the attic air and in the living space. We see the so-called “ping-pong” effect in the Fresno attic, where moisture is driven from the roof deck into the attic, and is then reabsorbed at nighttime. This is characterized by the cycling of roof deck vapor pressure substantially above the other nodes during daytime and below at nighttime. We see the same daytime spikes in roof deck vapor pressure during winter, but there is no nighttime vapor pressure depression, when the roof deck would re-absorb moisture from the other nodes. The

spikes in roof deck vapor pressure are also smaller in winter due to lower solar gains, typically in the 2000-3000 pa range compared with 3000-5000pa in summer. The spikes in the attic air and house air are also strongly damped or non-existent during the winter.

Figure 76 EW52, Fresno. Vapor pressure during the summer at the attic peak, attic air, living space air and outside.

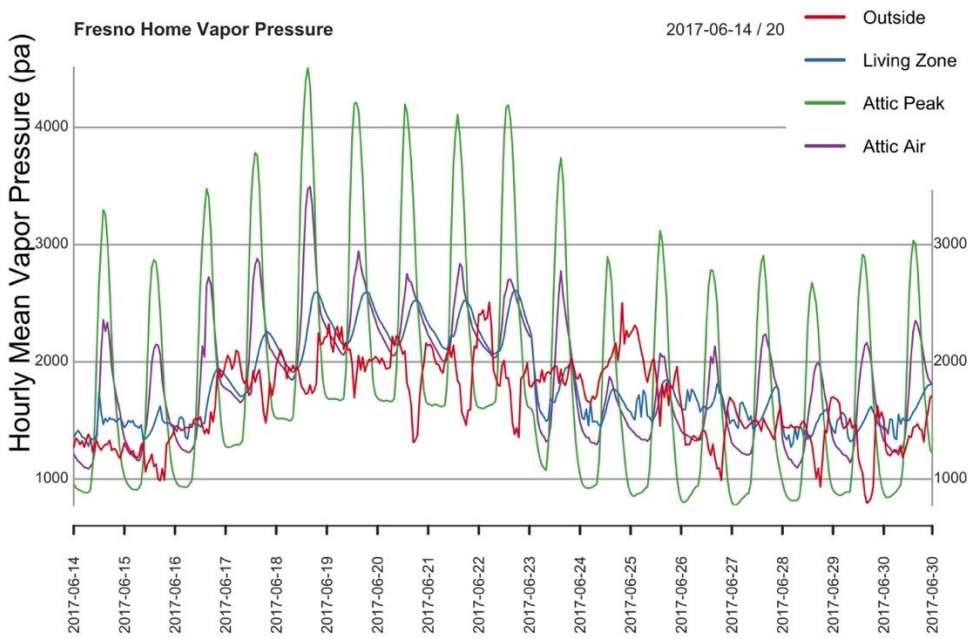

Figure 77 EW52, Fresno. Vapor pressure during the winter at the attic peak, attic air, living space air and outside.

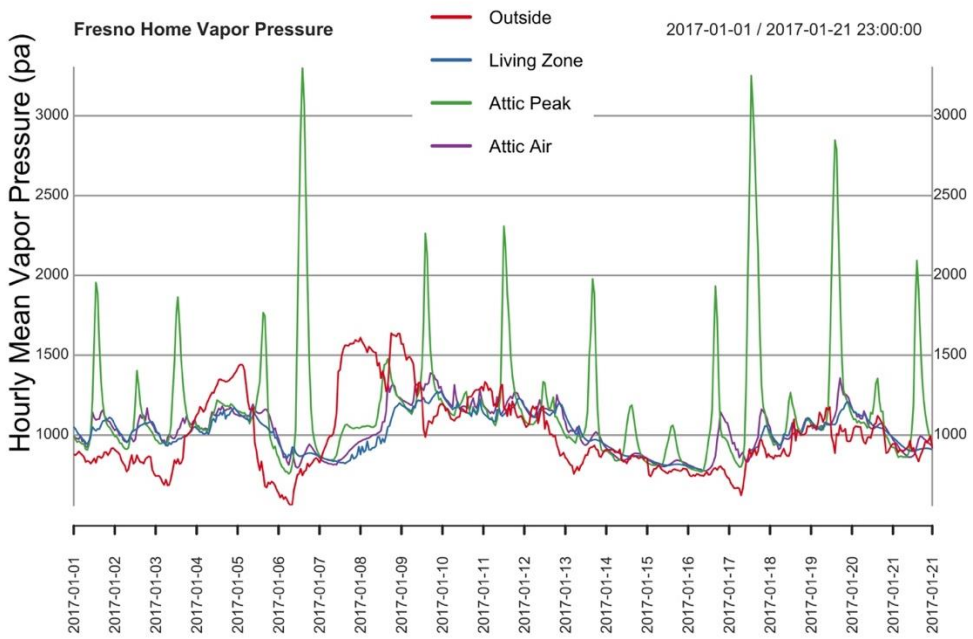

To estimate the net effect of these strong diurnal cycles of vapor pressure, the rolling monthly average vapor pressure is shown for the whole monitoring period in the Fresno EW52 attic in Figure 78. The attic air and living space air are well-coupled in terms of vapor pressure, except during the Spring season, when the attic has a markedly higher vapor pressure than the house (roughly 200-300pa). We hypothesize that this is the result of moisture mass stored in the OSB roof deck during the cold winter, which is then re-emitted into the attic air as conditions warm in spring. All indoor locations register their highest vapor pressure levels during spring time, including the living space, attic air and roof deck. The outside air has lower mean vapor pressure during all months of the monitoring period, except in August of 2017, when it roughly equals the living space and attic vapor pressures. As expected, this is consistent with the addition of moisture to the living space by occupant activities and building materials, which increases absolute humidity in conditioned space above outdoor ambient levels. The outside air is near-continuous source of drying potential for this home and attic. It is notable that even a very dry roof deck, like the Fresno home in Summer, can create high vapor pressures in adjacent attic air and insulation under high solar gain conditions.

Figure 78 EW52, Fresno. Rolling monthly average vapor pressure at the attic peak, attic air, living space air and outside.

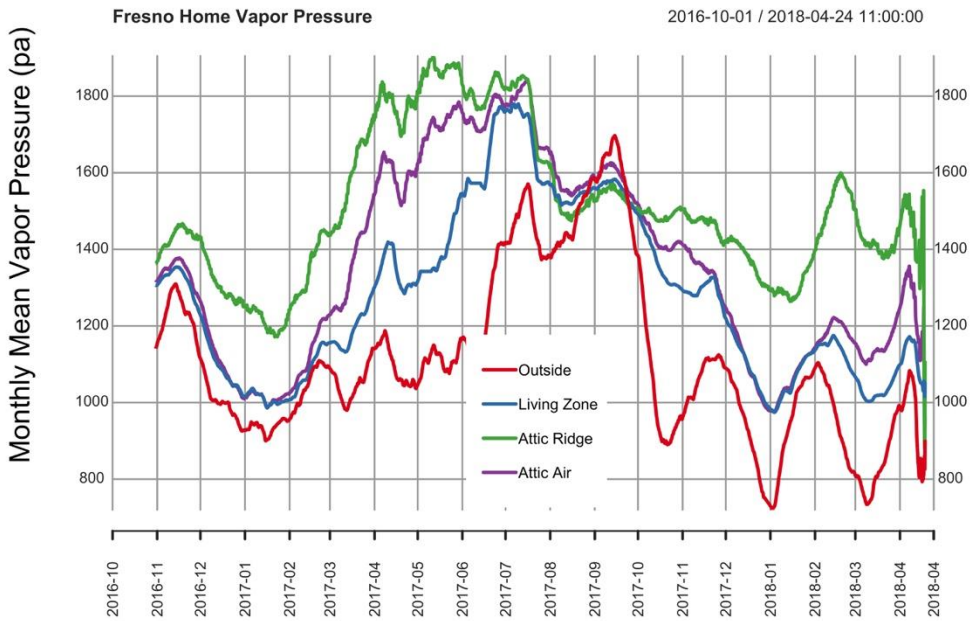

Vapor pressure time-series are plotted for the EW26N attic in the Clovis test home for summer and winter in Figure 79 and Figure 80, respectively, and the monthly mean vapor pressures are shown in Figure 81. As in the Fresno test home, there is evident ping-ponging of water vapor from the OSB roof deck to the attic air and back during the summer, while the winter is characterized by daytime vapor pressure peaks at the ridge sheathing and little difference at nighttime. In the rolling monthly mean plot, we note that once again the ridge sheathing has the consistently higher vapor pressure, while the outside vapor pressure is lower than indoors once occupancy begins in September. The attic and living zone vapor pressures are quite similar, once again with a short-term increase in the attic air vapor pressure during early spring. While during the peak winter months, the living space vapor pressure is marginally higher than in the attic, suggesting the living space could be a source of moisture for the attic.

Figure 79 EW26N Clovis. Vapor pressure during the summer at the attic peak, attic air, living space air and outside.

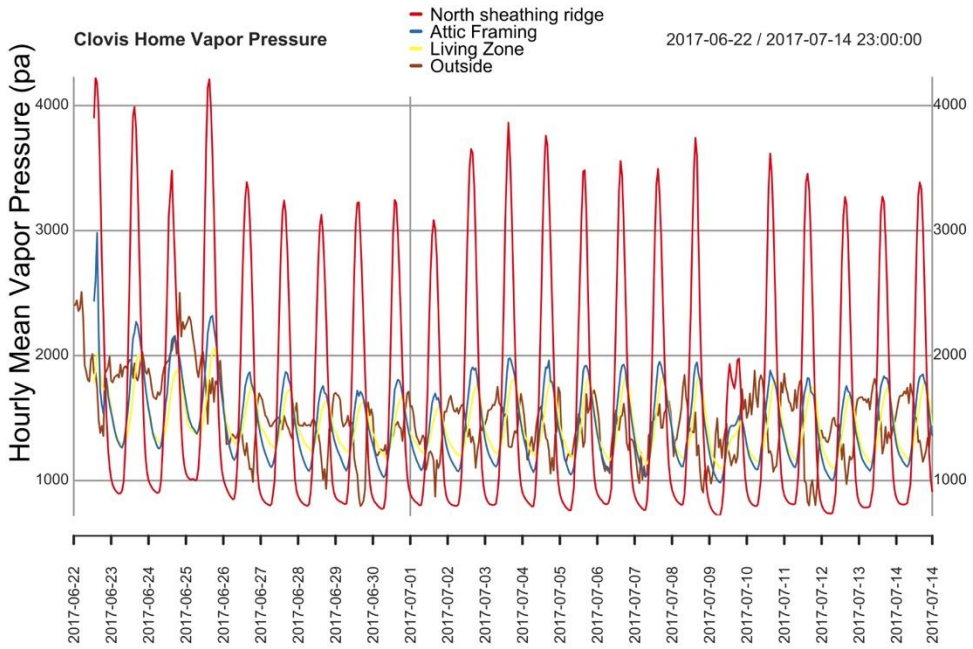

Figure 80 EW26N Clovis. Vapor pressure during the winter at the attic peak, attic air, living space air and outside.

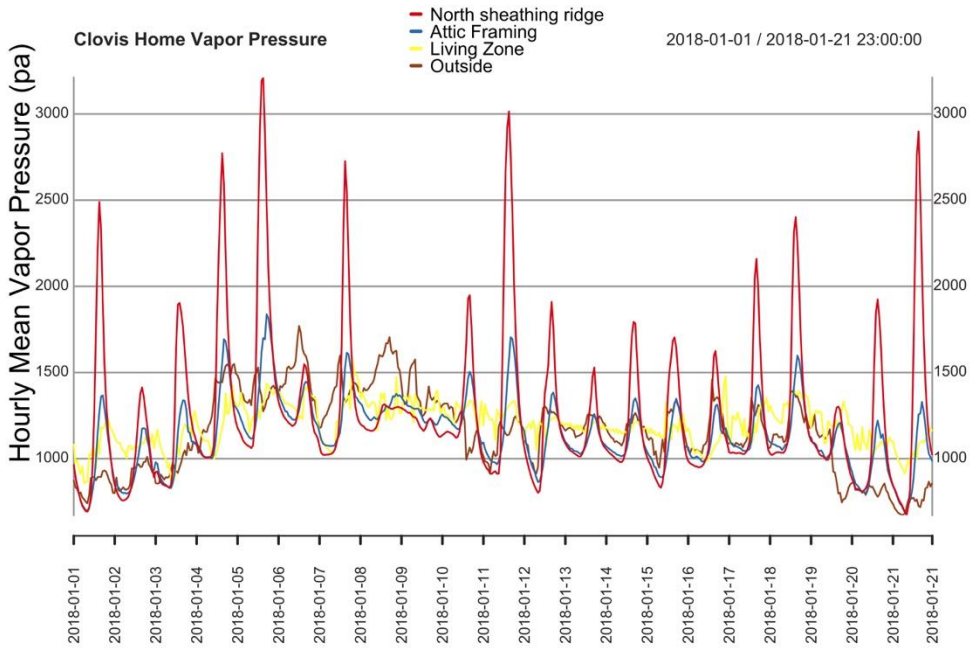

Figure 81 EW26N Clovis. Monthly average vapor pressure at the attic ridge OSB, ridge blocking, attic air, living space air and outside.

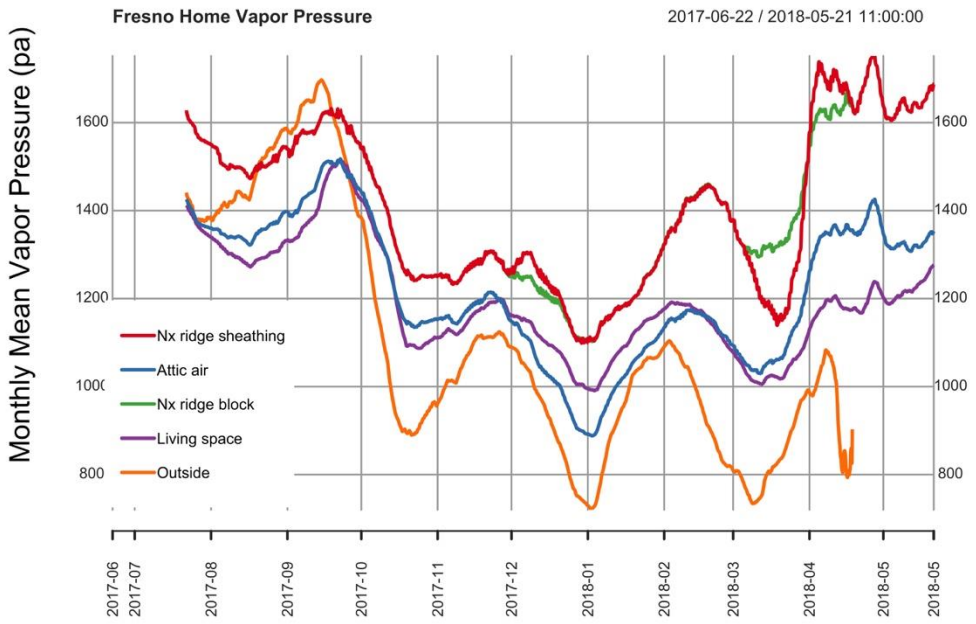

5.3.8 Vapor Pressure Differences, Attic vs. Living Space and Outside

In order to more clearly demonstrate the trends in monthly vapor pressure in the attic relative to the living space and relative to outdoors, we show monthly boxplot distributions of vapor pressure differences for the Fresno EW52 attic relative to outside (Figure 82) and the living space (Figure 84). With the sole exception of August, more than 50% of hours each month have vapor drive from the attic air to outside, and in most months, outside vapor pressure is higher than the attic for less than 25% of hours. The attic vs. living space vapor pressure differences are smaller overall, and the greatest vapor pressures differences occur in March through May, when the attic air is more moist than the living space air. As noted previously, we believe this is the result of seasonally stored moisture being baked out of the roof deck, as it warms and solar gains increase.

The Clovis EW26N attic monthly boxplots are shown in Figure 83 for attic vs. outside, and in Figure 85 for attic vs. living space. Overall vapor pressure differences between the attic and outside are smaller in the Clovis home, which is consistent with its greater levels of leakage area to outside (see Section 5.1). But the attic remains, on average, more humid than outside. Consistent with this, the living space vapor pressure is higher than the in the attic 50% or more of the hours in each month. Yet, overall, the living space and attic are very similar, with slightly positive mean annual values (29 pa, attic more humid than living space) and slightly negative median values (-47 pa, living space more humid than attic).

Given these monthly boxplot summaries and the average presented in the prior section, a few items become clear. First, the outside air is a source of potential drying for the living space, attic and roof deck, which means that outside air ventilation or diffusion venting should be beneficial. Second, during most of the year, the living space and attic air volumes have similar moisture contents, except in spring, when the attic air is humidified relative to the living space air; we hypothesize due to seasonal drying of stored moisture in the roof deck. Given these measured trends, we expect that intentional mixing of the living space and attic to have little impact on moisture levels in either space, except during spring, when mixing could facilitate drying of the attic air, or if this intentional mixing of the living space and attic also increased mixing in the attic air volume itself, reducing differences between the weighted attic air conditions and the conditions at the roof ridge.

Figure 82 EW52 Fresno, monthly vapor pressure difference boxplots between EW52 attic and outside air.

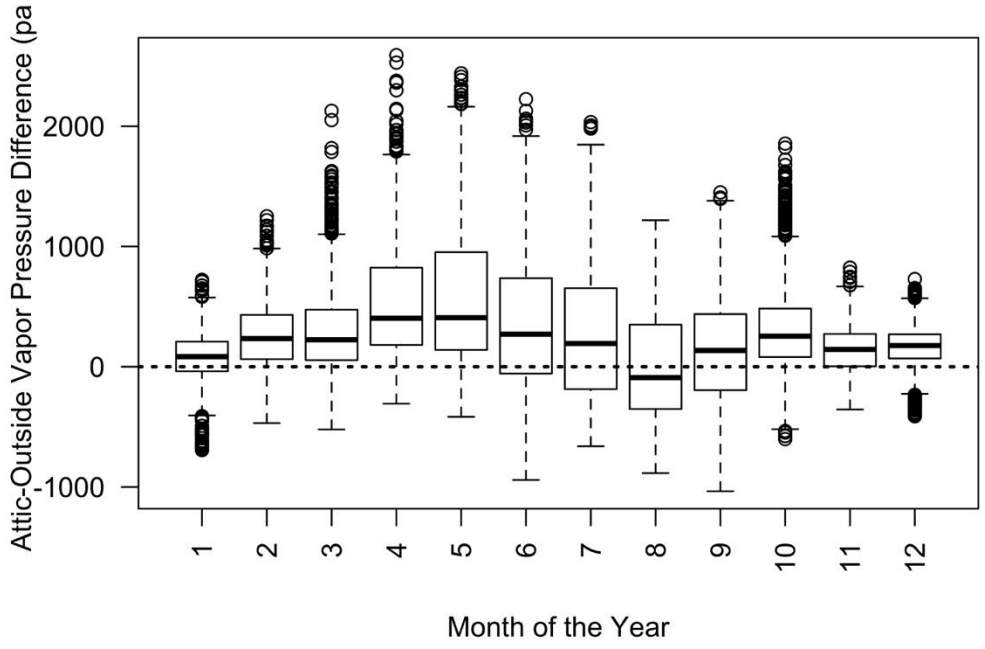

Figure 83 EW26N Clovis, monthly vapor pressure difference boxplots between EW26N attic and outside air.

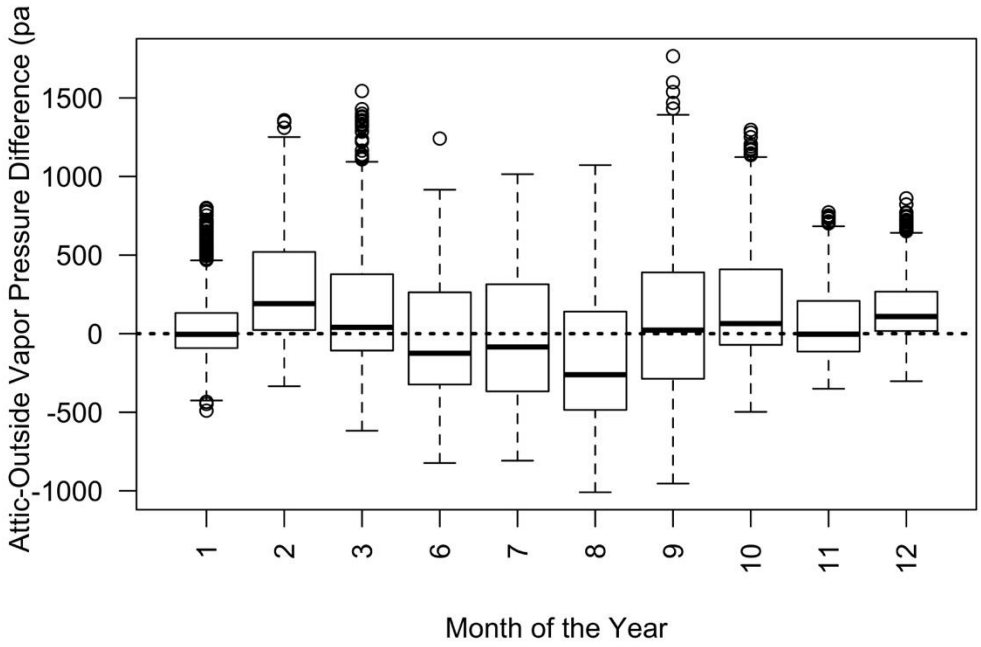

Figure 84 EW52 Fresno, monthly vapor pressure difference boxplots between EW52 attic and the living space air.

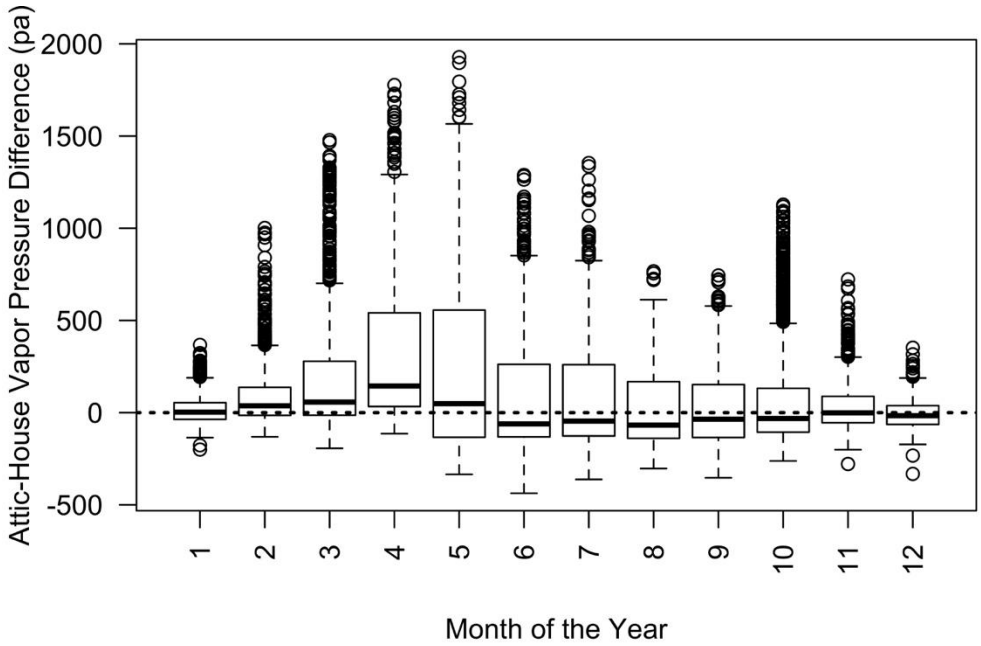

Figure 85 EW26N Clovis, monthly vapor pressure difference boxplots between EW26N attic and the living space air.

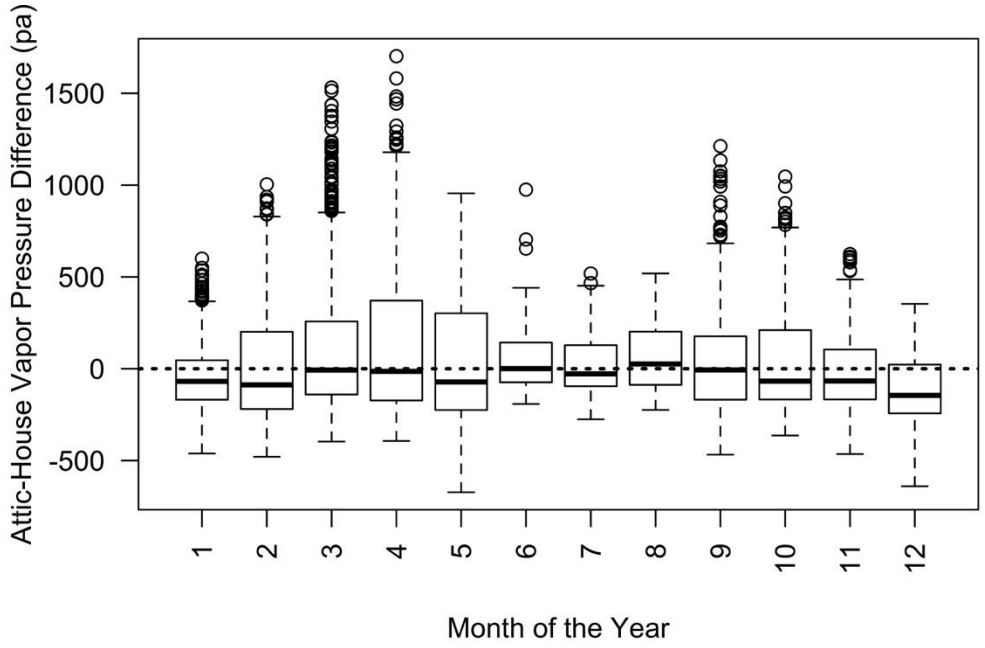

5.4 Energy Performance

HVAC energy consumption was monitored continuously in each sealed attic test home, though there is no similarly situated vented attic with which to compare energy use. The two test homes are discussed individually below in terms of their heating gas or electricity consumptions and runtime fractions for the furnace, cooling compressor and the central air handling unit (AHU).

5.4.1 Clovis Test Home

Overall, total HVAC energy use of 8,131 kWh was quite evenly distributed between the cooling compressor (2,884 kWh), the HVAC blower (2,806 kWh) and the gas furnace (2,441 kWh). HVAC system runtimes over the monitoring period were 2.6% for heating and 24.6% for cooling. The HVAC blower operated continuously, which means that 72.8% of its operation was during non-heating or cooling hours. This standby operation of the HVAC blower used 1,788 kWh (62% of total blower energy use). Total standby for the blower and compressor combined was 1,947 kWh or 24% of measured HVAC energy use.

The Clovis test home's monthly heating and cooling runtime fractions in Figure 86 illustrate that there is considerable air conditioning in this home from July-September and heating in December-February.

The results in Figure 87 show that the compressor energy increases as outside temperature increases, with peak hourly compressor power use of 2,820 watts. Most of the results fall in a consistent band. The peak data are from times when the multi-speed compressor was in high speed mode. The data below the band are from hours where

there was partial runtime. The compressor power consumption is not zero during non-cooling periods, due to the requirements of the HVAC system controls. We used a threshold of 100 watts of power consumption as the change point between standby and cooling operation. Compressor standby mode accounted for an estimated 6,271 hours out of 7,990 monitored hours, with an estimated standby energy use of 158.1 kWh, while the active cooling period used 2,718 kWh. The standby power for the compressor increased as outside temperatures decreased, suggesting some of this may due to a crankcase-heating element. With this approach to estimating standby time, we estimate the cooling runtime during the monitoring period was 21.5%. If we instead use the one-minute data and keep the 100-watt threshold for standby vs. cooling, the cooling runtime estimate is reduced to 15.5%, while standby energy use drops to 157 kWh and active cooling to increases to 2,726 kWh.

The diurnal compressor runtime for each month is shown in Figure 88 and compressor power is shown similarly in Figure 89. The hourly runtime plots show that during cooling months, runtimes are between 20 and 100% for every hour of the day. In the peak cooling months, the runtime fraction is at or near 100% from noon to midnight. Notably, this does not mean the compressor is working at maximum capacity during these hours, rather it is simply running continuously at a non-zero level. Figure 89 shows the compressor power use diurnally for each month, along with the peak power use of 2,820 watts, and we see that the hourly mean values are well below the peak capacity.

Figure 86 Clovis test home, HVAC runtime by month of the year, furnace and compressor.

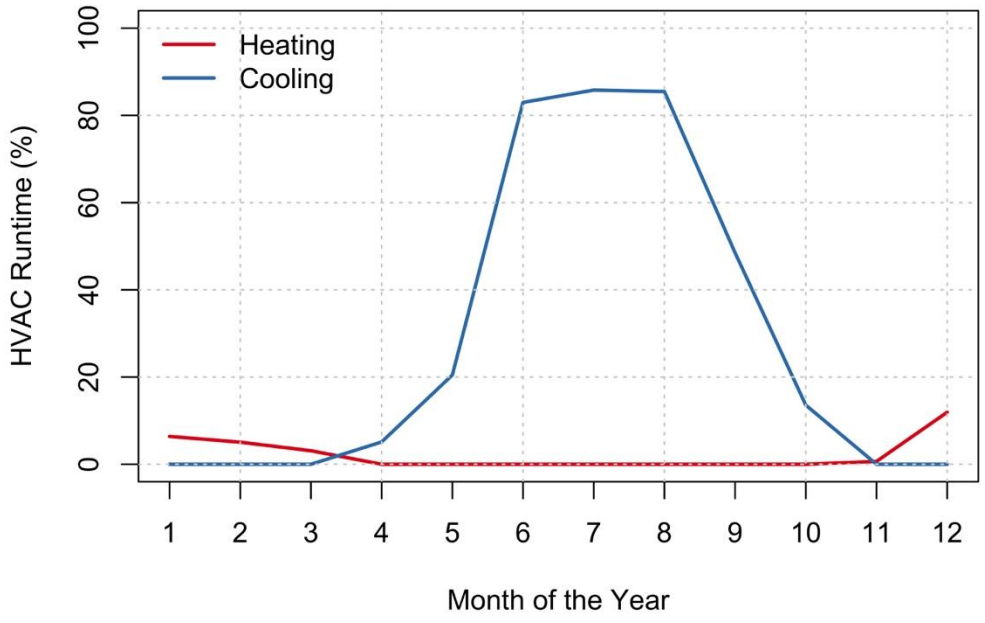

Figure 87 Clovis test home, hourly compressor power use vs. outdoor dry-bulb temperature, by compressor status.

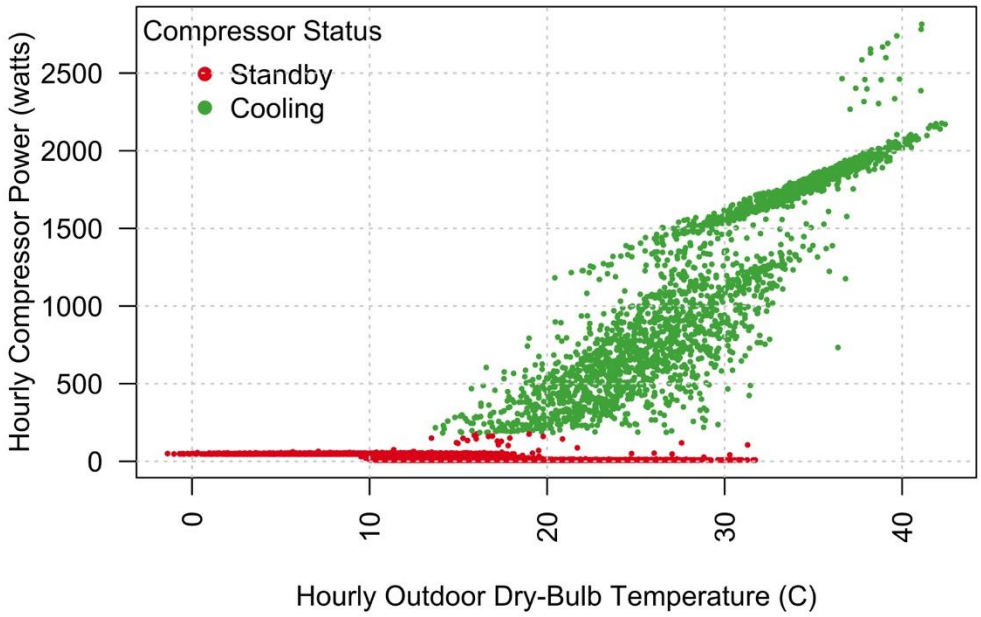

Figure 88 Clovis test home, compressor runtime by hour of the day, for each month of the year.

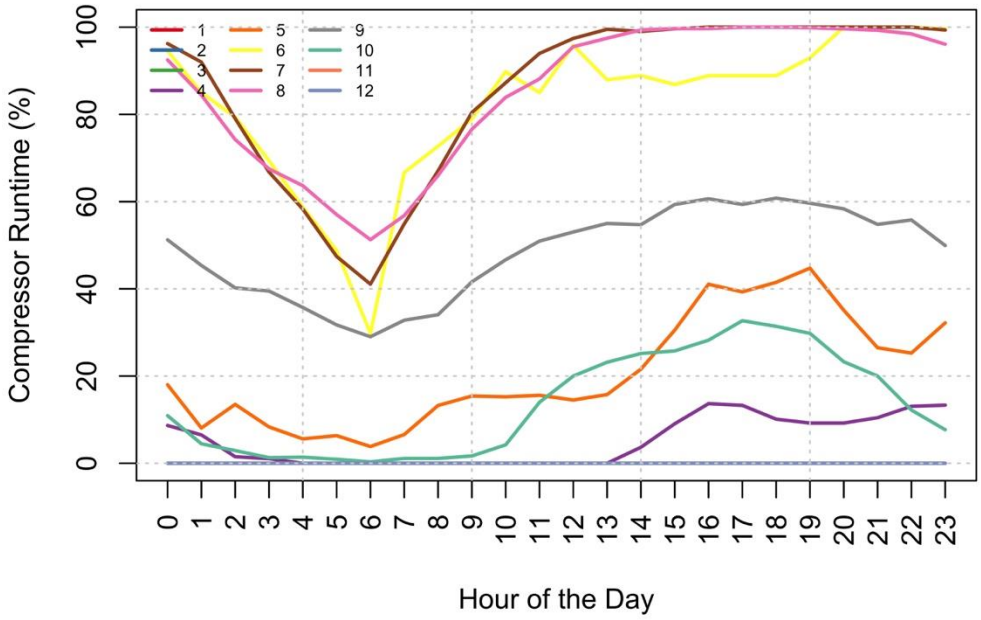

Figure 89 Clovis test home, mean compressor power consumption by hour of the day, for each month of the year.

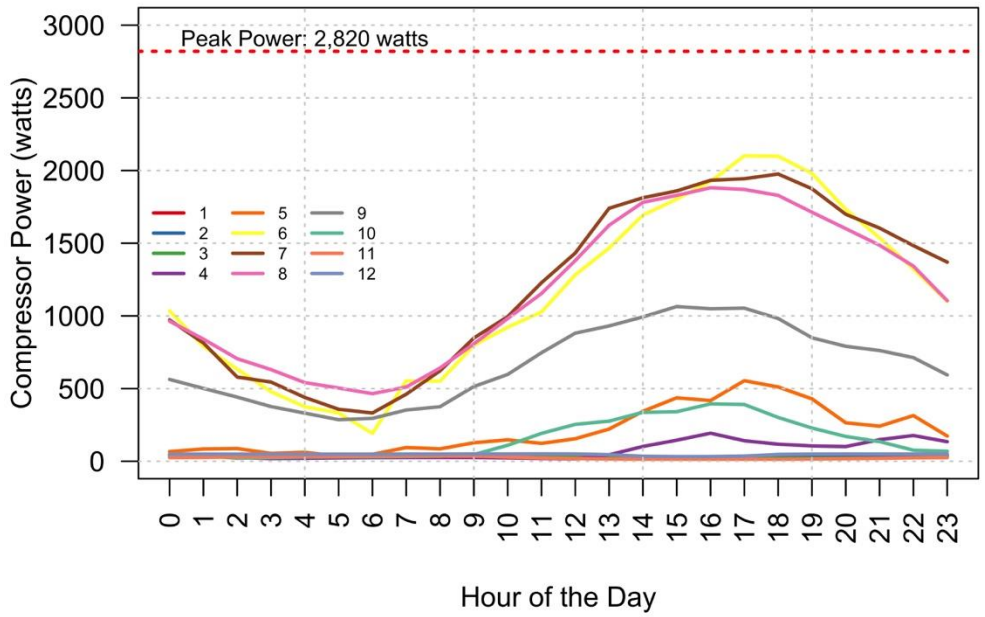

In Figure 90 the gas furnace shows very different behavior in response to outside dry-bulb temperatures compared to the cooling system. There is increasing consumption during colder hours, though the relationship is clearly less clean than in cooling. As expected, the gas furnace has no standby gas consumption, and we estimate total consumption for heating energy at 2,441 kWh (83.3 therms).

The heating system runtime shown in Figure 91 was determined from the difference between supply and return air temperatures. Heating was recorded for time steps when the supply air temperature was 2˚C or more above the return air temperature. The total heating runtime is estimated at 2.1% of the monitored time period.

Figure 90 Clovis test home, hourly gas furnace energy use vs. outdoor dry-bulb temperature, by furnace status.

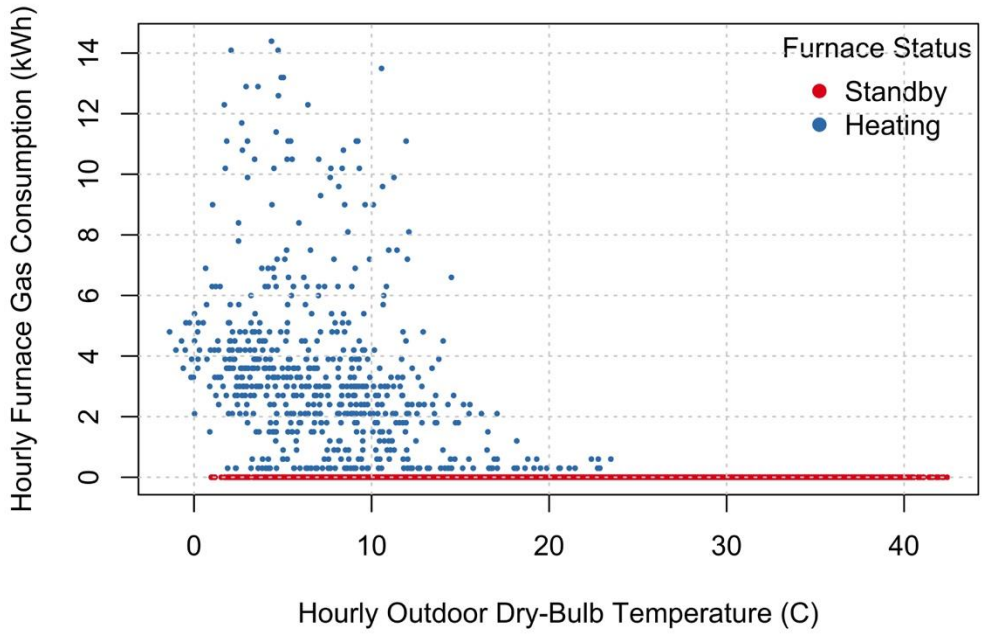

Figure 91 Clovis test home, gas furnace runtime by hour of the day, for each month of the year.

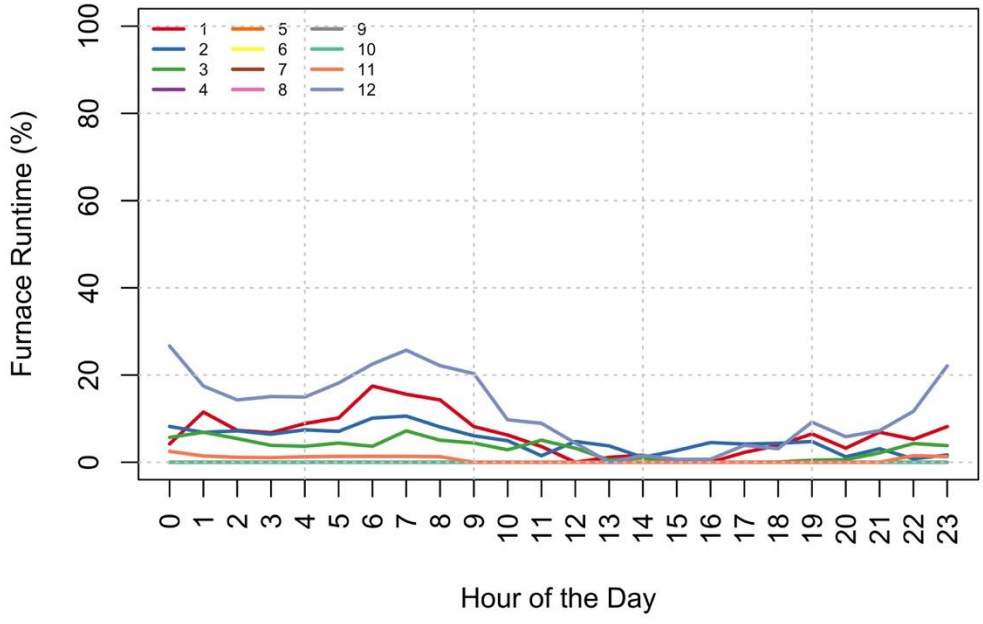

The HVAC blower fan was operated continuously for the purposes of mixing the indoor air as indicated in the diurnal monthly fan power in Figure 92. Note that the continuous fan operation is intended to be part of a central fan integrated supply system, but we could not identify any outside air duct into the system, despite reports by the builder

that one existed. Total HVAC blower energy use was 2,808 kWh. Mean hourly blower power consumption was between 300 and 400 watts, with distinct afternoon increases in power use during peak cooling periods in the summer months up to roughly 1 kW. Blower power in heating mode was quite similar to that used during recirculation/mixing hours, so no evident increase is shown during the nighttime hours of the heating season months. The majority of blower fan energy use was used for mixing indoor air during non-heating/cooling hours. We estimate blower energy use purely for mixing (and, potentially, ventilation) was 1,788 kWh, while blower fan energy during cooling and heating were 878 kWh and 104 kWh, respectively.

Figure 92 Clovis test home, mean HVAC blower power consumption by hour of the day, for each month of the year.

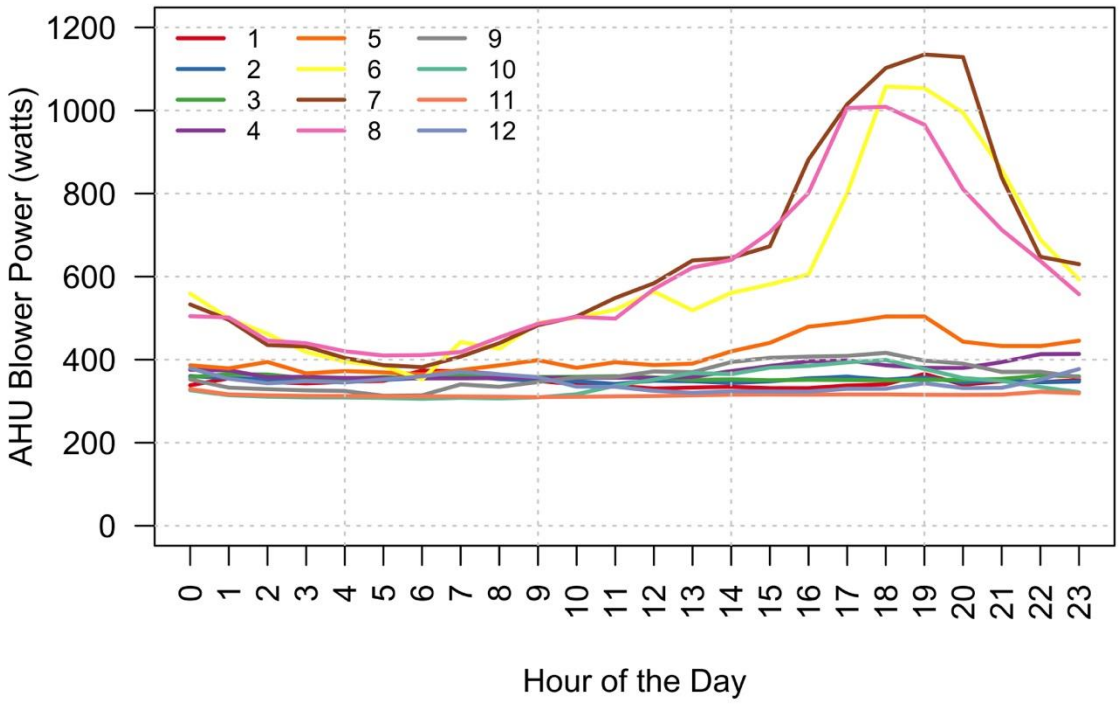

5.4.2 Fresno Test Home

The Fresno test home energy monitoring occurred between November 2016 and April 2018; we report here the consumption values for the 2017 Calendar year. Total heating, cooling and AHU energy use was 6,021, 3,477 and 1,429 kWh/year, for a total measured HVAC energy use of 10,927 kWh in 2017. We estimate that 10% (1,089 kWh) of total HVAC energy was used in standby or recirculation modes.

Estimated HVAC system runtime fractions are shown for each month of 2017 for heating and cooling in Figure 93. Heating season (November – February) runtime fractions varied between roughly 10 and 40% of monthly hours, while cooling runtime fractions were higher in peak cooling months (May – October) between 40 and 80% of

hours. The compressor hourly runtime fractions are shown for each month of the year in Figure 94 (hourly cooling power in Figure 95), and the heating hourly runtime fractions are shown in Figure 96. Hourly furnace and compressor energy use is shown against hourly outside temperature for reference in Figure 98 and Figure 99, respectively. Cooling runtime fractions were at or near 100% during many hours in the peak months of August and September, and through all summer months, peak hourly runtimes were in the 60-90% range. As noted in the Clovis home data, even though cooling runtimes are high, the power consumption for the compressor varies substantially between months and hours, because of its variable capacity. A clear cooling setback occurred between roughly 7am and noon in the cooling months, characterized by a drop in runtime fractions during those hours. Heating hourly runtime fractions were noticeably highest in December, as opposed to the other heating months of November and January. Heating operation was concentrated in two periods. First, in the early morning—presumably to recover from a nighttime thermostat setback—and second, in the early evening, possibly when occupants returned home from work (and before the nighttime setback began).

Again, as in the Clovis test home, the compressor energy use was almost never 0, due to the crank case heater and other energy consuming components. We estimate that 89% (3,101 kWh) of total compressor energy use was for active cooling, while the remaining 10.8% (377 kWh) was used in standby mode. We suspect the crank case heater drives this, as the energy use during non-cooling periods increases in the heating season and decreases in the warmer months.

Figure 93 Fresno test home, HVAC runtime by month of the year, furnace and compressor.

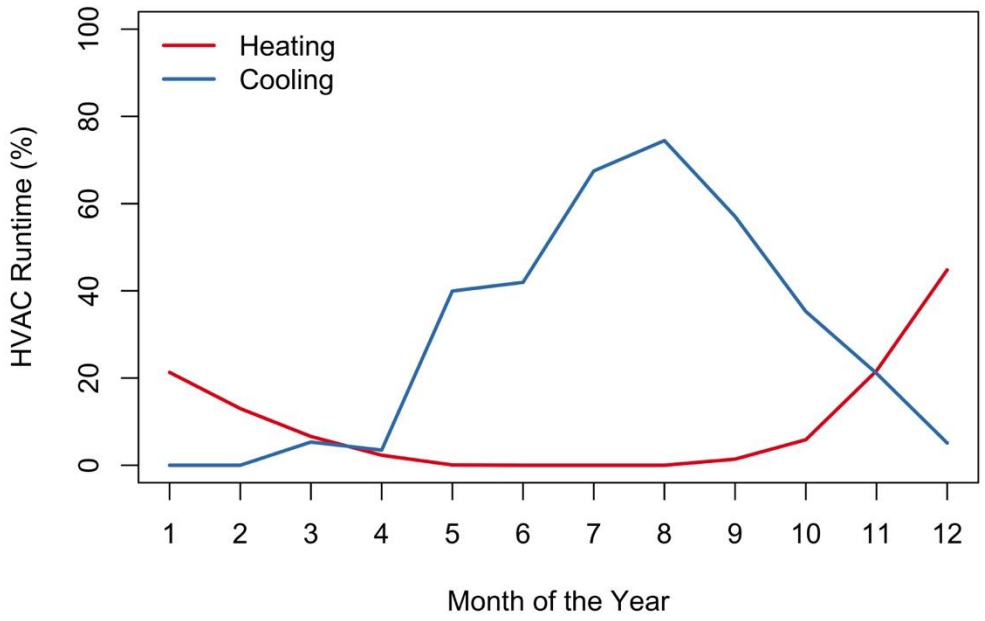

Figure 94 Fresno test home, compressor runtime by hour of the day, for each month of the year.

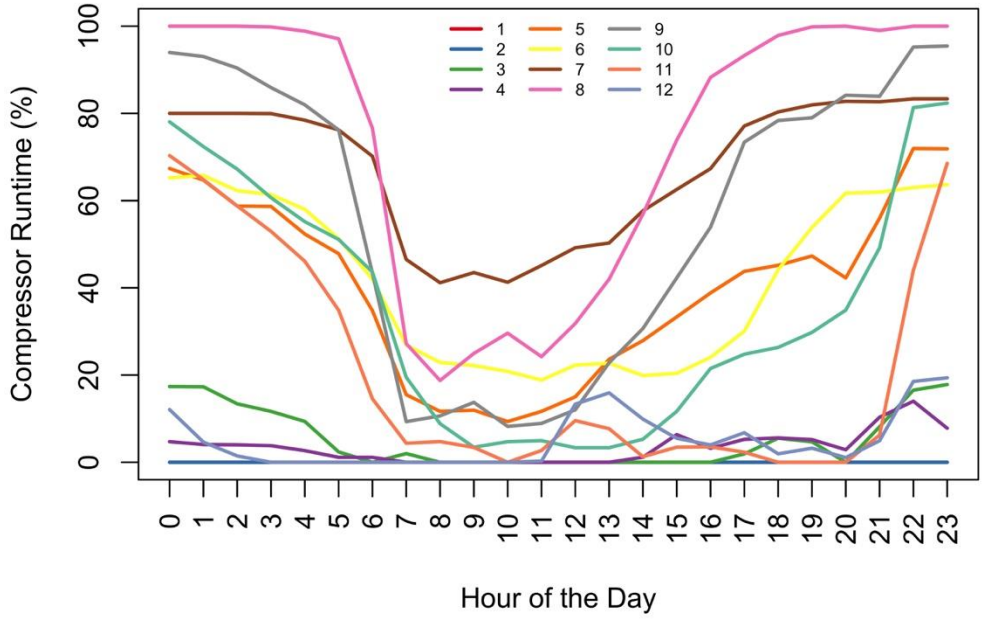

Figure 95 Fresno test home, mean compressor power consumption by hour of the day, for each month of the year.

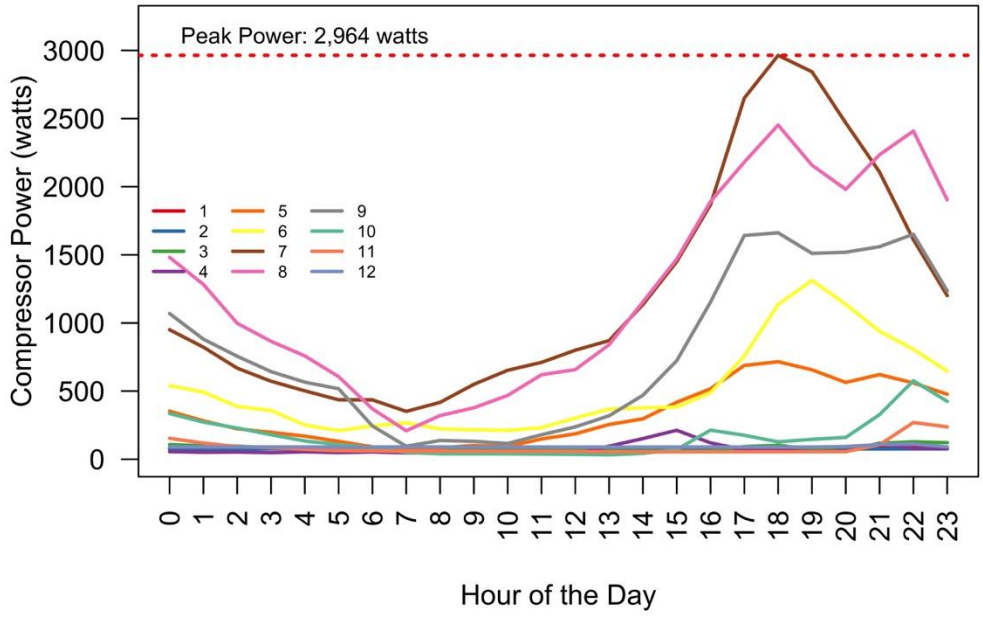

Figure 96 Fresno test home, gas furnace runtime by hour of the day, for each month of the year.

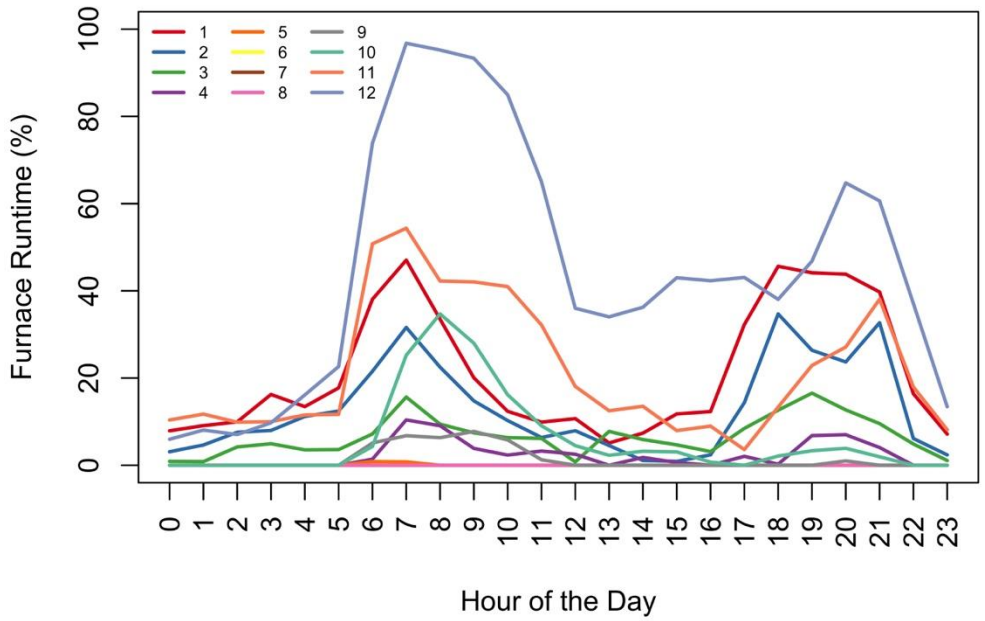

As in the Clovis test home, the Fresno home's AHU operated continuously at a low-speed, and we estimate the blower energy consumption during recirculating, heating and cooling periods. The fraction of blower energy use during each period was 46% (668 kWh) in recirculation, 37% (537 kWh) in cooling and 11% (155 kWh) in heating, with a remaining 6% (84 kWh) without runtime attribution. Hourly mean HVAC blower power for each month of the year is shown in Figure 97. First, we note that during November and December, the blower does not appear to have operated continuously in recirculation mode, which may be the result of occupant or builder intervention/preference. During these months, an evident increase is visible in AHU fan power during the early morning heating runs (roughly 5am to noon). During cooling months, the peak AHU fan power consumption is coincident with the peak compressor power shown in Figure 95 for 18:00 - 19:00.

Figure 97 Fresno test home, mean HVAC blower power consumption by hour of the day, for each month of the year.

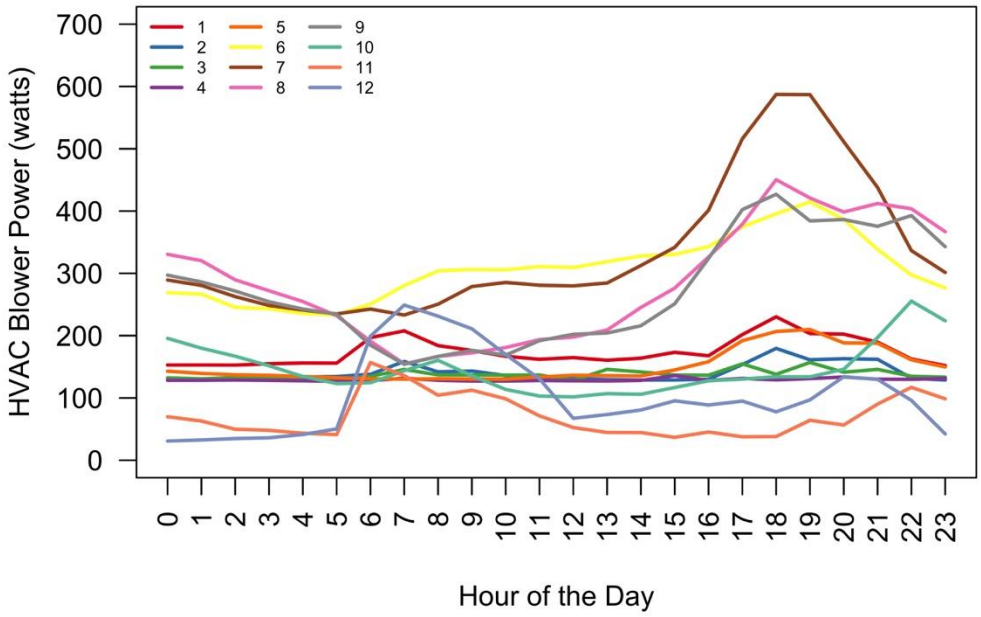

Figure 98 Fresno test home, hourly gas furnace energy use vs. outdoor dry-bulb temperature, by furnace status.

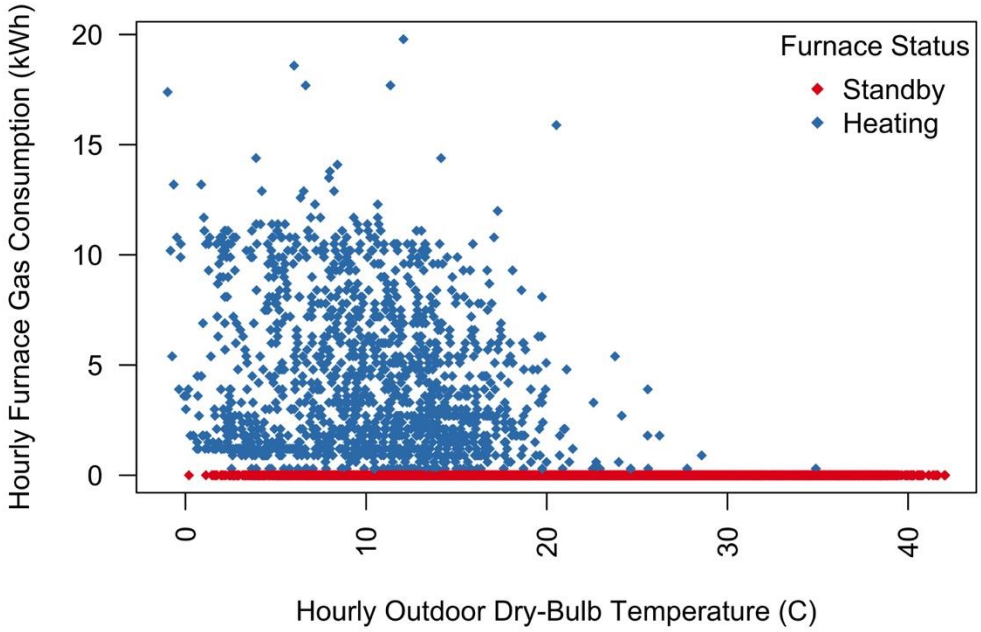

Figure 99 Fresno test home, hourly compressor power use vs. outdoor dry-bulb temperature, by compressor status.

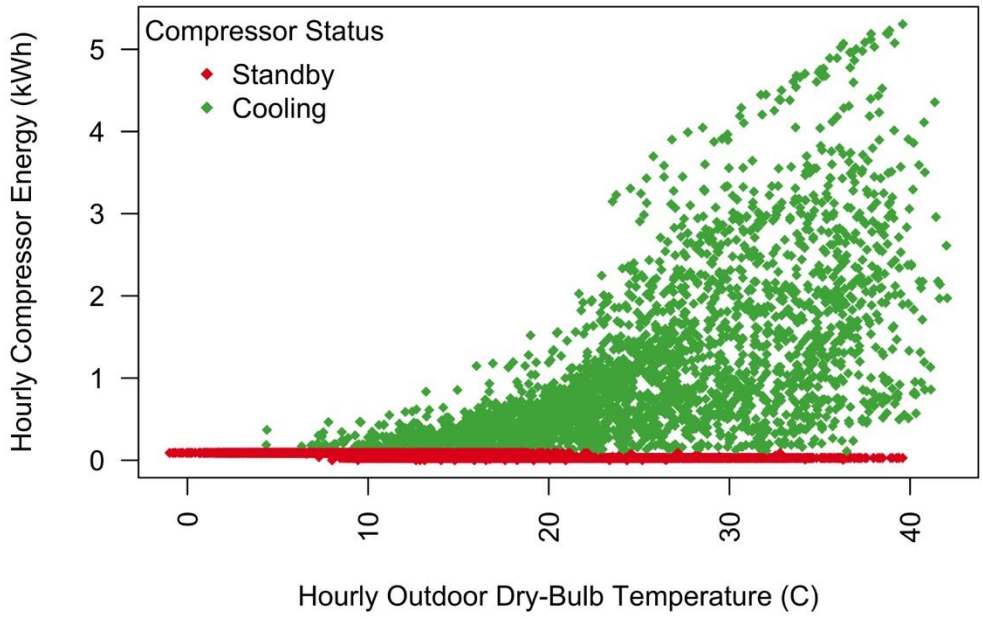

5.5 Summary of Field Study

5.5.1 Overall

- The sealed and insulated attics are the same temperature on average as the living space, such that they can be considered to be inside conditioned space from a modeling and T24 compliance perspective. But particularities of attic and house geometry, attic leakage, presence of HVAC equipment, and other factors can contribute to some sealed attics having widely varying thermal performance.
- Moisture risk at the North ridge sheathing is evident, and while mold index calculations predict safe assemblies, visual inspection revealed suspected mold growth in the Clovis home. This was particularly surprising, as the measured moisture parameters all appeared to be lower in the Clovis home. Measured wood moisture contents were in the safe range below fiber saturation at all measured locations. Current methods for predicting safe moisture performance in sealed attic assemblies may be inadequate to the complexities inherent in these assemblies, particularly when they are completely vapor and air permeable, as they were in this research.

5.5.2 Detailed Observations

- The construction approach to use foam to seal the attic had variable success. The Fresno attic was tighter than the home per unit of exterior surface area, but the Clovis attic was substantially leakier than the home.
- The glass fiber batt insulation performed as expected and thermally insulated the attic space from the roof deck resulting in average temperature differences between the home and the attic of less than 1˚C for the Fresno house and 2˚C for the Clovis house. The leakier Clovis home, with a higher

surface-area-to-volume and no HVAC equipment in the monitored attic, had much more variability between the attic and living space temperatures.
- Although temperature and moisture stratification was observed in the attics, it was very small during times of the year critical for moisture (i.e., in winter months and at nighttime) and therefore may not be a primary driver for moisture concerns.
- The attics were more humid than the living spaces and we observed the classic ping-ponging of moisture in and out of wood assemblies, because moisture leaving the wood is not vented away, as in a vented attic.
- From a moisture perspective, the critical location was at the roof ridge and for surfaces with lower solar exposure (North facing). This has been seen in other studies and indicates that future research studies and design specifications should focus on this location.
- Further study is needed to fully understand the moisture dynamics at play: for example, the coldest part of the roof deck was at the eaves, and yet this location did not display condensation or increase in wood moisture content.
- The Fresno test home has surface condensation (estimated at 23% of annual hours) and high surface wood moisture content (up to 26%) periodically at the roof ridge, but no surface mold or degradation upon visual inspection at the end of the test period.
- The Clovis test home showed less indication of high moisture levels at the measured ridge location – moderately high surface RH, no measured condensation and modest wood moisture content (maximum of 16.5%), but there was visible suspected mold on the inside of the North sheathing at the end of the field testing and other evidence of moisture, such as rusted roofing fasteners and raised OSB grain.
- Calculated mold index based on measured surface temperature and humidity was in the “safe” range at all locations in each test home, despite visible suspected mold growth on the North roof deck in the Clovis test attic.
- These results show the limitations of current moisture measurement techniques focused on wood moisture content, rather than potential for mold growth, and they also call into question the utility of the mold index as a metric for mold growth risk in sealed attic roof deck assemblies. They also indicate that our current field measurement metrics and equipment may be acceptable for determining the risk of wet wood and associated rot, but may not be adequate to predict mold issues with precision.

5.5.3 Implementation Challenges

We note some design, implementation and inspection issues with sealed and insulated attics. Some concerns apply to all sealed attic assemblies, independent of insulation type, while others are specific to fibrous insulation and batt installations.

- The need for careful design review and planning is universal. The failure that we observed to insulate the large garage ceiling that abutted the sealed attic in the Clovis home could occur in a home insulated with SPF, fiberglass or cellulose.
- Similarly, all sealed and insulated attic volumes should be accessible for inspection and potential remedial work, whereas a number of the Clovis home attic volumes are now completely inaccessible.
- Batt insulation may require additional quality control, such as the need to ensure that batts are installed and remain in direct contact with the underside of the roof sheathing.
- All insulation methods can be disrupted by other trades, but fiberglass batts hung in place may be uniquely susceptible to accidental disruption by plumbing

and HVAC venting and other activities. Inspection and review of the thermal boundary should be made after all other trades have completed their scopes of work.

- Similar to vented attic construction, the amount of insulation that is possible where the sloped roof intersects the above grade walls (at the eave) is limited. Raised heal trusses and other methods are commonly used in vented attics to increase insulation at this location, and the same should be done for sealed and insulated attics, to ensure their thermal boundary extends fully to the eave, as needed.

6 Simulation Study Methods

6.1 REGCAP Moisture Model

The REGCAP simulation tool was used to predict the performance of advanced attics in new California homes. The tool combines detailed models for mass-balance ventilation (including envelope, duct and mechanical flows), heat transfer, HVAC equipment and moisture. The details of this model have been presented elsewhere (Iain S. Walker, 1993; Iain S. Walker & Sherman, 2006; I.S. Walker, Forest, & Wilson, 2005). Two zones are simulated: the main house and the attic. Detailed hygrothermal calculations are performed for the attic air, wooden framing and roof assembly. REGCAP is implemented using a one-minute time-step to capture sub-hourly fan operation and the dynamics of cycling HVAC system performance. In order to capture longer-term moisture accumulation and mold risk, all simulations in this work are four-year periods, with one-year weather data repeated four consecutive times.

Critical model thermal and moisture assumptions include the following:

- No diffusion occurs between the roof and outside, moisture is exchanged solely between the roof sheathing nodes and the attic air and insulation nodes.
- The attic volume is a single, well-mixed zone, which ignores moisture and temperature stratification effects in the attic air volume.
- The sloped roof sheathing is represented by a single node for each orientation. Field evidence suggests that moisture accumulates at the roof ridge and less so along the mid-span and eave locations; however, the physical mechanisms that cause this are poorly understood and without a well understood physical process we have no practical way to include this localized effect in current modeling software[7].
- All cases assume a simplified roof geometry of two sloped roof surfaces, with vertical gable walls on each end. The ability to have pitched surfaces that have different orientations with respect to the sun has proven to be critical in previous simulations and field studies due to the strong effect of solar gains on attic thermal performance, e.g., the difference in moisture issues between north and south facing sheathing.
- Wood moisture calculations include separate surface and bulk wood nodes to better capture the moisture buffering of attic wood assemblies.
- Liquid moisture transport is ignored. This is not critical because attics rarely drain liquid moisture, and if they do the attic is heavily contaminated with large quantities of liquid moisture and will have failed by any reasonable criterion.
- Thermal effects of phase change in moisture are ignored. The magnitude of heat transfer due to phase change is negligible compared to the radiation, convection and conduction processes occurring in an attic space.
- The air flow network uses a mass-balance approach for the two zones (attic and house) that includes natural infiltration effects due to leaks distributed over the building envelope, mechanically driven flows (including duct leakage) and flows between the attic and home. This allows the model to include interactions between these effects and to track inflows and outflows separately as needed for the thermal and moisture balances.

[7] We analyzed the field data from this study to attempt to find some simple correlations between stratification and mean values but were unable to find a successful approach – even if only for the two attics we tested in the field. This remains a topic for future research.

- The thermal model has indoor temperature as an unknown (and a thermostat to control heating and cooling operation) and uses a true thermal balance rather than the forced loads approach used in most energy modeling software. This allows for correct interactions of natural and mechanical flows as well as thermal and moisture interactions with HVAC systems located in attics.

6.1.1 REGCAP Moisture and Thermal Network Nodes

The moisture and thermal network nodes estimated in the REGCAP model are summarized in Figure 100 and Figure 101, respectively. The moisture balance network contains 11 nodes, including house and attic air volumes, house bulk mass, insulation assembly nodes, and surface and inner wood nodes for attic bulk framing and two sloped roof deck sheathing surfaces. The thermal balance network contains 18 nodes, eleven from the moisture model, along with added thermal nodes for the attic gable wall, the attic floor (house ceiling), and sky-facing roof finish nodes.

Figure 100 REGCAP attic model moisture nodes.

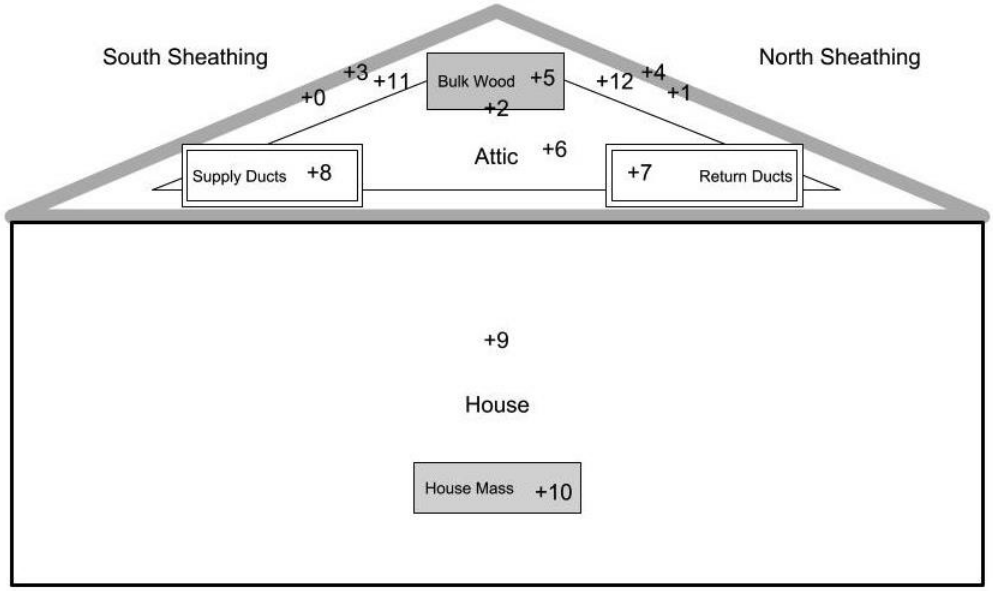

Figure 101 REGCAP attic model heat transfer nodes.

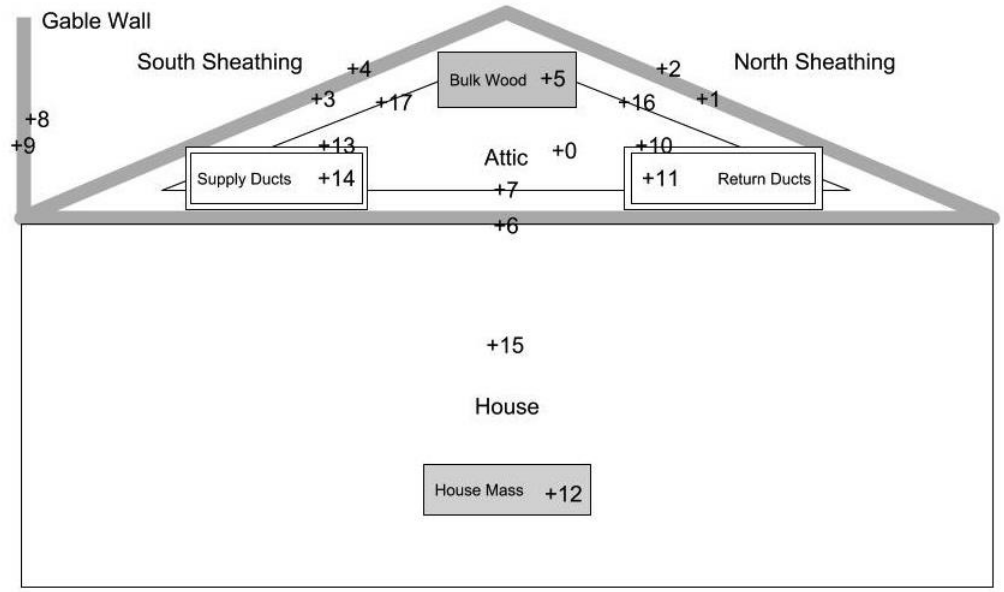

6.1.2 Verification of REGCAP Model Extensions Using Field Data

The REGCAP simulation model and its detailed attic mass, heat and moisture models have been validated in other contexts (Iain S. Walker, 1993; I.S. Walker et al., 2005), but these validations have focused on prediction of the performance of vented attics. The main goal of the verification step in this research is to confirm that REGCAP generates reliable results for predictions in advanced roof/attic assemblies in the context of new California homes. For this study we added nodes for assessing moisture transport through the insulated roof assembly, the key one being the tracking moisture diffusion through the insulation layer on the pitched roof surfaces. All of the fundamentals for this are already in place in the model, but additional nodes are required in the simulation to predict the complex roof assemblies used in unvented and HPVA assemblies.

We verified the REGCAP moisture model predictions for sealed and insulated attics by comparing measured sensor data from the Fresno test home against the REGCAP model predictions for the two-story CEC prototype home used in our parametric simulations. Crucially, these are not the same home, and they have different floor areas (2,700 ft^2 modeled vs. 3,605 ft^2 real), conditioned volumes, interior temperatures and moisture generation rates, exhaust fan schedules, etc. Furthermore, the REGCAP model includes no window opening, which we expect during mild times of the year in an occupied home. However, we attempted to select thermostat schedules and used our knowledge of occupancy to provide reasonable model inputs. Given these restrictions, the model verification is limited and we will focus on the predictions of surface conditions and wood moisture content. To facilitate more direct comparison, the monitored weather data for the 2017 calendar year was used in the REGCAP simulation, and the model moisture and thermal nodes were initialized at values that matched midnight on January 1st 2017 in the monitored sensor data for the Fresno test home.

Overall, it is worth nothing that the REGCAP model has much less moisture dynamics than the measurements. We believe this can be attributed to a much larger effective surface depth for the wood in the model, relative to the effective depth of the actual wood surfaces our instrumentation are mounted to. The model also averages thermal and moisture effects for the entire surface area of the roof deck material, whereas we know from our measured data that the thermal and moisture behavior vary substantially along the roof span and depending on location in the attic. Ultimately, the sensor vs. model node locations, and the way we are measuring vs. calculating moisture and thermal values are not perfectly comparable.

The thermostat schedule used in the REGCAP model was derived from the monitored data in the Fresno test home. The heating thermostat schedule was the hourly mean of the 2nd floor house temperature for the months of January, February, November and December of 2017. The cooling thermostat schedule used the months of May through September 2017.

We tested the REGCAP input files for two-story homes in CEC climate zone 13 that were to be used in the parametric simulation campaign. We selected 3 ACH_{50}, with 50% ceiling and attic leakage rates to align reasonably well with the physical characteristics of the actual Fresno test home. We then tried medium and high moisture gains, along with different IAQ fan airflows (None, 2008 Title 24 and current Builder Practice). The thermal predictions of air and surface temperatures were not noticeably affected by the moisture gains or fan airflows. The wood moisture content results were much more sensitive and we found that the combination of High moisture gain cases with a 2008 Title 24 exhaust fan was most similar to the measured results, and we will use that combination for the verification process described below.

6.1.2.1 Roof Deck Temperatures

The REGCAP model performed well in terms of predicting the temperature of the living space and attic volumes, along with surface temperature predictions at the roof deck locations. The seasonal variability is shown in Figure 102, and the modeled temperatures are typically within 1 or 2°C of the measured temperatures. The diurnal variability is shown in Figure 103, and the simulated and monitored roof deck temperatures are very similar at nighttime, but during the daytime hours, the REGCAP model predicts substantially higher roof deck temperatures than those measured at the field study home. The differences are greatest at the North roof deck, where the daily peak temperature in the REGCAP model exceeds the measured value by roughly 5°C. The South roof deck temperatures are closer aligned, though again the daily peak in the model exceeds that in the monitoring data by 2-3°C. The nighttime temperatures are critical for predicting surface relative humilities and wood moisture content at the roof deck, but the daytime values are still important.

Figure 102 Comparison of simulated (REGCAP) and measured (Fresno) roof deck surface, attic air and living space air temperatures, by month of the year.

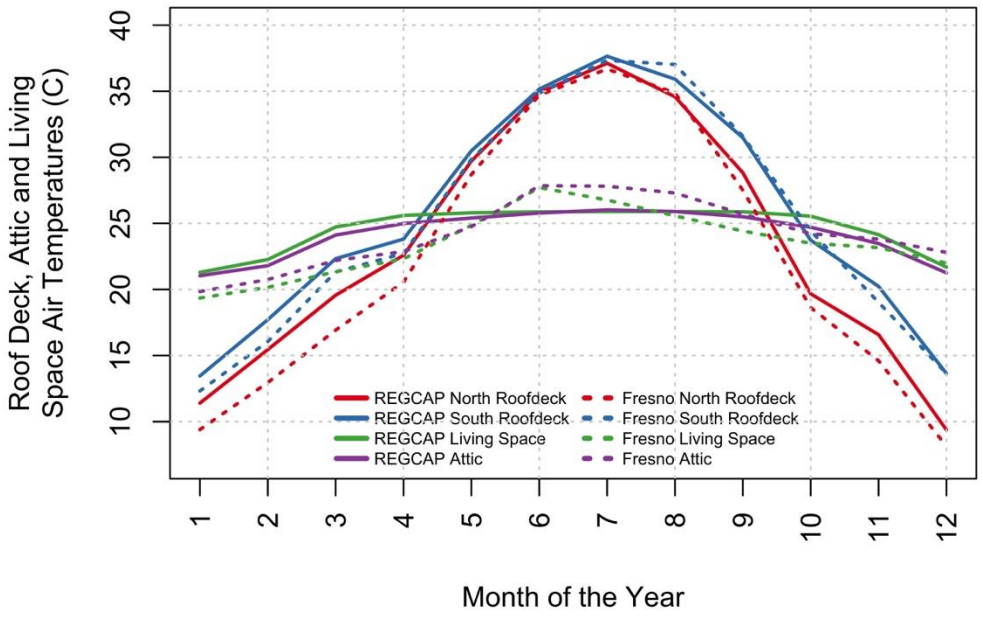

Figure 103 Comparison of simulated (REGCAP) and measured (Fresno) roof deck surface, attic air and living space air temperatures, by hour of the day.

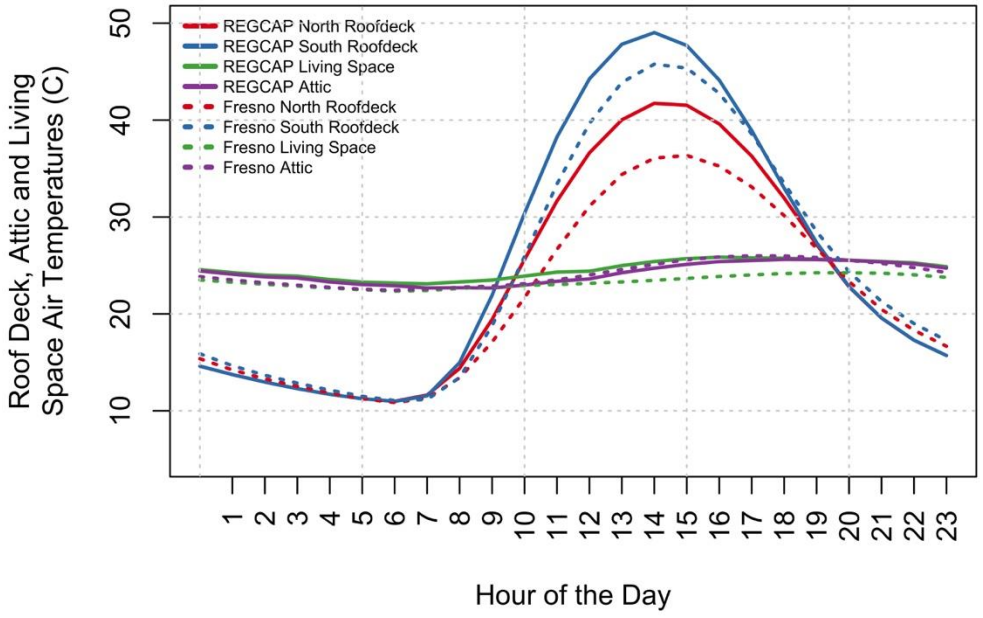

Time-series example plots are shown for the North roof deck in January 2017 in Figure 104 and the South roof deck in July of 2017 in Figure 105. These figures show how the model captures weather-induced dynamics of roof deck temperature. The thermal dynamics are extremely complex throughout the attic, varying spatially and temporally, and the REGCAP model consistently provides reasonable results.

Figure 104 January 2017 time-series plot of North roof deck surface temperatures in monitored and simulated Fresno home, including the mean surface temperature along the roof span at the insulation-roof deck interface, and at the bottom side of the roof tile at midspan.

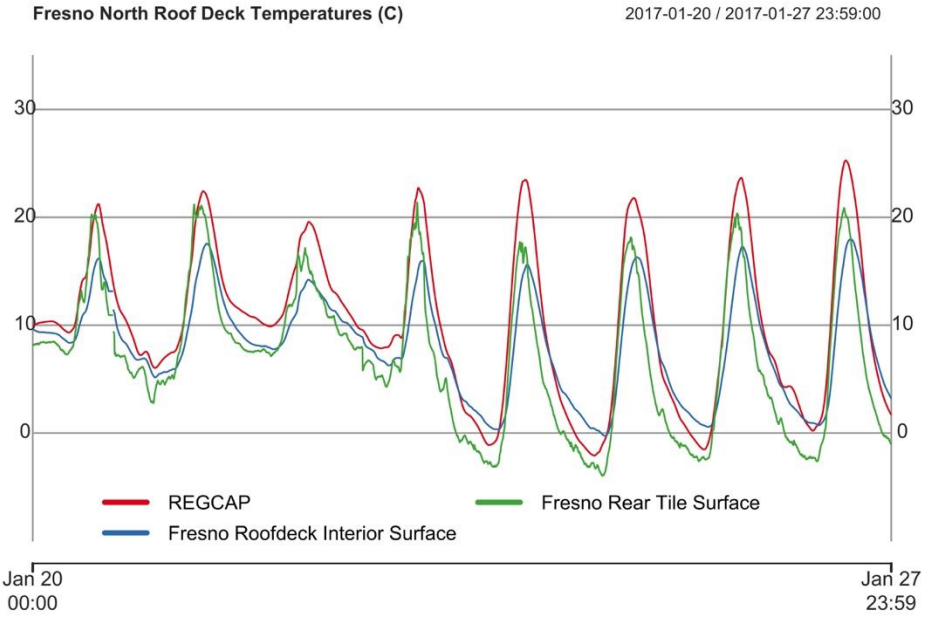

Figure 105 July 2017, time-series plot of South roof deck temperatures in monitored and simulated Fresno home, including the mean surface temperature along the roof span at the insulation-roof deck interface, and at the bottom side of the roof tile at midspan.

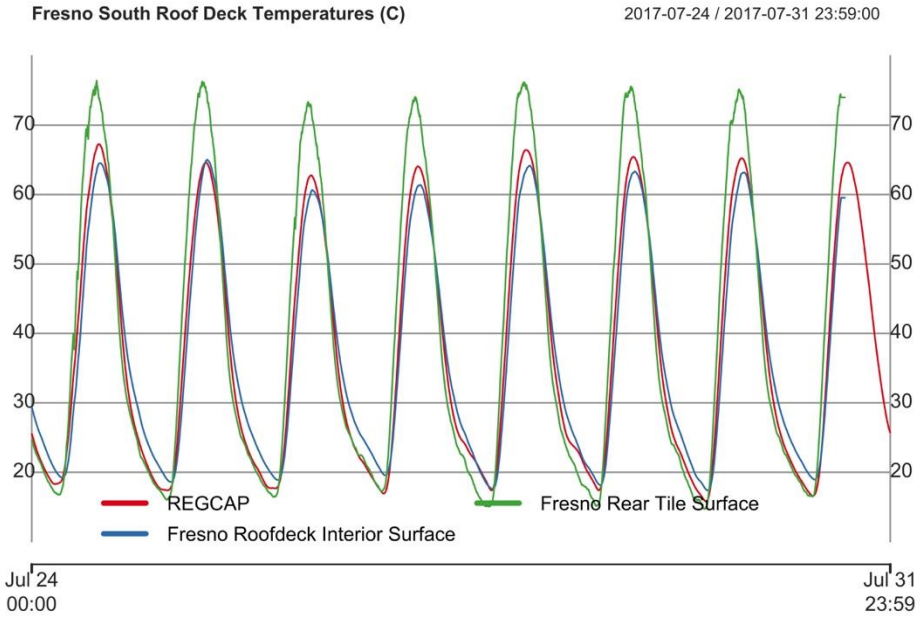

6.1.2.2 Wood Moisture Content

We show monitored and simulated wood moisture contents at the North roof deck surface in Figure 106 for the calendar year of 2017. The monitored results are shown for the ridge and eave locations on the North roof slope. The values begin the same, due to careful initialization of the moisture nodes in the REGCAP model. Both immediately decline in sync with one another, and their agreement remains reasonable through March. The values are not identical, but the trends and patterns are clearly matched in the simulations and monitored data, with up and down trends aligned in time, but not entirely in magnitude. At times, the model shows higher moisture contents, and at other times the monitored peaks are higher, which we hypothesize to be the result of surface condensation in the field study home. Both series show rapid drying beginning in March down to similar levels in April, and then the REGCAP model shows lower moisture contents during the entire summer cooling period. This under-prediction of moisture content during summer by the model is not very troubling, because both the REGCAP model and the WMC instrumentation have large uncertainties at dry wood conditions below 7%. It is better to say that both the measured and modeled results predict dry wood below about 7%. Beginning in November, the model predicts a rapid increase in the North roof deck moisture content, while the monitored data showed very little increase (in sharp contrast to the prior winter of 2016/2017).

Figure 106 Monitored and simulated North roof deck wood moisture content in the Fresno homes.

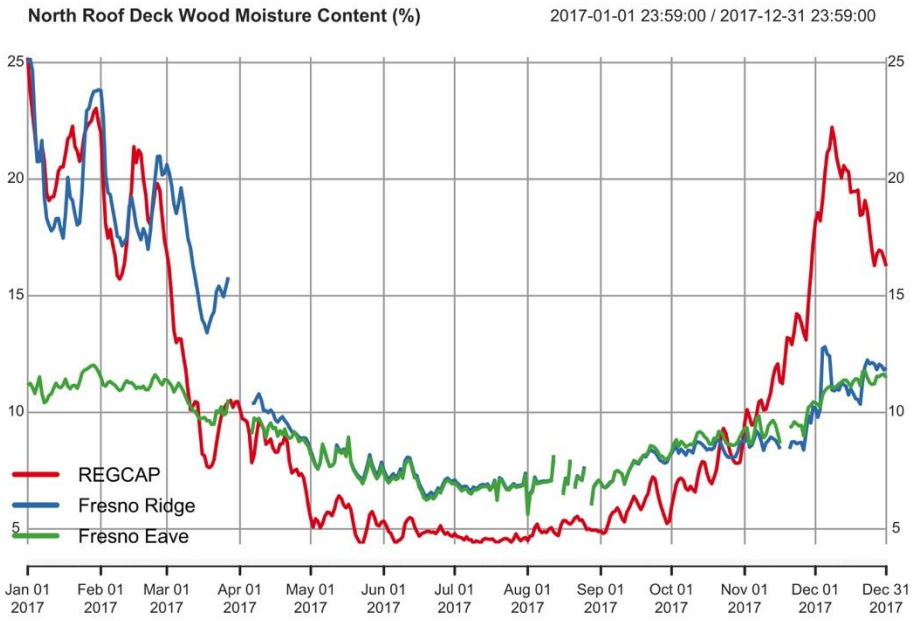

6.1.2.3 Surface Relative Humidity

We show weekly mean surface relative humidity for the south and North oriented roof slopes in the REGCAP model and the monitoring data in Figure 107, along with an indicator of Cooling system runtime in the REGCAP model. There is good agreement in North roof deck surface RH in the winter months, but during the summer the predicted RH is consistently low. The model

reflects the measured data showing that surface RH is higher at the North vs. South roof slopes. Similarly, the modeled and monitored data both show that surface RH are nearly identical between the two orientations during the entire summer cooling period from May through September. This shows that the model adequately captures the physical dynamics in this system, across seasons and orientations, even if the values are not in perfect agreement.

Figure 107 Monitored and simulated weekly mean roof deck surface relative humidity in the Fresno homes.

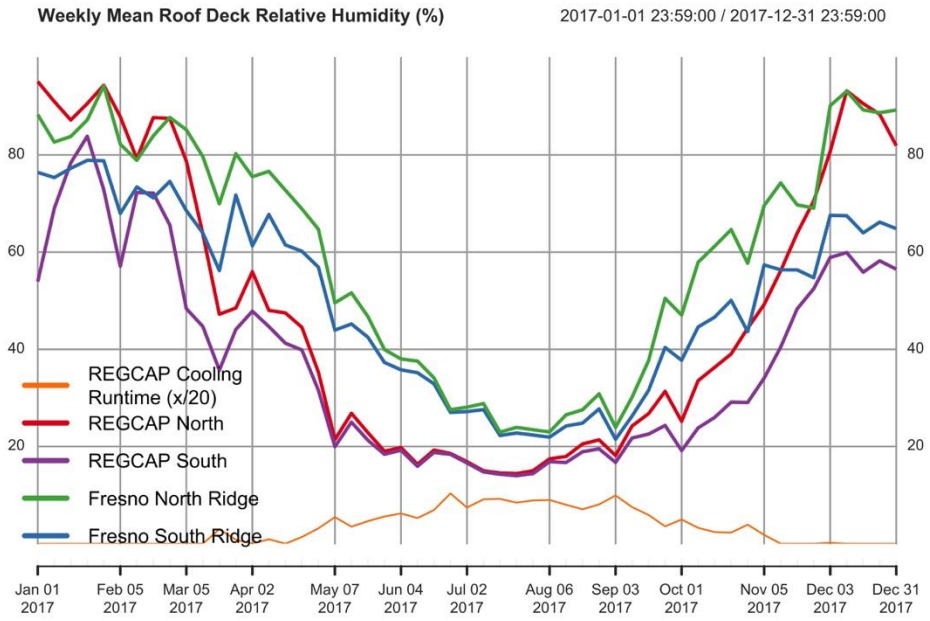

6.1.2.4 Mold Index

We show the monitored and simulated mold index values for this home, along with corresponding surface relative humidities, in Figure 108. Again, both values begin the same and increase in a nearly identical fashion until the end of February. The simulated surface RH values drop quickly below the critical 80% RH threshold, while the monitored data show continuing periods of RH exceeding the threshold, though not continuously. Accordingly, the monitored mold index reaches a maximum of 1.5 compared with roughly 1.2 in the 2017 winter. The same thing happens in the Fall when the surface RH in the monitored data stream increases more rapidly, often exceeding the 80% RH threshold. This stops the decline in the monitored mold index, which continues declining in the simulated data until roughly December 1st, when the simulated surface RH finally exceeds 80%. These results show how sensitive the mold index can be to patterns of simulated seasonal shifts in surface moisture, as well as to the dampening of surface RH that occurs in the model based on diffusion moisture transport. The surface RH values appear to agree quite well in this plot, yet their exact timing and up/down cycling has major impacts on the predicted mold index value. Given the REGCAP model's demonstrated tendency to exhibit less cycling of surface RH, as well as less time at saturation, we expect that the mold index may be under-predicted in the parametric simulations.

Figure 108 Comparison of monitored and simulated North roof deck mold index values, along with the monitored and simulated surface relative humidities.

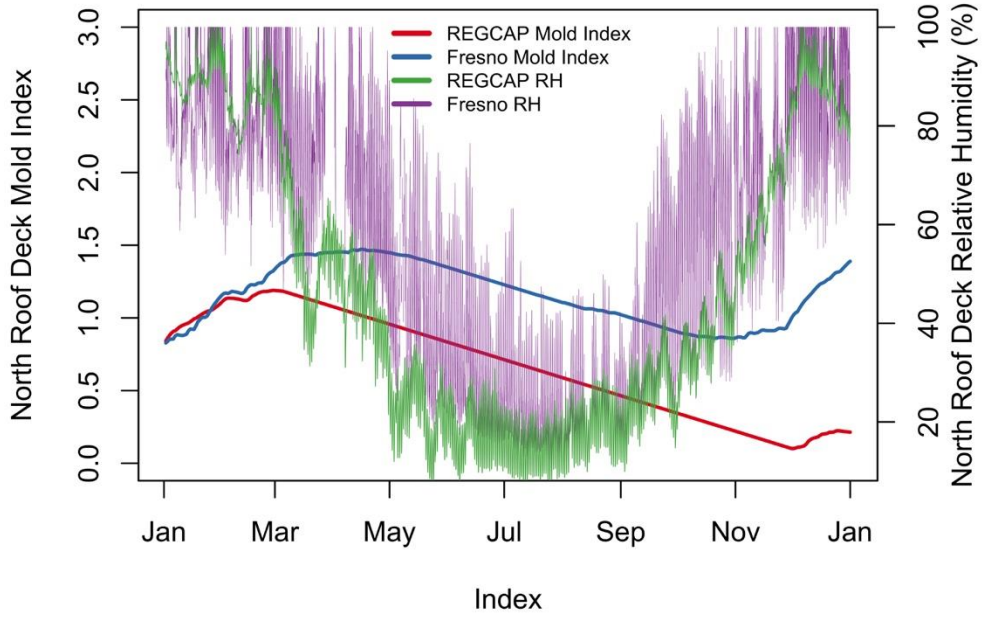

6.1.2.5 Roof Deck Vapor Pressure

North roof deck surface vapor pressure is plotted for monitored and simulated data for the month of January 2017 in Figure 109. We see very good agreement between monitored and simulated data in terms of the overall magnitudes and diurnal patterns of surface vapor pressure. During periods with substantial sky cover, the REGCAP model predicts higher vapor pressures by several hundred pascals at nighttime and up to 1,000 pa during peak solar hours. Conversely, when sky cover is minimal, and the night sky is clear and cold, the REGCAP model predicts lower North roof deck vapor pressures, again by 100-200 pascals. Daytime vapor pressures are very well-aligned during these clear sky periods. See Section 6.1.2.1 for a discussion of the temperature impacts of sky cover in the REGCAP model. Overall, the REGCAP model is better at predicting vapor pressures than relative humidity compared to the field data. This is likely a combination of the specific locations for relative humidity measurement (compared to spatially averaged value in the model) and simplifying assumptions about how the wood surface layer is modeled.

Figure 109 January 2017 time-series plot of North roof deck vapor pressure in monitored and simulated Fresno home.

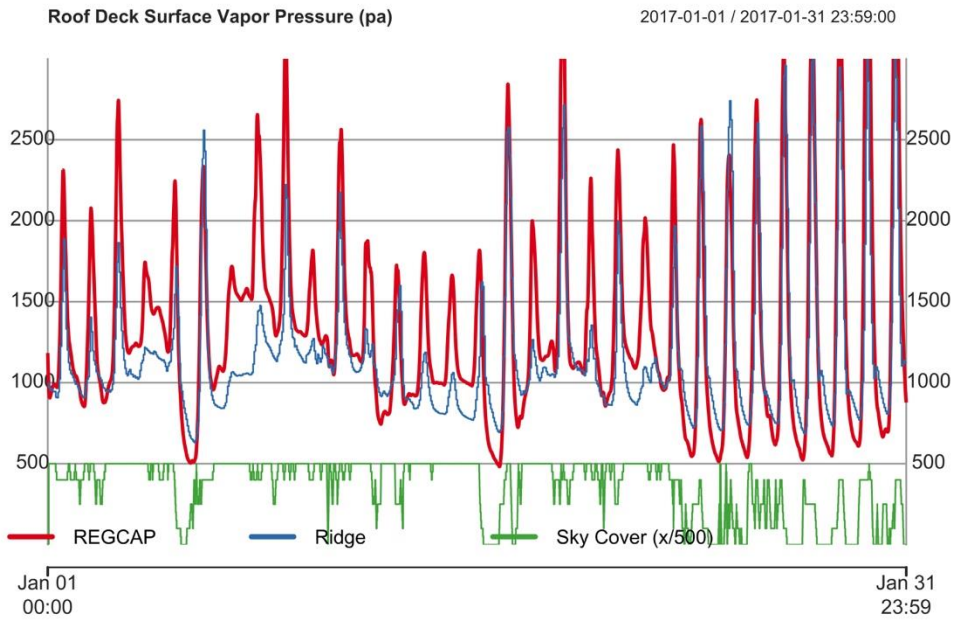

6.2 Parametric Simulation Parameters

We have selected a number of simulation parameters that are varied in this study, which reflect the expected ranges across the California new housing stock, while also fully exercising factors that affect moisture risk in these assemblies:

- Attic construction (vented, HPA, and sealed and insulated)
- House prototype (1-story, 2,100 ft^2 and 2-story, 2,700 ft^2)
- Climate zone (CEC Climate Zones 1 – 16)
- Envelope airtightness (1, 3, and 5 ACH_{50})
- Ceiling Leakage (20, 50 and 80% of whole house reference case leakage)
- Attic Leakage (20, 50 and 80% of whole house reference case leakage, with fixed living space leakage at 50% of whole house reference case leakage)
- Duct leakage (2, 5, and 8% of total system cooling airflow split evenly between supply and return ducts)
- Internal moisture gains (medium, 6.5 kg/day vs. high, 11.8 kg/day)
- IAQ ventilation fan sizing (None, T24 (2008), and current California building practice: T24 (2008) + 40%)
- IAQ fan type (exhaust vs. supply)
- Roof finish (tile vs. asphalt shingle)

To cover all combinations of the parameters we have identified would require a total of 93,312 simulations—an unmanageable amount. So, we target a reduced number using a process guided by identifying and investigating those scenarios with significant moisture risk, while still covering a wide range of potential new homes in the state. The simulation parameters are summarized by the counts for vented/HPA attics in Table 13 and for sealed and insulated attics

in Table 14. Overall, 2,632 cases were simulated, with 344 each vented and HPA, and 1,944 sealed and insulated cases.

To ease the total number of simulations, we have identified core values for most parameters (see the blue lettered entries in Table 14). These are, we believe, the most common and likely values for these parameters to take in new homes across the state. As such, the vast majority of cases use these core values, and when other parameters are varied, these core values remain fixed. For example, in order to assess internal moisture gains, we vary moisture gains between two options, while we fix house air leakage at 3 ACH_{50}, duct leakage at 5%, ceiling leakage at 50%, etc. Each of the parameters is described in further detail in subsections below. There are no core values for climate zone and house prototypes, as these are all simulated in all scenarios. In addition to these core characteristics, we also identified a set of values that would be used to assess moisture interventions. This was intended to exercise the critical parameters, namely IAQ fan sizing, internal moisture gains and climate zone, which cover the array of conditions that sealed and insulated attics face across new homes in the state.

Whenever we assess the impacts of a simulation parameter, we compare groups of simulations with the different parameter values. Many cases are filtered out in this comparison process, and only matching cases are included, which are identical to one another, aside from the specific parameter of interest. For example, when we assess the impacts of IAQ fan sizing on moisture risk, we exclude 984 cases and include only the 320 T24 2008 cases that are exact counterparts to the None and T24 2008 + 40% cases. This exact matching process allows a direct assessment of the impacts of the parameter on each individual case.

Table 13 Summary of the parameters used in all vented and HPA attic simulations, total of 688 simulated cases.

Prototype	**Count**	**IAQ Fan Sizing**	**Count**
1-story	172	T24 2008	312
2-story	172	T24 2008 + 40%	0
		None	32
Moisture Gains	**Count**		
High	64	**Attic Type**	**Count**
Medium	280	Sealed	0
		HPA	344
Envelope Airtightness	**Count**	Vented	344
1 ACH50	128		
3 ACH50	120	**CEC CZ**	**Count**
5 ACH50	96	1	24
		2	24
Duct Leakage	**Count**	3	24
5%	192	4	24
2%	76	5	24
8%	76	6	24
		7	24
Attic Leakage	**Count**	8	24
50%	344	9	24
20%	0	10	24
80%	0	11	24
		12	24
Ceiling Leakage	**Count**	13	24
50%	344	14	24
20%	0	15	24
80%	0	16	24

Table 14 Summary of the parameters used in all sealed and insulated attic simulations, total of 1,944 simulated cases. Core case parameters are highlighted in italicized blue lettering.

Prototype	**Count**	**IAQ Fan Sizing**	**Count**	**HVAC Supply Air in Attic**	**Count**
1-story	***972***	***T24 2008***	***1304***	No	1752
2-story	***972***	T24 2008 + 40%	320	Yes	192
		None	320		
Moisture Gains	**Count**			**CRC Air Impermeable Insulation Above Roof Deck**	**Count**
High (11.8kg/day)	608	**Attic Type**	**Count**	No	1752
Medium (6.5 kg/day)	***1336***	***Sealed***	***1944***	Yes	192
		HPA	0		
Envelope Airtightness	**Count**	Vented	0	**1 Perm Vapor Retarder on Batt Surface**	**Count**
1 ACH50	256			No	1752
3 ACH50	***1464***	**CEC CZ**	**Count**	Yes	192
5 ACH50	224	***1***	***124***		
		2	***124***	**Outdoor Air Supply Ventilation into Attic Volume**	**Count**
Duct Leakage	**Count**	***3***	***124***	No	1752
5%	***1920***	***4***	***124***	Yes	192
2%	12	***5***	***124***		
8%	12	***6***	***124***	**R20 Roof Deck**	**Count**
		7	***124***	No	1912
Attic Leakage	**Count**	***8***	***124***	Yes	32
50%	***1368***	***9***	***124***		
20%	288	***10***	***124***	**IAQ Fan Type**	**Count**
80%	288	***11***	***124***	***Exhaust***	***1880***
		12	***124***	Supply	64
Ceiling Leakage	**Count**	***13***	***124***		
50%	***1496***	***14***	***124***	**Roof Finish**	**Count**

20%	224	***15***	***124***	***Tile***	***1880***
80%	224	***16***	***124***	Asphalt Shingle	64

6.2.1 Attic Type

We varied the attic/roof construction to cover three of the most reasonable approaches that designers are expected to take in satisfying the attic/roof requirements of the California State Building Energy Standards. These include the following:

- Traditional vented attics with insulation on the flat ceiling and intentional attic venting at 1/300 ceiling area.
- High Performance Attics (HPA) with insulation on the flat ceiling, intentional venting, and insulation below the roof deck at R13 in CZ 4, 8-16.
- Sealed and insulated attics with insulation on the sloped roof deck at the same R-value as ceiling insulated in vented attics, uninsulated ceilings, and no intentional leakage.
-

Vented and HPA attics are simulated solely to provide appropriate baselines for energy and moisture performance, against which we compare sealed and insulated attics. Attic geometries are identical between attic types, solely their insulation and leakage characteristics are changed.

6.2.2 Prototype Home Geometry and Details

Two continuously occupied CEC prototype homes were simulated—one- and two-story, with conditioned floor areas of 2,100 and 2,700 ft^2 (195.1 and 250.8 m^2), respectively (Nittler & Wilcox, 2006). Geometry assumptions are detailed in Table 15 and thermal insulation values are detailed in Table 16. These values were made to align as well as possible with the prescriptive performance requirements (Option B) in the 2016 Title 24 energy code. Thermostat schedules were set to meet those specified in the 2016 ACM that include nighttime setback when heating and daytime setup when cooling. HVAC equipment was sized using ACCA Manual J load calculation procedures. An over-sizing of 33% was added on top of Manual J estimates, to ensure adequate cooling capacity to meet load. Sizing is not critical for this study; we simply wanted to ensure that loads were met in all cases to facilitate an apples-to-apples comparison. Current deviations from the Title 24 prescriptive path prototypes include no whole house economizer fans, internal gains based on RESNET calculation method (see Section 6.2.7) and increased HVAC equipment efficiencies. Equipment efficiency was increased beyond prescriptive minimums to SEER 16 A/C (EER of 12.8) and 92 AFUE gas furnaces in order to align with standard new construction practice encountered in the HENGH field study (Chan et al. 2018) and based on input from the project's Technical Advisory Committee.

As described below, the building envelope and HVAC system characteristics of these homes will be consistent with the Prescriptive Package A requirements for roof/attic Options A, B and C, as specified in Table 150.1-A of the Residential Compliance Manual (roof/attic requirements reproduced above in Table 3). Homes will be assumed to have tile roof finishes, as this finish predominates in the regions with most new housing starts.

Table 15 Living space geometry assumption for each prototype.

Element	**1-story, 2,100 ft^2**	**2-story, 2,700 ft^2**
Number of stories	1	2
Length of House (m)	15.2	15.2
Width of House (m)	14.0	8.8
Conditioned Floor Area (m^2)	195.1	250.8
1st Floor Area (m^2)	195.1	116.1
2nd Floor Area (m^2)	0.0	134.7
Perimeter of 1st Floor	58.5	48.2
Floor Framing Height (m)	0.0	18.6
Height Above Grade (m)	0.3	0.3
Story Height (m)	2.7	2.7
Floor Height Above Grade (m)	0.3	0.3
Soffit Height Above Grade (m)	3.4	6.1
Window Area (m^2)	39.0	50.2
Door Area (m^2)	3.7	3.7
Gross Above Grade Wall Area (m^2)	160.5	232.4
Net Above Grade Wall Area (m^2)	121.5	182.3
House Volume (m^3)	535	729

Table 16 Envelope thermal resistance values by CEC climate zone. Based on values in Title 24 Appendix B, Table 150.1-A.

CZ	Assembly Thermal Resistance (ft^2-°F/Btu)						
	Ceiling or Sloped Roof	Above Grade Walls	Windows	Windows SHGC	Doors	Raised floor	Slab perimeter
1	40	19.6	3.13	0.25	5	19	0
2	40	19.6	3.13	0.25	5	19	0
3	32.3	19.6	3.13	0.25	5	19	0
4	40	19.6	3.13	0.25	5	19	0
5	32.3	19.6	3.13	0.25	5	19	0
6	32.3	15.4	3.13	0.25	5	19	0
7	32.3	15.4	3.13	0.25	5	19	0
8	40	19.6	3.13	0.25	5	19	0
9	40	19.6	3.13	0.25	5	19	0
10	40	19.6	3.13	0.25	5	19	0
11	40	19.6	3.13	0.25	5	19	0
12	40	19.6	3.13	0.25	5	19	0
13	40	19.6	3.13	0.25	5	19	0
14	40	19.6	3.13	0.25	5	19	0
15	40	19.6	3.13	0.25	5	19	0
16	40	19.6	3.13	0.25	5	19	7

6.2.3 Attic Geometry and Details

All attics are assumed to have two gable end walls, connected by two pitched roof surfaces. The roof ridge is in the East-West cardinal orientation such that the pitched roof surfaces face North and South. This orientation was selected because thermal and moisture conditions of roof surfaces depend strongly on solar heating and the North and South facing surfaces represent the extremes of solar exposure for an attic. All attics contain HVAC ductwork. The attic air volume is not adjusted for estimated HVAC duct volume, which could lead to biases, particularly in small attics. The attic geometries are quite different between the two prototypes, largely due to being 1- vs. 2-story homes. Despite its smaller overall floor area, the 1-story home has a much larger ceiling area (2,100 vs. 1,450 ft^2), greater attic volume and a greater height above the soffit. The attic geometries are described in Table 17.

Table 17 Attic geometry assumptions for each prototype.

Attic Parameter	1-story, 2,100 ft^2	2-story, 2,700 ft^2
Roof Pitch (Degrees (Rise/Run))	22.6 (5:12)	18.4 (4:12)
Roof Ridge Height Above Soffit (m)	3.17	2.54
Attic Volume (m^3)	309.7	171.1
Roof Ridge Height Above Grade (m)	6.5	8.6
Attic Vent Height Above Grade (m), Vented Attics Only	4.9	7.4
Sloped Roof Surface Area (m^2)	211.3	142.0
Gable Wall Surface Area (m^2)	81.3	44.9
Ceiling Surface Area (m^2)	195.1	134.7
Attic Bulk Framing Surface Area (m^2)	195.1	134.7
Roof Sheathing Thickness (m)	0.015	
Roof Sheathing Surface Thickness (m)	0.003	
Bulk Attic Framing Thickness (m)	0.013	
Bulk Attic Framing Surface Thickness (m)	0.001	

Two roof finish materials are assessed in this work—cement tile and asphalt shingles. The thermal and physical properties used for each roof finish are summarized in Table 18.

Table 18 Roof finish thermal and physical values.

Roof Finish Parameter	Cement Tile	Asphalt Shingle
Absorptivity	0.8	0.92
Emissivity	0.9	0.91
Thermal Resistance (m^2-°K/watt)	0.5	0.078
Density (kg/m^3)	50	11
Specific Heat Capacity (J/kg-°C)	880	1260

6.2.4 Envelope and Attic Leakage

The air leakage of various components of the building envelope will be varied, because of their anticipated effects on air exchange, energy use and moisture conditions. The airtightness values selected—1, 3 and 5 ACH_{50}—reflect the common range of values seen in new California homes, as well as those we anticipate seeing in future zero energy homes. It should be noted that in

simulations with vented attics—the traditional vented attic and the HPVA Option B cases—builder-installed venting areas will comply with code requirements (i.e., a minimum of 1 in 300, assuming provision of high and low attic vents, per the 2013 California Residential Code (Title 24, Part 2.5 of the California Building Standards Code)).

Leakage area is specified in the REGCAP model for the: (1) living space walls and floor, (2) the ceiling, and (3) the sloped roof , gable end wall and soffit vents of the attic. All unintentional envelope leakage areas assume a leakage pressure exponent (*n*) of 0.67, which is typical for residences.

Whole house envelope leakage area is calculated based on the envelope airtightness (1, 3 or 5 ACH_{50}), using the living space volume (not including the attic air volume). All cases assume that 50% of this reference whole house envelope leakage is in the living space walls and floor. For the vented attic cases, the remaining 50% is in the ceiling as required by Title 24. For the unvented attic cases, the remaining 50% is in the attic leaks. This ensures that total leakage areas are the same for vented and sealed attic cases.

For sealed and insulated attics, we further varied the ceiling leakage and attic leakage rates. The ceiling leakage between the living space and the attic was varied between 20%, 50% and 80% of the reference whole house envelope leakage. The attic leaks were also set to 20%, 50% and 80% of the reference whole house envelope leakage to examine the effect of changing attic leakage without changing the leakage of the floor and walls below the attic. When attic leakage is 20%, whole house leakage is only 70% of the reference case (50% living space leakage + 20% envelope leakage). And for the 80% leakage attics, the whole house leakage is 130% of the reference case (50% living space leakage + 80% envelope leakage). So, attic leakage area is changing, as is whole house leakage area. This impacts living space and attic ventilation rates.

Vented attic leakages are specified differently. The ceiling area is multiplied by 0.003 to estimate the unintentional leakage areas in the sloped roof surfaces (based on measurements of attic leakage by Walker (1993). This is translated to a leakage coefficient used in the REGCAP model using an orifice flow factor of 0.6. Builder installed attic vents are also specified, at a size of 1/300 relative to the ceiling area. This intentional venting is specified as two equal sized leaks (one in the north sloped roof face and one in the south), with a fixed height set at half the total attic height (ridge – soffit). Pressure exponents (*n*) of 0.5 are assumed for intentional vents.

6.2.5 Duct Leakage

Duct leakage was varied over a range that includes good ducts (2% leakage), code compliant ducts (5% leakage) and a case (8% leakage) that exceeds the energy code. The values we chose roughly correspond to high-performance, code-compliant, and average, for unvented CA attics[8]. Levels of air leakage are important even inside unvented attics, because this leakage partially conditions the attic volume and enhances mixing of attic and house air. In this study we

[8] Based on data presented from duct testing in unvented attics (Hoeschele, Weitzel, German, & Chitwood, 2015).

specified duct leakage as balanced between supply and return ducts. So, for 5% leakage, there is 2.5% supply leakage and 2.5% return side leakage. When the air handler is not operating, these duct leaks allow flow between the living space and attic volumes, and under these conditions, a pressure exponent of 0.6 is used.

6.2.6 IAQ Fan Sizing and Type

We explored three different fan sizing approaches for IAQ fan ventilation. All cases had auxiliary fan operation, independent of the main IAQ fan sizing and operation. Cases with envelope leakage of 3 or 5 ACH_{50} were simulated with exhaust fans, while 1 ACH_{50} cases used balanced supply/exhaust systems. The balanced fans have increased fan energy consumption compared to exhaust fans. We also performed a few simulations with supply fans of the same flow rate at the exhaust fans. Fan airflows did not vary with airtightness. Select cases were also simulated with supply fans only, in order to assess the potential impacts of the direction of mass flow through the ceiling, induced by unbalanced ventilation fans. All fans were simulated with a fan efficacy of 0.44 Watts/L-s. All IAQ fan airflows and energy consumption are listed in Table 19.

1. No continuous IAQ fan. This is meant to represent the many new homes in the state, where the code-required IAQ fan ventilation system is installed but turned off by the occupants or otherwise non-operational. In these cases, the only air exchange occurs by natural infiltration and auxiliary fan operation (bathroom and kitchen exhaust fans and dryer exhaust). The simulations assume no window or door operation, so they result in lower in the overall air exchange estimates.

2. IAQ fans sized to the Fan Ventilation Rate Method (FVRM) in Title 24 (2008). This method does not account for infiltration. Fan airflow is calculated based on the home's conditioned floor area and number of bedrooms (a proxy for occupancy), as follows:

$$\boldsymbol{Q_{fan}} = \frac{\mathbf{A}_{\boldsymbol{floor}}}{\mathbf{100}} + \mathbf{7.5} \times (\mathbf{N}_{\boldsymbol{br}} + \mathbf{1})$$

Q_{fan} = calculated IAQ fan airflow, cfm

A_{floor} = conditioned floor area, ft^2

N_{br} = number of bedrooms

3. Current builder practice. Based on preliminary findings from the recent field study of ventilation in New California Homes (Chan, Kim, Less, Singer, & Walker, 2018), we increased the 2008 IAQ fan airflows by 40%[9]. Similar fan oversizing in new California homes was reported by Stratton, Walker, & Wray (2012). This over-sizing results in IAQ fan airflows that are roughly similar to those required by the current ASHRAE Standard 62.2-2016.

[9] Since the simulations were performed the HENGH field study has also been completed, and the average oversizing was in fact closer to 50%.

Table 19 IAQ fan airflows and energy consumption.

IAQ Fan Sizing Method	IAQ Fan Airflow (L/s, watts)	
	1-story, 2,100 ft^2	2-story, 2,700 ft^2
None	0 (0)	0 (0)
FVRM Title 24 (2008)	23.8 L/s (10.4 watts, 20.8 watts balanced fan)	30.0 L/s (13.1 Watts, 26.2 watts balanced fan)
Builder Practice	33.3 L/s (14.5 Watts, 29 watts balanced fan)	42.1 L/s (18.3 Watts, 36.6 watts balanced fan)

6.2.7 Internal Gains and Auxiliary Fan Operation

Internal moisture gains took one or two values—medium at 6.5 kg/day and high at 11.8 kg/day (see Table 20). This moisture load was emitted continuously at the same rate for each simulation time step, and the moisture is added to the living space air volume node. As in our previous work (Iain S. Walker & Sherman, 2007), the medium (or average) moisture generation rate is based on design values from ASHRAE Standard 160 (2009) which is 13.8 kg/day for a three bedroom four occupant home. We assume that bathing, cooking and dishwashing moisture is exhausted through local fans, so we subtract 4 kg/day (estimate from NIST (Emmerich, Howard-Reed, & Gupte, 2005)) from this design value. The resulting rate of 9.8 kg/day is then corrected to 6.5, with an assumption that the home is only occupied 2/3 of the time. The high occupancy level assumes continuous occupancy and additional gains for a total of 11.8 kg/day (9.8 + 2).

Sensible heat gains in the living space varied only by prototype, with 943 watts in 2-story homes and 775 watts in the 1-story homes. Sensible internal heat gains are calculated using the formula for the reference home in the Home Energy Rating System (HERS) Standards (RESNET, 2006) Table 303.4.1(3).

Table 20 Summary of sensible gains and moisture gains, by prototype and moisture gain parameters.

Prototype	Sensible Gains (watts)	Moisture Gains	Internal Moisture Gains (kg/day)
1-story	775	Medium	6.5
2-story	943	High	11.8

The auxiliary fans were bathroom and kitchen exhausts and a vented clothes dryer. The dryer is assumed to have airflow of 71 l/s, kitchen exhaust is 47 l/s and all bathroom fans are 24 l/s (equivalent to Title 24 and ASHRAE requirements of 100 and 50 cfm, respectively). Exhaust fan operation is distributed semi-randomly throughout the occupied periods of the day. The daily operation of the auxiliary exhaust fans in the home (e.g., kitchen exhaust, laundry, and

bathroom fans) are listed for each combination of house prototype and moisture gain value in Table 21. In the 1-story prototype with high moisture gains (higher occupancy), greater dryer usage is specified (77 vs. 52 minutes per day), while kitchen and bathroom exhausts remain the same. In the 2-story prototype with high gains, the laundry exhaust is increased and an additional bathroom exhaust fan flow is simulated at 40 minutes per day.

Table 21 Auxiliary fan minutes of operation for each prototype and moisture gain value.

Prototype	Internal Moisture Gains	Exhaust Fan Operation (Minutes per Day)				
		Dryer Exhaust	Kitchen Exhaust	Bath 1	Bath2	Bath3
1-story	Medium	52	69	80	80	0
	High	77	69	80	80	0
2-story	Medium	52	69	80	80	0
	High	77	69	80	80	40

6.2.8 Climate Zones

We simulated attic performance in all 16 CEC climate zones to assess risk across the entire state. The CEC climate regions are summarized in Table 22 that includes their mapping to the U.S. DOE climate zones (includes multiple DOE CZ designations where there is climate region overlap), single-family new construction estimates, and rough ranges for heating and cooling degrees days. Table 23 provides a more detailed summary of the annual weather data files used in CBECC-Res to demonstrate residential compliance with Title 24, including annual dry-bulb, wet-bulb, dew-point temperatures, wind speed, solar gains, and sky cover. CBECC-Res weather files were first converted to SI units and were then read into REGCAP, which performs a linear interpolation from one-hour to one-minute time steps for use in the simulation. We used the CEC weather files (.csw) used to demonstrate Title 24 residential compliance with CBECC-Res.

Table 22 Summary table of CEC climate regions, their US DOE CZ mappings, estimates of new construction rates, and rough heating and cooling degree-day estimates.

CEC CZ	DOE CZ	City	2017 New Single-Family Homes	2017 New Homes Fraction	Rough HDD_{65} Range	Rough CDD_{80} Range
1	3C/4C	Arcata	695	0.006	3800-4500	0-50
2	3C/4B/4C	Santa Rosa	2602	0.024	2600-4200	200-900
3	3C	Oakland	5217	0.048	2500-3800	10-500
4	3C	San Jose-Reid	5992	0.055	2300-2900	200-1000
5	3C	Santa Maria	1164	0.011	2300-3000	200-900
6	3B/3C	Torrance	4142	0.038	700-1900	500-1200
7	3B	San Diego-Lindbergh	6527	0.060	1300-2000	500-1100
8	3B	Fullerton	7110	0.066	1300-1800	700-1300
9	3B	Burbank-Glendale	8259	0.076	1100-1700	1300-1600
10	3B	Riverside	16620	0.154	1600-1900	1400-1900
11	3B	Red Bluff	5970	0.055	2500-4300	600-1900
12	3B/4B	Sacramento	19465	0.180	2400-2800	900-1600
13	3B	Fresno	13912	0.129	2000-2700	1000-2200
14	3B	Palmdale	3338	0.031	1900-2700	2000-4200
15	2B/3B	Palm Spring-Intl	3885	0.036	1000-1300	4000-6600
16	3B/4B/5B	Blue Canyon	3135	0.029	4300-6000	200-1000

Table 23 Annual weather parameters summarized for each CEC climate zone from CBECC-Res weather data files.

CZ	Dry Bulb Temp (°F)	Wet Bulb Temp (°F)	Dew Point Temp (°F)	Sky Temp (°F)	Wind Direction (degrees)	Wind Speed (mph)	GHI (btu/ft^2)	Total Sky Cover
1	51	49	47	27	206	6	53	5.5
2	57	51	46	29	204	5	65	3.2
3	57	52	48	32	228	9	64	5.3
4	59	52	47	31	276	7	67	4.0
5	56	51	47	29	241	7	69	4.2
6	61	56	52	37	255	6	66	4.8
7	62	57	53	40	227	6	68	5.8
8	63	56	51	36	179	5	67	2.9
9	64	55	48	34	183	6	69	2.4
10	64	54	47	33	223	5	70	2.2
11	63	52	43	31	230	8	66	2.2
12	61	53	47	30	212	6	66	2.1
13	64	54	47	36	232	6	67	4.2
14	62	49	37	23	210	10	75	0.9
15	75	57	43	40	233	7	73	1.1
16	52	41	30	11	160	6	68	2.1

6.3 Moisture Control Measures

We assessed five optional moisture mitigation measures:

- California Residential Code (CRC) (2016) air impermeable insulation above the roof deck, plus batt insulation to make up remaining thermal resistance.
- HVAC supply air provided to the attic volume at a rate of 50 cfm/1000 ft^2 of attic floor area.
- 1 perm-in vapor retarder on attic-facing surface of fibrous insulation.
- Mechanical outdoor air supply fan into the attic volume at 20 cfm per 1,000 ft^2 of ceiling area.
- Mechanical outdoor air supply fan into the attic volume at 50 cfm per 1,000 ft^2 of ceiling area.

These five mitigations are simulated in each prototype and climate zone, with both medium and high internal moisture gains and three IAQ fan sizes, for a total of 192 cases each. Core parameters are otherwise fixed, at 3 ACH_{50} envelope leakage, 5% duct leakage, 50% attic and ceiling leakage, exhaust fan, and tile roof.

6.3.1 Continuous Roof Deck Insulation.

All simulation cases were first run with air permeable, fibrous roof deck insulation. In some of California's colder climates, this approach is considered a moisture risk, and does not comply with the International Residential Code 2012 requirements in Table 806.5 (reproduced in Table 24) (ICC, 2012). The 2016 California Residential Code (CRC) Chapter 8, Section R806.5 contains

similar requirements specified using California's CEC climate zones, which have been overlaid with the IECC requirements in Table 24. The model code requires a continuous layer of air impermeable insulation, which increases the temperature of the first condensing surface in the roof assembly and provides some assurance that risk of condensation and moisture accumulation will be minimal. In cases with continuous roof deck insulation, we use the CEC Climate Zone values reproduced in Table 24. For cases where no air impermeable insulation is required (i.e., CZ6-15 with tile roofing), we specify the minimum R-5 air impermeable insulation in order to distinguish these prior simulations using solely air and vapor permeable insulation. In all cases, the remaining thermal resistance is comprised of air permeable insulation below to the roof deck, such that the total thermal resistance of the roof deck is identical between base and mitigation cases.

This approach was implemented in REGCAP by adding thermal resistance to the roof sheathing, which mimics the placement of air impermeable insulation above the roof deck. A common alternative approach is to place the air impermeable insulation in direct contact with the underside of the roof sheathing. These represent fundamentally different moisture dynamics. Namely, the insulation above the roof deck limits condensation, but still allows condensation on the wood sheathing, and it allows direct contact with water vapor in the attic air. Placing the air impermeable insulation on the underside of the roof deck effectively places a vapor retarder (depending on depth/material) between the attic air and the sheathing material. This has the added benefit of protecting the sheathing from high relative humidity and potential mold growth.

We note things two things about the IRC and CRC requirements. First, the air impermeable insulation requirements were developed in order to minimize the risk of condensation and elevated wood moisture content, not explicitly to limit mold growth. Effectively, the criteria are established such that the temperature at the roof sheathing will not be less than 7°C when assessed with an exterior temperature equal to the average outdoor temperature of the coldest three months and indoor condition of 20°C (CRC Section R806.5.1.4). This should limit but not eliminate condensation, and it should aid in controlling elevated RH, but again, it is not designed to do so in any controlled way. In essence, this is a rule-of-thumb approach based on basic engineering calculations. Second, the entire basis of this method depends on the fraction of the assembly thermal resistance that is made up by the air impermeable insulation and exterior elements. It is this ratio that determines the temperature at the sheathing surface. Because the total assembly resistances are different between the CRC and IRC, the required air impermeable insulation levels should vary as well. The CEC could consider a more California-specific assessment of these requirements, based on current code requirements and CEC climate zone analysis.

Table 24 2012 International Residential Code, Unvented Attics Table 806.5.

U.S. DOE Climate Zone	CEC Climate Zone	Minimum Air Impermeable Insulation R-Value	2012 IECC Required Total R-Value of Ceiling	CEC Required Total R-value of Ceiling
2B and 3B tile roof only	6-15 tile roof only	0	30	32 - 40
1, 2A, 2B, 3A-C	3-15	5	38	32 - 40
4C	1-2	10	38	40
4A-B	16	15	49	40
5		20	49	
6		25	49	
7		30	49	
8		35	49	

6.3.2 Intentional HVAC Supply Air in Attic

The most recent IRC in 2018 has added a requirement to supply conditioned air to all sealed attics at 50 cfm per 1,000 ft^2 of ceiling area. In climate zones 1-3, an optional path was added to use solely air permeable insulation (e.g., fiberglass or cellulose), provided that vapor diffusion vents are installed with more than 20 perms at the roof peak (1 unit diffusion vent area per 600 units of ceiling area) (BASC 2018). The REGCAP model is not currently able to simulate the diffusion vents in this new code provision, and the California building code does not include these new requirements and options. As such, we simulate the added HVAC supply air (which is required in all sealed and insulated attics), but not the diffusion venting.

We simulated the impacts of the intentional attic supply air as an additional supply leak located in the attic ductwork in the REGCAP model. This requires a 105 cfm supply leak in the 1-story prototype and a 73 cfm leak in the 2-story prototype attic. This increased leakage was specified as the fractional amount of the larger of the heating or cooling total HVAC airflows. For example, if the heating airflow was 600 cfm and the cooling was 1,100 cfm, then 105 cfm of leakage / 1100 cfm = 0.095. This same fractional leakage was applied for both heating and cooling operating modes. Thus, in cases where forced air system airflows were different for heating and cooling, it the lower flow mode the additional supply air was reduced. This leakage fraction was added to the base duct leakage already specified in the model (e.g., 0.02, 0.05 or 0.08). The supply duct leakage coefficient was similarly increased, which allows the REGCAP model to account for stack-driven airflows between the living and attic zones through the supply duct leak site during periods when the air handling system is non-operational. The intentional supply air leak results in large imbalances in return and supply leakage, which we expect will mix the house and attic air volumes substantially, and generally depressurize the home and pressurize the attic relative to outside.

6.3.3 Vapor Retarder at Insulation-Attic Air Interface

The 2016 California Residential Code (CRC) Chapter 8, Section R806.5 adds that a Class I or II vapor retarder be installed on the attic-side of any air permeable insulation, in order to provide for condensation control. The code language is not clear here, as it appears that this requirement in the CRC (Number 4.1, Section R806.5) may apply only in CEC CZ 14 and 16. It is also unclear if this requires a vapor retarder in attics that also use air impermeable insulation against or above the roof sheathing. Either way, this vapor retarder would limit the diffusion of water vapor through the insulation, from the attic air to the cold roof deck sheathing locations, hopefully limiting condensation and moisture accumulation. Moisture in the attic air would only contact the vapor retarder surface, which should be nearly identical to the attic air temperature, which is very similar to the house air temperature. Recent research reported in cold climate contexts has found that variable permeability "smart" vapor retarders (e.g., CertainTeed MemBrain, Intello, ProClima and DuPont AirGuard Smart). may in fact offer the best performance in sealed attic assemblies with fibrous insulation (Ueno & Lstiburek, 2018). These were not investigated in this work.

We simulated cases with the insulation material treated as having a vapor diffusion coefficient of 1 perm-in. The standard fibrous insulation in the model is assumed to have a vapor permeance of 106 perm-in, specified as a vapor diffusion coefficient of 2.12E-05 m^2/s[10]. The 1 perm-in vapor retarder is specified as a vapor diffusion coefficient of 2.2472E-07 m^2/s.

6.3.4 Outdoor Air Supply Fan Into Attic Volume

Two versions of this mitigation were tested, first with 50 cfm per 1,000 ft^2 of ceiling area introduced by mechanical supply into the attic, and then with only 20 cfm per 1,000 ft^2 introduced. The supply airflows are specified for the two prototypes and target airflows in Table 25. Due to time and resource constraints in modeling, these cases do not include added supply fan energy, nor do they add thermal energy to the supply air stream. In post-processing, we added the mechanical fan energy in Table 17 into these cases to ensure accurate savings estimates.

[10] Calculated as 106 perm-in * (1 m / 39.37 in) * (5.722E-11 kg/s-m^2-Pa/ 1 perm) * (462 J/kg-°K) * (298 °K) = 2.12E-5 m^2/s

Table 25 Supply fan airflows provided in attic volumes at 20 and 50 cfm per 1,000 ft^2 of ceiling area.

Prototype	Supply Airflow into Attic Volume (cfm (L/s))	
	50 cfm per 1,000 ft2	20 cfm per 1,000 ft2
2-story	72.5 cfm (34.2 L/s)	29 cfm (13.7 L/s)
1-story	105 cfm (49.6 L/s)	42 cfm (19.8 L/s)

Table 26 Attic OA supply fan power and energy estimates, for each target flow and prototype.

Prototype	50 cfm per 1,000 ft^2 ceiling		20 cfm per 1,000 ft^2 ceiling	
	Power (watts)	Energy (kWh)	Power (watts)	Energy (kWh)
2-story	14.9	130.7	6.0	52.6
1-story	21.6	184.0	8.6	75.7

7 Simulation Study Results and Discussion

Overall, 2,632 simulations were performed, in which we varied the factors believed to affect sealed and insulated attic hygrothermal performance, sufficiently to represent performance across a variety of newly constructed California single-family homes.

We begin with a brief overview of the temperature differences the REGCAP model predicts for sealed and insulated attics (Section 7.1.1). Next, we provide an overview of attic moisture performance in terms of mold index and maximum 7-day wood moisture content in vented, HPA and sealed and insulated attics (Section 7.2). This is followed by a brief examination of the correlation and behavior of three moisture performance criteria—mold index, prior ASHRAE 160 surface RH, and 7-day maximum wood moisture content (Section 7.2.1). Next we examine some example time-series plots of the simulated results, to provide the reader with a more intuitive understanding of the seasonal trends occurring in the simulations (Section 7.2.2). Subsequent sections focus solely on the North sheathing and bulk attic framing moisture nodes as they are the locations most at risk for moisture problems. We present a sensitivity analysis that summarizes the moisture risks across all of the simulation parameters, helping to identify which parameters are most important in determining risk (Section 7.2.3). We then proceed to examine moisture performance for each simulation parameter in isolation, highlighting mold index failures, maximum 7-day wood moisture contents, condensed moisture mass and other features of the data (Section 7.2.4). These sections are used to explore how and why each parameter affects sealed and insulated attic moisture performance. Moisture results are concluded by examining a variety of mitigation measures that could be used to reduce moisture risks in sealed and insulated attics using fibrous insulation materials, including HVAC supply air in the attic, air impermeable insulation per the CRC 2016, a 1-perm vapor retarder on the surface of the fibrous insulation, and an outdoor air supply fan into the attic at 50 and 20 cfm/1,000ft^2 of ceiling area (Section 7.2.5). The results section finishes with an examination of the energy use for all attic types, and of the energy savings for sealed and insulated attics across California climate regions (Section 7.3).

7.1 Thermal Performance

7.1.1 House-to-Attic Temperature Differences

In our simulations, the attic and living space air volume temperatures were very closely connected, as was expected for these assemblies and has been a verified using field data measurements (see Section 5.2.4). For all sealed attic cases, annual mean temperature differences between the attic and living space were -0.7˚C (from -1.9˚C to 0.15˚C), meaning the attics were on average 0.7˚C colder than the living space. In the measured field study homes, annual differences were also small, but the attics were slightly warmer than the living space (rather than cooler)—annually by 0.1˚C (NS33 Fresno), 0.7˚C (EW52 Fresno) and 1.7˚C (EW26N Clovis).

In Figure 110, we show the monthly distribution of temperature differences between the attic and living space air volumes for an example simulation case in CZ13 (Fresno). We see that the attic and living space are most often within roughly 0.5°C of one another. The attic is a thermal buffer zone between the directly conditioned living space and the outside air, so we expect it to be somewhat colder than the house in heating season and warmer than the house in cooling season. We see this exact trend in this case. For comparison, we show a corresponding vented attic in the same climate zone in Figure 111, and we see that in the heating season the attic is typically 5 to 15°C colder than the living space, and in cooling season the attic is from 0 to 15°C warmer than the living space. Eliminating these temperature differences and drastically reducing thermal losses from the HVAC distribution system are the key benefits of sealed and insulated attics.

Figure 110 Temperature. Attic vs. living space air temperature distributions by month for a sealed and insulated attic. Negative values mean living space is warmer than attic.

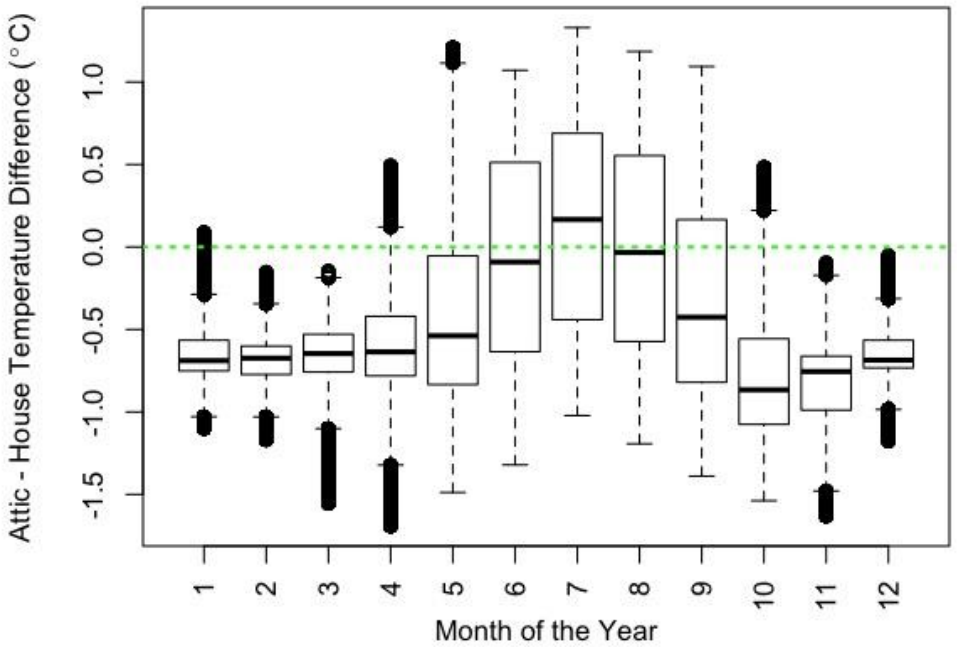

Figure 111 Temperature. Attic vs. living space air temperature distributions by month for a vented attic case.

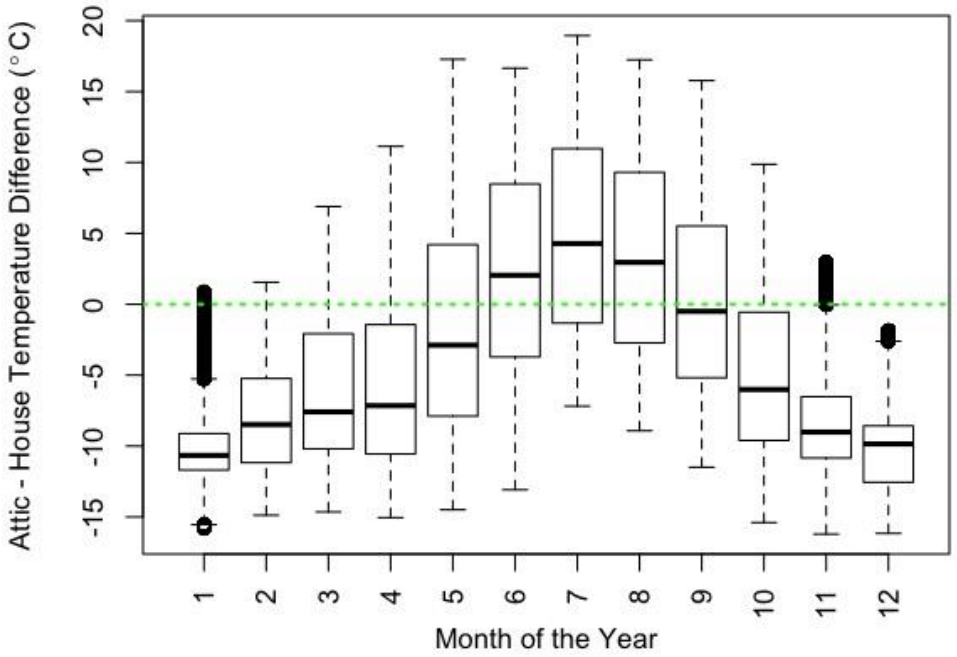

The temperature patterns on a daily basis are driven by solar radiation incident on the roof surfaces. In Figure 112, we show hourly time-series plots for an example sealed attic case for 2 weeks in winter and summer. We see that the sheathing nodes have significant diurnal temperature swings, elevating well above ambient temperature during daytime and depressing below outside air temperatures at night. The south and north sheathing surfaces are at similar nighttime temperatures, but the south surface heats up much more during daytime hours. The attic air is very close to the living space temperature. During the cooling season, the south sheathing node experiences temperatures in excess of 70°C, while cooling to just below ambient temperatures during nighttime. We also see that the attic air cycles just above the living space temperature during daytime periods and drops just below during nighttime.

Measured field data from this study (from the same Climate Zone as these simulations, but not the exact same weather) show wider temperature excursions for the attic relative to the living space during daytime hours in the cooling season, with maximum temperature differences around 4°C (see Section 5.2.4). Heating season temperature patterns show tighter agreement with the simulation results, with very little temperature deviation between the two air volumes.

Figure 112 Temperature. Example time-series plot showing hourly temperatures at sheathing and air nodes during two summer and two winter weeks.

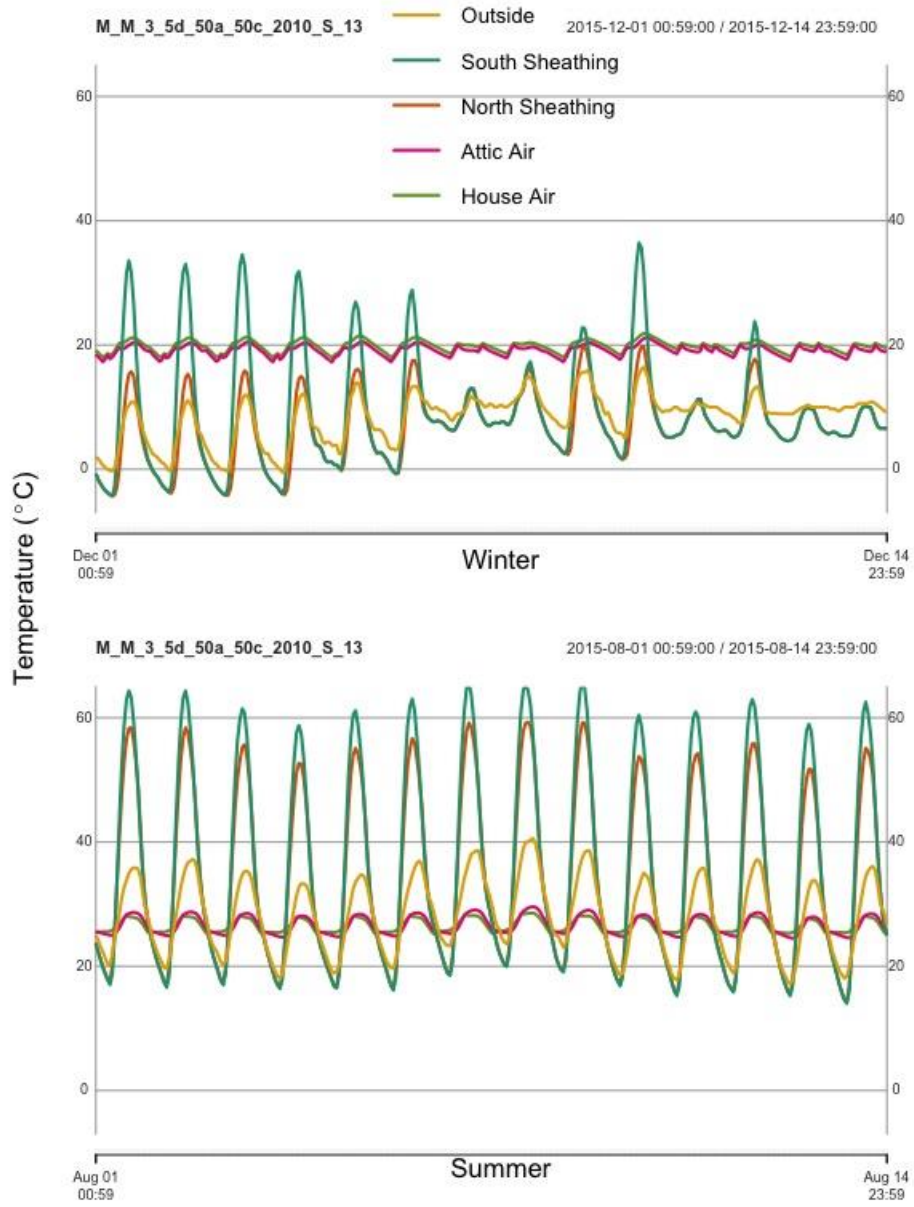

7.2 Moisture Performance

In these results we focus on the surface of the wood, either from a surface mold, surface wood moisture content or surface condensation. It should be noted that the interior of the wood members in the attics never had elevated wood moisture content (always below 10%). This may be acceptable from a purely structural point of view, however, even surface degradation and mold growth must be avoided on homes from both a potential health hazard perspective (mold) from our desire to be conservative when dealing with structural issues. The majority of simulated cases performed acceptably from a moisture perspective, and the higher risks cases had results that were highly variable, with very little risk in many contexts and substantial risks in others. In Figure 113, we show the maximum values for 7-day running average surface wood moisture content and mold index for the North sheathing moisture node in each simulated case, including vented, HPA and sealed and insulated attics. We also note numerous performance thresholds for each metric.

Figure 113 Comparison of the maximum 7-day surface wood moisture content and maximum mold index values for the North sheathing location in all simulated homes. Performance threshold levels are indicated and notated, as appropriate.

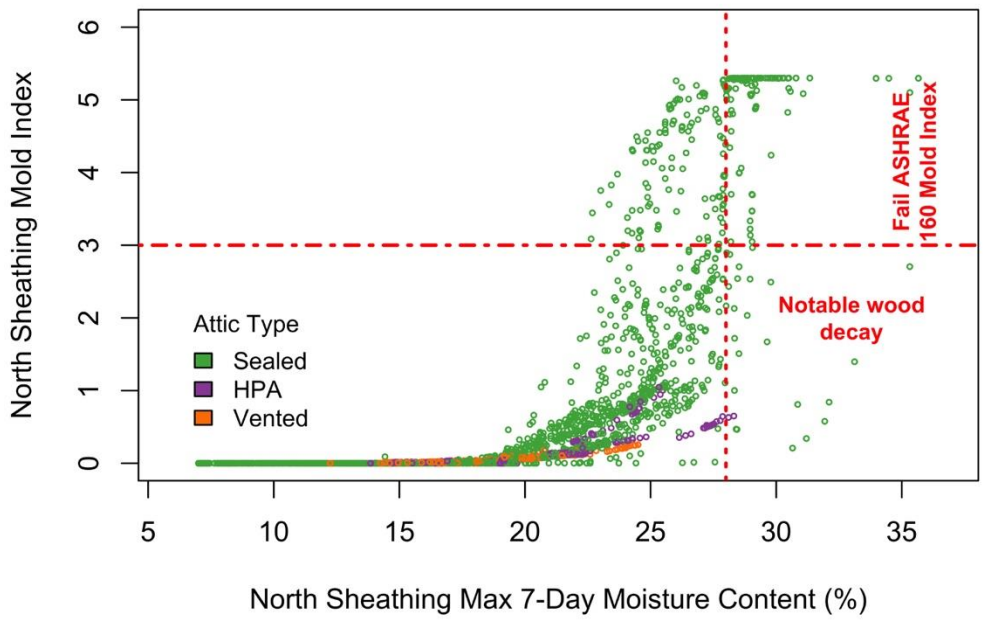

All mold index failures occurred in sealed and insulated attics, while all vented and HPA attics passed the ASHRAE 160 criteria. In sealed and insulated attics, mold index failures were most common in the North sheathing location (18% failure rate) and bulk attic framing (19% failure rate) locations, and were less frequent at the South sheathing (4% failure rate) node. We see in Figure 113 how all the vented and HPA cases had mold index values below 1, indicating no mold growth. Some HPA attics had elevated 7-day wood moisture content at the North sheathing, but none peaked above the threshold for wood rot/decay. In contrast, sealed and insulated attics experienced higher wood moisture contents and a number of failures of the

wood rot threshold. Of all sealed and insulated attic cases, 10% exceeded the 28% moisture content threshold at the North sheathing, while failures at the bulk framing and South sheathing were much lower, at 1% and 0%, respectively.

Similar data are plotted for the bulk attic framing moisture nodes in Figure 114. Overall, maximum 7-day wood moisture contents are lower in the bulk attic framing. Bulk framing for the vented and HPA attics reached at most 25%, with the HPA having somewhat high WMC than the traditional vented attics. Sealed and insulated attics had marginally higher bulk framing WMC, but their mold index values were much higher. A notable pattern occurs here for sealed and insulated attics, where cases either fail very badly, with mold indices of 6 indicating near total mold coverage on all visible surfaces, or they pass the criteria with values below 3. There are some in-between cases, but this moisture node is marked by lower failure rates, but when there is failure, it is severe.

Figure 114 Comparison of the maximum 7-day wood moisture content and maximum mold index values for the bulk attic framing location in all simulated homes. Performance threshold levels are indicated and notated, as appropriate.

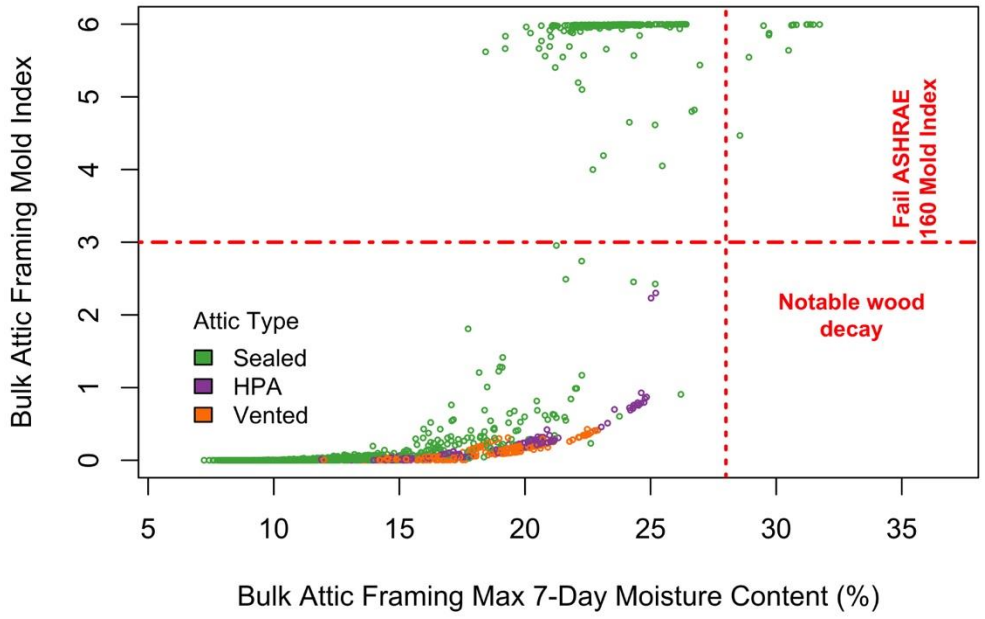

These findings are consistent with past research in attic moisture and ventilation, namely that sealed and insulated attics insulated with vapor permeable insulation increase the risk of mold growth and wood rot, relative to vented attic assemblies, and that the focus should be on risk assessment on the North sheathing. All subsequent moisture results will focus solely on the North sheathing and bulk framing moisture nodes in sealed and insulated attics.

7.2.1 Comparison of Moisture Performance Metrics

We use a variety of moisture performance metrics in this work as detailed in Section 3. The first is the ASHRAE 160 mold index, which is the only criteria for acceptability in the ASHRAE 160

standard. We also assess whether cases 7-day mean wood moisture content exceeded 28%, as a threshold for structural wood rot. Finally, we also considered the former ASHRAE 160 criteria, that 30-day running mean surface RH must remain below 80% while 30-day running mean surface temperature is between 5 and 40°C.

To assess these moisture metrics, we generated confusion matrices for all simulated cases. Each case either passed or failed each of the three moisture criteria. Table 27 shows the confusion matrix for the mold index and prior ASHRAE 160 criteria. As others have noted, the prior ASHRAE 160 criteria fails many assemblies, fully 47.9% of all cases failed this criteria, while only 10.5% of cases failed the current mold index criteria. Notably, all cases that failed the current mold index also failed the prior ASHRAE 160 criteria, whereas the prior 160 failed 37.4% of cases that the mold index deem acceptable. This analysis suggests that, as previously noted by others, the prior ASHRAE 160 was much more likely to fail these types of assemblies. Note, this does not address which criteria ultimately assesses risk correctly; it could be that the majority of these cases do in fact have risk of mold growth.

Table 27 North Sheathing, mold index vs. prior ASHRAE 160.

		Mold Index		Total
		Pass	Fail	
Prior ASHRAE 160	Pass	1,471 (52.1%)	0 (0%)	1,471 (52.1%)
	Fail	1,057 (37.4%)	296 (10.5%)	1,353 (47.9%)
Total		2,528 (89.5%)	296 (10.5%)	2,824 (100%)

We compared the criteria for mold index against the surface wood moisture content (threshold of 28% over 7-day running mean) for the North sheathing (see Table 28). There is improved overall agreement here, with each criteria failing a small subset of cases—10.5% fail the mold index and 7.2% fail the WMC criteria. The two criteria agree that 6.3% of cases fail, but in the other failures, the criteria give differing results. The mold index fails 4.2% of cases that pass the WMC criteria, and the mold index passes 0.9% of cases that fail the WMC criteria. If we look more closely at these specific cases of disagreement, we observe that the disagreement cases are tightly clustered above and below the criteria.

Another way to frame this issue, is that the 28% WMC threshold is imperfect for mold prediction, yet the values are highly correlated. In all cases that fail the mold index, wood moisture content is also elevated. For example, in all cases failing the mold index criteria at the North sheathing, the maximum 7-day WMC is at least 23% and averages 28%.

Table 28 North Sheathing, mold index vs. 7-day WMC > 28%.

		Mold Index		Total
		Pass	Fail	
WMC > 28%	Pass	2,502 (88.6%)	119 (4.2%)	2,621 (92.8%)
	Fail	26 (0.9%)	177 (6.3%)	203 (7.2%)
Total		2,528 (89.5%)	296 (10.5%)	2,824 (100%)

This analysis was repeated for the bulk framing moisture nodes in Table 29 and Table 30. For bulk framing we find that the prior ASHRAE 160 and the current mold index model agree very well on which cases are risky. They both estimate that roughly 10% of cases will fail (9.3 vs. 10.4%), and they agree on the vast majority of those cases (8.6%), with disagreement in only 20-30 cases. The WMC threshold is almost never exceeded at the bulk framing, yet there are a number of mold index failures (9.3%), so they metrics disagree in those cases. This is likely the result of the mold index being reached due to long-term elevated moisture in the attic air, which is not sufficient to bring the moisture content above 28%. For example, mold can begin growing at 80% RH, but that corresponds to WMC values of roughly 16%. At the bulk framing node, we conclude that the prior and current ASHRAE 160 methods agree well, and the WMC metric does not add any value on top of the mold index calculation.

Table 29 Bulk framing, mold index vs. prior ASHRAE 160.

		Mold Index		Total
		Pass	Fail	
Prior ASHRAE 160	Pass	2,510 (88.9%)	20 (0.7%)	2,530 (89.6%)
	Fail	50 (1.8%)	244 (8.6%)	294 (10.4%)
Total		2,560 (90.7%)	264 (9.3%)	2,824 (100%)

Table 30 Bulk framing, mold index vs. 7-day WMC > 28%.

		Mold Index		Total
		Pass	Fail	
WMC > 28%	Pass	2,560 (90.7%)	249 (8.8%)	2,809 (99.5%)
	Fail	0 (0.0%)	15 (0.5%)	15 (0.5%)
Total		2,560 (90.7%)	264 (9.3%)	2,824 (100%)

7.2.2 Overall Moisture Trends and Dynamics in Simulated Time-Series Data

When interpreting the results presented in subsequent sections, it is helpful for the reader to be more familiar with the time-series behavior of moisture in sealed and insulated attics, as represented in the REGCAP simulation model. In this section, we provide some illustrations of these dynamics and we discuss them, as appropriate.

7.2.2.1 Relative Humidity

Surface relative humidity drives mold index behavior, which is the most likely path to moisture failure for sealed and insulated attic using vapor permeable insulation in new California homes. We show three examples of daily mean RH over 4-year simulation periods for a likely safe 2-story home in CZ6 (Figure 115), a questionable 2-story home in CZ13 (Figure 116) and a clearly failing 1-story home with no IAQ fan in CZ1 (Figure 117). All cases show elevated RH at the North sheathing location, relative to the attic and living space air volumes. This elevated surface RH occurs during the heating season and is driven by cold outside temperatures and reduced daytime solar gains. In the safe case, attic and living space RH are in the 40-55% range on most days, and the North sheathing just barely peaks above the critical threshold of 80% for a few days at a time. The questionable case has bigger differences between living space and attic RH, likely due to its being a central valley climate, as opposed to a south coastal location. Yet, the house air never exceeds 55% on a daily basis. The North sheathing clearly exceeds the critical mold growth level of 80% and does so for roughly three months each winter, with daily averages in the 80-95% range. A failure is likely in this case, though not guaranteed. Finally, Figure 117 shows a clear failure, where North sheathing surface RH is at saturation for more than half of each year. Notice how the attic and living space RH are also very high in this home, which is located on the very humid North Coast (CZ1 Arcata)—a location notorious for mold growth in residences.

Figure 115 Relative humidity. Example time-series plot of daily mean relative humidity calculated at the North sheathing, attic air and living space air volumes over 4-year simulation period. This case has RH below critical levels at all nodes and is likely to be moisture-safe.

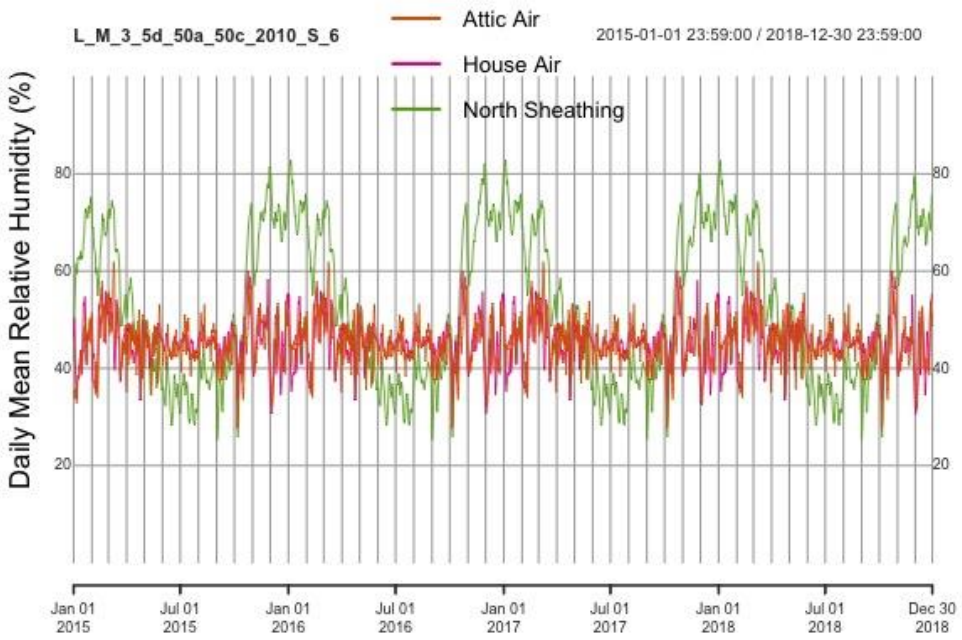

Figure 116 Relative humidity. Example time-series plot of daily mean relative humidity calculated at the North sheathing, attic air and living space air volumes over 4-year simulation period. This case has typical elevated RH at the North sheathing, which may or may not lead to mold index failure.

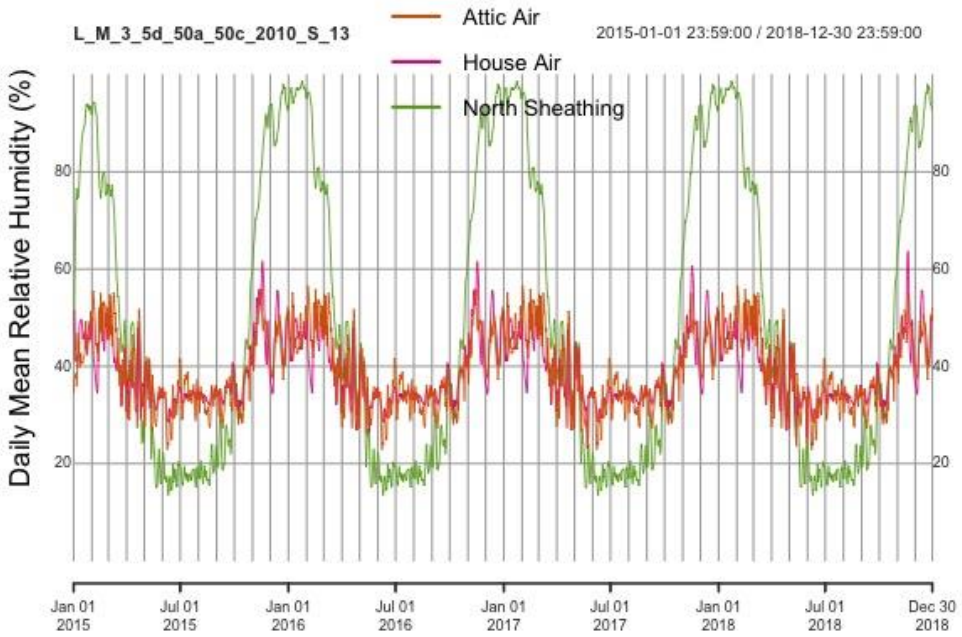

Figure 117 Relative humidity. Example time-series plot of daily mean relative humidity calculated at the North sheathing, attic air and living space air volumes over 4-year simulation period. This case has critically elevated RH at the North sheathing at saturation for more than half the year, certainly leading to failure.

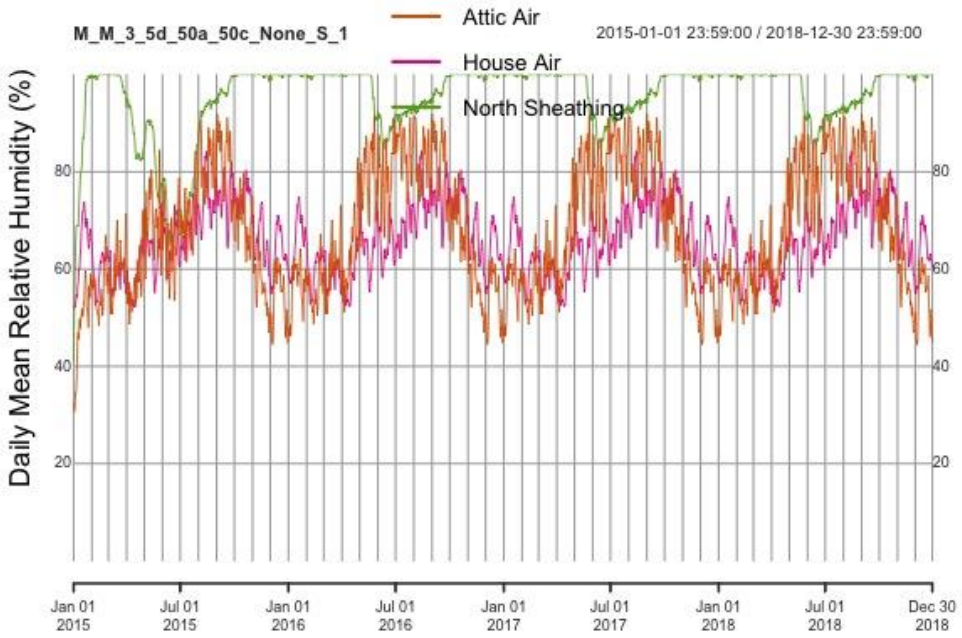

7.2.2.2 Mold Index

Mold index values generally change rather slowly over the course of weeks and months with seasonal trends that are related to relative humidity trends at the moisture node location. In Figure 118, we show an example time series plot of a sealed attic case with no IAQ fan in CZ4 that fails the ASHRAE 160 mold index criteria at the North sheathing location. As the mold index increases, the risk of mold growth increases. We see that a seasonal pattern dominates, where mold risk increases during the heating season (roughly November through March in this case) and is reduced in the cooling season. This cycle repeats year-after-year, eventually stabilizing at a steady maximum value. The mold index is driven by surface relative humidity, which is driven largely by surface temperature in a given attic, and we see that the coldest surface (North sheathing) is the only place to experience mold risk. Notably, the South sheathing and bulk framing experience some elevated RH, but it occurs during the late-winter/early-spring. This pattern is common and is due to the seasonal storage and release of moisture in the wood of the attic. During winter, wood moisture contents increase, storing moisture mass in the structure, and when the structure heats up during spring, that moisture is steadily released into the attic air leading to high attic air moisture and potential risk at all locations.

Figure 118 Mold index. Example time-series plot of mold index values calculated at the North sheathing, South sheathing and bulk attic framing over 4-year simulation period. The North sheathing fails the ASHRAE 160 criteria that mold index remain below 3.

7.2.2.3 Surface Wood Moisture Content

Wood moisture content follows very similar seasonal trends as the mold index and RH values, with increased WMC in the sheathing surfaces during the heating season, followed by drying down to roughly kiln-dry levels below 8%. We show a reasonably moisture safe example in Figure 119 of a 1-story home in CZ3 with a T24 (2008) exhaust fan, where WMC peaks briefly above 20%, while the example in Figure 120 demonstrates a very likely moisture failure, with North sheathing WMC at or above 30% for months consecutively. This latter case is a similar home but with no IAQ fan, located in CZ16.

In nearly all cases, there is a rapid drying to low levels in summer. This drying occurs even in cases with very high winter WMC values, as shown in Figure 120. This rapid and complete drying is facilitated by the vapor permeability of the insulation assembly, which allows both rapid accumulation and removal. This illustrates how these assemblies are at risk of moisture accumulation in the surfaces of the sheathing and bulk framing, but they also benefit from enormous drying potential. As with mold index, we see that the North sheathing has the greatest moisture accumulation, followed by the South sheathing and then the attic framing. Figure 120 shows an exception to this rule, when during the late-spring/early-summer, all three nodes experience very high moisture content, again we hypothesize this is due to the temperature-driven removal of moisture from the North sheathing, which is redistributed to the all nodes.

Figure 119 Wood moisture content. Example time-series plot of surface wood moisture content calculated at the North sheathing, South sheathing and bulk attic framing over 4-year simulation period. This case has somewhat elevated wood moisture content that does not constitute failure.

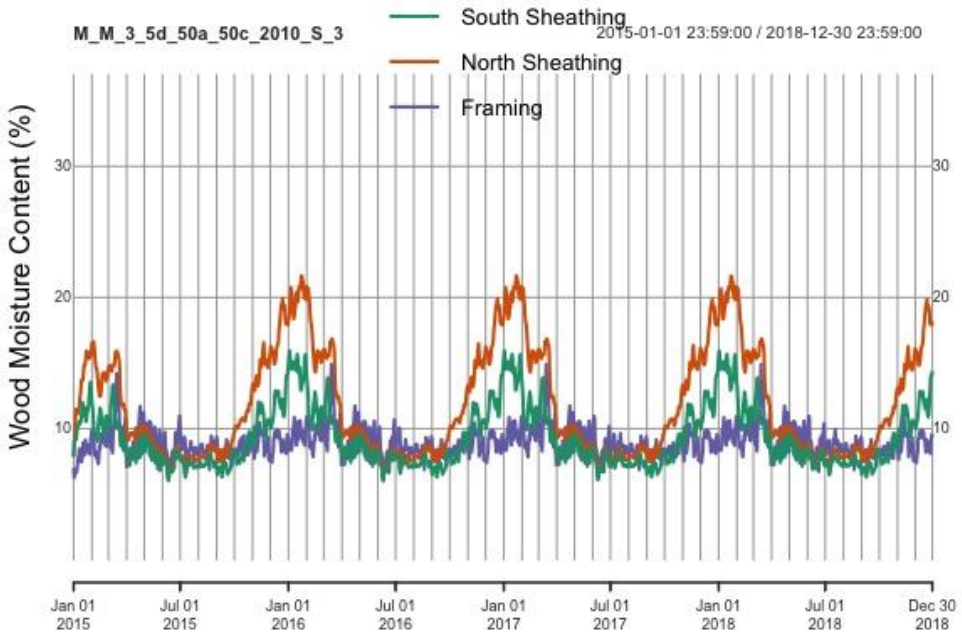

Figure 120 Wood moisture content. Example time-series plot of surface wood moisture content calculated at the North sheathing, South sheathing and bulk attic framing over 4-year simulation period. This case has elevated wood moisture content that constitutes failure.

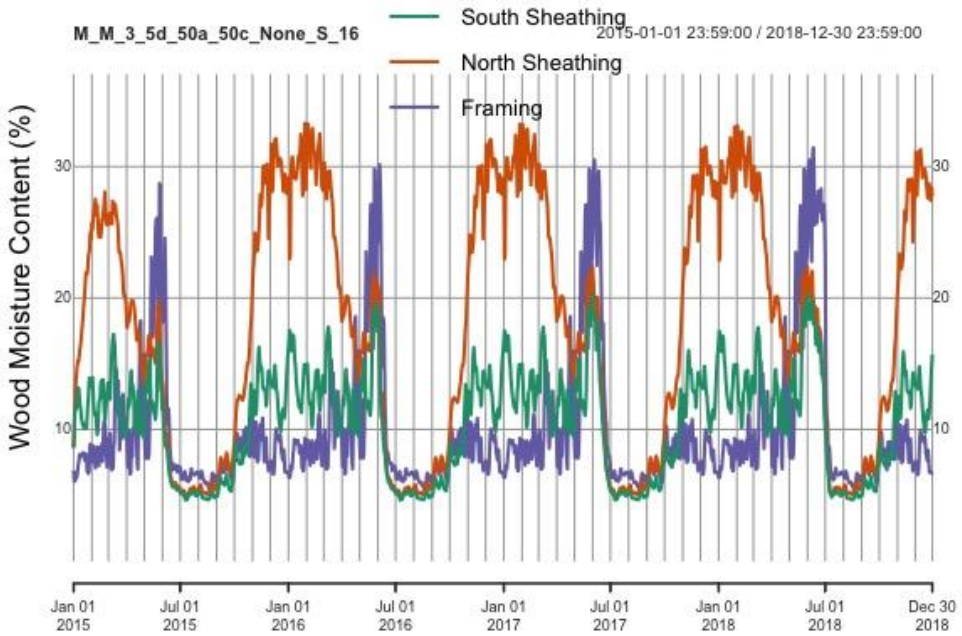

7.2.2.4 Condensed Moisture Mass

Finally, we show the mass that condensed at each time-step for sealed and insulated attics in the REGCAP simulation model on the sheathing and bulk attic framing moisture nodes. Most cases showed little or no hours of condensation through the simulated periods.

Yet, some were clearly problematic, as shown in Figure 121 where the North roof deck surface has substantial condensation occurring from roughly November through March. This is a 1-story home with high moisture gains and an exhaust fan sized to T24 (2008) located in CZ1 Arcata. In this bad case, there are also marginal periods of condensation at the South roof deck and attic framing nodes, which are obscured in this plot by the dominant North roof deck condensation. In most situations, condensation events occurred only in the heating season, driven by cold outside temperatures and typically associated with clear night sky conditions.

Yet, as shown in Figure 122, condensation also occurred in some cases during warmer weather and at the South roofdeck sheathing surface. This example home is 1-story with high moisture gains in CZ13 (Fresno). We note that condensation is occurring at the South roofdeck not during the coldest heating season periods, but rather in the springtime. This result was unexpected, so we assessed some example periods where we observed this South roof deck condensation. They occurred when south roofdeck moisture content was high (e.g., 24%) and the surface temperature was being warmed by the sun up to above 40°C. This drove the vapor pressure at the surface above the saturation vapor pressure, and moisture then condensed on the hot roofdeck.

This effect is similar to the elevated springtime attic air humidity levels we identified in the prior sections, which we hypothesize are the result of moisture that has been stored in the roof deck during the heating season being driven into the attic air during relatively warmer periods.

Figure 121 Time-series of condensed mass in a sealed and insulated attic at each roof deck and attic framing node for an example 1-story home with high moisture gains in CZ1 (Arcata) with a T24 (2008) exhaust fan.

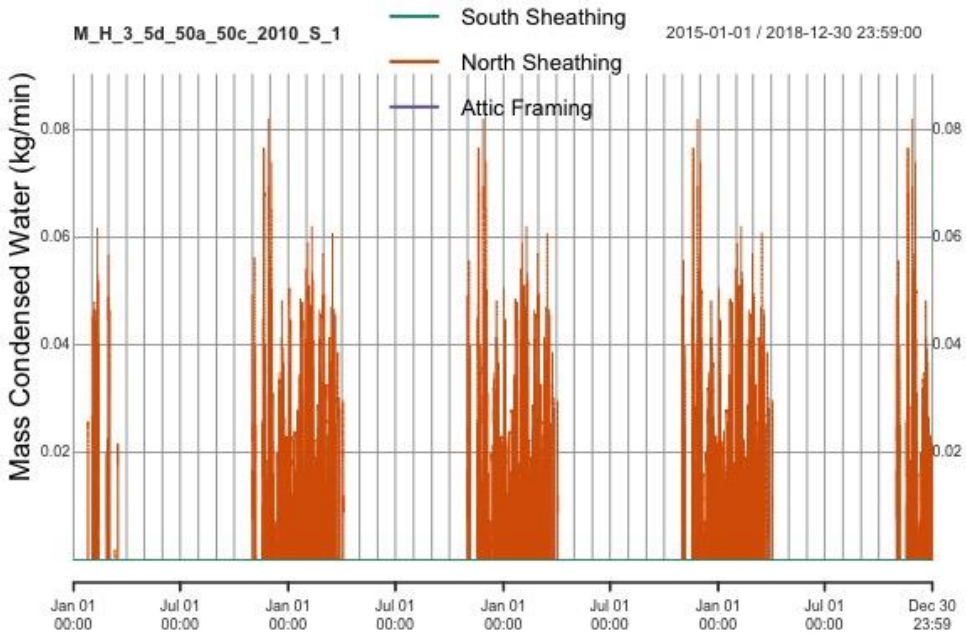

Figure 122 Time-series of condensed mass in a sealed and insulated attic at each roof deck and attic framing node for an example 1-story home with high moisture gains in CZ13 (Fresno) with a T24 (2008) exhaust fan. Note condensation occurring on South roofdeck sheathing and attic framing during early spring.

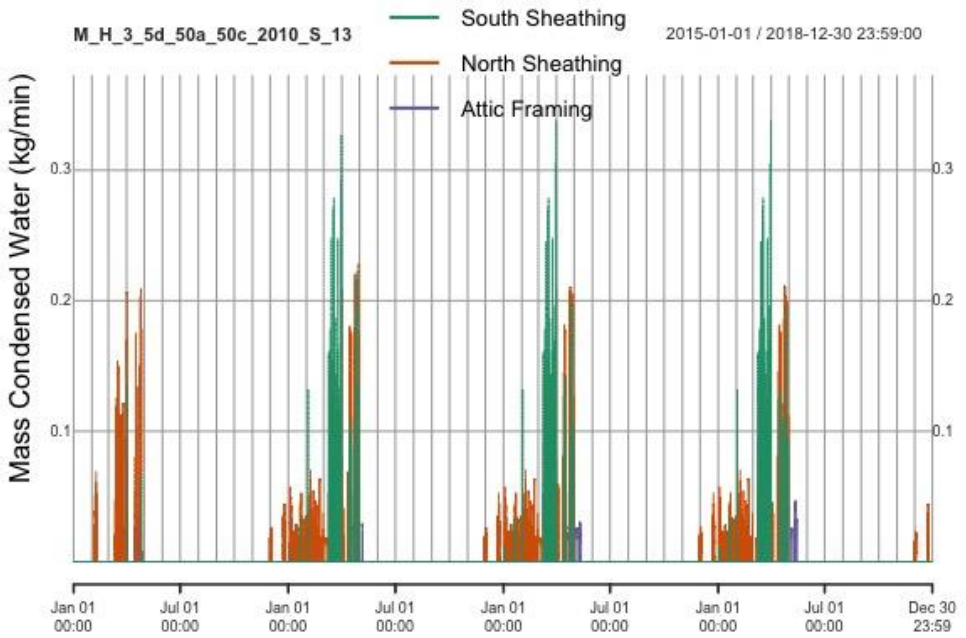

7.2.2.5 Vapor Pressure

The vapor pressure relationship between the attic and living space air volumes is also quite important in this modeling work, as the mixing of these air volumes and their moisture contents can be a key determinant in moisture failure or robustness. In Figure 123 we show a 4-year time-series plot showing the daily average vapor pressure difference between the attic and living space. This is a 1-story home with a T24 (2008) exhaust fan in CZ13. Most of the time, the living space has a vapor pressure that is equal to or higher than the attic (negative values in plot), which suggests that overall the house is the source of moisture for this attic. Each year, this trend is reversed during early-spring, when as noted previously, moisture stored in the roof sheathing is baked out by rising temperatures into the attic air. During these times, the attic has much higher vapor pressure than the house. This plot suggests that for this case, mixing the living space and attic volumes will increase moisture in the attic air during winter, and should facilitate drying of the attic air during spring. Intentional mixing should therefore be avoided during the heating season and encouraged during the spring.

We show a daily diurnal vapor pressure plot for an example home in Figure 124, which illustrates the ping-pong effect commonly referenced in the attic moisture literature. When the sun shines on the roof, moisture is baked out of the sheathing, dramatically increasing the vapor pressure relative to the attic and living space air nodes. When the sun goes down, the trend reverses and the sheathing re-absorbs the water vapor from the attic air at a lower vapor pressure. A similar though less pronounced pattern also occurs with the attic and living space air volumes, where daytime solar heating of the attic (and moisture drive from the sheathing) elevates the attic relative to the living space during daytime hours, and again the reverse occurs at night, with the house transferring moisture back to the attic, and from the attic air to the sheathing.

Figure 123 Vapor pressure difference Attic - Living Space. Example time-series plot of the calculated vapor pressure difference between the attic and living space air volumes. Positive values indicate attic has higher vapor pressure than living space.

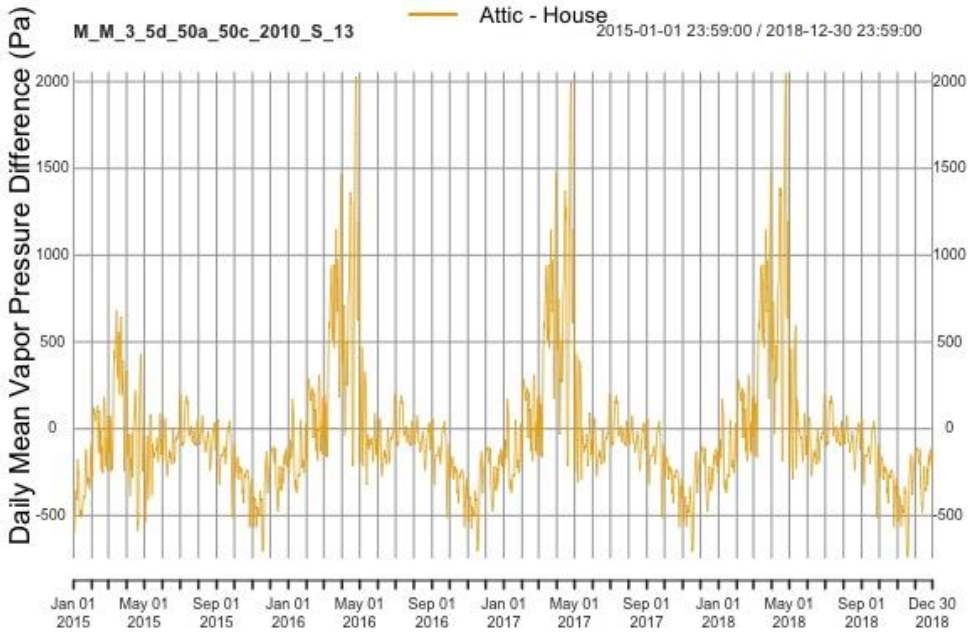

Figure 124 Vapor pressure diurnal trends for example sealed attic, showing hourly averages over the hours of the day for sheathing, attic, living space and outside air.

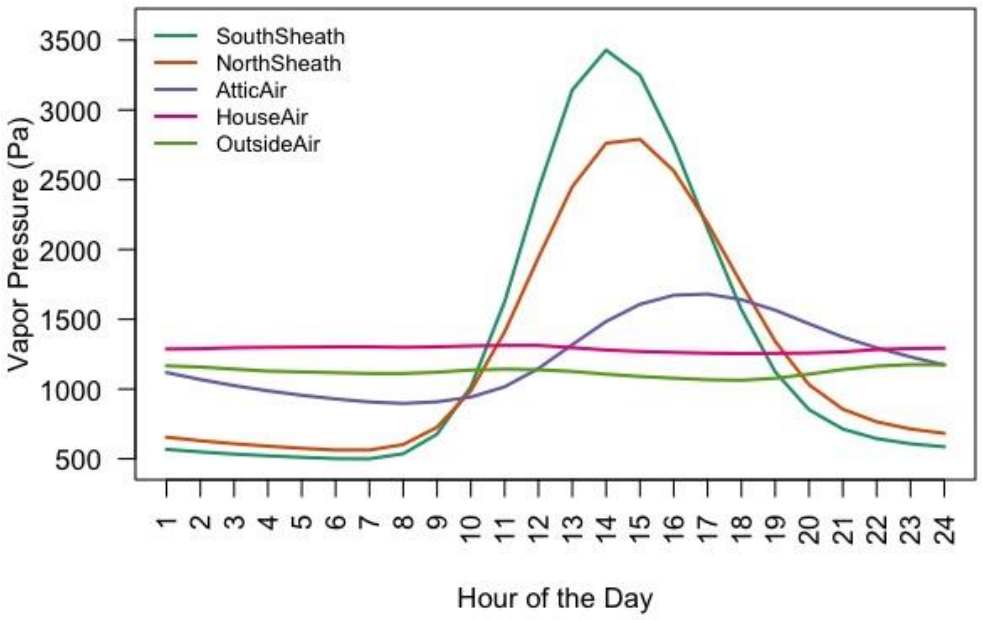

7.2.3 Simulation Parameter Sensitivity Analysis

In Table 31 we show the mean values for each moisture outcome aggregated by the simulation parameters at each moisture node (North and South sheathing and attic framing), including mold index failure rate, maximum mold index, maximum 7-day wood moisture content and total condensed mass[11] over the 4-year simulation period. The parameters include the moisture intervention measures outlined in Section 6.3, as well as the simulation parameters described in Section 6.1.2. Within a single parameter category, all cases are matched identically aside from the parameter value, but the simulated cases do vary between the parameters. For example, the cases simulated with and without air impermeable insulation per the CRC (2018) are different than the cases simulated with different IAQ fan airflows. See Section 6.1.2 for a discussion of the simulated parameters in Table 13 and Table 14. The values for each parameter are sorted according to the North sheathing mold index failure rates within that parameter category (e.g., CZ1 had the highest mold index failure rates, so it is listed first in climate zone category, followed by CZ13, 2, 5, etc.). This table does not show the variability of results within a parameter category, but it facilitates an overall understanding of the impacts of the parameter on the various moisture metrics and locations in the attic (as discussed briefly below and in greater details in Section 7.2.4.1 through 7.2.4.11).

As expected, sealed attics had far and away the highest levels of moisture risk across moisture outcomes. The differences were smallest for the 7-day wood moisture content metrics, where HPA and vented attics were within a few percent of the sealed attic North sheathing, and in fact had marginally higher 7-day moisture contents at the South sheathing and attic framing relative to the sealed attic cases.

Climate zone was a primary driver of moisture risk in the sealed attic simulations, with more than a third of all cases in CZ1, 13 and 2 failing the mold index metric at the North sheathing. Notably, the order of climate zone risk is not intuitive based on simple climate parameters. For example, high sheathing moisture risk is typically associated with colder weather, yet the coldest climate in the state—CZ16 (Blue Canyon) in the Sierra Nevada mountains—is among the safest of locations. This runs counter to design guidance in the CRC Table R806.5, which assumes that moisture risk increases with colder climates. In addition, the CRC (2016) requires a vapor retarder on the surface of fibrous insulation in CZ14 and 16, both of which appear to be some of the safest locations, from a mold risk perspective. In general, it appears that Coastal climates up and down the state, as well as some central valley locations had the highest moisture risk at the North sheathing. Wood moisture and condensation risks by climate zone are similar though not exactly aligned with the North sheathing mold index risk. For example, CZ5 has the second highest condensation levels, yet in terms of mold risk, it is only the fourth most risky. The climate regions are sorted by the North sheathing mold index risk, yet the ordering is substantially different for the bulk attic framing mold index risks, where CZ 2, 3, 5-

[11] As described in Section 3.1.3, the total condensed mass is the sum of cyclic periods of wetting and subsequent re-evaporation. The condensed moisture does not all remain in the wood; this is not a cumulative sum of moisture in the wood.

8 and 13 had the highest risks. So, the climate drivers of mold risk may be different at sheathing locations vs. the general attic framing.

Moisture risks are much higher in 1-story prototype homes, as well as in homes with high internal moisture generation rates. Both of these parameters drove all moisture metrics up substantially relative to the larger 2-story homes with medium moisture gains. Again, the wood moisture metrics appear to be the least sensitive to changes in the simulation parameters. Increased internal moisture gains increase indoor moisture levels and increase overall moisture risks in the sealed attic. The 1-story prototype homes have higher risk, because they are smaller homes with the same moisture generation rates, and their ventilation rates are lower, due to less natural infiltration and smaller IAQ fan airflows.

A number of parameters are related to outside air exchange, and these consistently show that increased outside air exchange reduces moisture risk in sealed and insulated attics. This is evident as envelope leakage increases from 1 to 3 and 5 ACH_{50}, moisture risk is reduced. Similarly, increasing the airflow through the IAQ fan reduces moisture risks, as does increasing the leakage area in the sealed attic from 20 to 50 and 80% of house envelope leakage. When outside air was mechanically introduced into the attic volume, moisture risks dropped dramatically.

While increased outside air exchange reduced moisture risk, greater levels of mixing of the living space and attic air volumes tended to marginally increase risk. This is evident that as ceiling leakage increases from 20 to 50 and 80% of envelope leakage, moisture risks increase slightly. Increasing duct leakage also enhances mixing of the living space and attic volumes, as does the introduction of an HVAC supply register in the attic. Both of these parameters showed increased moisture risks when mixing was increased, such that moisture risks were highest at 8% duct leakage and with a supply register in the attic (vs. no register).

Much moisture risk was driven by cold roof sheathing temperatures, and as expected, parameters that increased roof deck temperatures during cold nights reduced moisture risks. Both the placement of air impermeable insulation above the roof deck per the CRC (2018), and the use of tile roofing vs. asphalt shingles, showed reduced moisture risks. These features add thermal resistance towards the exterior of the sheathing, which warms the first condensing surface temperatures in the roof assembly—reducing surface RH, condensation and mold risk at the wood sheathing.

Table 31 Mean moisture outcomes aggregated by each simulation parameter, sorted from worst to best in terms of North sheathing mold index failure rates. Within a single parameter category, all cases are matched identically aside from the parameter value, but cases do vary between parameters.

	Mold Index Failure (%)			Max Mold Index			Max 7-Day WMC (%)			Condensed Mass, 4-Year Total (kg)		
Parameter	**North Sheathing**	**South Sheathing**	**Attic Framing**	**North Sheathing**	**South Sheathing**	**Attic Framing**	**North Sheathing**	**South Sheathing**	**Attic Framing**	**North Sheathing**	**South Sheathing**	**Attic Framing**
Attic Type												
Sealed	22%	3%	19%	1.5	0.5	1.1	22%	16%	14%	1331	514	109
HPA	0%	0%	0%	0.2	0.1	0.1	19%	17%	17%	41	3	2
Vented	0%	0%	0%	0.0	0.0	0.1	17%	17%	17%	0	0	0
CEC Climate Zone												
1	58%	16%	15%	3.7	1.0	1.0	28%	20%	15%	3569	711	60
13	41%	1%	34%	2.5	0.6	2.1	25%	20%	16%	1617	598	161
2	37%	1%	27%	2.3	0.6	1.7	27%	20%	17%	1807	734	215
5	26%	20%	24%	1.5	1.1	1.5	22%	15%	14%	2968	1804	354
6	26%	7%	37%	1.4	0.7	2.2	19%	16%	16%	1059	814	193
3	24%	12%	23%	1.9	0.8	1.4	24%	18%	15%	1534	627	178
12	20%	1%	12%	1.9	0.4	0.8	25%	20%	13%	1112	247	59
7	14%	1%	27%	0.9	0.4	1.6	18%	14%	14%	521	471	115
4	13%	1%	13%	0.9	0.2	0.8	21%	15%	13%	791	302	70
8	10%	1%	30%	0.8	0.5	1.8	18%	15%	15%	798	693	125
11	9%	0%	6%	0.7	0.1	0.4	24%	16%	12%	460	135	37
16	3%	0%	18%	0.2	0.1	1.0	20%	15%	14%	417	187	77
9	1%	0%	7%	0.2	0.1	0.4	15%	12%	12%	225	203	36
14	1%	0%	7%	0.1	0.0	0.4	16%	11%	10%	235	128	27
10	1%	0%	20%	0.4	0.3	1.3	17%	14%	15%	390	534	105
15	0%	0%	0%	0.0	0.0	0.0	12%	9%	9%	11	2	1
Prototype Home												
1-story, 2,100 ft^2	27%	8%	35%	1.7	0.7	2.1	22%	16%	16%	1909	968	215
2-story, 2,700 ft^2	8%	0%	3%	0.8	0.1	0.2	20%	15%	11%	296	54	12
Internal Moisture Gains												
High (11.6 kg/day)	33%	8%	25%	2.1	0.7	1.5	23%	17%	15%	2445	795	150
Medium (6.5 kg/day)	13%	2%	11%	1.0	0.2	0.7	20%	15%	13%	729	157	36
Envelope Air Leakage												
1 ACH50	30%	7%	40%	1.8	0.8	2.4	22%	17%	16%	1541	1142	254

3 ACH50	10%	4%	15%	0.8	0.3	0.9	19%	15%	13%	654	403	97
5 ACH50	9%	0%	9%	0.7	0.1	0.6	19%	15%	12%	418	166	50
Duct Leakage												
8%	8%	0%	0%	1.1	0.0	0.1	22%	16%	12%	391	2	7
5%	0%	0%	0%	0.9	0.0	0.1	22%	16%	12%	317	2	7
2%	0%	0%	0%	0.8	0.0	0.1	21%	16%	12%	243	1	6
Attic Leakage												
20%	26%	8%	38%	1.6	0.8	2.3	21%	17%	16%	1458	1026	236
50%	7%	1%	8%	0.7	0.2	0.5	19%	14%	12%	138	1	3
80%	4%	0%	4%	0.5	0.1	0.3	19%	14%	11%	201	42	16
Ceiling Leakage												
20%	17%	4%	22%	1.1	0.5	1.3	20%	15%	14%	871	597	139
50%	15%	3%	20%	1.0	0.4	1.2	20%	15%	14%	783	495	116
80%	13%	3%	18%	1.0	0.4	1.1	20%	15%	13%	719	432	102
IAQ Ventilation Fan Sizing												
None	56%	20%	38%	3.2	1.5	2.3	26%	20%	17%	4306	1424	212
T24 2008	9%	0%	5%	0.9	0.1	0.3	20%	15%	12%	399	31	15
T24 2008 + 40%	2%	0%	0%	0.3	0.0	0.0	18%	13%	10%	107	2	0
IAQ Fan Type												
Supply	38%	6%	17%	2.2	0.6	1.1	24%	18%	15%	2158	417	80
Exhaust	9%	0%	5%	0.9	0.1	0.3	20%	15%	12%	399	31	15
Roof Finish Material												
Tile	9%	0%	5%	0.9	0.1	0.3	20%	15%	12%	399	31	15
Asphalt Shingles	6%	0%	19%	0.8	0.1	1.2	20%	14%	14%	732	95	68
R20 Roof Deck Insulation vs. T24 (2016)												
R20	3%	0%	3%	0.5	0.0	0.2	19%	14%	11%	NA	NA	NA
T24 2016	0%	0%	0%	0.4	0.0	0.0	19%	14%	11%	143	1	3
Moisture Interventions												
HVAC Supply Register in Attic (50 cfm per 1,000ft^2 ceiling area)	27%	7%	16%	1.7	0.6	1.0	22%	17%	14%	1816	467	71
None	22%	7%	14%	1.5	0.5	0.9	21%	16%	13%	1604	486	76
Air Impermeable Insulation Above Roof Deck (per CRC 2018)	15%	5%	8%	1.0	0.4	0.5	19%	15%	12%	524	100	28
Outdoor Air Supply Fan into Attic (20	5%	0%	0%	0.4	0.0	0.0	18%	14%	10%	198	4	0

cfm per 1,000 ft^2)												
Outdoor Air Supply Fan into Attic (50 cfm per 1,000 ft^2)	0%	0%	0%	0.1	0.0	0.0	17%	14%	10%	38	0	0
Vapor Retarder on Batt Insulation	0%	0%	1%	0.0	0.0	0.0	9%	7%	11%	0	0	0

Based on this sensitivity analysis, the following parameters were consistently the most important in determining moisture risk at the North sheathing (presented in order of importance):

- Climate zone
- IAQ fan sizing
- House prototype
- Envelope airtightness
- Attic leakage
- Internal moisture gains
- IAQ fan type (supply vs. exhaust)

The critical variables for predicting moisture risk at the bulk attic framing node were similar, yet distinct from the North sheathing, as follows:

- House prototype
- Attic leakage
- Envelope leakage
- Climate zone
- IAQ fan sizing
- Internal moisture gains

Overall, we observe the following:

- Outside air ventilation by infiltration and/or mechanical ventilation of the home can mitigate moisture risk, though fan type can be important, as well.
- Higher interior moisture gains place the home at risk (though substantially less than having reduced ventilation rates).
- Smaller, single-story homes increase risks for two reasons—higher moisture loads per units volume and reduced ventilation rates due to limited stack effect.
- Climate zones with higher average outdoor RH and less sunshine in California pose particular risks due to outdoor moisture and temperature conditions, and risk is not necessarily greatest in the coldest locations.
- Ceiling leakage and duct leakage had marginal impacts on moisture risk, in either direction.
- Risk factors are different for North sheathing and bulk framing locations. They overlap substantially, but are not identical. Yet, trends are similar, for example, the 1-story homes have increased risk at both locations, and increasing fan airflow or envelope leakage reduces risk at both locations.

7.2.4 Factors Affecting Mold Index Failure Risk

7.2.4.1 Location in the attic

Three relevant moisture nodes were simulated in the sealed and insulated attics—north ridge sheathing, south ridge sheathing and attic bulk framing. The sheathing nodes were located at the interface between the insulation and the roof sheathing, which forms the first condensing surface in these assemblies. The bulk attic framing represents the moisture conditions for general wood throughout the attic, including truss framing, blocking, etc. These nodes differ mainly by their heating due to solar exposure, cooling at night by radiation and exposure to outdoor temperatures. The south sheathing experiences more solar heating compared to the north sheathing. The bulk wood is isolated from these radiation and external weather effects.

Location within the attic had strong impacts on ASHRAE 160 mold index failures, as shown in Figure 125. The north sheathing failed in 18% of all cases, while the bulk attic framing failed in 19% of cases and 4% for the south sheathing. We assessed if North sheathing failures were related to South sheathing failures using a confusion matrix. We found that both nodes were safe in 939 cases, and both nodes failed mold index criteria in 46 cases, while in 159 solely the North sheathing failed. In no cases did the South sheathing fail, unless the North sheathing also failed. In fact, the south sheathing failures only occurred in those cases that also had the very highest north sheathing mold index values (i.e., > 5). We performed a similar analysis comparing North sheathing and bulk framing nodes. We found that both nodes were safe in 864 cases, and both nodes failed in 140 cases. There were then 65 cases where North failed and bulk passed, and there were 75 cases where bulk failed and North was safe. The North and bulk nodes are clearly related, but the behavior is distinct enough that we will report moisture metrics for both nodes from here onward.

We note that the sealed and insulated attics research literature does not contain numerous accounts of mold growth and related moisture failures on bulk attic framing (Less et al. (2016)). Yet, these results suggest these locations are at least as risky, if not more so, than the north sheathing location.

One possible explanation is that most moisture and durability assessments in sealed attics have occurred in cold climates, where outside moisture levels are sufficiently low in the heating season, that living space and attic air are quite dry. It could be the particularly cold ambient temperatures that drive failures at the North roof deck, despite relatively low moisture levels in the attic and living space air.

Furthermore, most sealed and insulated attic studies have focused on sheathing wood moisture content and have not measured (or reported) attic framing moisture content or investigated the possibility of surface mold at this location. One exception is Ueno & Lstiburek (2016) who showed visual observation of mold on a vertical truss member in an Orlando, FL attic insulated at the roof deck with a netted and blown fiberglass insulation. They also observed daytime solar driven moisture at or near saturation in the sealed attic. In another comparison of sealed attics insulated with open and closed cell spray polyurethane foam insulation, Miller, Railkar, Shiao, & Desjarlais (2016) found that open cell insulation led to attic air at or near saturation

from 12pm to 8pm on warm/hot days. Stored moisture was being driven from the roof deck out through the vapor permeable insulation and into the attic air. Closed cell foam, due to its lower vapor permeability, did not exhibit this behavior. They did not report mold growth or long-term mold index estimates. Nevertheless, these findings elsewhere in the literature support our result that sealed and insulated attics with highly air and vapor permeable materials can experience high attic moisture levels and potential mold growth, driven by solar irradiance and warm/hot ambient temperatures.

Figure 125 Overall mold index failure rates across the three moisture node locations in sealed and insulated attics.

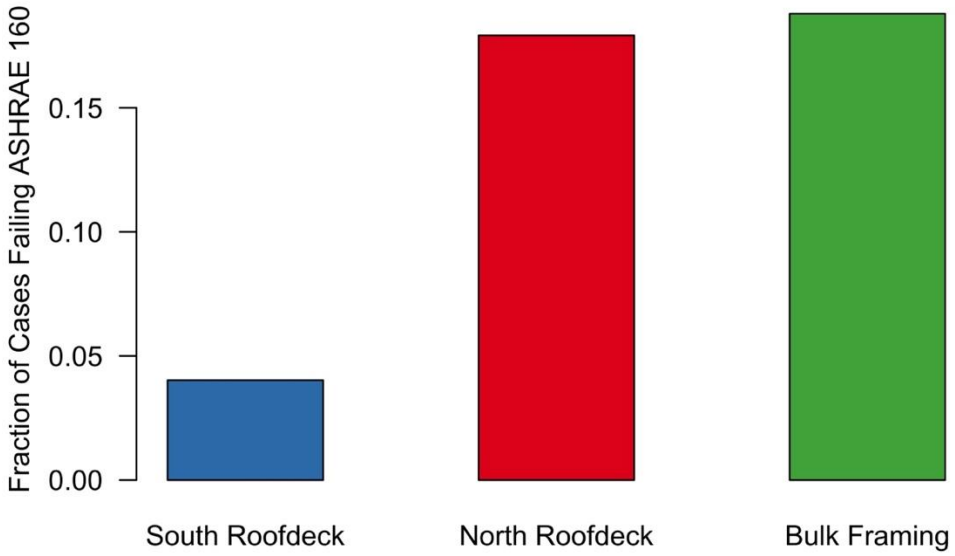

The North sheathing failures are driven largely by cold outside temperatures, and are exacerbated by elevated outdoor and indoor humidity levels. Mold index values increase at the North sheathing during the coldest periods of winter, driven by condensation and elevated RH near saturation at the insulation-sheathing interface.

In contrast, the bulk attic framing mold index values were more likely to increase during the spring and very early summer periods. These were caused by the seasonal storage and release of moisture in sealed and insulated attics. Wood moisture content increased at the sheathing locations during winter in the attics, and this stored moisture was then baked out of the wood by warmer ambient temperatures and solar radiation on the roof deck during the spring. This springtime moisture release, coupled with very low ventilation rates in the attics, led to elevated RH in the general attic air volume (see an example plot in Figure 117).

Condensation occurred predominantly on the North sheathing surfaces, with smaller amounts on the South sheathing, and the least condensation on the bulk framing (see Figure 126). Despite this lack of condensation at the general attic framing, the attic air volume was elevated at or above 80% RH for long periods in some cases (see an example plot in Figure 117), which explains the number of bulk framing mold index failures.

Figure 126 Annual condensed moisture mass across the three moisture node locations in sealed and insulated attics.

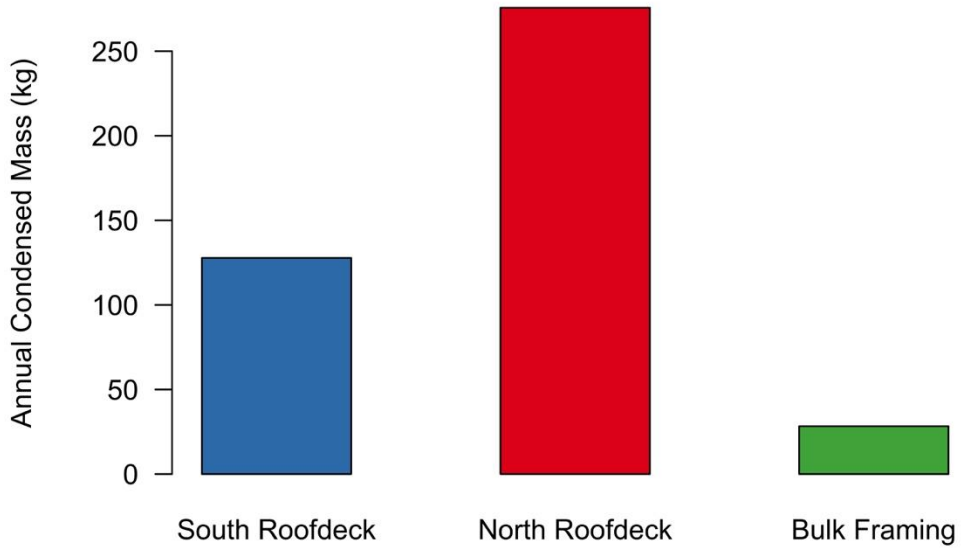

These seasonal mold index dynamics are illustrated quite clearly in the example time series plot in Figure 127, which shows the mold index values at all three moisture nodes for an example home over the simulation period of 4-years. This home has both north sheathing and bulk attic framing failures, but these increase during different time periods, as described above. The north sheathing location (orange line) rises rapidly each winter, beginning roughly in November and finally declining again each April. This corresponds with cold outside temperatures. The attic bulk framing (purple line) follows a similar, though seasonally shifted pattern. Its behavior is largely dormant during each winter, but it rises rapidly every year beginning in late-February and March. These periods correspond with the seasonally stored moisture being baked out of the roof deck and into the sealed attic air volume, where moisture levels can exceed the 80% critical mold growth threshold and air temperatures are conintuously supportive of mold growth (18-25˚C).

Past work in sealed and insulated attics has largely highlighted the moisture risks in cold locations. Yet, even in cold climates, average winter temperatures are often cold enough to suppress mold growth entirely, despite increasing wood moisture content and surface condensation events. This is not the case in California, where many locations have winter nighttime temperatures that are sufficient to drive condensation, while daily average temperatures are not cold enough to suppress mold growth. This opens nearly the entire winter and early spring periods as susceptible mold growth on sheathing surfaces. Similarly, in sealed and insulated attics, the bulk framing and attic air should more or less always be within the temperature range amenable to mold growth (roughly 5-40°C), so that all hours with elevated RH are problematic, whereas at the North sheathing, the highest RH often occurs during periods below 5°C, which dampens mold growth potential.

Figure 127 Time-series illustration of mold index behavior by season and location. An example 1-story home with high interior moisture gains, 3 ACH_{50}, and 5% duct leakage in CEC climate zone 3 (Oakland).

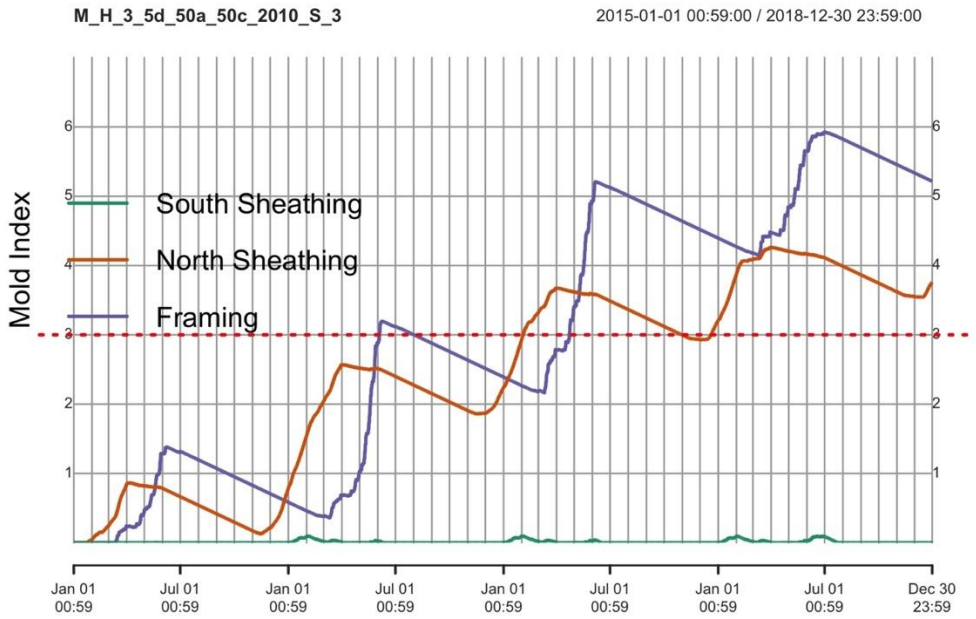

7.2.4.2 Climate Zone

Climate zone was one of the most important factors in determining moisture risk in sealed and insulated attics. We show the fractions of cases that failed in each CEC climate zone, for each moisture node in Figure 128. North sheathing and bulk framing locations show strong climate zone trends, but the trends are not the same.

For the north ridge sheathing location, the highest risk location is clearly CZ 1 (Arcata), which is the second coldest overall climate zone (after CZ16). CZ1 is situated west of the Northern Coastal Range and has a moist, cool climate influenced greatly by the conditions of the Pacific Ocean. Past work in attic moisture research, has consistently shown that cold marine climates along the west coast of the U.S. and Canada have particularly high moisture risks (Finch, LePage, Ricketts, Higgins, & Dell, 2015; Forest & Walker, 1993; Morrison Hershfield, 2014; Roppel, Norris, & Lawton, 2013). Even vented attics can have mold problems in these climates, due to a combination of high ambient relative humidity and less solar heating of attic surfaces.

Elevated risk in CZ 1 is not surprising, given past work on attic moisture in cold marine climates, but locations like CZ 13 (Fresno) had unexpectedly high moisture risk. Similar surprises came with bulk framing failures in CZ 6-8. These climates are mild coastal zones, which have the highest dew point temperatures of all CEC zones, suggesting the outside air is quite humid (relative to the rest of the state). This may drive elevated living space and attic moisture loads, combined with low cooling levels and minimal dehumidification. It is not clear why CZ13 is high risk. It does not stand out on any particular weather factor (see summary in Table 23), being neither the coldest, nor hottest, most humid, windy (or still). Ventilation air

flow rates are average in CZ13 cases. These results show that risk is driven by a complex interaction of building and weather-related factors that are not straightforward or intuitive.

Figure 128 Fraction of all cases ran in each CEC climate zone that failed the ASHRAE 160 mold index criteria (>3) for each moisture node.

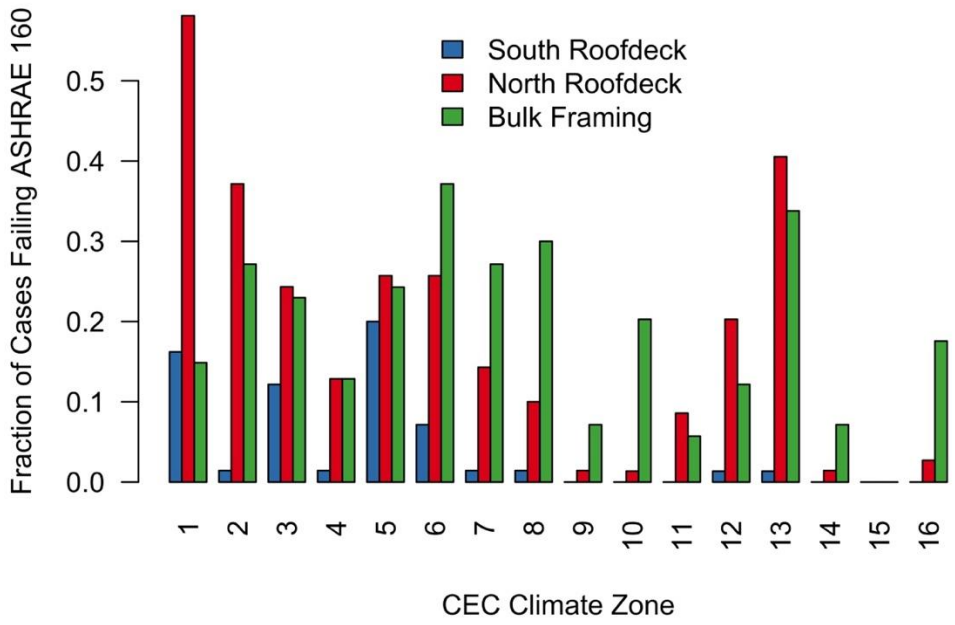

7.2.4.3 House Prototype

In Figure 129 (North Sheathing) and Figure 130 (Bulk Framing), we illustrate the increased risk of mold index failure in 1-story prototype homes by comparing the fraction of cases that failed for the 1- and 2-story prototype homes in each CEC climate zone. For North sheathing failures (excepting CZ1), we see that the 1-story homes consistently fail the mold index criteria at rates of 5-70%, while the 2-story homes are consistently safe in most locations, except CZ1-6 and 12-13. Overall failure rates are 8% and 27% for 2- and 1-story homes, respectively. The attic bulk framing failures show an even more stark contrast between house prototypes, with the 2-story homes having 3% failures, while 1-story cases failed in 35% of all cases, spread across nearly all climate zones.

Figure 129 North sheathing mold index failures comparison by house prototype in each CEC Climate Zone.

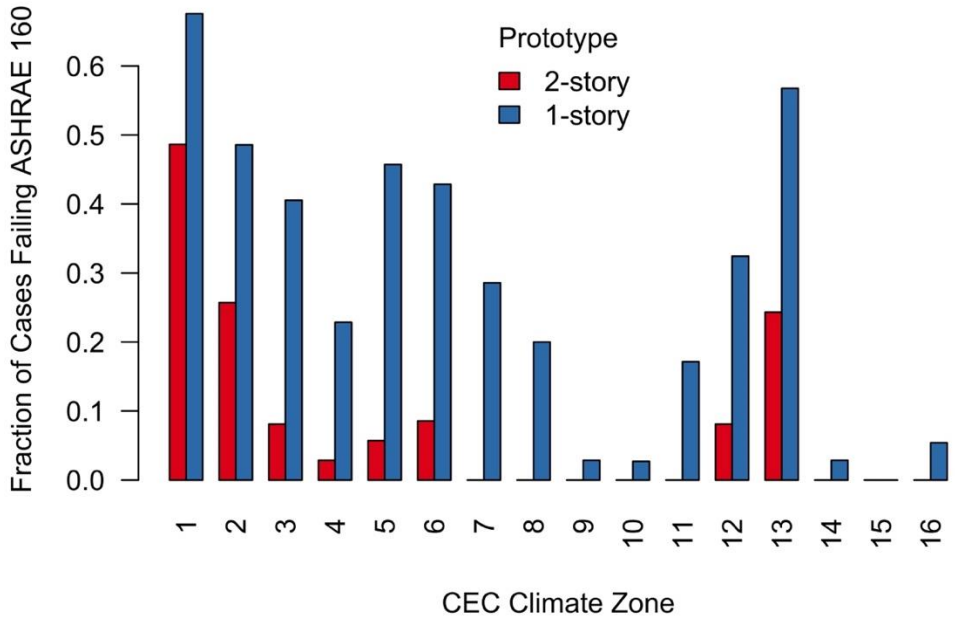

Figure 130 Attic bulk framing mold index failures by house prototype in each CEC Climate Zone.

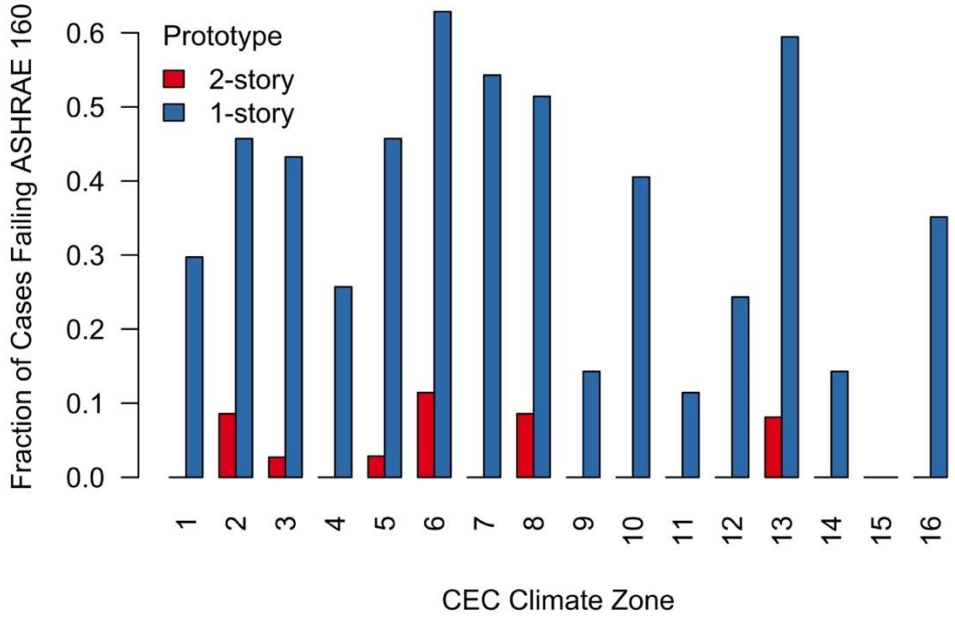

Maximum 7-day mean wood moisture content is compared between house prototypes for North sheathing (Figure 131) and bulk framing (Figure 132) locations, and we see that values are quite similar between prototypes at the North sheathing, while the bulk framing shows substantially lower maximum WMC in the 2-story homes. Annual condensed moisture mass, on the other hand, shows trends similar to the mold index calculations (see North sheathing in Figure 133

and South sheathing in Figure 134). North sheathing condensation is elevated in CZ 1-8 and 12-13, primarily for 1-story homes, while South sheathing condensation was elevated in the majority of climates for 1-story prototype homes.

Figure 131 North sheathing maximum 7-day wood moisture content by house prototype in each CEC climate zone.

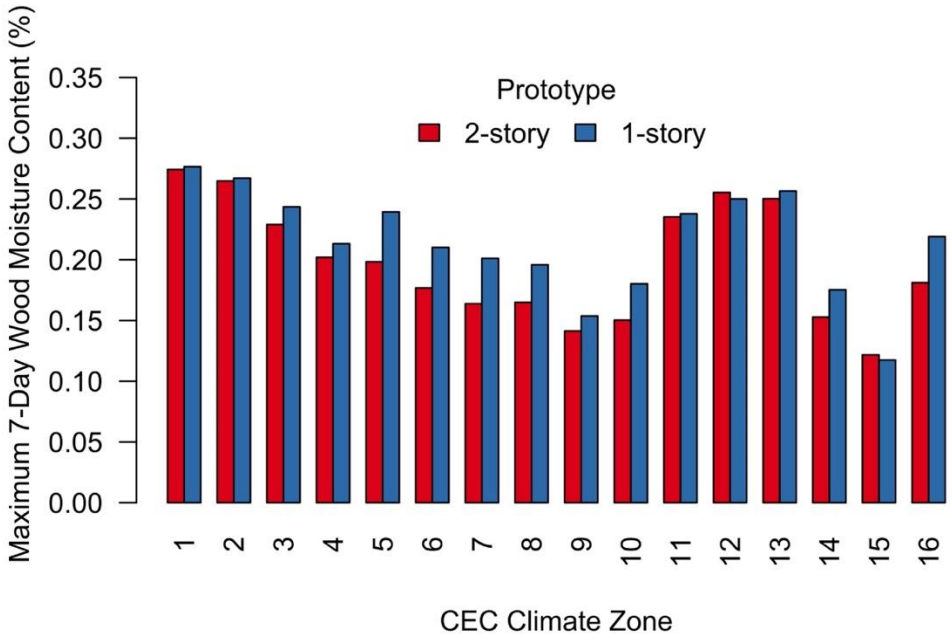

Figure 132 Attic bulk framing maximum 7-day wood moisture content by house prototype in each CEC climate zone.

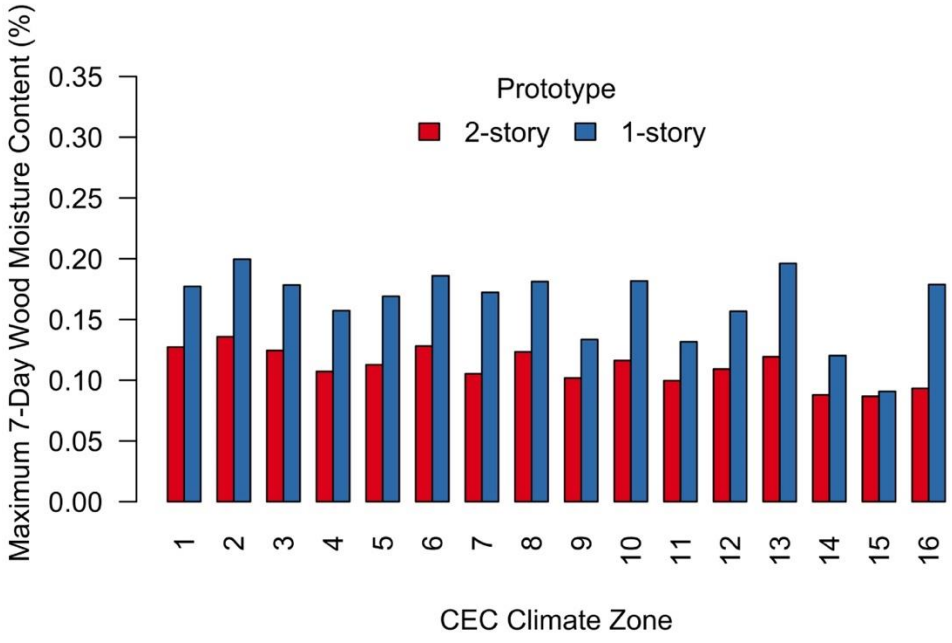

Figure 133 North sheathing annual condensed mass of water by house prototype in each CEC climate zone.

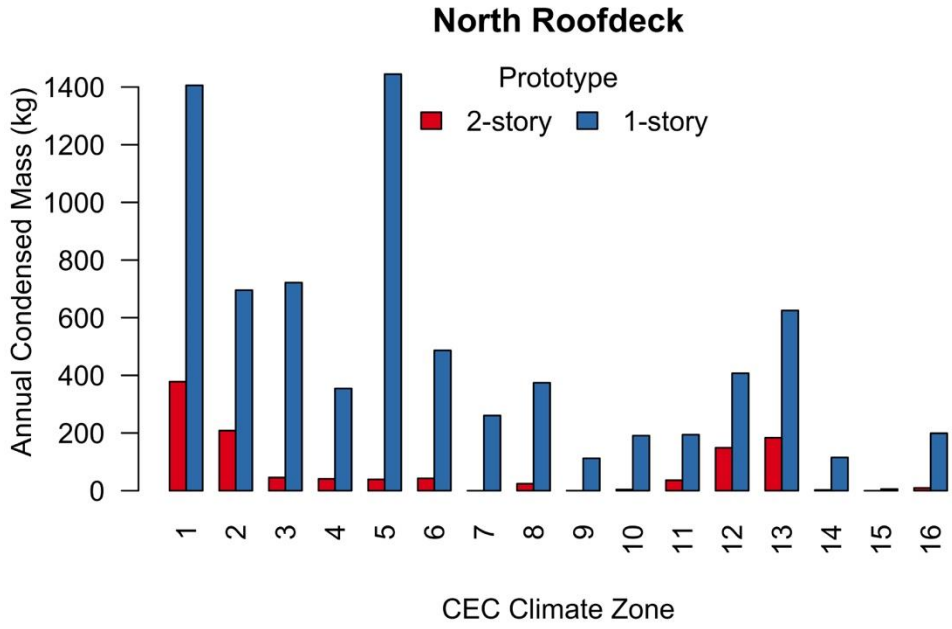

Figure 134 South sheathing annual condensed mass of water by house prototype in each CEC climate zone.

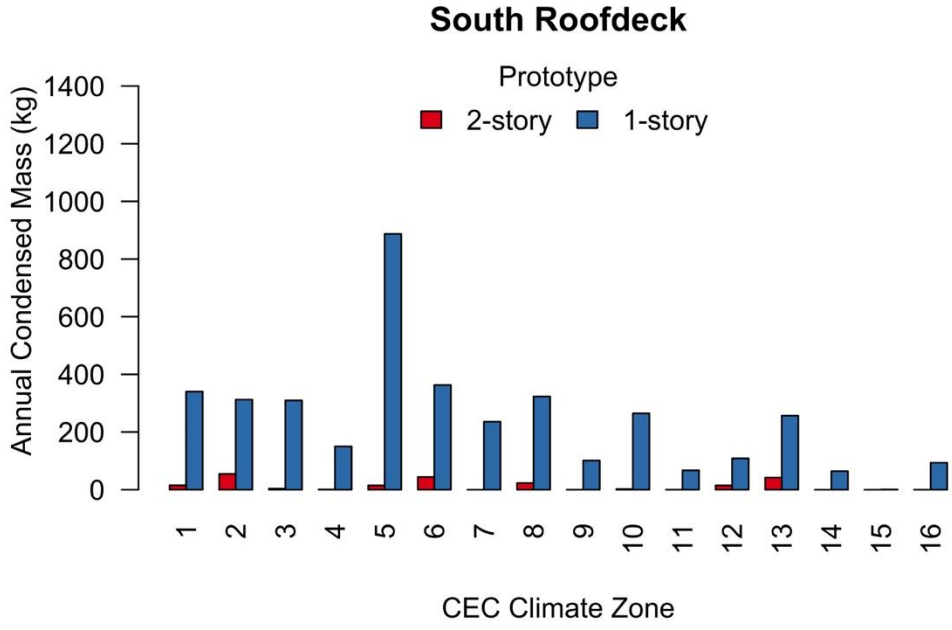

We show the monthly mean exchange rates for the attic and living space, compared between house prototypes in Figure 135. We see clearly that the 2-story homes have higher mass exchange rates. In the 1-story homes, the house and total mass flows are roughly 30% lower than their 2-story counterparts, and the attic mass flows are roughly 55% lower. The monthly

mean vapor pressures in the attic and living space are pictured in Figure 136. We see that 1-story homes have higher vapor pressures both in the living space and attic, which is especially accentuated in the 1-story attic volume during late winter and spring. The 2-story homes have similar vapor pressure in the attic and living space during winter, whereas the 1-story have elevated moisture in the living space air. This trend then reverses in spring.

Why is risk of mold growth and condensation so elevated in 1-story homes? First, they are smaller, yet have the same indoor moisture emissions as the larger 2-story homes. This leads to elevated living space moisture, which then leads to elevated attic moisture. Second, 1-story homes have much lower stack-induced natural infiltration, so their ventilation rates are lower. Finally, the attic exterior envelope has much more leakage area per unit surface area in the 2- vs. 1-story home. In essence, while the 1-story attic volume is nearly double the 2-story attic volume, the leakage areas are similar. In combination, this leads to dramatically lower mass exchange rates in the 1-story homes. The total conditioned volume (living space + attic) gets 29% less exchange in 1-story homes; the living space gets 8% less mass exchange; and the attic volume receives 51% less mass exchange in 1- vs. 2-story homes.

Some of these results are driven by the assumptions about home and attic leakage distribution in Title 24. Attic exterior surface leakage that is normalized by surface area is unlikely to be very different between 1- and 2-story homes. However the leakage distribution requirements for Title 24 compliance modeling, where 50% of envelope leakage is placed in the exterior envelope of the attic means that the leakage per unit exterior area is very different for 1 and 2 story homes. It may be 2-story attics that appear artificially moisture “safe” in this work due to their unnaturally leaky attic surfaces, rather than 1-story attics that appear artificially “risky”.

The IAQ fan sizing requirements in the 2019 Title 24 now require an estimate of infiltration be made for each home assuming a 2 ACH_{50} envelope. This calculation will require larger fan airflows in 1-story homes, due to their reduced natural stack-driven airflows. This may also alleviate some of the 1-story moisture risk.

Figure 135 Monthly mean outdoor air mass exchange rates for the attic, living space and total conditioned volumes.

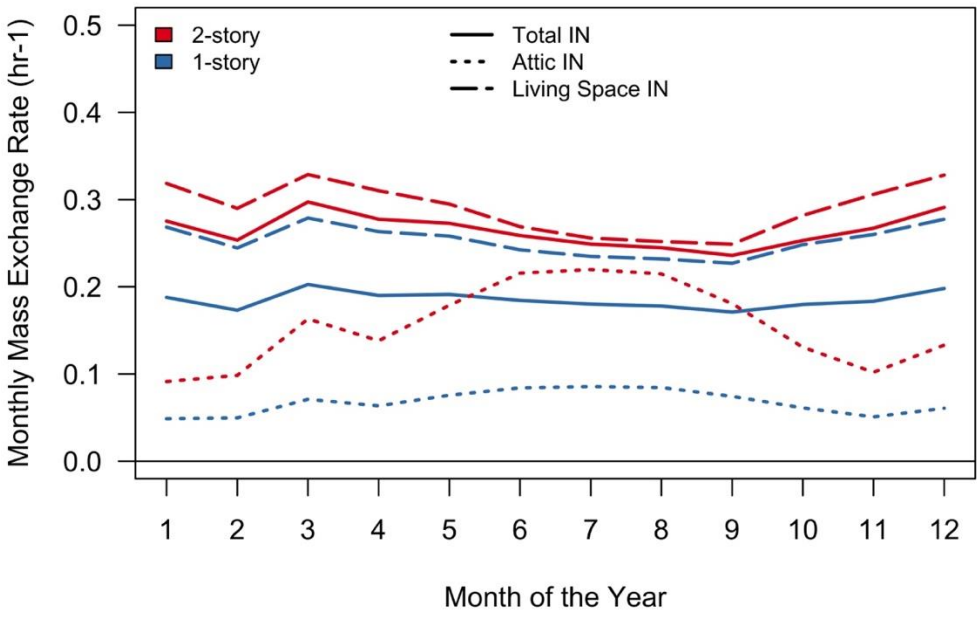

Figure 136 Monthly mean vapor pressure in the attic and living space of each prototype home.

7.2.4.4 Internal Moisture Gains

The internal moisture gains were varied between medium and high rates, with continuous water emissions in the living space of 6.5 and 11.2 kg/day. The moisture generation indoors is a critical factor in determining the moisture content of the air in the living space and the sealed attic.

For both medium and high moisture gains, we show the fraction of cases in each climate zone that failed to meet the ASHRAE 160 mold index criteria on the North sheathing (Figure 137) and the attic bulk framing (Figure 138). As expected, failure rates were substantially higher in the cases with greater moisture gains. Overall, 33% of high gains cases failed at the North sheathing, while only 13% of cases failed with medium moisture gains. Bulk framing failures occurred in 25% of high gain cases and only 11% of medium gain cases.

Internal moisture gains also had strong impacts on wood moisture content failures (7-day mean MC exceeding 28%), specifically on the North sheathing, where 31% of high gain cases failed vs. 8% of medium gain cases. Maximum 7-day MC values were generally reduced by between 2 and 7% when comparing medium with high gain cases (e.g., 28% with high gains vs. 26-21% with medium gains). Mean values are shown for each climate zone in Figure 139. Wood moisture failures were rare in the bulk framing and South sheathing nodes. Surface condensation on the North sheathing surfaces was reduced on average by 70% with medium vs. high moisture gains, while South sheathing and attic framing condensation were reduced by 80 and 78%, respectively.

Figure 137 North sheathing mold index failures comparison by indoor moisture generation rates in each CEC Climate Zone.

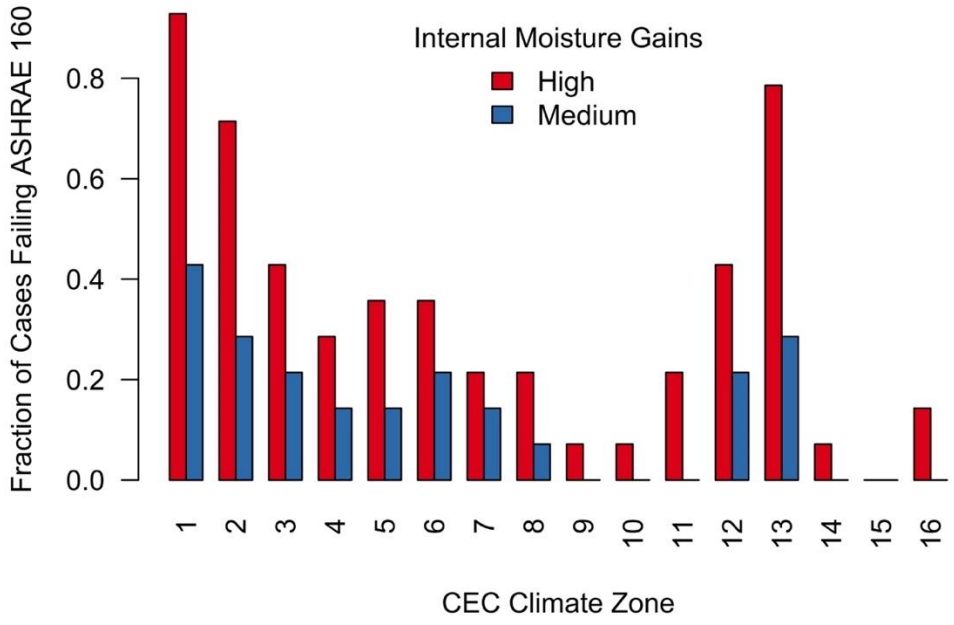

Figure 138 Bulk framing mold index failures comparison by indoor moisture generation rates in each CEC Climate Zone.

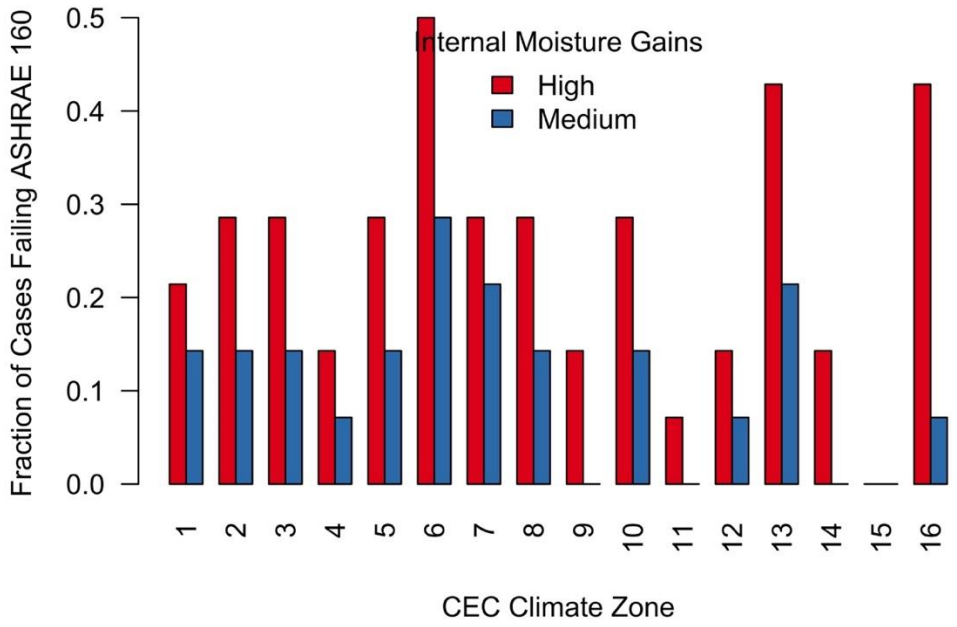

Figure 139 North sheathing maximum 7-day wood moisture content by internal moisture gains in each CEC climate zone.

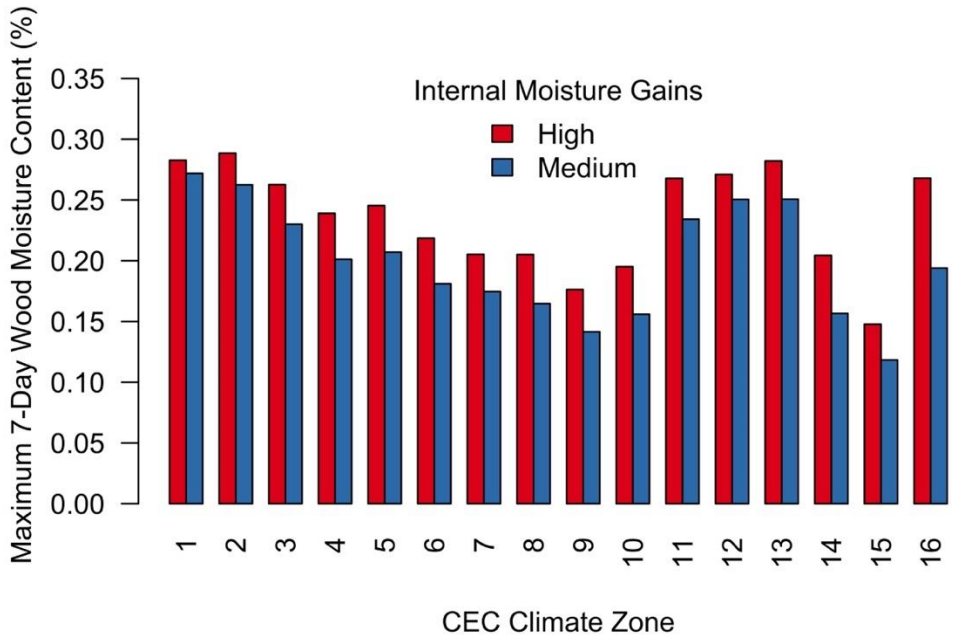

Increased internal moisture gains led to moisture-related failures because of elevated indoor and attic moisture levels. We show the mean monthly vapor pressure in living spaces and attics averaged over all cases and differentiate by moisture gains in Figure 140. Monthly mean vapor pressures are consistently between 100 and 300 pa higher in the high gain cases. This

difference is greatest in spring, when water stored in the attic sheathing during winter is baked into the attic air by increasing temperatures and insolation. Air exchange rates are effectively identical between cases with medium and high moisture gains. Figure 140 also shows the effects of seasonal moisture storage. From July-February the attic wood is absorbing moisture that is then released in the spring.

Figure 140 Monthly mean vapor pressure in the attic and living space of sealed attic homes with medium and high internal moisture gains.

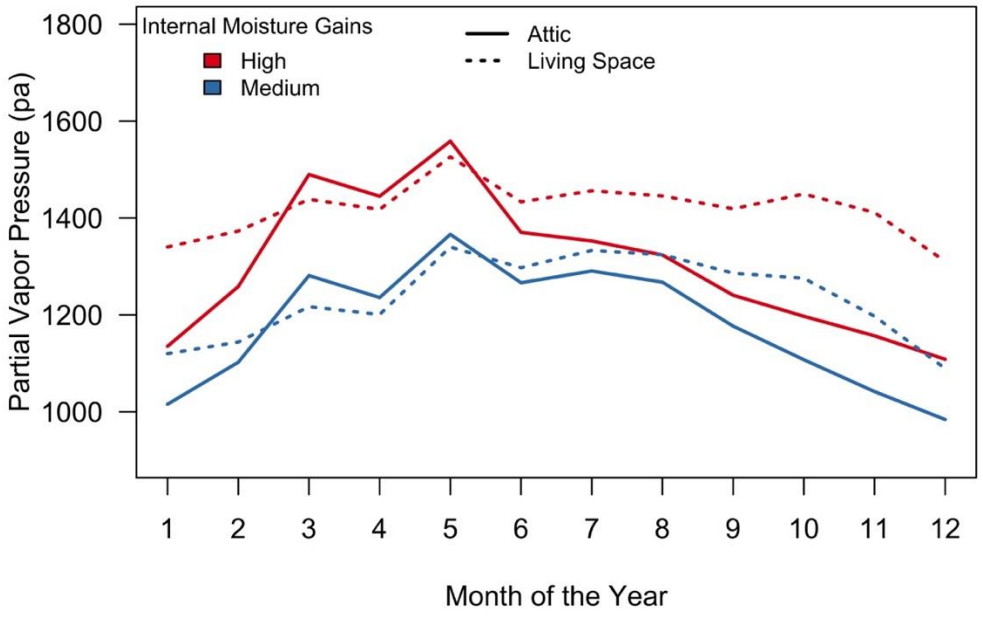

We show the comparison of total HVAC site energy consumption for medium and high gain cases in Figure 141 (TDV energy use is shown in Figure 142). We see marginally greater energy use of 80 kWh/year site energy in the high moisture gain cases, which is due to the increase in latent moisture load placed on the compressor with elevated indoor humidity (compressor energy use accounts for 90% of the difference between medium and high moisture gains).

Figure 141 Relative total HVAC site energy use for each climate zone by internal moisture gains.

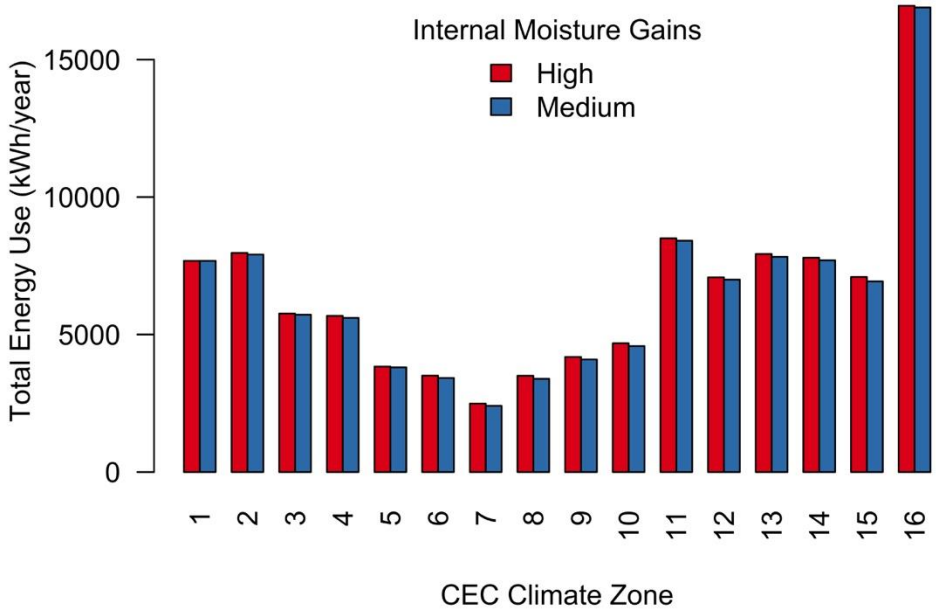

Figure 142 Relative total HVAC TDV energy use for each climate zone by internal moisture gains.

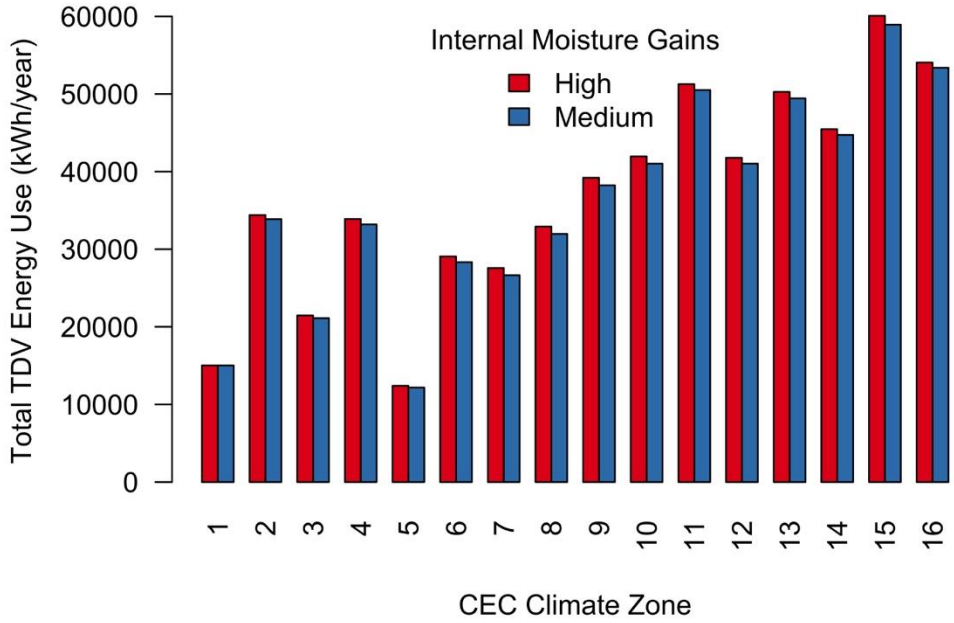

7.2.4.5 IAQ Fan Ventilation

Because increasing outdoor air exchange is expected to reduce moisture risk in sealed and insulated attics using vapor permeable insulation, we tested three common IAQ fan sizing scenarios for new CA homes—no IAQ fan, a fan sized to the 2008 T24, and an IAQ fan that is 40% greater than the 2008 T24 requirement. The upcoming 2019 Title 24 contains new IAQ fan

sizing requirements that are different from those simulated here. For 2019, all homes calculate a target total ventilation rate (combined mechanical and natural airflows), and they then take an infiltration credit using the assumption that the home envelope is 2 ACH_{50}. This sizing method results in code required fan airflows that are substantially larger than the T24 (2008) Fan Ventilation Rate Method, and they are more in-line with our largest simulated fan size.

For all three IAQ fan sizes, we show the fraction of cases in each climate zone that failed to meet the ASHRAE 160 mold index criteria on the North sheathing (Figure 143) and the attic bulk framing (Figure 144). As expected, failure rates were substantially higher in the cases with no IAQ fan, and they dropped as fan sizes increased. When a T24 (2008) fan was used, failures occurred only in CZ1, 2 and 13, and when the 40% larger fan was used, only CZ1 showed a North sheathing failure. Overall, 56% of no fan cases failed at the North sheathing, while only 9 and 2% of cases failed with T24 2008 and T24 (2008) + 40% fans, respectively. Even at the South sheathing location, 20% of no fan cases failed ASHRAE 160 criteria. Bulk framing failures occurred in 38% of no fan cases and only 5% of the T24 (2008) cases, while no bulk framing failures were predicted with the largest IAQ fans.

Surface condensation was also drastically reduced through use of either IAQ fan size (see Figure 145). North sheathing condensation was reduced by 91% and 98% for T24 (2008) and T24 (2008) + 40% fan sizes, respectively. South sheathing reductions in condensation were 98% and 100%, and attic framing reductions were 93% and 100%.

For each individual case that failed mold index criteria with no fan, we show the North sheathing and bulk framing maximum mold indices with each of three fan sizes in Table 32 and Table 33. All cases that failed the North sheathing mold index criteria after addition of the T24 (2008) fan were high moisture gain cases in CZ 1, 2 and 13. Similarly, remaining bulk framing failures after addition of the T24 (2008) fan were high moisture gain cases in CZ6, 13 and 16. The larger fan eliminated all bulk framing failures and all but one at the North sheathing, even at the higher moisture generation rate.

Figure 143 North sheathing ASHRAE 160 mold index failures for each climate zone, by IAQ fan sizing.

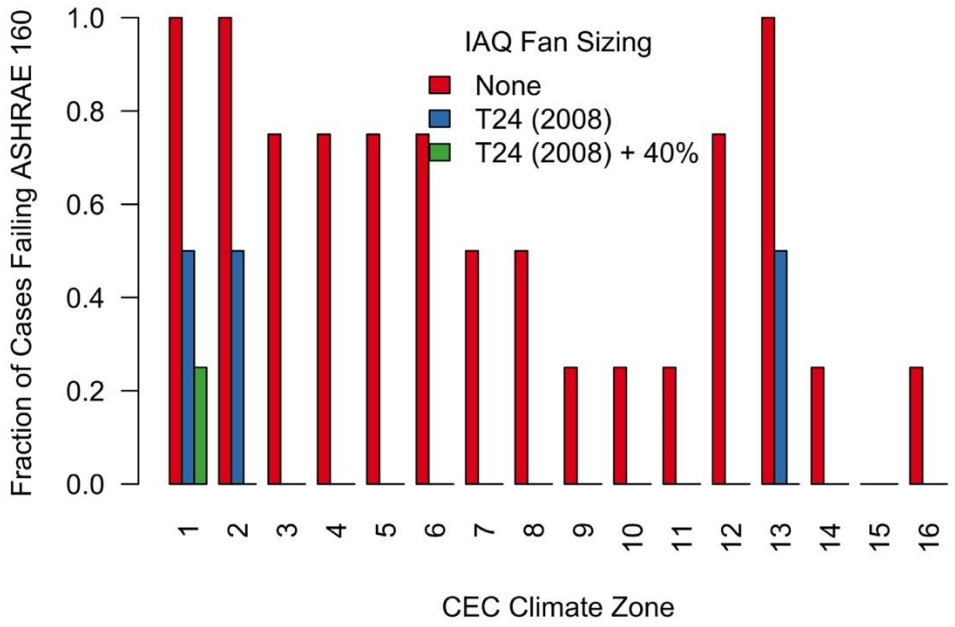

Figure 144 Bulk framing ASHRAE 160 mold index failures for each climate zone, by IAQ fan sizing.

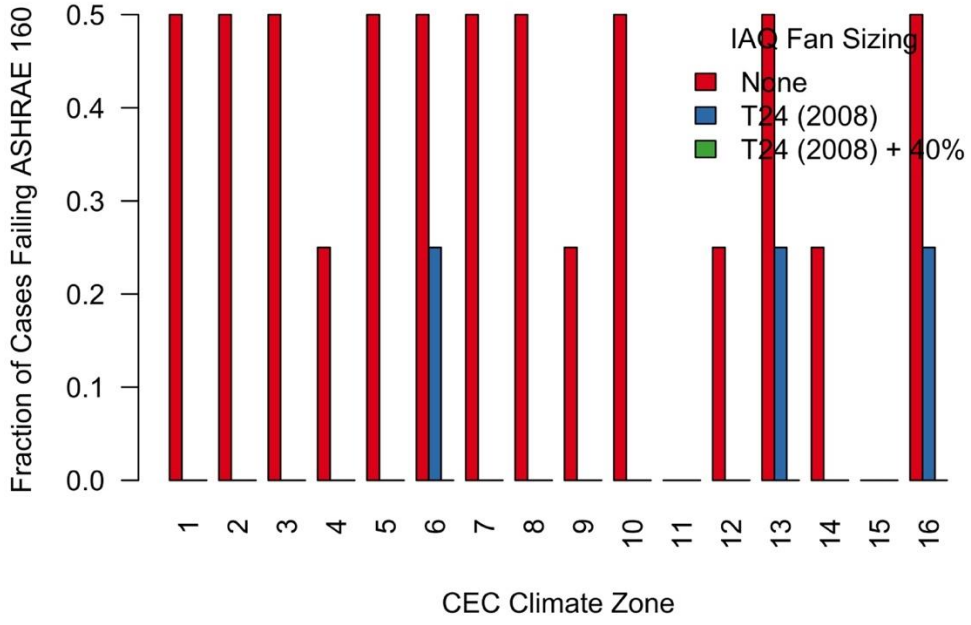

Figure 145 Annual condensed mass on attic moisture nodes, by IAQ fan sizing.

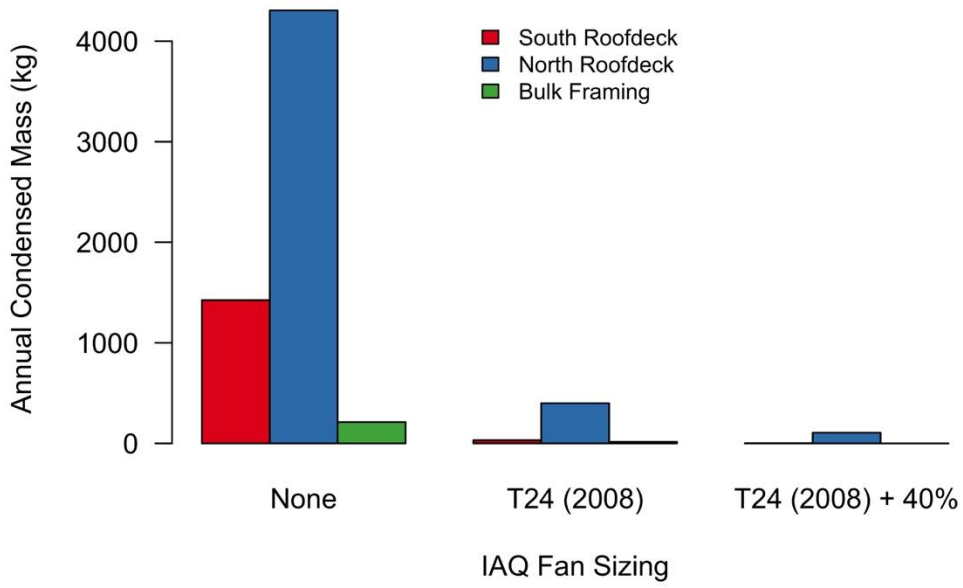

Table 32 North sheathing mold index failure cases, response by IAQ fan sizing.

Prototype	Moisture Gains	ACH_{50}	Duct Leakage	Attic Leakage	Ceiling Leakage	CZ	IAQ Fan Sizing		
							None	T24 (2008)	T24 (2008) + 40%
L	H	3	5d	50a	50c	1	5.3	5.29	4.81
M	H	3	5d	50a	50c	1	5.3	5.28	1.5
M	H	3	5d	50a	50c	13	5.3	5.08	0.34
L	H	3	5d	50a	50c	13	5.3	3.99	2.11
L	H	3	5d	50a	50c	2	5.3	3.47	1.72
M	H	3	5d	50a	50c	2	5.3	3.22	0.49
L	H	3	5d	50a	50c	12	5.29	2.89	1.68
L	M	3	5d	50a	50c	1	5.29	2.81	1.65
M	H	3	5d	50a	50c	12	5.3	2.7	0.46
M	M	3	5d	50a	50c	1	5.3	2.65	0.71
L	H	3	5d	50a	50c	3	5.3	2.42	0.97
M	H	3	5d	50a	50c	3	5.3	1.85	0.15
M	M	3	5d	50a	50c	13	5.3	1.69	0.04
L	M	3	5d	50a	50c	13	3.05	0.99	0.59
L	M	3	5d	50a	50c	2	3.05	0.94	0.64
M	H	3	5d	50a	50c	11	5.3	0.84	0.14
M	H	3	5d	50a	50c	5	5.3	0.78	0
L	H	3	5d	50a	50c	5	5	0.75	0.19
M	M	3	5d	50a	50c	2	5.3	0.75	0.18
M	M	3	5d	50a	50c	12	5.29	0.74	0.19
L	H	3	5d	50a	50c	4	4.87	0.73	0.28
M	H	3	5d	50a	50c	4	5.3	0.62	0.01
M	H	3	5d	50a	50c	6	5.3	0.53	0
M	H	3	5d	50a	50c	16	5.3	0.47	0
M	M	3	5d	50a	50c	3	5.3	0.43	0.03
M	M	3	5d	50a	50c	5	5.3	0.08	0
L	H	3	5d	50a	50c	6	4.27	0.05	0
M	M	3	5d	50a	50c	4	5.05	0.02	0
M	H	3	5d	50a	50c	10	4.89	0	0
M	H	3	5d	50a	50c	14	5.3	0	0
M	H	3	5d	50a	50c	7	5.3	0	0

M	H	3	5d	50a	50c	8	5.3	0	0
M	H	3	5d	50a	50c	9	5.3	0	0
M	M	3	5d	50a	50c	6	5.3	0	0
M	M	3	5d	50a	50c	7	5.12	0	0
M	M	3	5d	50a	50c	8	5.05	0	0

Table 33 Bulk framing mold index failure cases, by IAQ fan sizing.

Prototype	Moisture Gains	ACH_{50}	Duct Leakage	Attic Leakage	Ceiling Leakage	CZ	IAQ Fan Sizing		
							None	T24 (2008)	T24 (2008) + 40%
M	H	3	5d	50a	50c	13	5.99	5.97	0
M	H	3	5d	50a	50c	6	5.99	5.9	0
M	H	3	5d	50a	50c	16	5.99	5.85	0
M	M	3	5d	50a	50c	13	5.97	1.22	0
M	H	3	5d	50a	50c	2	6	0.34	0.01
M	H	3	5d	50a	50c	3	6	0.14	0
M	H	3	5d	50a	50c	12	5.98	0.09	0
M	M	3	5d	50a	50c	2	5.99	0.06	0
M	H	3	5d	50a	50c	4	5.99	0.04	0
M	H	3	5d	50a	50c	5	5.99	0.03	0
M	H	3	5d	50a	50c	8	5.99	0.02	0
M	M	3	5d	50a	50c	3	5.99	0.02	0
M	H	3	5d	50a	50c	1	5.99	0.01	0
M	H	3	5d	50a	50c	10	5.99	0.01	0
M	H	3	5d	50a	50c	7	5.99	0.01	0
M	M	3	5d	50a	50c	1	5.96	0.01	0
M	M	3	5d	50a	50c	5	5.99	0.01	0
M	M	3	5d	50a	50c	6	5.99	0.01	0
M	H	3	5d	50a	50c	14	5.84	0	0
M	H	3	5d	50a	50c	9	5.98	0	0
M	M	3	5d	50a	50c	10	5.99	0	0
M	M	3	5d	50a	50c	16	4.47	0	0
M	M	3	5d	50a	50c	7	5.98	0	0
M	M	3	5d	50a	50c	8	5.98	0	0

IAQ fan sizing and operation is clearly critical to the moisture performance of sealed and insulated attics, due to its impact on outdoor air exchange and moisture removal. As home's ventilation rates are increased, the indoor vapor pressures will more closely resemble those outside, which are almost always lower than indoors in California climates. Indoor air is essentially outdoor air with moisture added to it by occupant activities (e.g., cooking, bathing and breathing) and building materials (e.g., from concrete in foundations or structural lumber). We show the monthly mean vapor pressure in the attic and living spaces for cases with the three IAQ fan sizes in Figure 146. We see that vapor pressures in the living space and attic get progressively lower as IAQ fan airflow is increased. This difference disappears in the living space during the cooling season, largely because moisture removal by the cooling system overwhelms the effects of the IAQ fan. Similarly convergence occurs in the attic volumes, but moisture removal is less, due to tight HVAC ducts (5%), so the no fan cases remain elevated.

Figure 146 Monthly mean vapor pressure in the attic and living space of sealed attic homes with three different IAQ fan airflows.

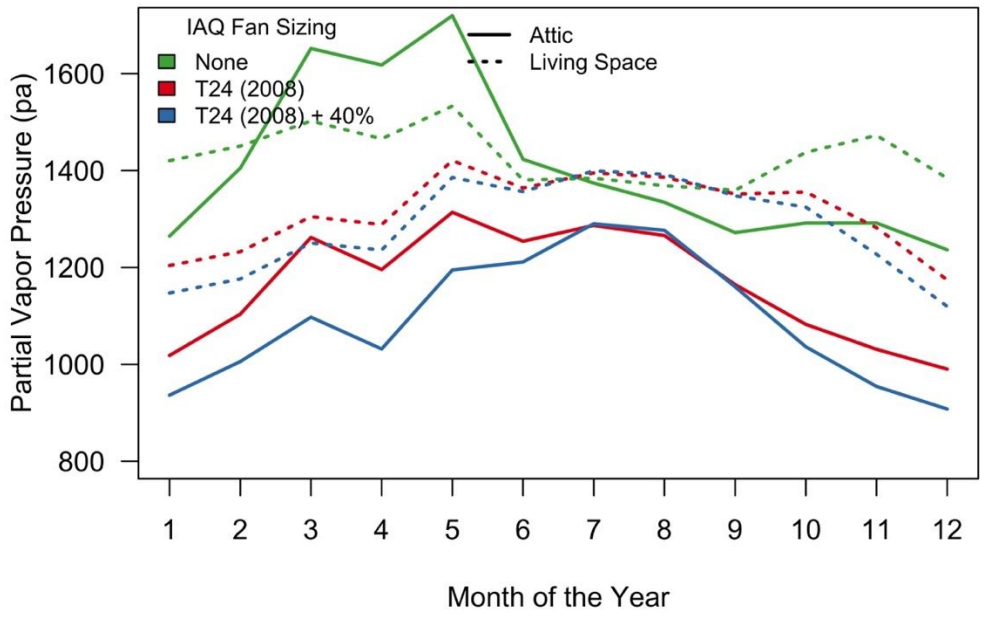

This difference in vapor pressure is driven by the air exchange with outside that occurs with and without IAQ fan ventilation. We show monthly mean air exchange rates for the attic, living space and total volumes in Figure 147, and we show what fraction of air flow into each volume comes from outside air in Figure 148. We see that with no IAQ fan installed, air exchange rates are substantially reduced and very little of the air flow into the attic comes from outside compared to an exhaust fan which can depressurize the house relative to the attic. As the IAQ fan sizes increase, the attics get proportionally more of their total air flow from outside, such that the cases with the largest IAQ fans get between 50-90% of attic ventilation flow from outside. When a sufficiently large fan is installed, it depressurizes the living space volume relative to the attic, such that nearly all flow is from the attic to the living space, which in turn

draws outside air in through leaks in the attic exterior envelope. Note that in all cases, the living space is predominantly vented with outside air, while the attics get more air from the living space. Given these results we performed additional simulations using a supply fan that pressurizes the house relative to the attic with more air from the house to the attic. These added tests are discussed later in Section 6.3.4.

Figure 147 Monthly mean mass exchange rates in cases with varying IAQ fan sizing.

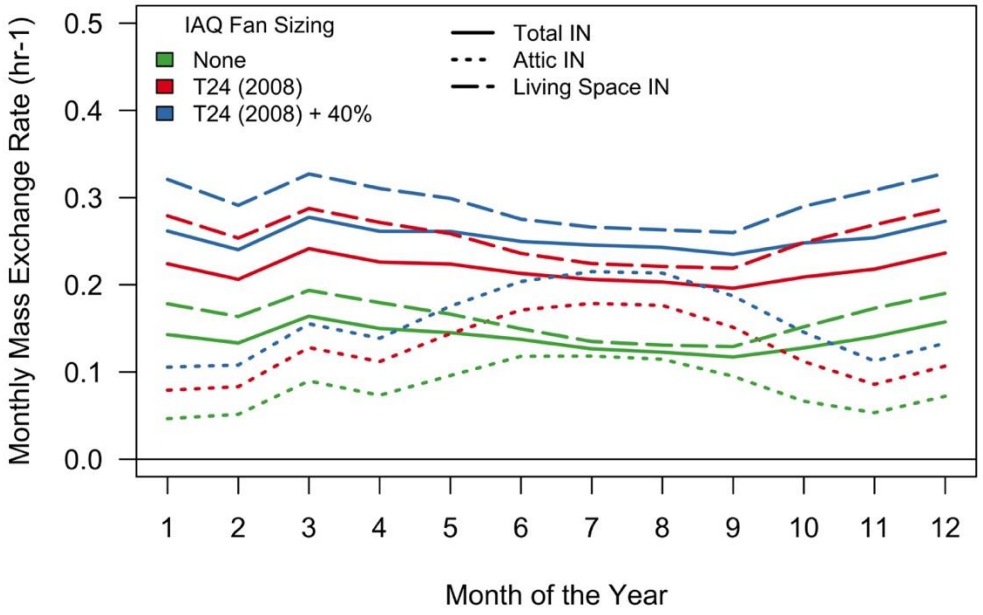

Figure 148 Fraction of mass flows into the attic and living spaces that come from outside, as opposed to the other zone.

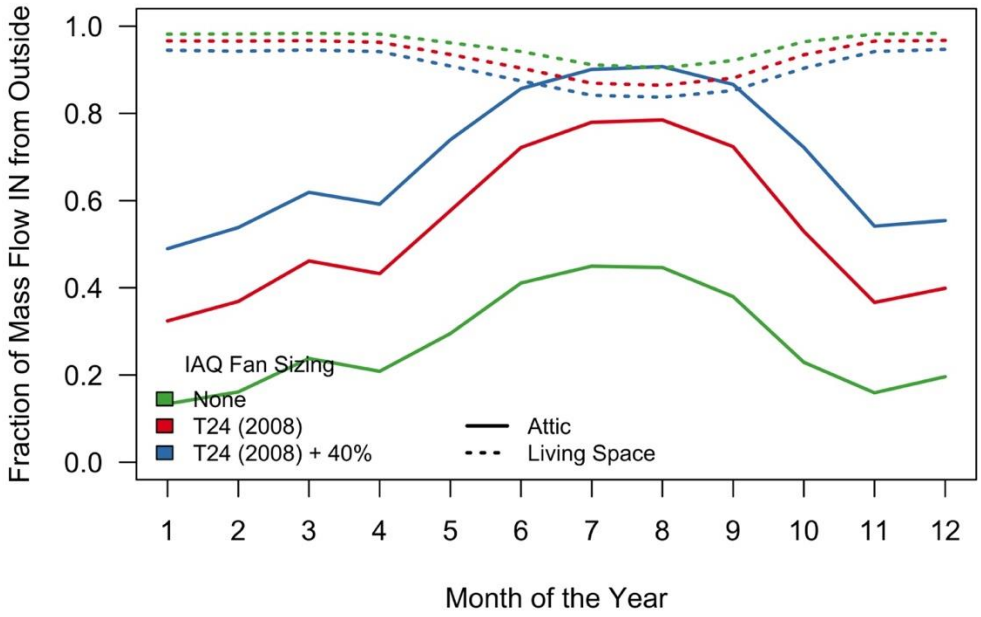

Increased IAQ fan ventilation airflow is clearly beneficial from a moisture performance perspective, but it comes with increased energy consumption, due to the need to condition the ventilation air. We compare total HVAC site energy consumption for each climate zone with each of the three IAQ fan sizing methods in Figure 149. Changes in TDV energy use are shown in Figure 150. As expected, the site and TDV energy consumptions increase in each case as IAQ fan airflows are increased. The mean increase from None to T24 (2008) was 625 kWh/year (1,848 TDV kWh/year), while an additional 40% fan airflow further increased energy use by 916 kWh/year (2,639 TDV kWh/year). Given the IAQ and moisture control benefits of IAQ fan ventilation, these energy use increases are a very reasonable cost.

Figure 149 Total HVAC site energy use for each IAQ fan sizing method, by climate zone.

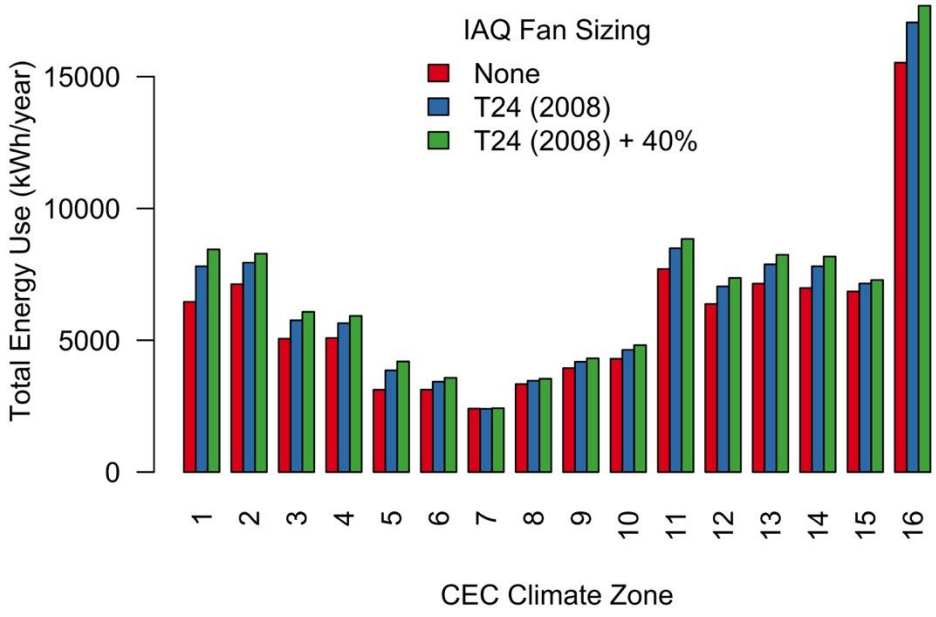

Figure 150 Total HVAC TDV energy use for each IAQ fan sizing method, by climate zone.

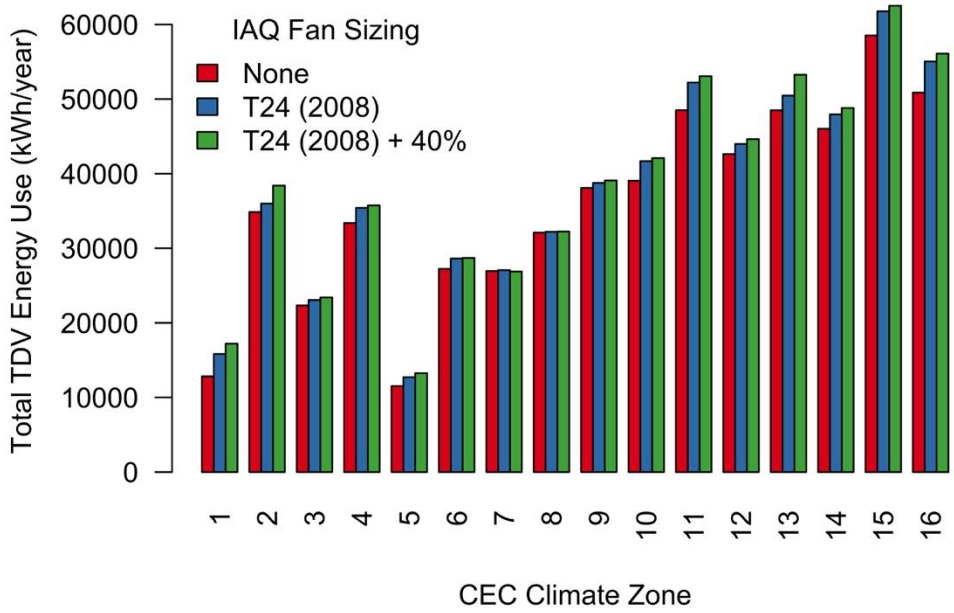

7.2.4.6 Envelope Airtightness

In this work, IAQ fan sizes were not varied with envelope airtightness, therefore leakier homes have greater air exchange. This is consistent with IAQ fan sizing in Title 24 (2008) using the Fan Ventilation Rate Method, which serves as the reference IAQ fan size used in all compliance calculations. The proposed 2019 fan sizing method will work in the same way, in that fan

airflows will not be affected by envelope air leakage. While target fan airflow did not vary with envelope leakage, the 1 ACH_{50} cases were simulated with balanced IAQ fans. As well as total leakage we varied the attic and total leakage and distribution. This is discussed in a later section.

We show the fraction of cases that failed the ASHRAE 160 mold index criteria at the North sheathing for each climate zone and level of envelope airtightness in Figure 151 (see Figure 152 for bulk framing failures). The highest failure rates for both North sheathing and bulk framing are in the 1 ACH_{50} cases. Overall, North sheathing failure rates drop from 30% at 1 ACH_{50} down to 10% and 9% at 3 and 5 ACH_{50}, respectively. Bulk framing failure rates drop even more dramatically from 40% to 15% and 9%. In both locations, the additional benefit of increasing leakage from 3 to 5 ACH_{50} is much reduced relative to the benefit of going from 1 to 3 ACH_{50}. It appears that only the most airtight of homes suffer from undue risk at these levels. Our results show that is would be better to target a minimum total air flow as is done in ASHRAE 62.2-2016 rather than a fixed fan flow with variable envelope leakage as is done here, and will continue to be done with the proposed 2019 Title 24 ventilation requirements. To have the same indoor moisture levels, smaller homes need bigger fans. This is true even though in our simulations the tightest home used a balanced ventilation system that will result in a higher total air flow rate than an unbalanced system of the same air flow in the same house.

Cases where 7-day mean wood moisture content exceeded the 28% threshold were rare in all of these cases, because only medium moisture gains were assessed in cases with varying envelope leakage. North sheathing WMC failures did decrease as leakage increased, from 7% to 4% and 3% of cases at 1, 3 and 5 ACH_{50}. Condensation at the North sheathing was reduced by 58% and 73% when increasing leakage from 1 to 3 and 5 ACH_{50} (see Figure 153). Reductions in condensation at the south sheathing and attic framing nodes were even larger, in the 60-85% range.

For each individual case that failed mold index criteria at 1 ACH_{50}, we show the North sheathing and bulk framing maximum mold indices with each of airtightness levels in Table 34 and Table 35. Numerous cases still failed the mold index criteria at the North sheathing as leakage was increased, but these were all cases where attic leakage was artificially reduced to 20% of envelope leakage. These occurred in CZ 1, 2, 3, 5, 6, 7, 12 and 13. The reduced attic leakage was clearly detrimental to moisture performance (see further discussion of varying attic leakage in Section 7.2.4.9). The bulk framing mold index failures performed similarly, with numerous failures when increasing envelope leakage, which nearly universally occurred in the 20% leakage attic cases.

Figure 151 North sheathing mold index failures for each level of envelope airtightness, by climate zone.

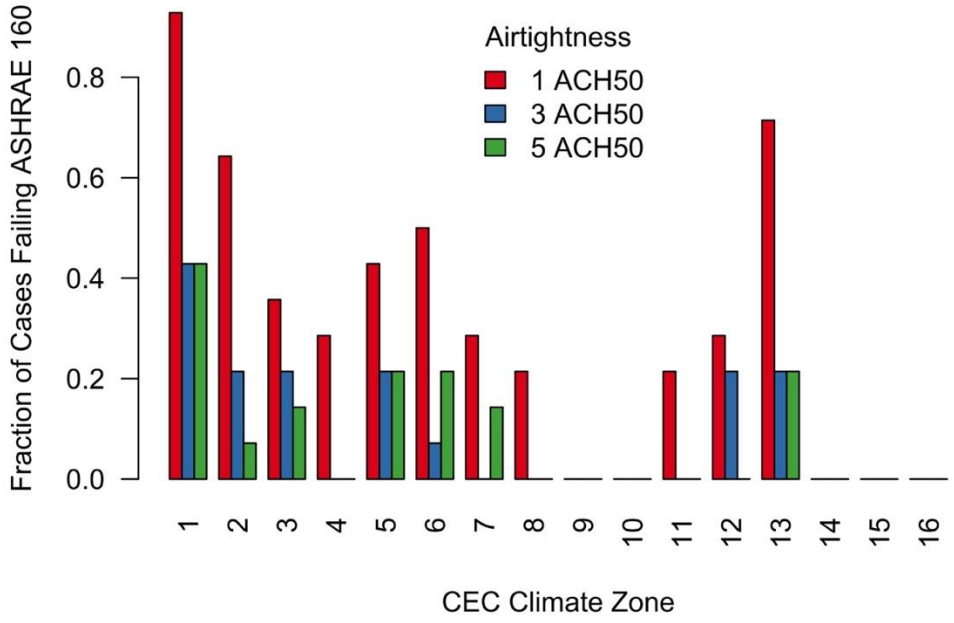

Figure 152 Bulk framing mold index failures for each level of envelope airtightness, by climate zone.

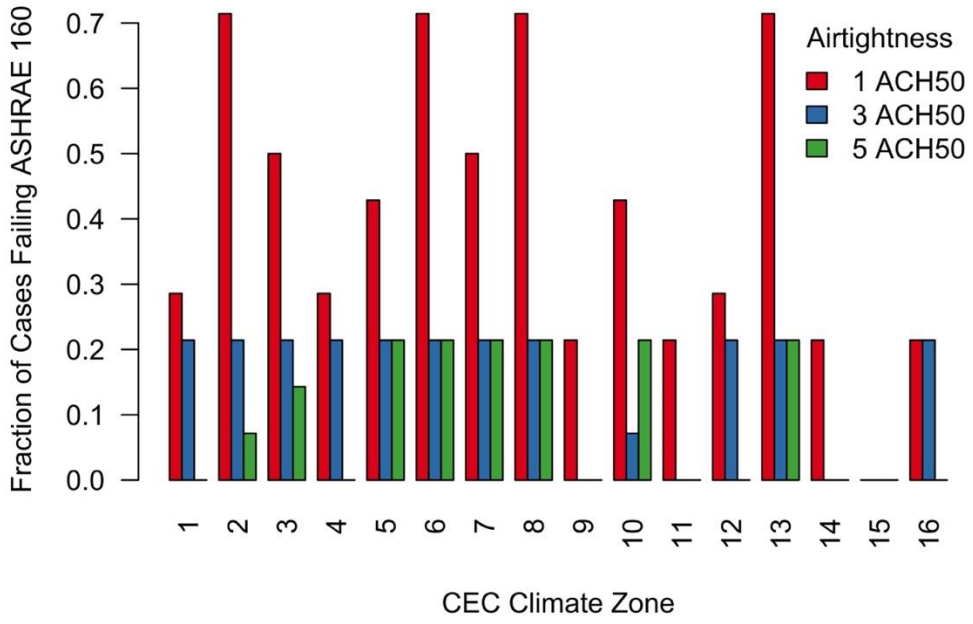

Figure 153 Annual condensed mass at each attic moisture node, by envelope airtightness.

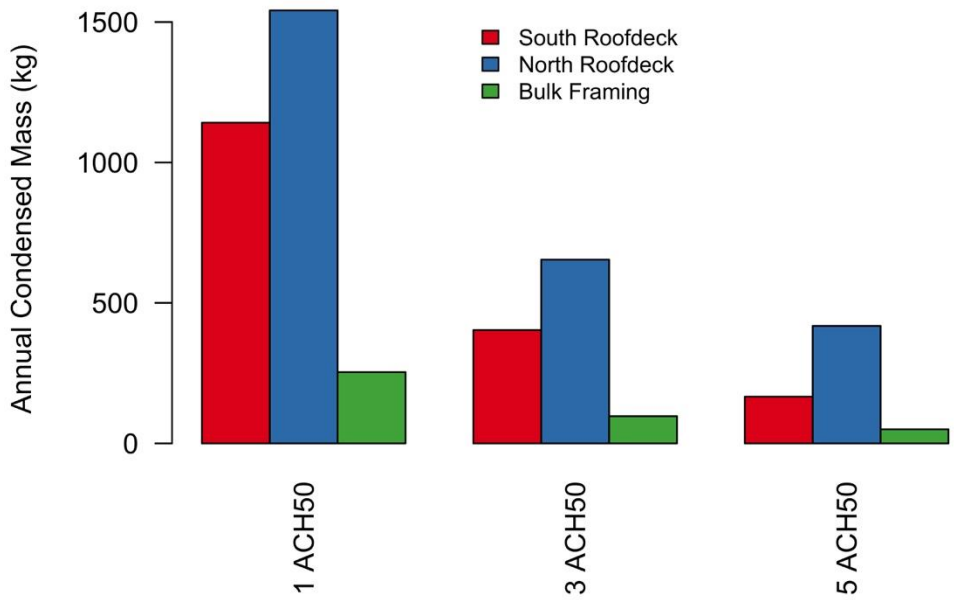

As with IAQ fan sizing, the envelope airtightness affects natural infiltration and ventilation rates, which when lowered lead to increased moisture levels indoors and elevated risk of mold and high WMC. We show the monthly mean partial vapor pressure in the attic and living spaces for 1, 3 and 5 ACH_{50} cases in Figure 154. While the 3 and 5 ACH_{50} attics are similar, the 1 ACH_{50} space has very high vapor pressures, particularly during later winter and spring. As in other cases, this is the result of stored moisture in the roof deck during winter being baked out by increasing sunshine and ambient temperatures as weather warms in the spring.

These seasonal moisture storage and release effects couple with very low attic outdoor air exchange rates to produce high moist air conditions. Monthly mean mass exchange rates are shown for the living space, attic and combined volumes for varying airtightness levels in Figure 155. We see that the attic mass exchange rate is particularly low in the 1 ACH_{50} cases. The 1 and 3 ACH_{50} cases have somewhat similar mass exchange rates for the living space and total conditioned volumes, but the attic is distinctly under vented for the most airtight cases. A contributory factor to the 1 and 3 ACH_{50} cases being close together is a combination of balanced fans resulting in higher total air flow rates than unbalanced fans and that the balanced fan airflows, which connect directly to the living space and only indirectly to the attic volume (through ceiling leakage areas), tend to ventilate the living space at the target rate, but they do not drive any mass exchange for the attic volume. Exhaust fans will depressurize the living space relative to the attic, which results in less moist indoor air entering the attic and more dry outdoor air entering the attic. Conversely, a supply fan would drive moist indoor air into the attic.

Figure 154 Monthly partial vapor pressure in the house and attic volumes, 1, 3 and 5 ACH50 (green, orange and purple lines, respectively).

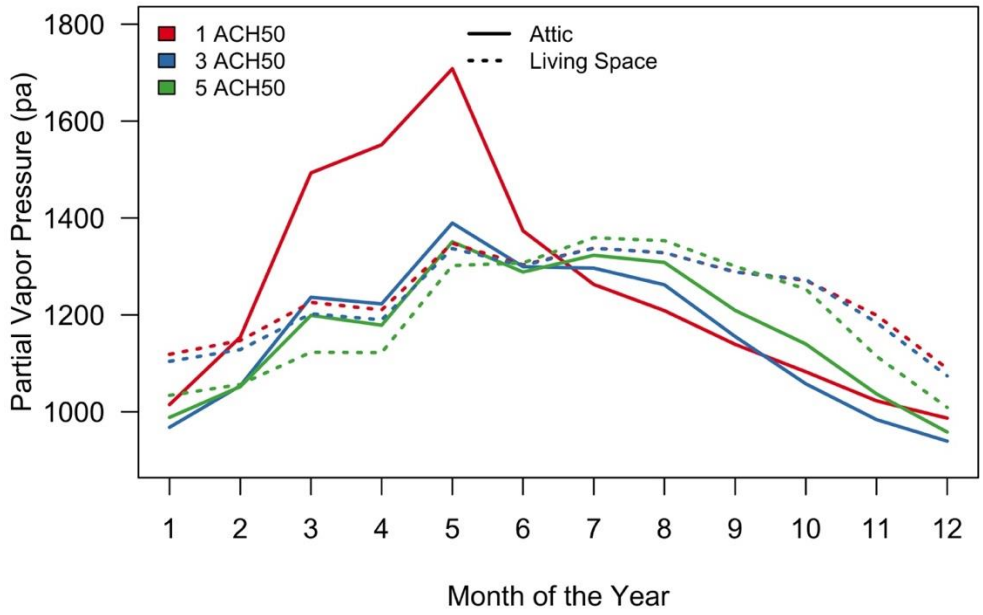

Figure 155 Monthly mean mass exchange rates in cases with varying envelope airtightness.

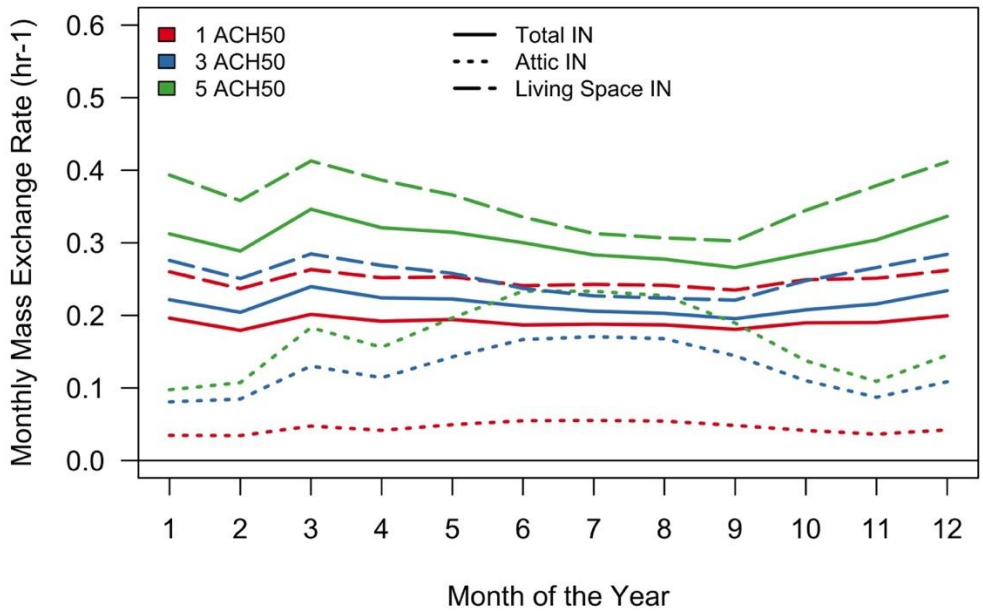

The most airtight cases have increased moisture risk, but we expect the primary motivation for designers and builders to increase the airtightness of homes to be energy savings and performance. We show the total HVAC site energy consumption for each climate zone and leakage level in Figure 156 (TDV energy shown in Figure 157). We see that in most cases, the total energy use increases with increasing air leakage. In select climates, the 3 ACH_{50} cases

actually use the least energy, which is likely due to the use of balanced fans in the 1 ACH_{50} cases and higher resulting ventilation rates. The increase in energy consumption averages 154 and 931 kWh/year when going from 1 to 3 and from 1 to 5 ACH_{50}, respectively. Absolute site HVAC savings increase similarly as leakage increases, from 1,337 to 1,423 to 1,696 kWh/year. The 3 ACH_{50} cases appear to be ideal here, with only roughly 150 kWh greater annual consumption than the 1 ACH_{50} cases, they have similar moisture risk to the 5 ACH_{50} homes which consume 800 kWh more energy than their 3 ACH_{50} counterparts.

Figure 156 Total HVAC site energy use predicted for each combination of climate zone and envelope leakage level.

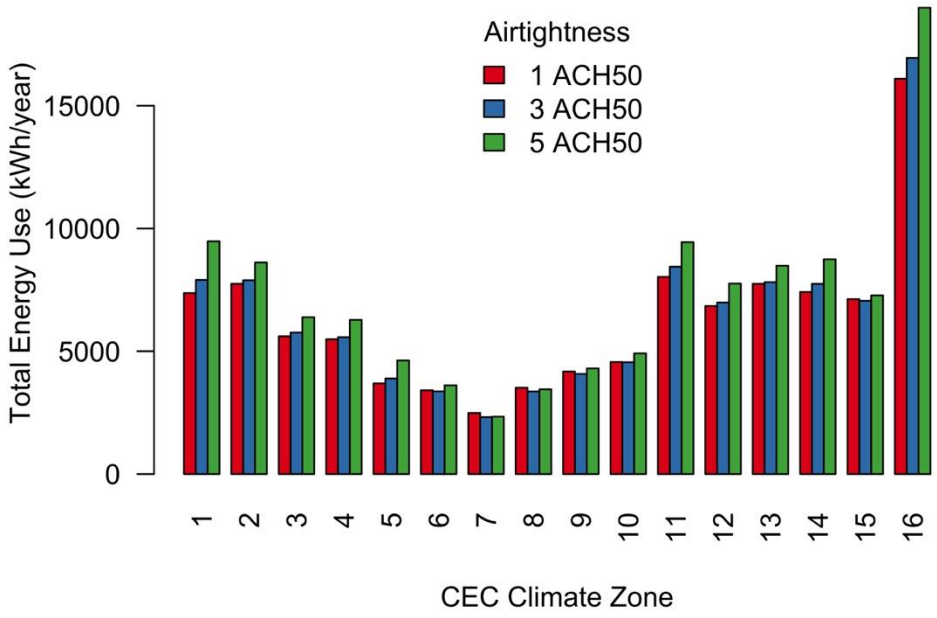

Figure 157 Total HVAC TDV energy use predicted for each combination of climate zone and envelope leakage level.

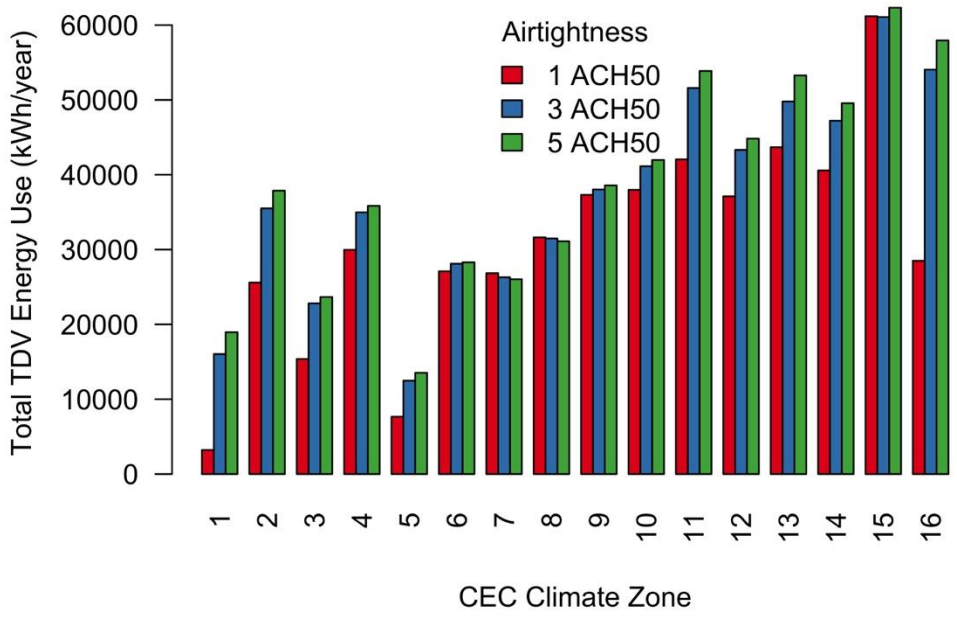

Table 34 North sheathing mold index failure cases, by envelope airtightness.

Prototype	Moisture Gains	Duct Leakage	Attic Leakage	Ceiling Leakage	Vent Fan Sizing	CZ	Envelope Airtightness (ACH_{50})		
							1	3	5
M	M	5d	20a	20c	2010	5	5.3	5.3	5.3
M	M	5d	20a	20c	2010	1	5.3	5.3	5.29
M	M	5d	20a	50c	2010	1	5.3	5.3	5.29
M	M	5d	20a	80c	2010	1	5.3	5.3	5.29
M	M	5d	20a	50c	2010	5	5.3	5.3	5.26
M	M	5d	20a	80c	2010	5	5.3	5.3	4.89
M	M	5d	20a	20c	2010	3	5.3	5.3	4.36
M	M	5d	20a	50c	2010	3	5.3	5.3	3.1
M	M	5d	20a	80c	2010	3	5.3	5.3	1.8
M	M	5d	20a	20c	2010	2	4.95	4.55	3.65
M	M	5d	20a	50c	2010	2	4.99	4.55	2.16
M	M	5d	20a	80c	2010	2	5	4.38	1.5
M	M	5d	20a	50c	2010	13	4.66	4.36	4.57
M	M	5d	20a	80c	2010	13	4.7	4.31	3.46
M	M	5d	20a	20c	2010	13	4.59	4.29	4.62
L	M	5d	20a	50c	2010	1	5.21	3.95	2.33
M	M	5d	20a	50c	2010	12	4.92	3.83	1.62
M	M	5d	20a	20c	2010	12	4.87	3.75	1.42
L	M	5d	20a	80c	2010	1	5.2	3.69	2.49

L	M	5d	20a	20c	2010	1	5.21	3.67	2.12
M	M	5d	20a	80c	2010	12	4.93	3.56	1.03
M	M	5d	20a	20c	2010	6	5.09	3.19	4.49
M	M	5d	20a	50c	2010	6	5.1	2.95	4.32
M	M	5d	20a	80c	2010	6	5.09	2.95	3.16
M	M	5d	20a	20c	2010	4	4.67	2.89	0.41
L	M	5d	50a	50c	2010	1	3.96	2.81	1.73
M	M	5d	20a	50c	2010	4	4.71	2.81	0.56
M	M	5d	50a	50c	2010	1	5.3	2.65	4.47
L	M	5d	80a	80c	2010	1	3.57	2.37	1.48
M	M	5d	20a	80c	2010	4	4.71	2.35	0.38
L	M	5d	80a	50c	2010	1	3.38	2.22	1.48
M	M	5d	20a	20c	2010	7	4.58	2.19	3.54
M	M	5d	80a	80c	2010	1	5.29	2.14	3.78
M	M	5d	20a	50c	2010	7	4.63	2.04	3.48
M	M	5d	80a	50c	2010	1	5.29	1.98	3.5
M	M	5d	20a	80c	2010	7	4.63	1.91	1.65
M	M	5d	20a	20c	2010	8	3.25	1.74	2.47
M	M	5d	50a	50c	2010	13	4.55	1.69	1.61
M	M	5d	80a	20c	2010	1	5.29	1.52	2.41
M	M	5d	20a	50c	2010	8	3.28	1.3	2.39
M	M	5d	20a	80c	2010	8	3.22	1.27	1.12
L	M	5d	20a	50c	2010	13	4.31	1.17	0.66
L	M	5d	20a	50c	2010	2	4.68	1.13	0.78
L	M	5d	20a	80c	2010	13	4.14	1.11	0.7
L	M	5d	20a	20c	2010	13	4.44	1.11	0.64
L	M	5d	20a	20c	2010	2	4.79	1.02	0.75
L	M	5d	20a	80c	2010	2	4.45	1	0.99
M	M	5d	50a	50c	2010	2	4.73	0.75	1.33
M	M	5d	80a	80c	2010	13	3.92	0.74	1.33
M	M	5d	50a	50c	2010	12	3.85	0.74	1.14
M	M	5d	80a	50c	2010	13	4.06	0.69	1.24
M	M	5d	80a	50c	2010	2	3.09	0.63	1.04
M	M	5d	80a	20c	2010	13	4.15	0.55	0.95
M	M	5d	80a	20c	2010	2	3.74	0.49	0.79
M	M	5d	50a	50c	2010	3	5.26	0.43	0.93
M	M	5d	80a	20c	2010	3	4.29	0.26	0.49
M	M	5d	20a	50c	2010	11	3.66	0.22	0.34
M	M	5d	20a	80c	2010	11	3.8	0.19	0.26
M	M	5d	20a	20c	2010	11	3.57	0.18	0.27
L	M	5d	20a	20c	2010	5	5.14	0.1	0.01

M	M	5d	50a	50c	2010	5	5.3	0.08	0.25
M	M	5d	50a	50c	2010	4	3.09	0.02	0.21
M	M	5d	80a	20c	2010	5	5.3	0	0.02
M	M	5d	50a	50c	2010	7	3.48	0	0.01
L	M	5d	20a	20c	2010	6	3.2	0	0
M	M	5d	50a	50c	2010	6	4.43	0	0
M	M	5d	80a	20c	2010	6	3.48	0	0
M	M	5d	80a	50c	2010	6	3.2	0	0

Table 35 Bulk framing mold index failure cases, by envelope airtightness.

Prototype	Moisture Gains	Duct Leakage	Attic Leakage	Ceiling Leakage	Vent Fan Sizing	CZ	Envelope Airtightness (ACH_{50})		
							1	3	5
M	M	5d	20a	20c	2010	2	6	6	6
M	M	5d	20a	20c	2010	10	6	4.05	5.99
M	M	5d	20a	20c	2010	13	6	6	5.99
M	M	5d	20a	20c	2010	3	6	6	5.99
M	M	5d	20a	20c	2010	5	6	6	5.99
M	M	5d	20a	20c	2010	6	5.99	5.99	5.99
M	M	5d	20a	20c	2010	7	5.99	5.99	5.99
M	M	5d	20a	20c	2010	8	5.99	5.99	5.99
M	M	5d	20a	50c	2010	13	6	5.99	5.99
M	M	5d	20a	50c	2010	5	6	6	5.99
M	M	5d	20a	50c	2010	6	5.99	5.99	5.99
M	M	5d	20a	50c	2010	7	5.99	5.99	5.99
M	M	5d	20a	50c	2010	8	5.99	5.98	5.99
M	M	5d	20a	50c	2010	10	6	2.43	5.98
M	M	5d	20a	50c	2010	3	6	6	5.98
M	M	5d	20a	80c	2010	5	6	6	5.98
M	M	5d	20a	80c	2010	6	5.99	5.99	5.98
M	M	5d	20a	80c	2010	7	5.99	5.99	5.97
M	M	5d	20a	80c	2010	8	5.99	5.98	5.66
M	M	5d	20a	80c	2010	13	6	5.99	5.55
M	M	5d	20a	80c	2010	10	5.99	1.17	4.65
M	M	5d	20a	50c	2010	2	6	6	2.49
M	M	5d	20a	20c	2010	1	5.99	5.99	0.99
M	M	5d	20a	50c	2010	1	5.99	5.99	0.99
M	M	5d	20a	80c	2010	1	5.99	5.98	0.63
M	M	5d	20a	80c	2010	3	5.99	5.99	0.52
M	M	5d	20a	80c	2010	2	6	6	0.14
M	M	5d	20a	20c	2010	12	5.99	5.99	0.09

M	M	5d	20a	50c	2010	12	5.99	5.99	0.09
M	M	5d	20a	20c	2010	4	6	5.99	0.07
M	M	5d	20a	50c	2010	4	6	5.99	0.07
M	M	5d	50a	50c	2010	6	5.99	0.01	0.05
M	M	5d	20a	80c	2010	12	5.99	5.99	0.04
M	M	5d	20a	80c	2010	4	5.99	5.98	0.04
M	M	5d	50a	50c	2010	8	5.98	0	0.04
M	M	5d	50a	50c	2010	13	5.99	1.22	0.03
M	M	5d	50a	50c	2010	2	6	0.06	0.03
M	M	5d	50a	50c	2010	1	5.98	0.01	0.02
M	M	5d	50a	50c	2010	3	5.99	0.02	0.02
M	M	5d	80a	50c	2010	6	5.99	0	0.02
M	M	5d	80a	80c	2010	6	5.99	0	0.02
L	M	5d	20a	20c	2010	5	5.99	0.01	0.01
L	M	5d	20a	20c	2010	6	5.99	0.03	0.01
L	M	5d	20a	20c	2010	8	5.96	0.02	0.01
L	M	5d	20a	50c	2010	6	5.98	0.02	0.01
L	M	5d	20a	50c	2010	8	5.91	0.02	0.01
L	M	5d	20a	80c	2010	6	5.98	0.02	0.01
L	M	5d	20a	80c	2010	8	5.4	0.02	0.01
M	M	5d	20a	20c	2010	11	5.99	0	0.01
M	M	5d	20a	50c	2010	11	5.99	0	0.01
M	M	5d	20a	50c	2010	9	5.99	0	0.01
M	M	5d	50a	50c	2010	10	5.99	0	0.01
M	M	5d	50a	50c	2010	12	5.98	0.01	0.01
M	M	5d	50a	50c	2010	5	5.99	0.01	0.01
M	M	5d	50a	50c	2010	7	5.99	0	0.01
M	M	5d	80a	20c	2010	3	5.99	0.01	0.01
M	M	5d	80a	20c	2010	6	5.99	0	0.01
M	M	5d	80a	20c	2010	8	5.98	0	0.01
M	M	5d	80a	50c	2010	10	4.61	0	0.01
M	M	5d	80a	50c	2010	2	6	0.01	0.01
M	M	5d	80a	50c	2010	3	5.98	0.01	0.01
M	M	5d	80a	50c	2010	8	5.98	0	0.01
M	M	5d	80a	80c	2010	2	5.1	0.01	0.01
M	M	5d	80a	80c	2010	8	5.97	0	0.01
L	M	5d	20a	20c	2010	13	5.99	0.01	0
L	M	5d	20a	20c	2010	2	6	0.04	0
L	M	5d	20a	20c	2010	3	5.57	0.01	0
L	M	5d	20a	50c	2010	13	5.99	0	0
L	M	5d	20a	50c	2010	2	6	0.03	0

L	M	5d	20a	80c	2010	13	5.99	0	0
L	M	5d	20a	80c	2010	2	6	0.02	0
M	M	5d	20a	20c	2010	14	5.44	0	0
M	M	5d	20a	20c	2010	16	6	5.99	0
M	M	5d	20a	20c	2010	9	5.99	0	0
M	M	5d	20a	50c	2010	14	4.82	0	0
M	M	5d	20a	50c	2010	16	6	5.99	0
M	M	5d	20a	80c	2010	11	5.99	0	0
M	M	5d	20a	80c	2010	14	4.8	0	0
M	M	5d	20a	80c	2010	16	6	5.98	0
M	M	5d	20a	80c	2010	9	5.99	0	0
M	M	5d	50a	50c	2010	4	5.98	0	0
M	M	5d	80a	20c	2010	10	5.96	0	0
M	M	5d	80a	20c	2010	13	5.99	0.02	0
M	M	5d	80a	20c	2010	2	6	0.01	0
M	M	5d	80a	20c	2010	5	5.99	0	0
M	M	5d	80a	20c	2010	7	5.98	0	0
M	M	5d	80a	50c	2010	13	5.99	0.01	0
M	M	5d	80a	50c	2010	7	5.95	0	0
M	M	5d	80a	80c	2010	13	5.98	0.01	0
M	M	5d	80a	80c	2010	7	5.88	0	0

7.2.4.7 Duct Leakage

Duct leakage has previously been reported as a critical feature in determining the energy savings value of sealed and insulated attics. Namely, very airtight and well insulated duct systems have not shown measurable energy savings in field testing (Less et al., 2016). We also expect some variability in moisture performance with duct leakage, as increased leakage should mix the living space and attic air volumes more thoroughly. During the cooling season, dry air is delivered to the attic through leakage sites, which can dehumidify the attic. A limited set of cases were run with varying duct leakage, solely in CZ 1, 3, 10, 12, 13 and 16. All cases use medium moisture gains in the living space and T24 (2008) IAQ fans.

For the limited set of cases run with varying duct leakage, the sole mold index failure was in CZ1 with 8% duct leakage at the North sheathing. There were no bulk framing failures. The maximum mold indices increase from 0.76 to 0.91 and 1.05 in 2%, 5% and 8% leakage duct cases showing that increasing duct leakage increased moisture risk. Condensation at the North sheathing also consistently increased as duct leakage increased from 2 to 5 and 8% (see Figure 158). This increase was evident in each simulated climate zone where condensation occurred.

CZ1 has previously been shown to have the highest risks of moisture damage, and increasing duct leakage to 8% further increased mold risk relative to either 2% or 5% leaky duct systems. The marginal increase in risk was small, such that in CZ1, the 2%, 5% and 8% ducts had maximum mold indices of 2.3, 2.7 and 3.2, respectively. In all likelihood, distinguishing

between 2.7 and 3.2 is beyond the precision offered by the mold index calculation method. Yet, in this case, it was enough to push the simulation into failure.

Figure 158 Annual condensed mass at each attic node, by duct leakage rate.

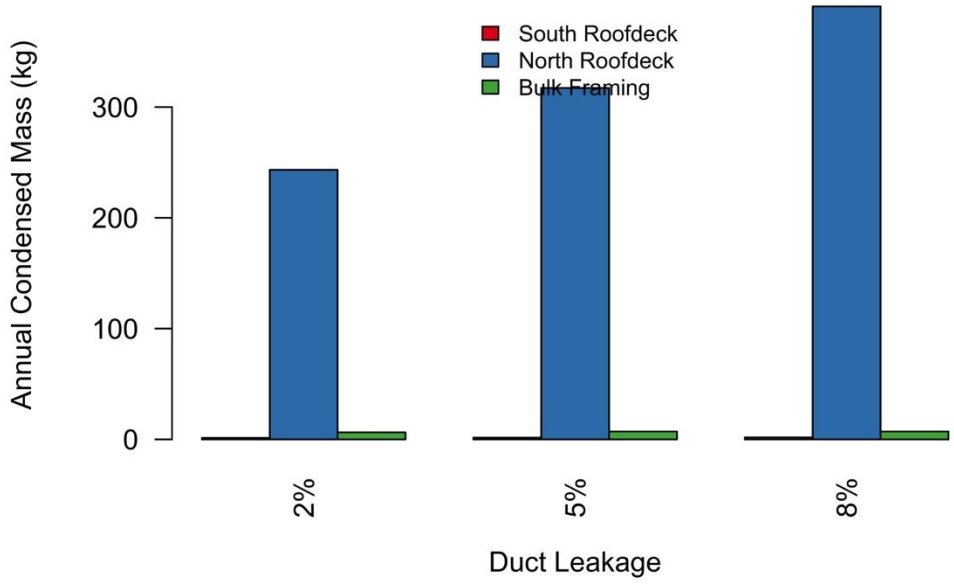

These results indicate that mixing slightly increases moisture risk more than the added summer time dehumidification decreases risk. To investigate this, we show the monthly mean partial vapor pressures in the living space and attic at the three duct leakage rates in Figure 159. We see that duct leakage rates have little impact on the monthly mean vapor pressures in the living space of the simulated homes, but the attic volumes are affected. The attic vapor pressure increases marginally as duct leakage increases, such that the 8% leakage attics have the highest attic vapor pressure in winter. This trend is reversed in the cooling months, when the 8% duct leakage cases have the lowest attic vapor pressures, due to delivery of dehumidified air to the attic. Vapor pressure increases in the winter, because the vapor pressure in the living space is higher than in the attic, so mixing introduces an additional moisture source to the attic air and insulated roof assembly. The difference in attic air vapor pressure is small, which explains why the changes in mold risk are also quite small.

Figure 159 Monthly mean vapor pressure in the living space and attic of homes with varying duct leakage.

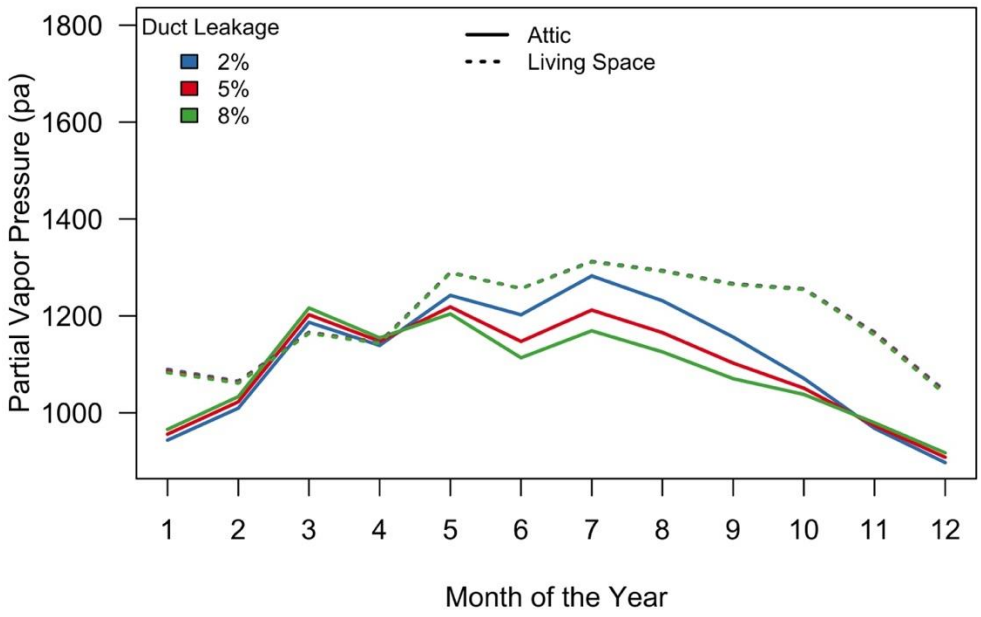

Increased duct leakage appears to marginally increase mold risk, though energy savings are also increased with greater duct leakage, as shown in Figure 160. Total site energy consumption remains steady across levels of duct leakage for sealed attics (see Figure 161), with only 33 and 63 kWh/year increased site energy use for the 5% and 8% leakage cases relative to the 2% cases (101 and 174 kWh/year TDV energy). This confirms that duct leakage into the conditioned attic has effectively no energy penalty in the sealed attic model. Rather the energy savings increase, because the vented attic cases increase energy use as duct leakage increases. The increment is approximately equal in each climate zone and at each duct leakage level. Reducing duct leakage from 8 to 2% decreases energy savings by roughly 2-3% per year.

Figure 160 Total HVAC site energy savings for each climate zone and level of duct leakage.

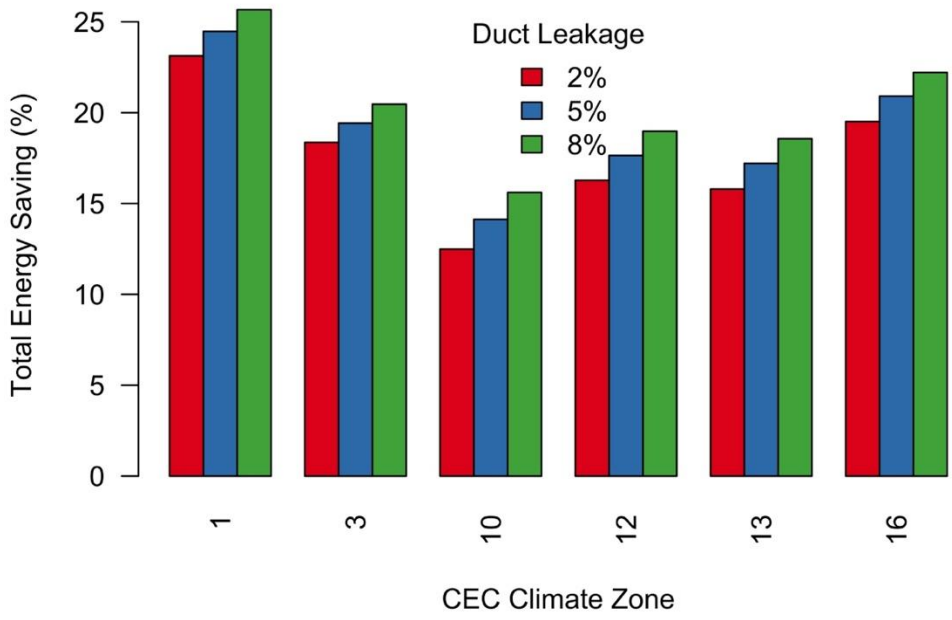

Figure 161 Total HVAC site energy use for each climate zone and level of duct leakage.

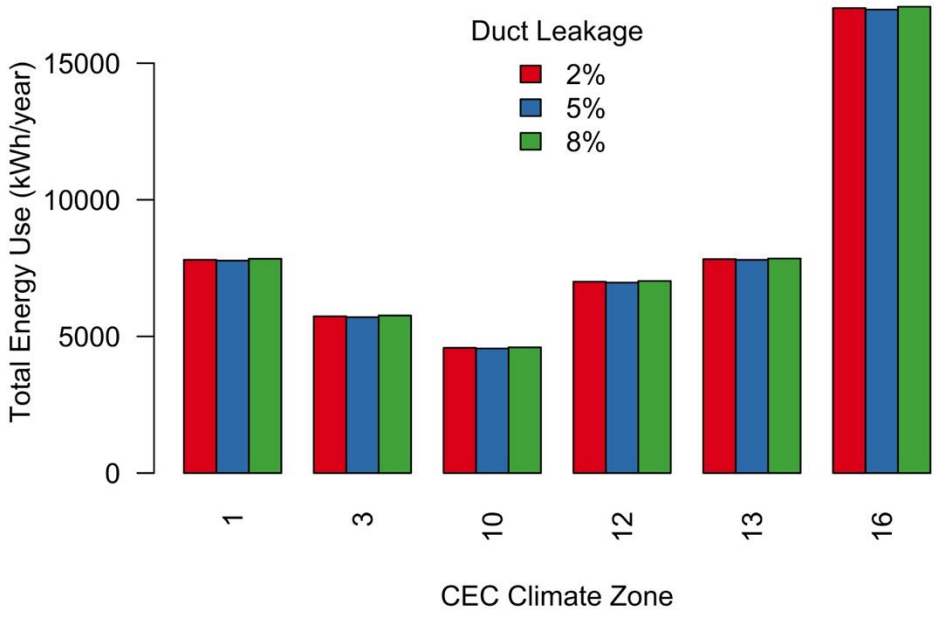

7.2.4.8 Ceiling Leakage

The ceiling leakage was varied in our simulations to account for variability in the efforts made by builders to seal the ceiling plane, even though it is no longer required as an air barrier in homes with sealed and insulated attics. Based on our observations from the duct leakage cases, we expect that increased ceiling leakage will lead to greater mixing and introduction of additional moisture into the attic volumes. This may increase mass flow from the house to the attic, increasing attic moisture levels and overall moisture risk. No energy savings comparisons are possible with the varying ceiling leakage, but we can assess how sealed attic energy use changed as ceiling leakage varied. We expect small impacts on energy consumption, as the ceiling does not form the primary pressure boundary for the condition space of the home.

To assess this hypothesis, we show the fraction of cases that failed the mold index criteria at the North sheathing for each climate zone and ceiling leakage rate in Figure 162. We see that in some climate zones, increasing ceiling leakage appears to reduce North sheathing mold risk (CZ2, 3, 5, 6 and 7), and in others it increases risk (CZ1) or risk remains the same (CZ4, 8-16). The impact of ceiling leakage is unclear. When we look at the maximum mold index values, rather than at failure rates, we see that changing ceiling leakage has very marginal impacts on the mold index, generally < 0.1 difference between leakage levels. Similarly, increased ceiling leakage was associated with reduced condensation mass at each moisture node in the sealed attic, but reductions were quite small (10-17% reductions from 20 to 50% ceiling leakage, and 17-28% reductions from 20% to 80% leakage).

We find some interesting and contradictory results when looking at the mass flow rates in these cases in Figure 163. The model predicts somewhat higher overall mass exchange rates for the living space and conditioned volumes in cases with leakier ceilings. This is paired with very slightly lower mass exchange rates for the attics with leaky ceilings. In addition to this, we see in Figure 164 that cases with tight ceilings get fractionally more mass from outside for both the living space and attic volumes, whereas the leaky ceilings have less mass from outside for both volumes. Mass exchange with outside has a drying effect. The balance between increased mass fraction from outside with a tight ceiling, and overall increased mass exchange with a leaky ceiling, appear to have balancing impacts that limit the overall effect of ceiling leakage in either direction. In some locations, increased ceiling leakage reduces mold index and in others increases it. Overall, we conclude that ceiling leakage is not a key variable in determining moisture performance of sealed and insulated attics.

Total site energy use is shown for each climate zone and level of ceiling leakage in Figure 165. In most locations, varying ceiling leakage had little impact on the site energy use, with an average of 58 and 100 kWh/year increased site energy use for 50 and 80%, relative to the 20% celling leakage cases. Overall, the 80% leakage ceilings had the highest energy consumption. In select climates (e.g., CZ16 Blue Canyon), the energy use increased by as much as 318 kWh/year site energy from 20 to 80% ceiling leakage. As expected, ceiling leakage has very little impact on the energy performance of sealed attic homes, because the ceiling does not form the primary pressure boundary between inside and outside.

Figure 162 North sheathing fraction of cases failing mold index criteria, by climate zone and ceiling leakage rates.

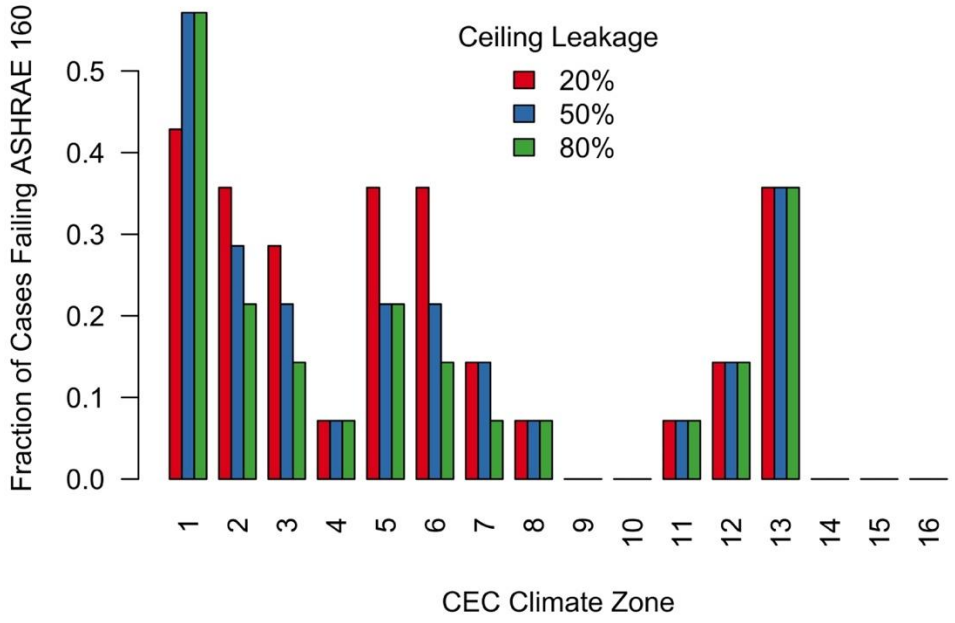

Figure 163 Monthly mean mass exchange rates for the attic, living space and conditioned volumes in each climate zone and ceiling leakage level.

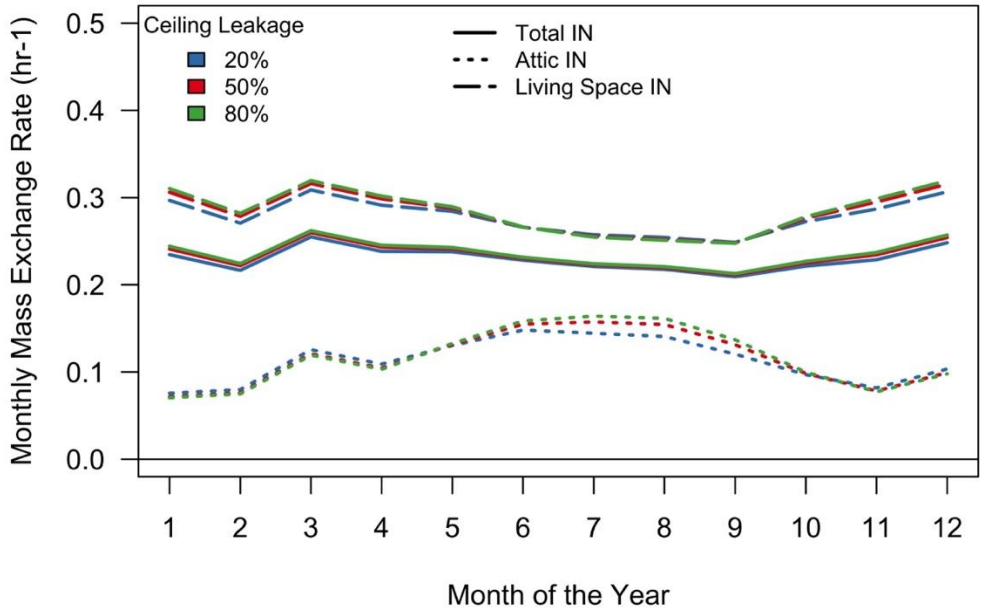

Figure 164 Fraction of monthly mean mass exchange that comes from outside air, by ceiling leakage rate.

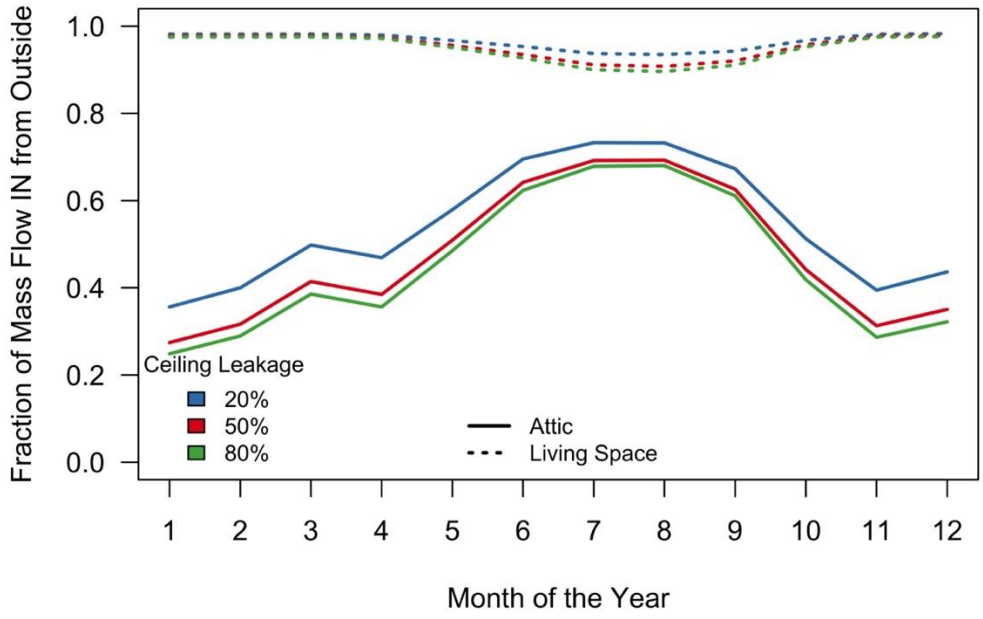

Figure 165 Total HVAC site energy use for each climate zone and level of ceiling leakage.

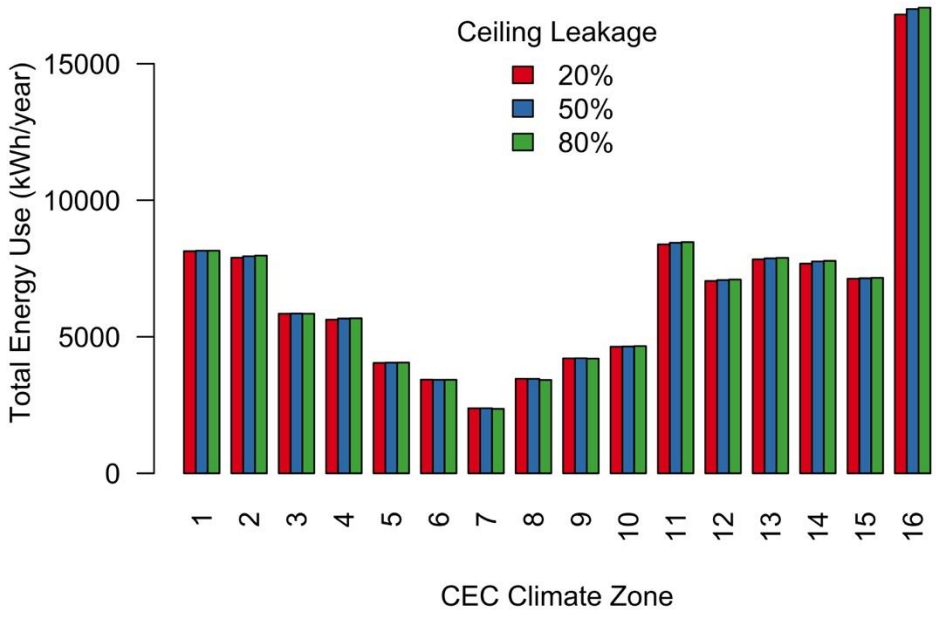

7.2.4.9 Attic Leakage

Attic leakage levels were intermingled with airtightness levels, making their analysis challenging. As noted in Methods Section 6.2.4, the varied attic leakage levels all have the same living space leakage areas, so the only difference between these cases is the amount of leakage

in the sealed attic. This leads to different overall envelope leakage areas. Overall, they follow the same patterns seen in other parameters, that is increased attic ventilation rates and house ventilation rates tend to reduce moisture risk through introduction of dry outside air. When the attic leakage was varied, so too was total envelope leakage, which means we have no baseline vented or HPA cases to compare these against, so we have no estimate of impact on energy savings. We do however, report the total energy use between varying levels of attic leakage.

We show the fraction of cases with North sheathing mold index failures in each climate and attic leakage level in Figure 166. As prior sections have suggested, increased attic leakage rates appear to reduce risk of mold growth. Overall, 26%, 7% and 4% of cases failed at the North sheathing with 20%, 50% and 80% attic leakage. The 20% leakage attic was particularly risky, while the 50 and 80% attics performed similarly from a mold risk perspective. Bulk framing failures (shown in Figure 167) showed even worse performance with the tight 20% attics, with 40-50% failure rates in most climate zones. Again, increased attic leakage reduced these risk across the board to 0-10% of cases.

Similar reductions in North sheathing condensation were observed when increasing attic leakage rates, as shown in Figure 168. The 50% leakage attics had the lowest condensed moisture mass in all climate zones, with a 91% reduction at the North roof deck (reductions at 80% attic leakage were lower—86%). Overall, the 50 and 80% attic leakage cases generally had very similar condensed moisture masses.

In relatively dry and mild California climate zones, increased outside air exchange reduces moisture levels in the living space and attic. We see in the monthly mean vapor pressures in Figure 169 that the leaky attics have the lowest moisture levels, while the most airtight attics have a massive increase in moisture content during late winter and spring, paired with overall slightly higher vapor pressure during the heating season. The 50% attic leakage cases experience some springtime increase, while the leakiest cases respond very little. This is confirmed by looking at the monthly mean air exchange rates in Figure 170. We see that while living space and conditioned volume air exchange rates remain reasonably similar across attic leakage rates, the airtight attics have roughly one-quarter of the air exchange experienced by the 50% and 80% cases.

Total site energy use is shown for each climate zone and level of attic leakage in Figure 171. As expected, total energy use increases with greater attic leakage rates in all climate zones, with the greatest increases in the coldest locations with the most infiltration. Mean energy use increased by 161 kWh/year from 20 to 50% attic leakage, and by 272 kWh/year from 20 to 80% attic leakage, respectively.

Figure 166 North sheathing fraction of cases that failed mold index criteria for each climate zone and attic leakage rate.

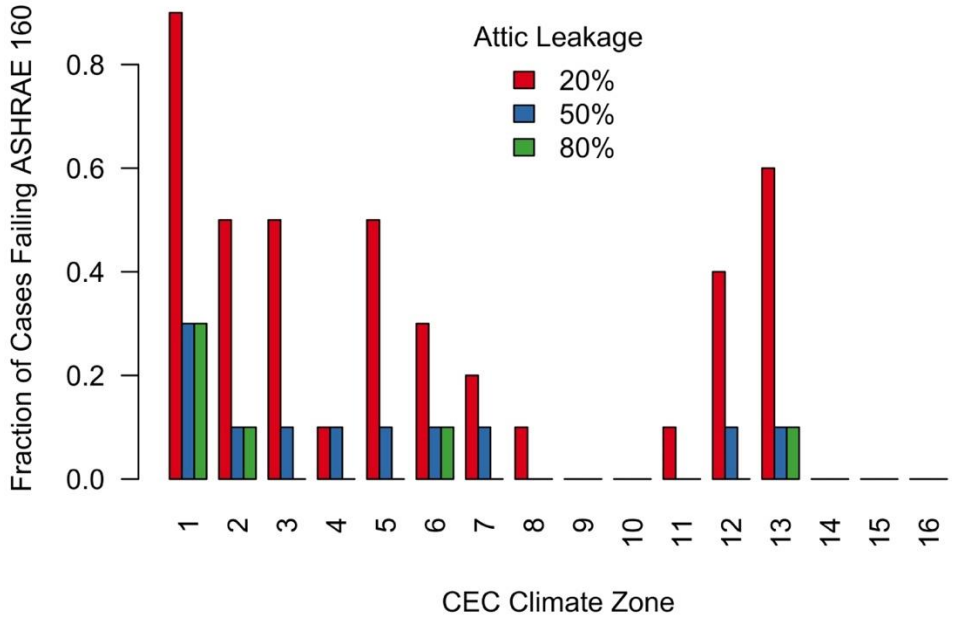

Figure 167 Bulk framing fraction of cases that failed mold index criteria for each climate zone and attic leakage rate.

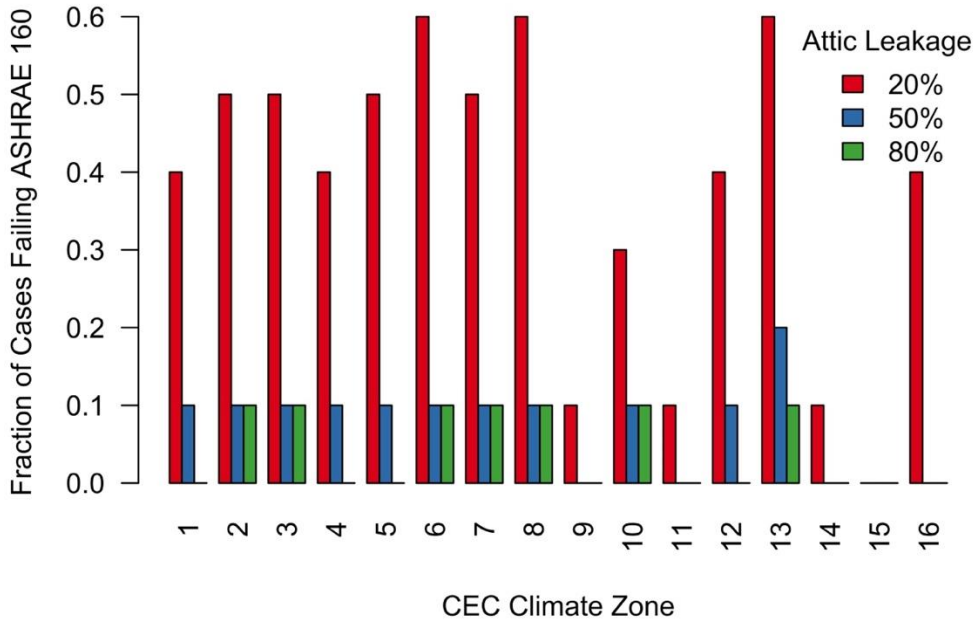

Figure 168 North sheathing average condensed mass by attic leakage rate for each climate zone.

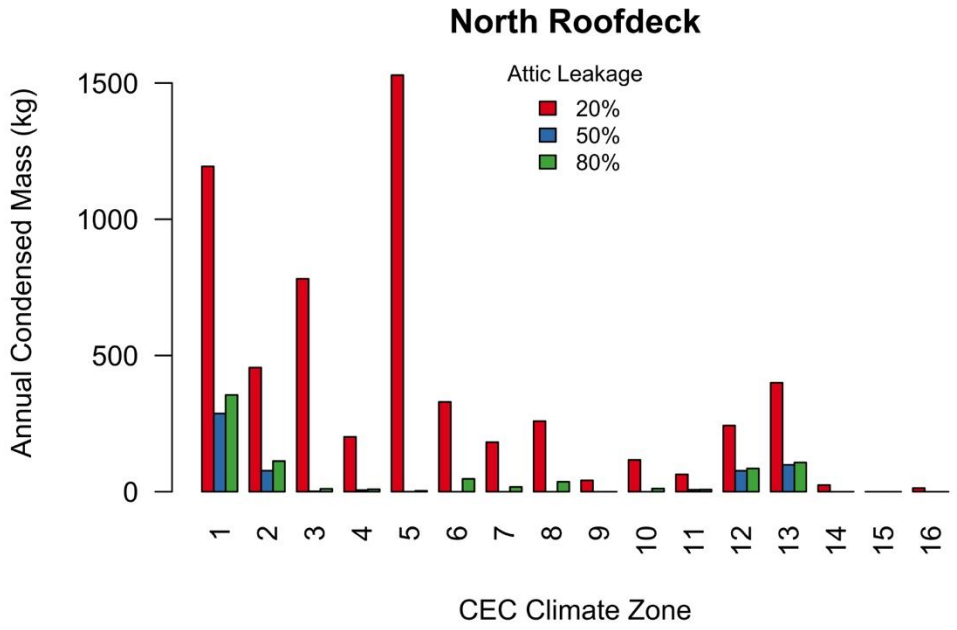

Figure 169 Monthly mean partial vapor pressure in the house and attic volumes for cases with varying attic leakage rates.

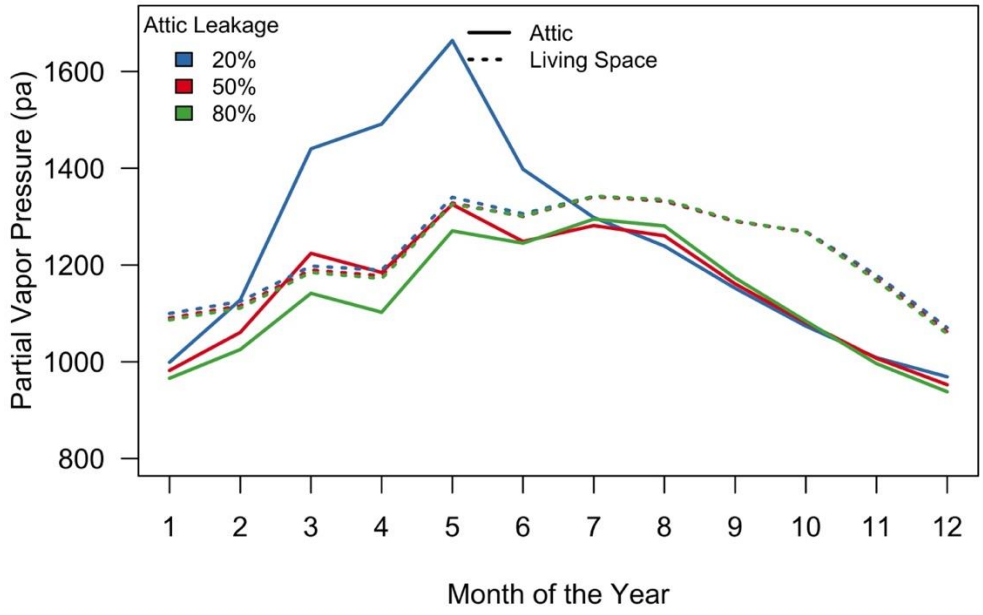

Figure 170 Monthly mean mass exchange rates for the attic, living space and conditioned volumes, with varying attic leakage rates.

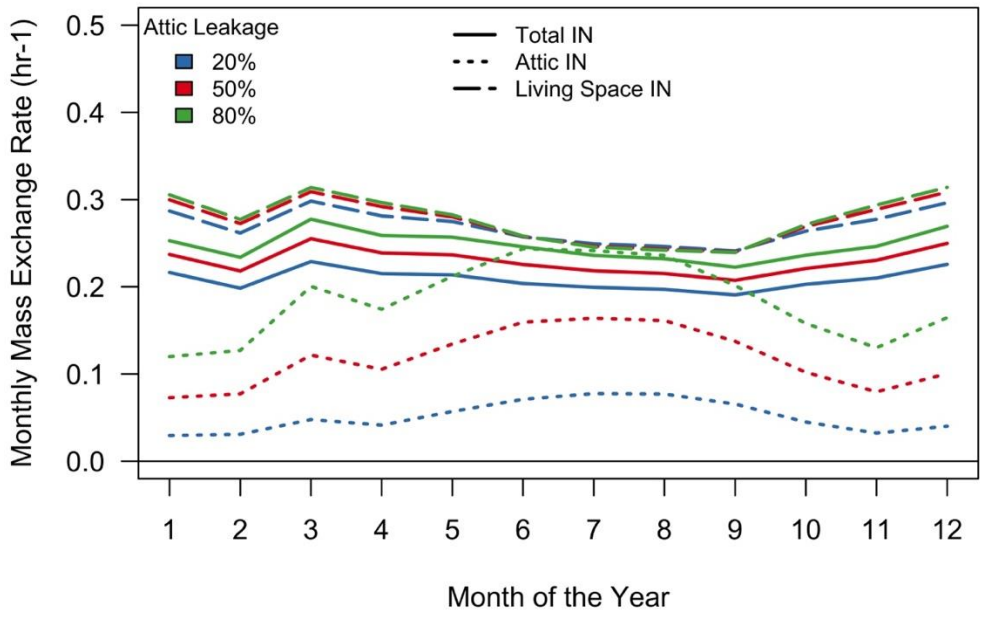

Figure 171 Total HVAC site energy use for each climate zone and level of attic leakage.

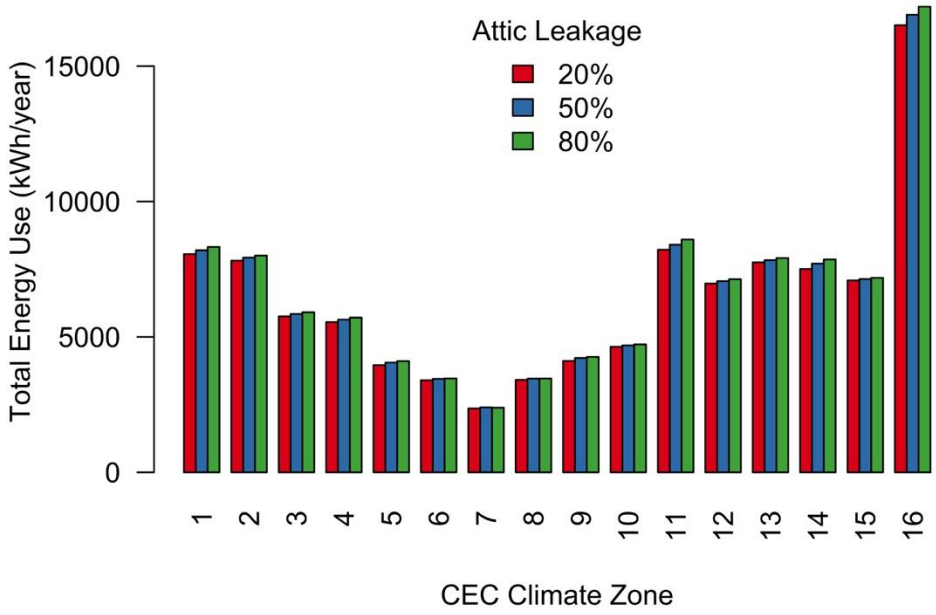

7.2.4.10 IAQ Fan Type (supply vs. exhaust)

Due to the sensitivity of the direction of mass flow through the ceiling, we anticipated that IAQ fan type would be an important parameter. Most cases were simulated with exhaust fans, so we added some runs that used an identically sized supply fan instead. A supply fan in the living

space should pressurize the living space relative to the attic, likely driving mass from the living space to the attic and then to outside. This means moisture generated indoors ends up in the attic, where it can contact the cold sheathing surface in winter. We hypothesis that supply fans will increase the risks of mold growth and moisture damage.

In Figure 172, we show the fraction of cases in each climate zone that failed the mold index criteria at the North sheathing with exhaust and with supply IAQ fans (see bulk framing failures in Figure 173). As expected, the use of supply ventilation fans substantially increases mold risk in most locations throughout the state. In comparison, exhaust fan failures occurred only in the most risky locations—CZ1, 2 and 13. Overall, North sheathing failure rates were 38% vs. 9% for supply and exhaust fans, while bulk framing failure rates were 17% and 5%. North sheathing cases that exceeded the 7-day 28% moisture content threshold were similarly increased from 11% to 31% with exhaust and supply fans, respectively. Notably, exhaust fans did not change the risk of bulk framing failures in CZ13 or 16. Condensation mass at the North sheathing was reduced by 82% when using exhaust ventilation fans compared with supply IAQ fans (see Figure 175), and similar reductions were recorded at the other attic moisture nodes (South sheathing (93%) and attic framing (81%)).

We show in Figure 175 how attic air vapor pressures were much higher in the homes using supply IAQ fans. In contrast, the vapor pressure in the living spaces were very similar, as they had similar outdoor air exchange rates using either exhaust or supply fans. When attic vapor pressure is elevated in springtime, the exhaust fan increases the living space vapor pressure, but only slightly. The source of the mass flows into the attic explains these differences, as shown in Figure 176. We see that when using an exhaust fan, between 40 and 80% of mass exchange in the attic is with outside, while the supply fan cases are dominated by flow from the living space, such that outside air makes up only roughly 10-20% of attic mass exchange. One caveat to these results is that they are for California climates: i.e. homes where there is less dehumidification than moisture added by occupants and building materials. In some extreme climates in a home with lots of dehumidification the indoor air may have less moisture than outdoor air and these effects may diminish or even be reversed.

Figure 172 North sheathing fraction of cases that failed mold index criteria for each climate zone and IAQ fan type.

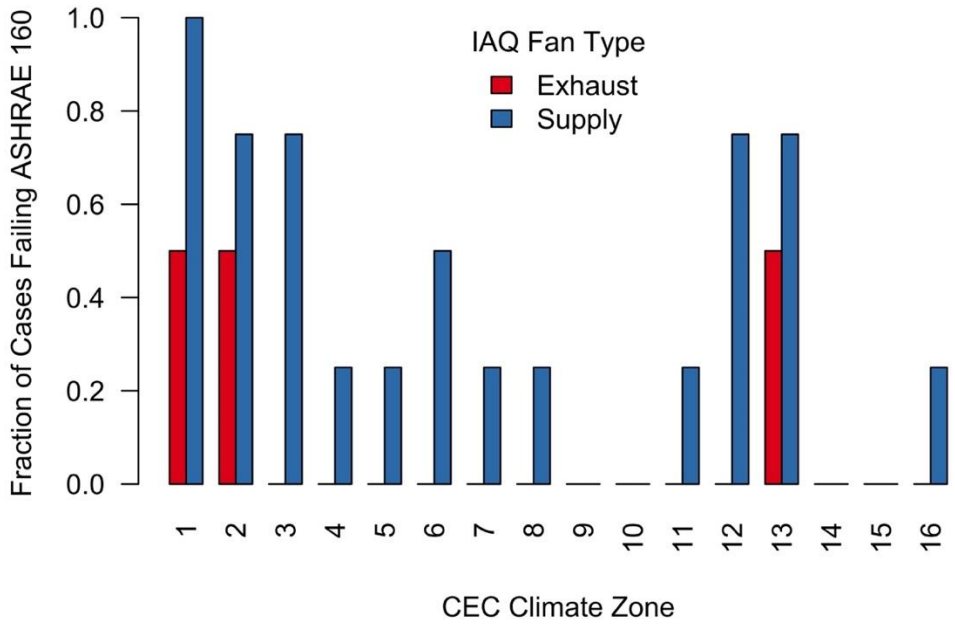

Figure 173 Bulk framing fraction of cease that failed mold index criteria for each climate zone and IAQ fan type.

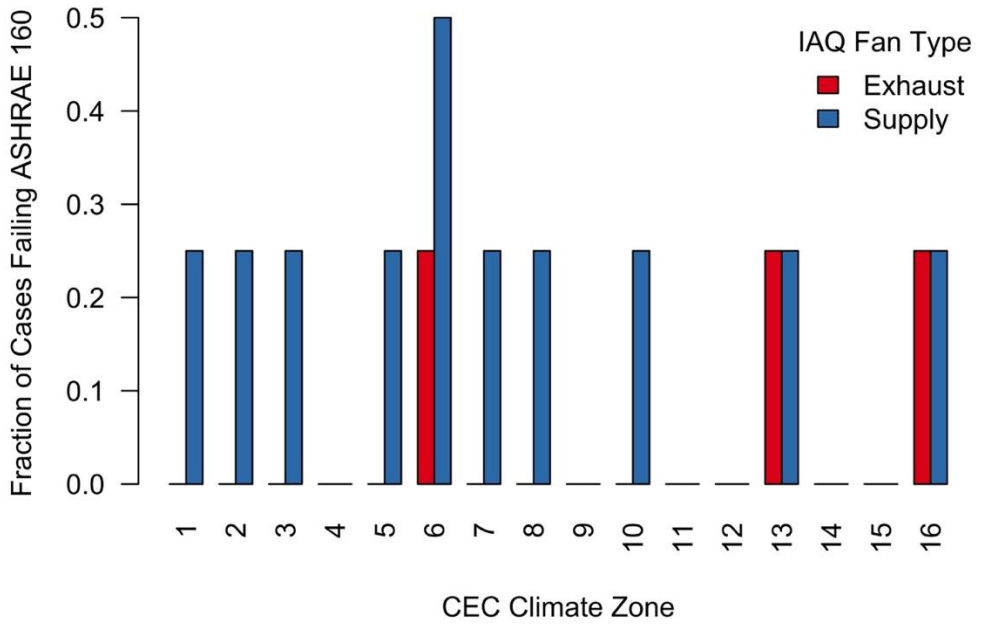

Figure 174 Annual condensed mass at the attic moisture nodes, by IAQ fan type.

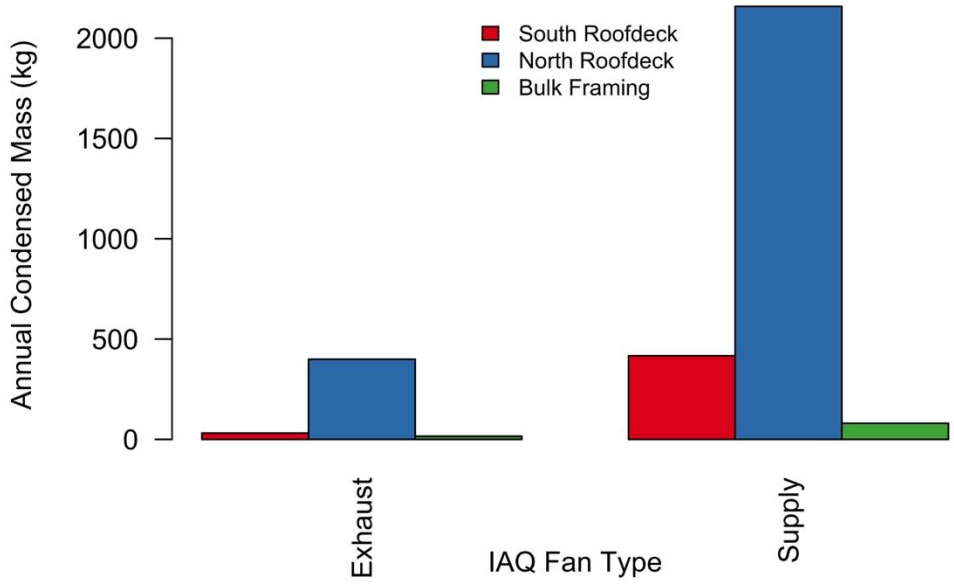

Figure 175 Monthly mean partial vapor pressures in the attic and living space for cases using exhaust vs. supply IAQ fans.

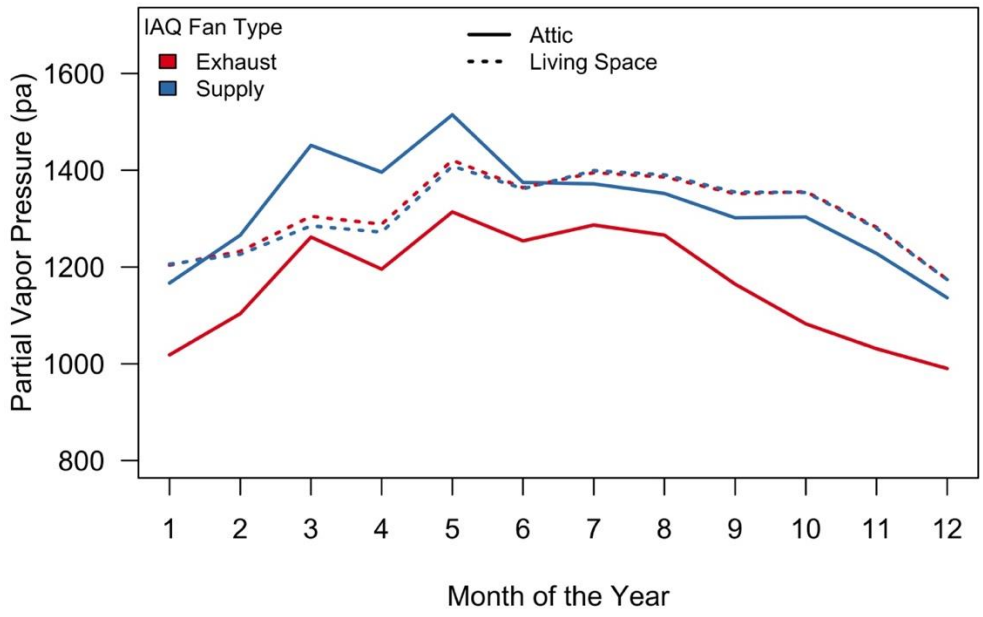

Figure 176 Monthly mean fraction of mass exchange for living space and attic that comes from outside for cases using exhaust vs. supply IAQ fans.

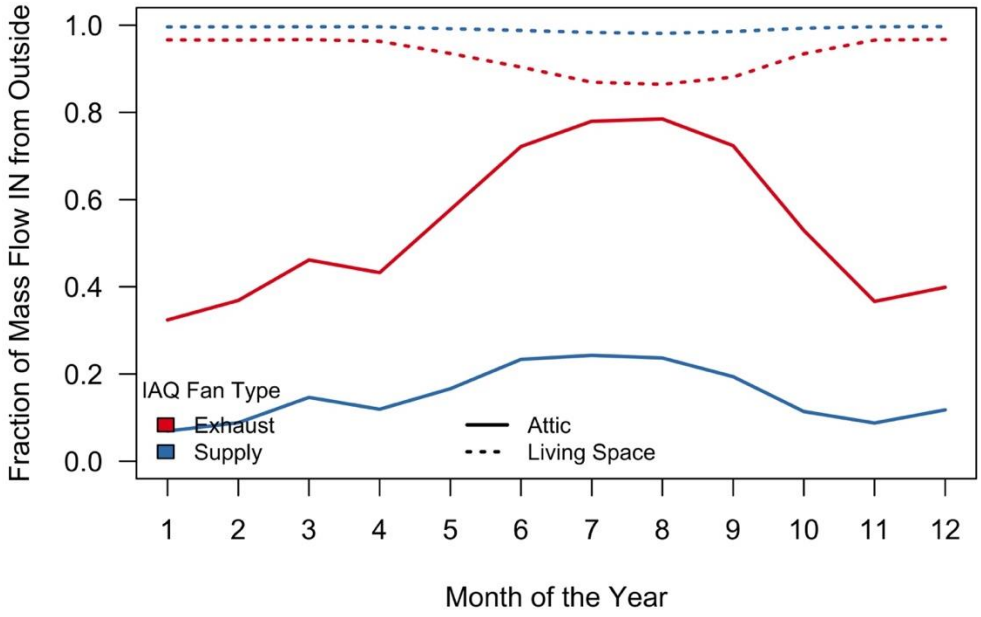

Sealed attic energy consumption was higher when using an exhaust ventilation fan compared with a supply fan. Energy use for each climate zone and fan type are shown in Figure 177. Mean increase consumption for exhaust fans was 82 kWh/year site energy. We hypothesize this benefit was the result of warmer attics in the heating season and cooler attics in the summer. The main mass flows into the attic were from the living space air, rather than the outside air, and this will reduce the loads on the attic and HVAC equipment contained inside.

Figure 177 Total HVAC site energy use for each climate zone and IAQ fan type.

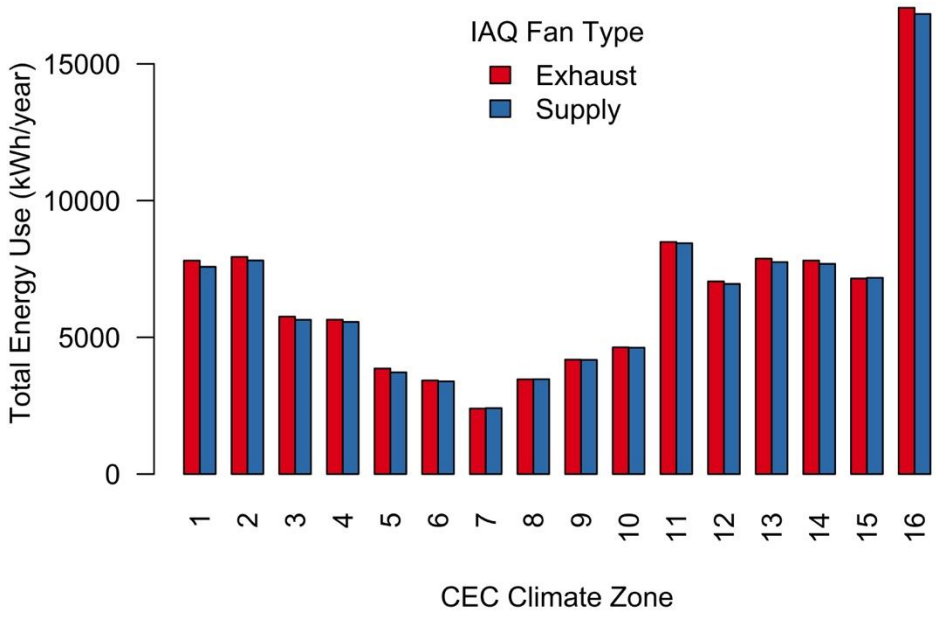

7.2.4.11 Roof Finish (Tile vs. Asphalt Shingles)

Roof finish is expected to affect the moisture performance of sealed and insulated attic assemblies. In fact, they are treated distinctly different in the model codes and the CRC (2016) in terms of how much air impermeable insulation is required to control condensing surface temperatures. Namely, tile roofs are allowed to use no air impermeable insulation (i.e., all fibrous insulation) in select climate zones, including CEC CZ 6-15 per the 2016 CRC (and DOE CZ 2B and 3B per the IECC). So, we tested a subset of cases with tile vs. asphalt shingle roof finishes.

The fraction of cases that failed the mold index criteria at the North sheathing for each climate zone and roof finish type are plotted in Figure 178. The results are mixed, with more failures on tile roofs in CZ2 and 13, more asphalt shingle failures in CZ5 and no difference in CZ1. Bulk framing results in Figure 179 are different, with consistently increased mold risk in the asphalt shingle cases. Overall, more tile roofs failed the mold index at the North sheathing, with 9 vs. 6% failure rate, while bulk framing showed 19% failure rate in shingle roofs vs. 5% in tile roofs. Shingle roofs also experienced substantially fewer cases of high wood moisture content at the North sheathing, where 11% of tile roof cases exceeded the 28% WMC threshold and only 3% of asphalt shingle cases. Condensation at the North sheathing was reduced across all climate zones for tile roofs, by an average of 45%. Condensation was also reduced at the other moisture nodes for cases with tile roofing by 67% and 77% at the South sheathing and attic framing nodes, respectively (see Figure 180).

Figure 178 North sheathing fraction of cases that failed mold index criteria for each climate zone and roof finish.

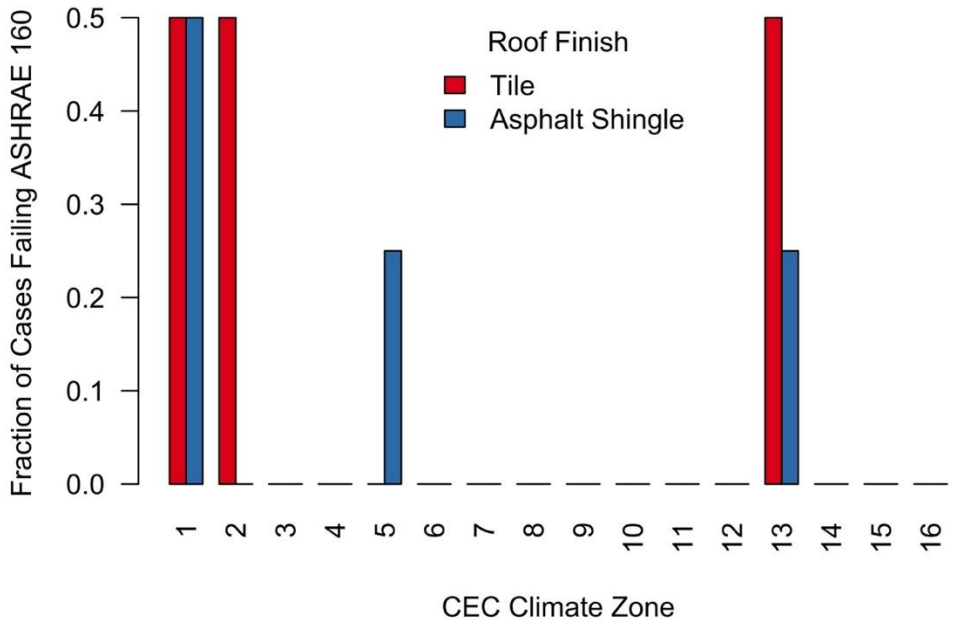

Figure 179 Bulk framing fraction of cases that failed mold index criteria for each climate zone and roof finish.

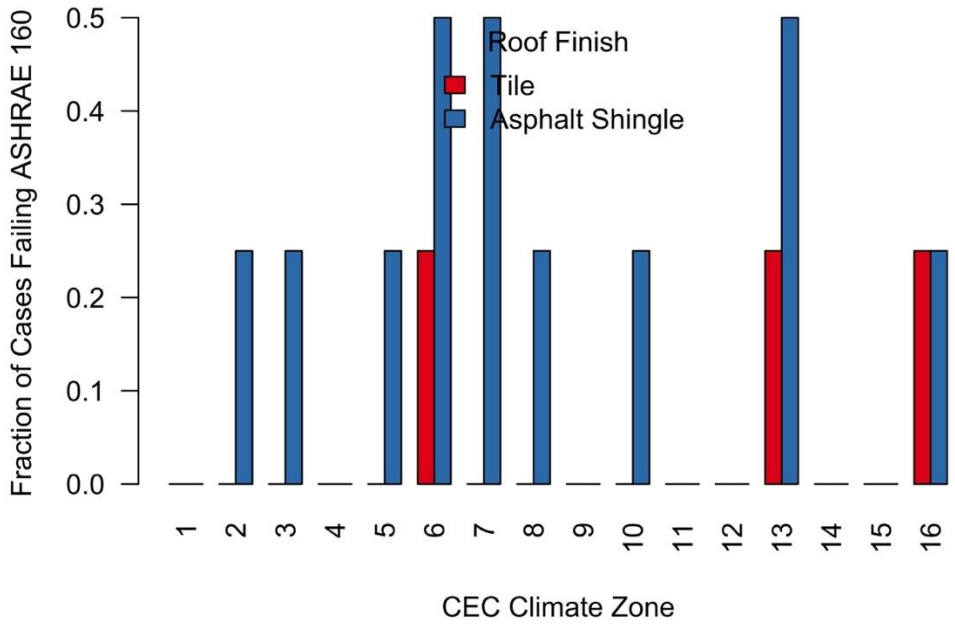

Figure 180 Total condensed mass at each attic moisture node, by roof finish (tile vs asphalt shingle).

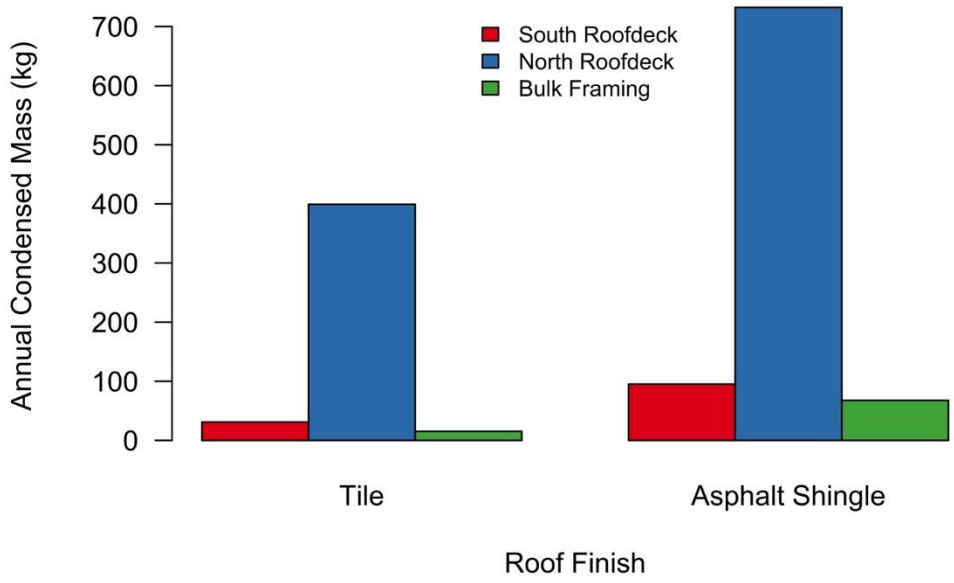

In the REGCAP model, the tile roof system has a greater thermal resistance than the shingle system (shingles 0.078 m^2-K/W (R-0.4 IP) vs. tile roof 0.5 m^2-K/W (R-2.8 IP)). This thermal resistance is to the exterior of the roof sheathing moisture node, so that the tile roof effectively acts as outboard insulation, which raises the surface temperature at the sheathing moisture nodes, and we would expect this to reduce local RH and moisture content while lessening condensation. The tile roof also has greater thermal mass, such that heat transfer is lagged and less extreme conditions are met, which again can limit periods of condensation, as very low temperature values are buffered by the thermal mass of the roofing.

To illustrate the protective effects of tile roofing, Figure 181 shows an example home in CZ5 with shingles and tile roof finishes (1-story, medium moisture gains, 3 ACH_{50}, 5% duct leakage, T24 (2008) exhaust fan). We see that the shingle roof gets both hotter in daytime and colder at night, because of the lower thermal resistance outboard of the roof sheathing. Consistent with that, the shingle roof experiences condensation (pink highlighted regions), while the tile roof never reaches saturation during this time period.

Median total HVAC energy use is shown for each climate zone and roof finish in Figure 182. The tile roof finish has lower energy use in each climate zone, which we believe is the result of increased roof deck thermal resistance (more insulated) and thermal mass, as well as from increase roof surface temperatures with single roof finishes. The mean increase in site energy use for asphalt shingle roofs was 81 kWh/year (539 kWh/year TDV energy).

Figure 181 Time series comparison of North roof deck surface temperature, RH and condensation for a week in winter in cases with tile roofing vs. asphalt shingles.

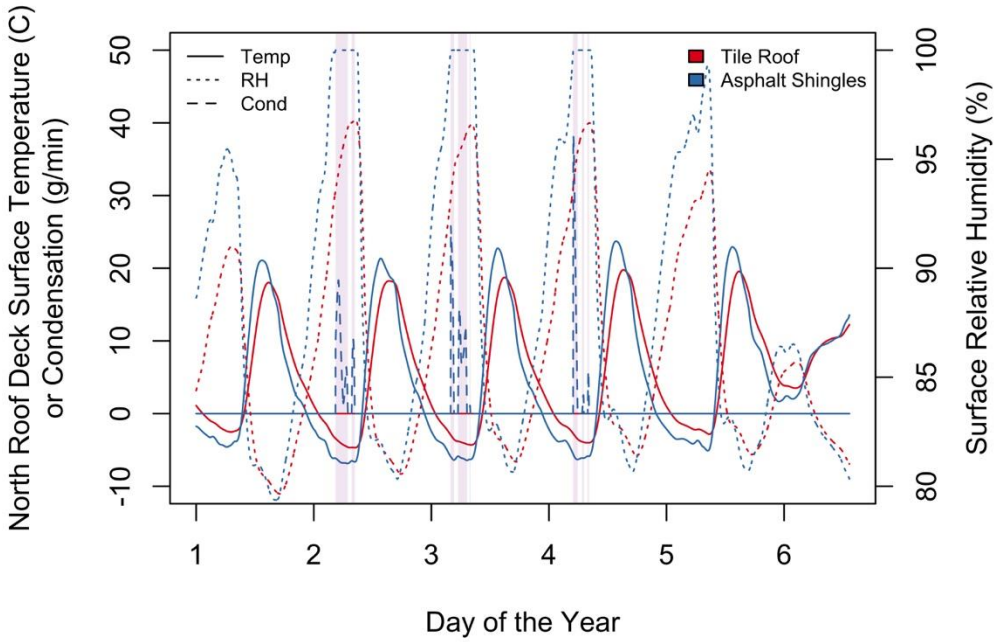

Figure 182 Total HVAC site energy use for each climate zone and roof finish.

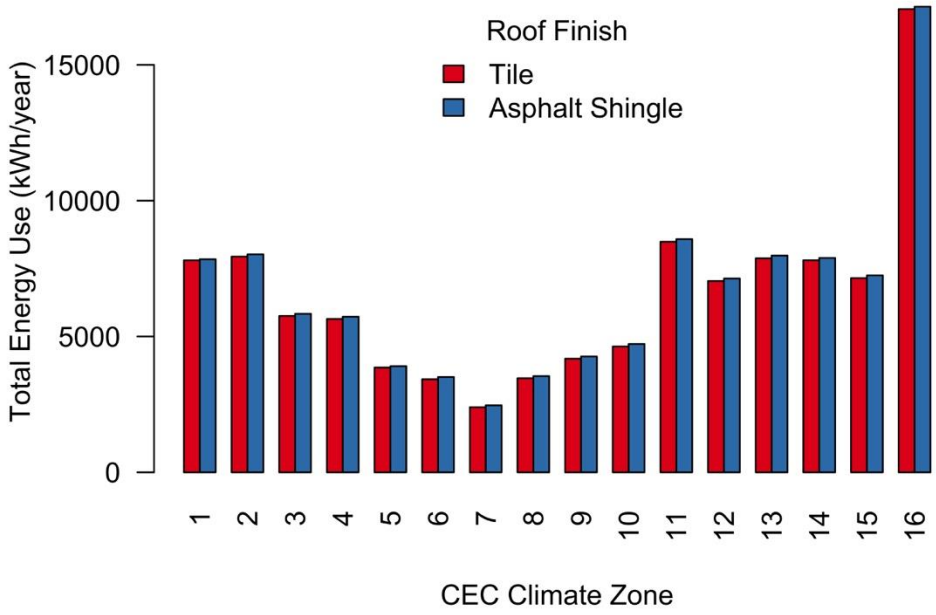

7.2.5 Moisture Mitigations

A core set of simulations was performed for a variety of moisture mitigation strategies. These included both prototypes, both internal moisture gains, three IAQ fan sizes in all 16-climate zones. All other factors were fixed at 3 ACH_{50}, 5% duct leakage, 50% attic and ceiling leakage, and exhaust fan with a tile roof finish. Each mitigation was simulated in 192 cases. The efficacy of the mitigation measures are assessed by what fraction of previously failing cases the measure fixes, with a mold index value below 3 and wood moisture content below 28%.

The following moisture mitigation measures were implemented in the REGCAP simulations:

1. HVAC supply air provided to the attic volume at a rate of 50 cfm/1000 ft^2 of attic floor area.
2. Air impermeable insulation at the roof deck per California Residential Code (2016) requirements, plus batt insulation to make up remaining thermal resistance.
3. 1-perm inch vapor retarder batt insulation.
4. Mechanical supply fan into the attic volume at 20 cfm per 1,000 ft^2 of ceiling area.
5. Mechanical supply fan into the attic volume at 50 cfm per 1,000 ft^2 of ceiling area.

7.2.5.1 HVAC Supply Air to Attic at 50 cfm/ 1000 ft2 of Attic Floor Area

Provision of HVAC supply air directly into the attic volume is a mandatory requirement in the 2018 IECC model code for all homes using a sealed and insulated attic approach. The intention is to eliminate moisture accumulation in the attic volume by directly conditioning it, just as for the living space. The intentional HVAC supply in the attic air was tested only in cases with medium moisture gains, 3 ACH_{50}, 5% duct leakage, core batch attic and ceiling (50a and 50c). This included 1- and 2-story prototypes, 2010 FVRM and no IAQ fans, and all climate zones.

North sheathing and attic bulk framing mold index failures are shown for baseline and added supply air cases in Figure 183 and Figure 184, respectively. These simulations suggest that this provision of HVAC supply air into the attic either increases or does not change mold risk at the North sheathing. Similar results were found for the bulk wood nodes, where the only successful cases were in CZ16, where failure rates were reduced from 25% to roughly 17%. Overall, North sheathing failure rates increased from 22% to 27% when adding the supply air, and bulk framing failures increased from 14% to 16% of cases. Very similar increased risk was seen for the wood moisture content threshold of 28%. Condensation at the North sheathing also increased by 12% when HVAC supply air was introduced into the attic volume.

We show the maximum mold index values for each case where the North and bulk framing mold indices failed with and without HVAC supply in Table 36 and Table 37. Consistent with the results previously reported, most cases would have failed with our without the HVAC supply in the attic, and in a handful of cases, the HVAC supply air forced a mold index failure that would not otherwise occur. Overall, this strategy is harmful in a small subset of cases, and is otherwise ineffective at addressing mold risks. This strategy was originally developed for homes in very humid climates in an effort to dehumidify the attic and may be a viable strategy in those locations. Outside very humid climates, moisture in attics is a winter problem when outside air is dryer than indoors and there is no mechanical dehumidification.

Figure 183 North sheathing mold index failure rates in each climate zone, with and without HVAC air supplied to the attic.

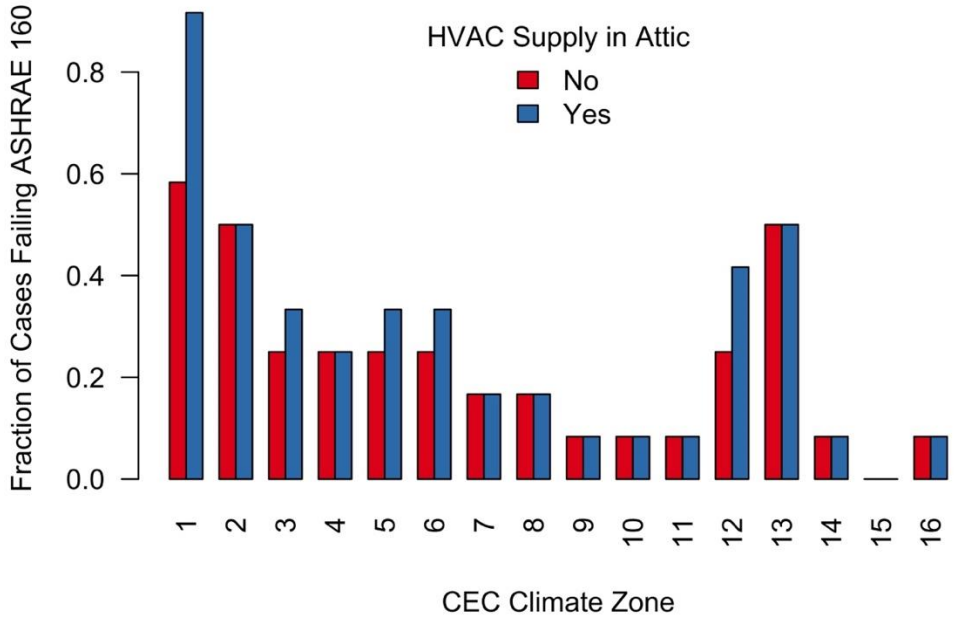

Figure 184 Bulk framing mold index failure rates in each climate zone, with and without HVAC air supplied to the attic.

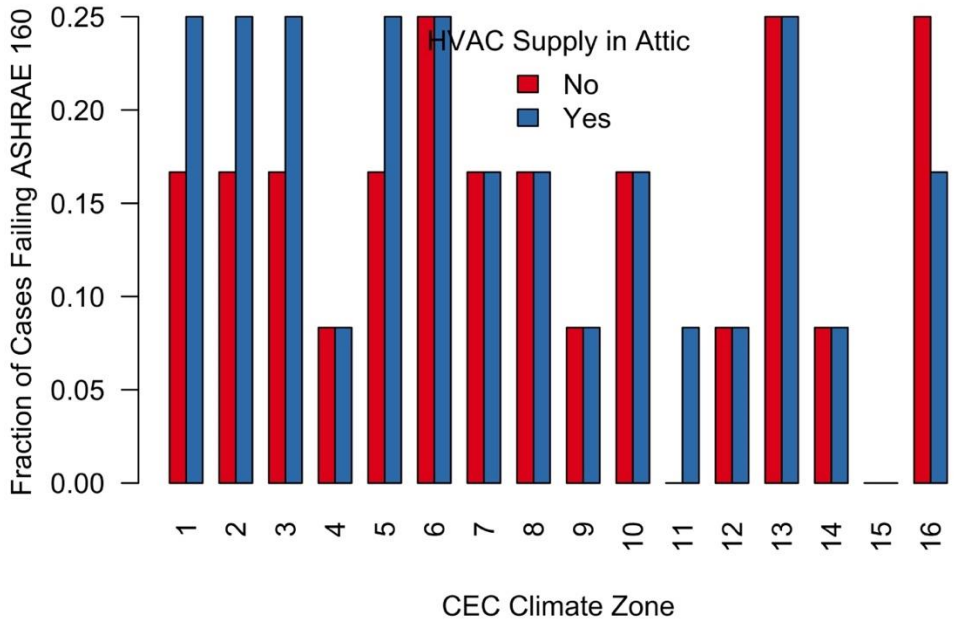

We plot the monthly mean partial vapor pressures in the attic and living space volumes for cases with and without HVAC air supplied in the attic in Figure 185. We see that vapor pressure is somewhat higher during the heating season in attics with intentional supply air, while these attics have much lower attic vapor pressure in the cooling season, when dehumidified air is

forced into the attic. Vapor pressure in the living space are quite similar, if somewhat lower in the cases with intentional supply air, because some of the moisture content in the living space air is being redistributed to the attic air. Clearly this strategy works to dehumidify the attic during the cooling season, but it appears to humidify the attic during the risky heating season when moisture accumulates in sealed attic roof deck assemblies. This effect assumes that the house is at a higher vapor pressure than the attic; if that were not the case, then we expect that mold risk would not worsen, but would also not improve. The only situation where this would be beneficial would be when the attic has substantially higher vapor pressure than the living space. For example, when seasonally stored moisture is baked out of the roof deck during spring, this strategy could facilitate more rapid drying. It would also provide dehumidification of attics in hot and humid climates, where daytime attic air can be at or near saturation during the cooling season, due to higher outdoor moisture and the emission of water vapor from the roof deck when heated by the sun. We also expect this strategy to mix the attic air during system operation, which would tend to reduce temperature and moisture stratification. It is possible that this mixing would limit the transport of moisture to the roof ridge, where past work has shown moisture accumulates most rapidly (Less et al. (2016)). The REGCAP model treats the attic and living spaces as well-mixed zones, because no valid models exist to predict the stratification and redistribution of thermal energy and moisture in attics. Without additional knowledge of the physics of stratification in attics we cannot provide more concrete discussion or conclusions.

Figure 185 Monthly mean partial vapor pressure in the house and attic volumes, with and without HVAC air supplied to the attic.

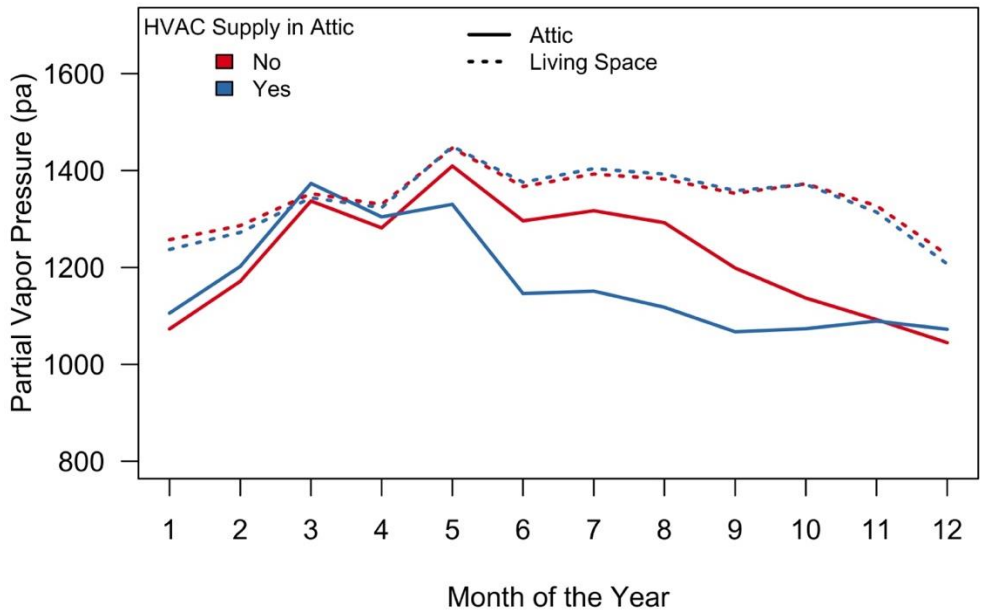

While its impacts of moisture performance were mostly negative, this strategy also increased total HVAC energy use and reduced energy savings, because rather than being allowed to float, the attic is actively conditioned. Supply air is diverted from the living space, which also requires

more system runtime to meet a given set point in the living zone. In Figure 186 Total HVAC site energy savings for each climate, with and without HVAC air supplied to the attic., we show median total HVAC site energy savings for each climate with and without intentional HVAC supply air in the attic (total consumption is shown in Figure 187). Indeed, energy savings are reduced by this strategy, on average from 18% to 16%. For matched cases, this strategy increased total HVAC energy use by an average of 161 kWh/year (389 kWh/year TDV energy).

Figure 186 Total HVAC site energy savings for each climate, with and without HVAC air supplied to the attic.

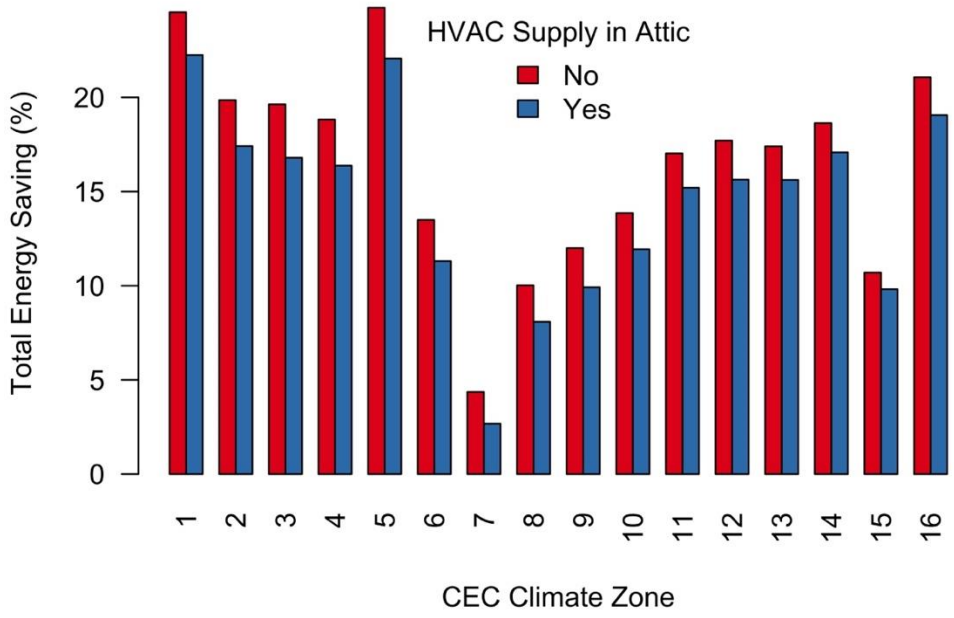

Figure 187 Total HVAC site energy use for each climate zone , with and without HVAC air supplied to the attic.

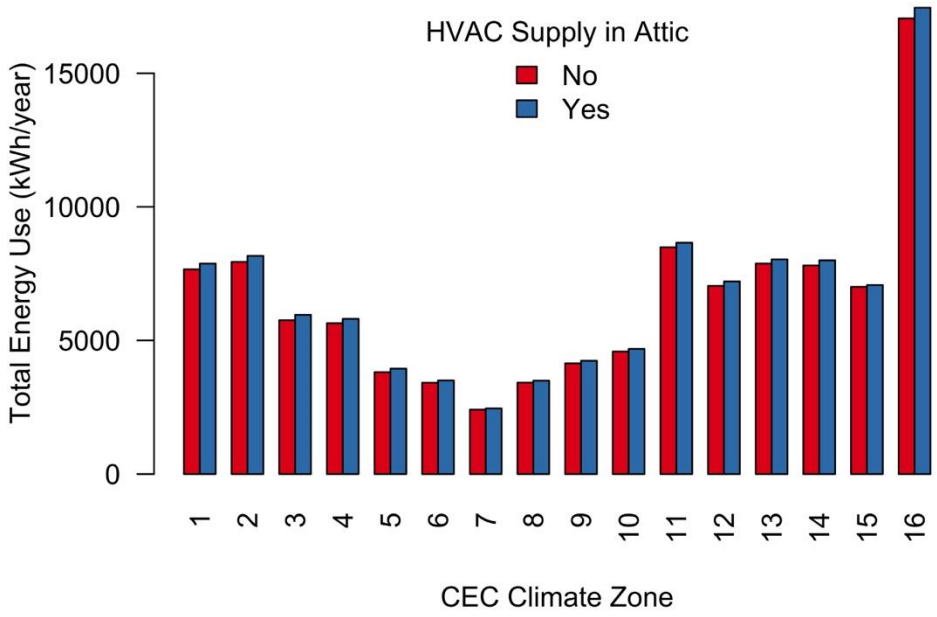

Table 36 North sheathing, mold index failures with and without HVAC supply air in the attic.

Prototype	Moisture Gains	ACH_{50}	Duct Leakage	Attic Leakage	Ceiling Leakage	Vent Fan Sizing	CZ	HVAC Supply Air In Attic?	
								Yes	No
L	H	3	5d	50a	50c	None	1	5.3	5.3
L	H	3	5d	50a	50c	None	13	5.3	5.3
L	H	3	5d	50a	50c	None	2	5.3	5.3
L	H	3	5d	50a	50c	None	3	5.3	5.3
M	H	3	5d	50a	50c	None	1	5.3	5.3
M	H	3	5d	50a	50c	None	11	5.3	5.3
M	H	3	5d	50a	50c	None	12	5.3	5.3
M	H	3	5d	50a	50c	None	13	5.3	5.3
M	H	3	5d	50a	50c	None	14	5.3	5.3
M	H	3	5d	50a	50c	None	16	5.3	5.3
M	H	3	5d	50a	50c	None	2	5.3	5.3
M	H	3	5d	50a	50c	None	3	5.3	5.3
M	H	3	5d	50a	50c	None	4	5.3	5.3
M	H	3	5d	50a	50c	None	5	5.3	5.3
M	H	3	5d	50a	50c	None	6	5.3	5.3
M	H	3	5d	50a	50c	None	7	5.3	5.3
M	H	3	5d	50a	50c	None	8	5.3	5.3
M	H	3	5d	50a	50c	None	9	5.3	5.3
M	M	3	5d	50a	50c	None	1	5.3	5.3

M	M	3	5d	50a	50c	None	13	5.3	5.3
M	M	3	5d	50a	50c	None	2	5.3	5.3
M	M	3	5d	50a	50c	None	3	5.3	5.3
M	M	3	5d	50a	50c	None	5	5.3	5.3
M	M	3	5d	50a	50c	None	6	5.3	5.3
L	H	3	5d	50a	50c	2010	1	5.29	5.29
L	H	3	5d	50a	50c	None	12	5.29	5.29
L	M	3	5d	50a	50c	None	1	5.29	5.29
M	M	3	5d	50a	50c	None	12	5.29	5.29
M	H	3	5d	50a	50c	2010	1	5.3	5.28
M	M	3	5d	50a	50c	None	7	5.06	5.12
M	H	3	5d	50a	50c	2010	13	5.3	5.08
M	M	3	5d	50a	50c	None	4	5.27	5.05
M	M	3	5d	50a	50c	None	8	4.85	5.05
L	H	3	5d	50a	50c	None	5	4.74	5
M	H	3	5d	50a	50c	None	10	4.83	4.89
L	H	3	5d	50a	50c	None	4	4.79	4.87
L	H	3	5d	50a	50c	Buil	1	5.15	4.81
L	H	3	5d	50a	50c	None	6	4.05	4.27
L	H	3	5d	50a	50c	2010	13	4.06	3.99
L	H	3	5d	50a	50c	2010	2	3.69	3.47
M	H	3	5d	50a	50c	2010	2	5.29	3.22
L	H	3	5d	50a	50c	2010	12	3.06	2.89
L	M	3	5d	50a	50c	2010	1	3.02	2.81
M	H	3	5d	50a	50c	2010	12	5.16	2.7
M	M	3	5d	50a	50c	2010	1	5.28	2.65
M	H	3	5d	50a	50c	2010	3	5.3	1.85
M	M	3	5d	50a	50c	2010	13	3.4	1.69
M	H	3	5d	50a	50c	Buil	1	5.29	1.5
M	H	3	5d	50a	50c	2010	5	4.88	0.78
M	M	3	5d	50a	50c	Buil	1	4.26	0.71
M	H	3	5d	50a	50c	2010	6	3.38	0.53
M	H	3	5d	50a	50c	Buil	2	3.14	0.49

Table 37 Bulk framing, mold index failures with and without HVAC supply air in the attic.

Proto type	Moisture Gains	ACH50	Duct Leakage	Attic Leakage	Ceiling Leakage	Vent Fan Sizing	CZ	HVAC Supply Air in Attic?	
								No	Yes
M	H	3	5d	50a	50c	None	2	6	6
M	H	3	5d	50a	50c	None	3	6	6
M	H	3	5d	50a	50c	None	1	5.99	5.99

M	H	3	5d	50a	50c	None	13	5.99	5.99
M	H	3	5d	50a	50c	None	16	5.99	5.99
M	H	3	5d	50a	50c	None	5	5.99	5.99
M	H	3	5d	50a	50c	None	6	5.99	5.99
M	H	3	5d	50a	50c	None	7	5.99	5.99
M	H	3	5d	50a	50c	None	8	5.99	5.99
M	M	3	5d	50a	50c	None	2	5.99	5.99
M	M	3	5d	50a	50c	None	3	5.99	5.99
M	M	3	5d	50a	50c	None	5	5.99	5.99
M	M	3	5d	50a	50c	None	6	5.99	5.99
M	H	3	5d	50a	50c	None	10	5.98	5.99
M	H	3	5d	50a	50c	None	4	5.98	5.99
M	M	3	5d	50a	50c	None	10	5.94	5.99
M	H	3	5d	50a	50c	None	12	5.98	5.98
M	M	3	5d	50a	50c	None	7	5.97	5.98
M	H	3	5d	50a	50c	None	9	5.96	5.98
M	M	3	5d	50a	50c	None	8	5.95	5.98
M	H	3	5d	50a	50c	2010	13	5.97	5.97
M	M	3	5d	50a	50c	None	13	5.96	5.97
M	M	3	5d	50a	50c	None	1	5.95	5.96
M	H	3	5d	50a	50c	2010	6	5.99	5.9
M	H	3	5d	50a	50c	2010	16	5.64	5.85
M	H	3	5d	50a	50c	None	14	5.57	5.84
M	H	3	5d	50a	50c	None	11	4	2.74
M	H	3	5d	50a	50c	2010	2	6	0.34
M	H	3	5d	50a	50c	2010	3	5.56	0.14
M	H	3	5d	50a	50c	2010	5	5.99	0.03
M	H	3	5d	50a	50c	2010	1	5.96	0.01

7.2.5.2 IECC Air Impermeable Insulation

The installation of air impermeable insulation above the roof deck of each case is meant to reflect the requirements in CRC Table R806.5 (2016) (see Table 1). Between R-5 and R-15 air impermeable insulation was added above the roof deck, depending on climate zone. For those CEC climate zones with no air impermeable insulation requirement in Table R806.5, we specified R-5 insulation, in order to distinguish these cases from the prior runs using solely fibrous insulation. This strategy was tested with a mix of medium and high moisture gains in cases with 1, 3 and 5 ACH_{50}, 5% duct leakage, core batch attic and ceiling (50a and 50c). This included 1- and 2-story prototypes, three IAQ fan sizes, and all climate zones.

North sheathing and attic bulk framing mold index failures are shown with and without added air impermeable insulation in Figure 188 and Figure 189, respectively. North sheathing failure rates were cut roughly in half in CZ1, 2 and 13, while reductions were modest or non-existent in

other locations. Overall, addition of air impermeable insulation per the CRC reduced mold index failure rates at the North sheathing node from 22% to 15% of all cases, and bulk framing failure rates went from 14% down to 8%. Similar reductions were seen on the North sheathing for cases that exceeded the 28% wood moisture content criteria. For North sheathing locations, use of air impermeable insulation per the CRC reduced maximum wood moisture content from an average of 22% to 18%.

We show maximum mold index results for each individual case that failed the North sheathing or bulk framing mold index criteria in Table 38 and Table 39. It is clear that for most of the no IAQ fan cases that failed using solely fibrous insulation, the provision of air impermeable insulation above the roof deck does not reduce the risk of mold growth to safe levels. In some conditions, this strategy clearly helps, for example in several cases in CZ1 and 2.

At its core, this strategy is designed to limit condensation, and condensation was by far the greatest on the North sheathing. So, we show the reduction in annual condensed moisture mass on the North sheathing for each climate zone in Figure 190. The inclusion of air impermeable insulation as specified in Table R806.5 of the CRC drastically reduces surface condensation on all moisture nodes, with an average reduction of 89% at the North sheathing, and 92% and 78% at the South sheathing and attic framing nodes (these values are the mean reduction in each case where there was condensation; the values in Table 31 are the reduction in the mean values across all cases). Clearly provision of insulation above the roof deck provides very strong assurance against condensation, but its control of mold index and surface RH, along with WMC, are not as valuable.

We illustrate why the mold index values remain fairly high when implementing this strategy with an example time series plot in Figure 191. We see that indeed the air impermeable insulation above the roof deck substantially warms the sheathing surface relative to solely fibrous insulation. Overnight temperatures are as much as 5°C colder at the solely fiberglass roof deck. We see that the fiberglass roof has condensation (pink highlighted regions), while the foam board roof deck has no condensation. Yet, the roof deck with foam board above the sheathing still has substantially elevated surface RH. The Surface RH is clearly lower than the solely fiberglass roof, yet the weekly average RH in this plot is still around 90% as compared with roughly 95% for the solely fiberglass roof deck. 90% is well above the critical mold growth level of 80% used in the mold index model, so the mold index still increments and considers some of these assemblies to be at risk.

Figure 188 North sheathing mold index failure cases in each climate zone with and without air impermeable insulation per the CRC Section R806.5.

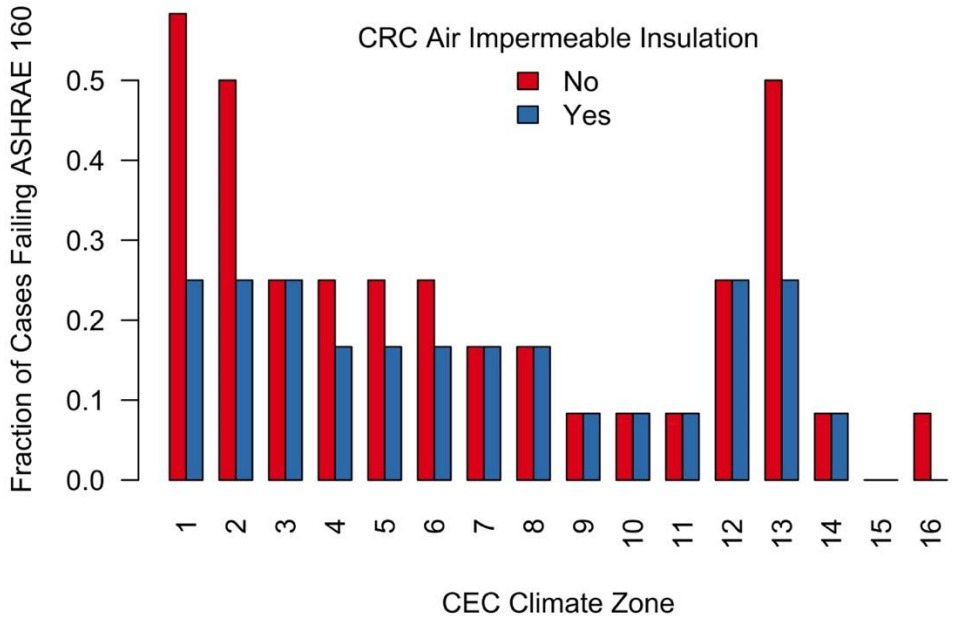

Figure 189 Bulk framing mold index failure cases in each climate zone with and without air impermeable insulation per the CRC Section R806.5.

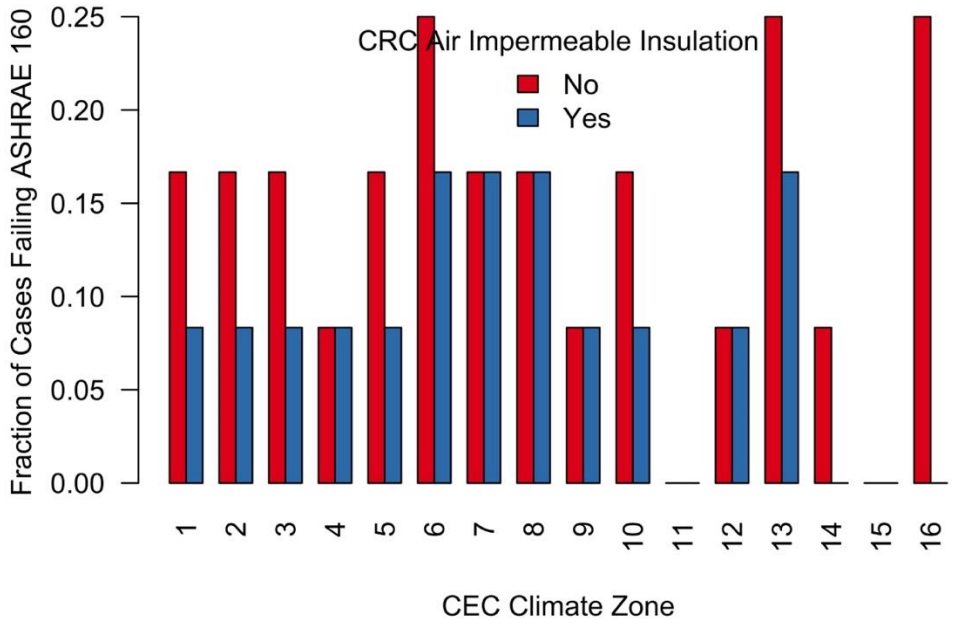

Figure 190 North sheathing % reduction in total condensed moisture mass for each climate zone with and without air impermeable insulation per the CRC Section R806.5.

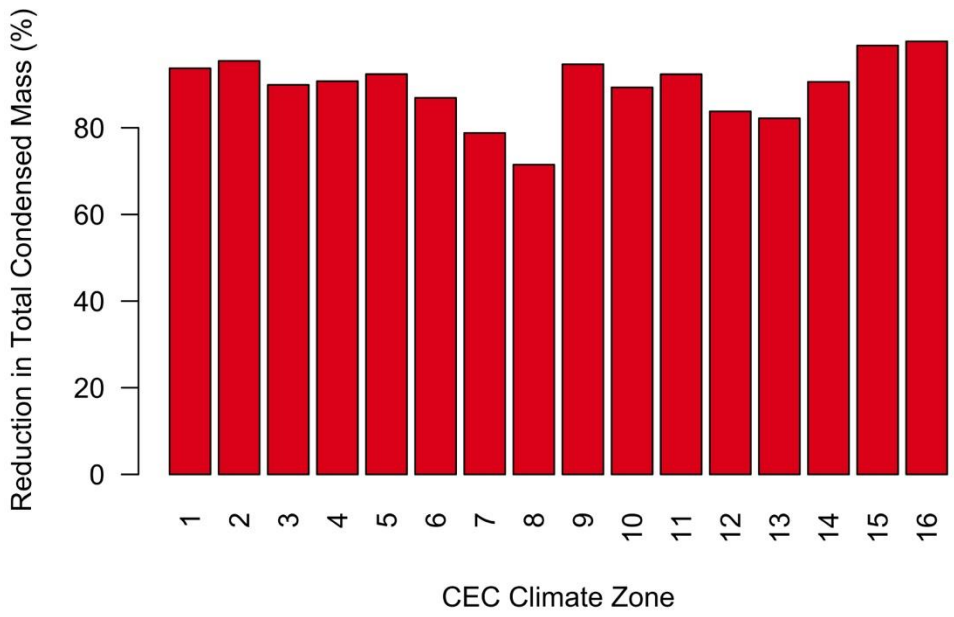

Figure 191 Time series illustration of North sheathing surface temperature, RH and condensed mass for an example case with and without CRC foam board insulation above the roof deck.

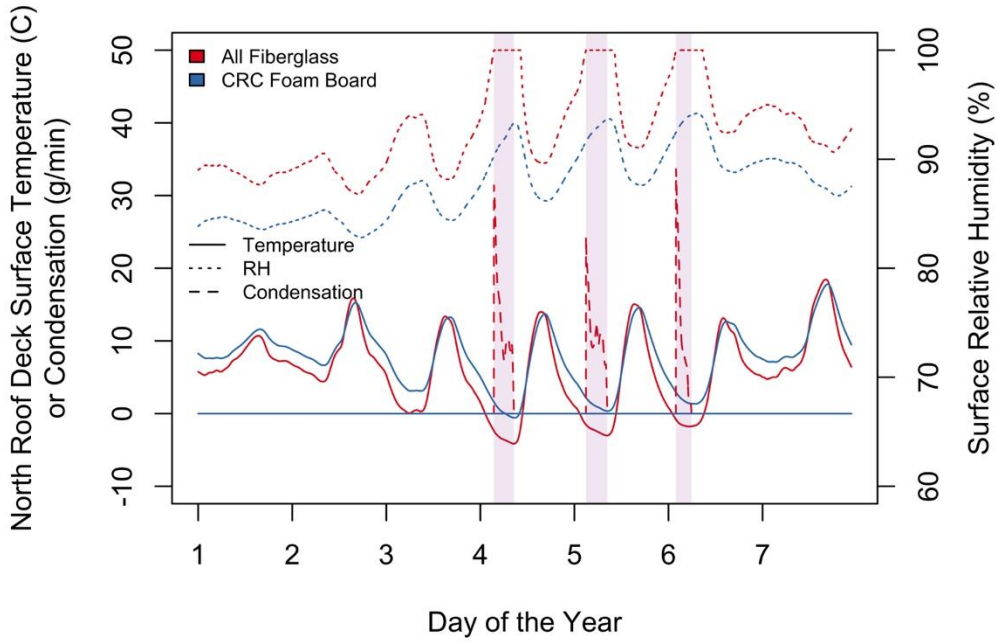

Table 38 North sheathing, mold index failures with and without IECC air impermeable insulation on the roof deck.

Prototype	Moisture Gains	ACH_{50}	Duct Leakage	Attic Leakage	Ceiling Leakage	Vent Fan Sizing	CZ	Air Impermeable Insulation Above Roof Deck?	
								Yes	No
L	H	3	5d	50a	50c	None	1	5.3	5.3
L	H	3	5d	50a	50c	None	13	5.3	5.3
M	H	3	5d	50a	50c	None	1	5.3	5.3
M	H	3	5d	50a	50c	None	11	5.3	5.3
M	H	3	5d	50a	50c	None	12	5.3	5.3
M	H	3	5d	50a	50c	None	13	5.3	5.3
M	H	3	5d	50a	50c	None	14	5.3	5.3
M	H	3	5d	50a	50c	None	2	5.3	5.3
M	H	3	5d	50a	50c	None	3	5.3	5.3
M	H	3	5d	50a	50c	None	4	5.3	5.3
M	H	3	5d	50a	50c	None	5	5.3	5.3
M	H	3	5d	50a	50c	None	6	5.3	5.3
M	H	3	5d	50a	50c	None	7	5.3	5.3
M	H	3	5d	50a	50c	None	8	5.3	5.3
M	M	3	5d	50a	50c	None	1	5.3	5.3
M	M	3	5d	50a	50c	None	13	5.3	5.3
L	H	3	5d	50a	50c	None	12	5.28	5.29
L	H	3	5d	50a	50c	None	3	5.27	5.3
M	M	3	5d	50a	50c	None	3	5.27	5.3
M	M	3	5d	50a	50c	None	12	5.23	5.29
M	M	3	5d	50a	50c	None	2	5.16	5.3
L	H	3	5d	50a	50c	None	2	5.12	5.3
M	H	3	5d	50a	50c	None	9	5.08	5.3
M	M	3	5d	50a	50c	None	6	5.01	5.3
M	M	3	5d	50a	50c	None	5	4.57	5.3
M	H	3	5d	50a	50c	None	10	4.24	4.89
M	M	3	5d	50a	50c	None	8	4.2	5.05
M	M	3	5d	50a	50c	None	7	3.76	5.12
M	M	3	5d	50a	50c	None	4	3.64	5.05
L	H	3	5d	50a	50c	None	4	2.95	4.87
L	H	3	5d	50a	50c	None	5	2.91	5
M	H	3	5d	50a	50c	2010	13	2.89	5.08
M	H	3	5d	50a	50c	None	16	2.71	5.3
L	H	3	5d	50a	50c	2010	13	2.52	3.99
M	H	3	5d	50a	50c	2010	1	2.18	5.28
L	H	3	5d	50a	50c	None	6	1.85	4.27

L	M	3	5d	50a	50c	None	13	1.68	3.05
L	H	3	5d	50a	50c	2010	1	1.66	5.29
L	M	3	5d	50a	50c	None	1	1.31	5.29
M	H	3	5d	50a	50c	2010	2	0.81	3.22
L	H	3	5d	50a	50c	2010	2	0.73	3.47
L	H	3	5d	50a	50c	Buil	1	0.53	4.81
L	M	3	5d	50a	50c	None	2	0.52	3.05

Table 39 Bulk framing, mold index failures with and without IECC air impermeable insulation on the roof deck.

Prototype	Moisture Gains	ACH50	Duct Leakage	Attic Leakage	Ceiling Leakage	Vent Fan Sizing	CZ	Air Impermeable Insulation Above Roof Deck?	
								Yes	No
M	H	3	5d	50a	50c	None	2	6	6
M	H	3	5d	50a	50c	None	3	6	6
M	H	3	5d	50a	50c	None	13	5.99	5.99
M	H	3	5d	50a	50c	None	5	5.99	5.99
M	H	3	5d	50a	50c	None	6	5.99	5.99
M	H	3	5d	50a	50c	None	7	5.99	5.99
M	H	3	5d	50a	50c	None	8	5.99	5.99
M	H	3	5d	50a	50c	None	10	5.98	5.99
M	M	3	5d	50a	50c	None	6	5.98	5.99
M	H	3	5d	50a	50c	None	4	5.94	5.99
M	H	3	5d	50a	50c	None	1	5.93	5.99
M	H	3	5d	50a	50c	None	12	5.9	5.98
M	M	3	5d	50a	50c	None	7	5.77	5.98
M	M	3	5d	50a	50c	None	8	5.69	5.98
M	M	3	5d	50a	50c	None	13	5.66	5.97
M	H	3	5d	50a	50c	None	9	5.2	5.98
M	H	3	5d	50a	50c	None	16	0.91	5.99
M	M	3	5d	50a	50c	None	3	0.54	5.99
M	M	3	5d	50a	50c	None	10	0.43	5.99
M	H	3	5d	50a	50c	None	14	0.23	5.84
M	M	3	5d	50a	50c	None	1	0.21	5.96
M	H	3	5d	50a	50c	2010	13	0.16	5.97
M	M	3	5d	50a	50c	None	2	0.07	5.99
M	M	3	5d	50a	50c	None	5	0.05	5.99
M	H	3	5d	50a	50c	2010	6	0	5.9
M	H	3	5d	50a	50c	2010	16	0	5.85
M	M	3	5d	50a	50c	None	16	0	4.47

7.2.5.3 Vapor Retarder on Attic Surface of Batt Insulation

The CRC (2016) has a requirement for placement of a vapor retarder on the attic air side of any air permeable insulation in sealed and insulated attics. It appears to only require this mitigation in CZ 14 and 16. Nevertheless, the addition of a vapor retarder to the face of the fibrous insulation is an integral part of the High Performance Attic package offered by Owens Corning. We evaluated the use of 1 perm-in vapor retarders on the attic face of the insulation in each CEC climate zone.

The use of a vapor retarder eliminated all cases of mold index failure and all cases of elevated wood moisture content at the North sheathing (see Figure 192 North sheathing mold index failure rate for each climate zone with and without a class II vapor retarder on the attic air side of the insulation.), and condensation was completely eliminated. Results were nearly as dramatic for bulk framing in Figure 193, where only a single failure remained in CZ1 after application of the vapor retarder. This result indicates that the seasonal moisture storage in the sheathing and release into the attic air volume is a very important moisture dynamic for the whole attic and not just the sheathing surfaces. The source of moisture for the insulated roofdeck is the attic air and the living space air, so when a vapor retarder blocks transport across the insulation assembly, very little water vapor ever reaches the sheathing. During cold weather periods, when the solely fiber glass roof deck is averaging 90% RH, the vapor barrier batts maintain surface RH at the roofdeck around 40%. This intervention appears very promising, though the REGCAP model does not include introduction of bulk water from rain leaks. If this were to occur, the vapor retarder would limit the drying potential to the attic air. Other research of this application in cold climates has reported preliminary findings that support the use of variable permeability “smart” vapor retarders, which had improved moisture resilience over fixed 1-perm products (Ueno & Lstiburek, 2018).

As expected, use of a vapor barrier had very little impact on the energy use of the simulated homes. Cooling energy use was very marginally reduced with use of a vapor retarder, because of its tendency to reduce attic and living space air humidity levels, which lessens the latent load on the cooling compressor. The median reduction was 16 kWh/year site energy.

Figure 192 North sheathing mold index failure rate for each climate zone with and without a class II vapor retarder on the attic air side of the insulation.

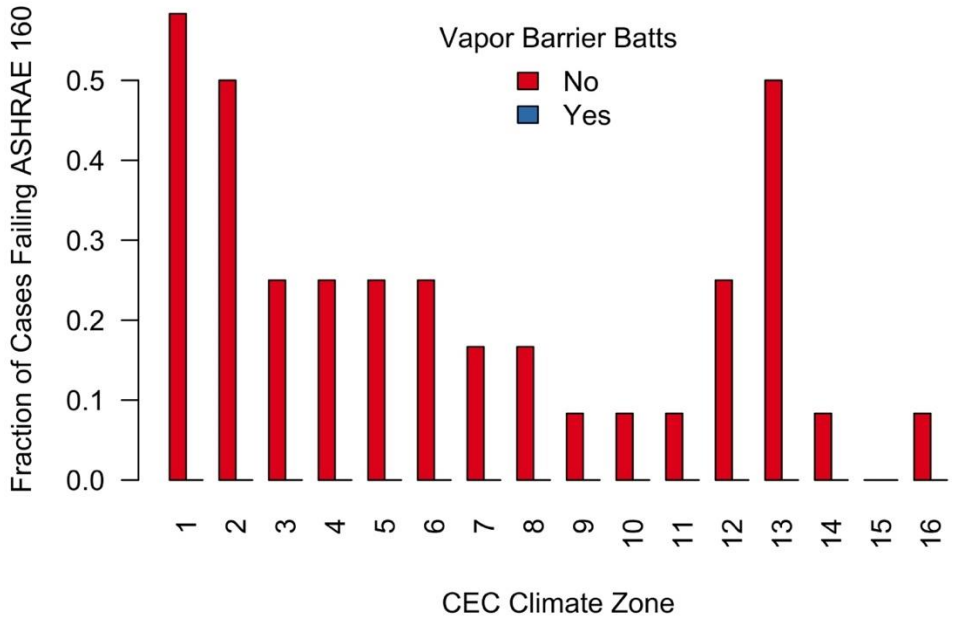

Figure 193 Bulk framing mold index failure rate for each climate zone with and without a class II vapor retarder on the attic air side of the insulation.

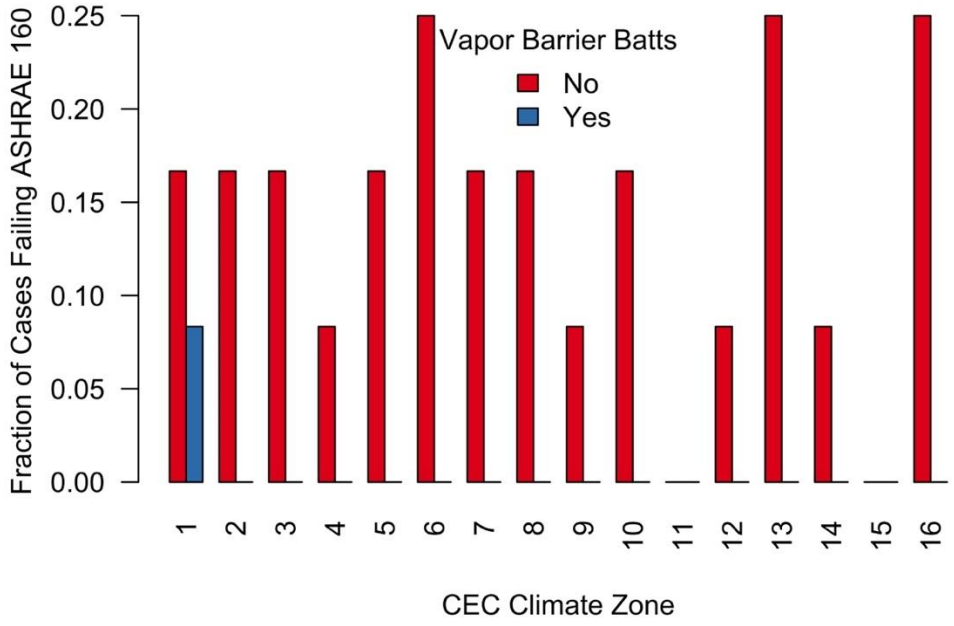

7.2.5.4 Outdoor Air Supply Fan Into Attic Volume

Our results have shown that increasing living space and attic outdoor air ventilation rates can reduce moisture risk in sealed and insulated attics. Furthermore, we have demonstrated that sealed attics have much lower air exchange rates than the living spaces they are attached to. In

line with these results, we reasoned that providing mechanical air exchange with outside supplied directly into the attic volume would be beneficial. These flows were implemented as airflows from outside into the attic volume, all hours of the year. This method was imperfect in that no fan energy was accounted for in the REGCAP model, nor was fan heat added to attic air volumes. We have added the mechanical fan energy back into the consumption totals in post-processing in order to better estimate the impacts on energy savings of these outdoor air supply fans, but we were unable to account for the addition of fan waste heat. See the estimates for mechanical supply fan power and energy use in Table 26. Energy savings are de-rated by this additional fan energy consumption.

In Figure 194 North sheathing mold index failures for each climate zone, with and without an outdoor air supply fan in the attic., we show the fraction of cases that failed the mold index criteria at the North sheathing for no attic supply fan along fans at 20 and 50 cfm per 1,000 ft^2 of attic floor area (see bulk framing failures in Figure 195). We found that providing 50cfm of outside air per 1,000 ft^2 of ceiling area fixed all mold index failures, while supply air at 20 cfm fixed the majority of failures. Overall, North sheathing failures dropped from 22% of all cases with no attic supply fan, down to 5% and 0% of cases with 20 and 50 cfm per 1000 ft^2 supplies, respectively. Bulk framing failures dropped from 14% of all cases down to 0% for either supply flow. Reductions in wood moisture failures were very similar in magnitude, and 7-day maximum wood moisture content at the North sheathing was reduced from an average of 21% down to 18% and 17% for 20 and 50 cfm per 1,000 ft^2 supply fans.

Condensation was also sharply reduced through introduction of outside air into the sealed attic volumes, as shown for the North sheathing location in Figure 196 Annual condensed mass at attic moisture nodes for each climate zone, by outdoor supply fan airflow into attic.. North sheathing condensed mass was reduced by 88% and by 98% at 20 and 50 cfm per 1,000 ft^2 supply fans. Condensed mass at the South sheathing and attic framing were effectively eliminated by either of the target supply fan airflows.

We have listed each individual case that failed the mold index criteria at the North sheathing with no supply attic fan in Table 40, along with matching counterparts with attic supply fans. Nearly all cases where the 20 cfm target supply fan did not remove risk of mold growth had no IAQ fan operating and most were high indoor moisture gain cases in the most risk-prone climates. Only in this subset of the most risky homes was the 50 cfm target flow required to achieve moisture resilience. We expect that in many cases, flows below 20 cfm per 1,000 ft^2 could also alleviate mold risk.

Figure 194 North sheathing mold index failures for each climate zone, with and without an outdoor air supply fan in the attic.

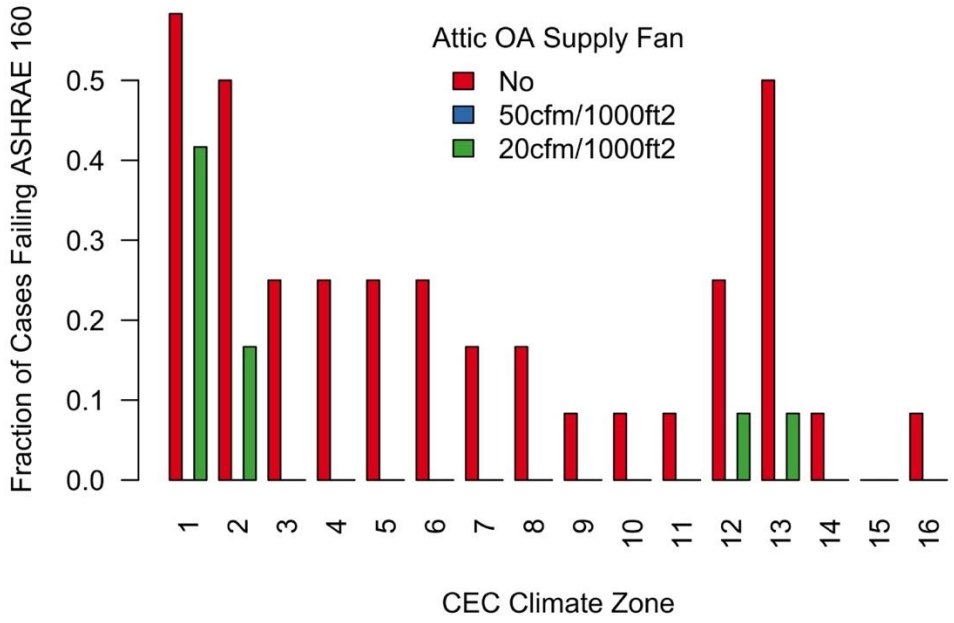

Figure 195 Bulk framing mold index failures for each climate zone, with and without an outdoor air supply fan in the attic.

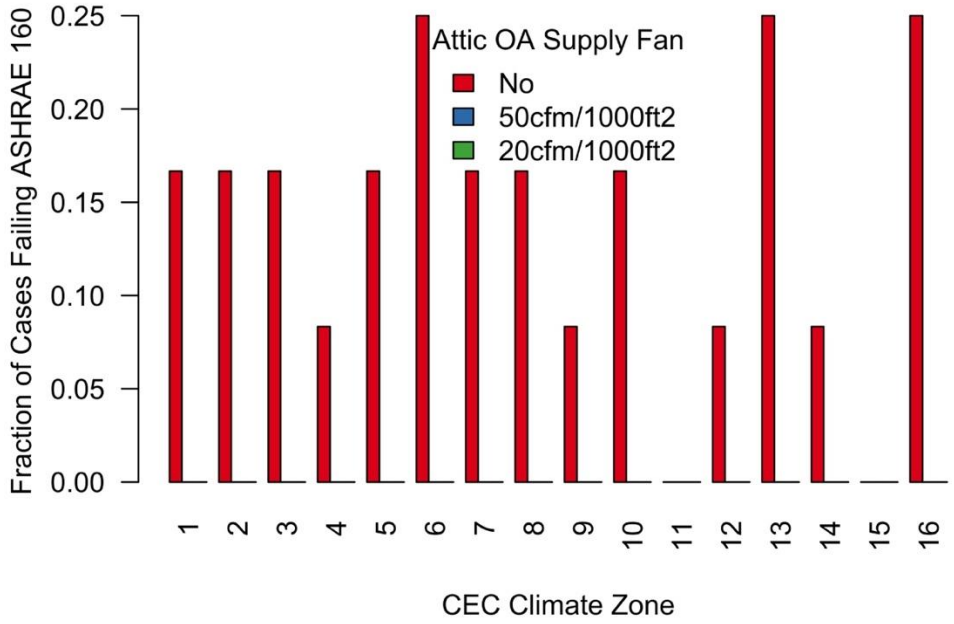

Figure 196 Annual condensed mass at attic moisture nodes for each climate zone, by outdoor supply fan airflow into attic.

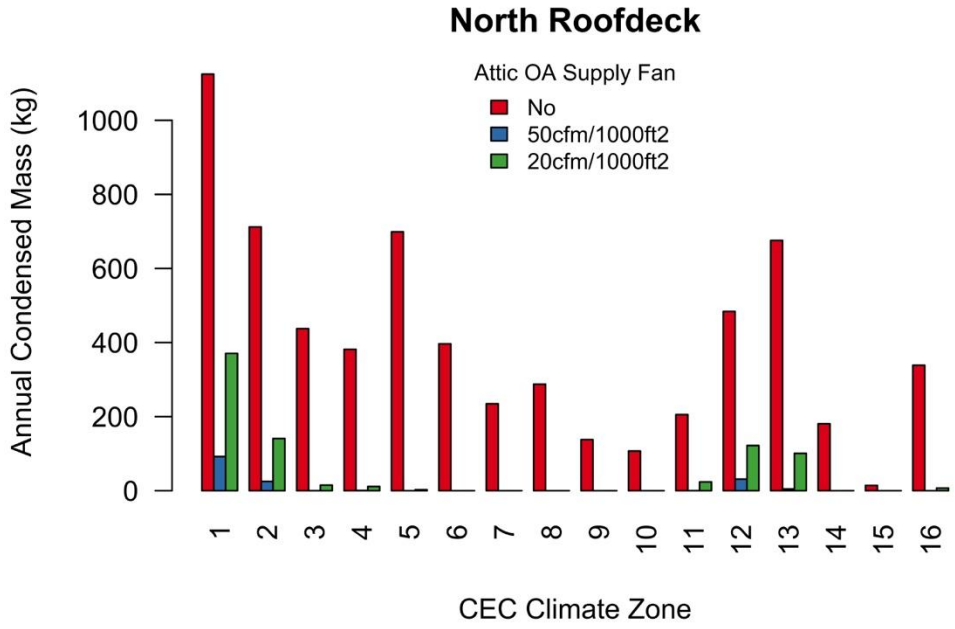

These attic supply fans led to drastically altered vapor pressure patterns in the attics and living spaces, as illustrated in Figure 197 Monthly mean vapor pressure in the attic, living space and outside of homes with and without an outdoor air supply fan in the attic.. This is especially clear in the heating season, where the provision of outside air into the attic volume reduces attic air vapor pressure between 100 and 200 pa relative to the standard sealed attic cases. With greater outside air ventilation, the attic vapor pressures look more and more like the ambient annual pattern, which is highlighted here as a dashed black line. The monthly mean mass exchange rates plotted in Figure 198 show how these attic supply fans have brought mass exchange rates in the attics up to a level just greater than the living space for the 20 cfm target, and more than double the living space with the 50 cfm target flow. We expect that most cases would have adequate moisture performance if the attic mass exchange were made to be equivalent to rates in the living spaces, or roughly 0.2 to 0.3 hr^{-1}. For comparison, the vented and HPA attics had annual average attic mass exchange rates between 2 and 6 hr^{-1}.

Figure 197 Monthly mean vapor pressure in the attic, living space and outside of homes with and without an outdoor air supply fan in the attic.

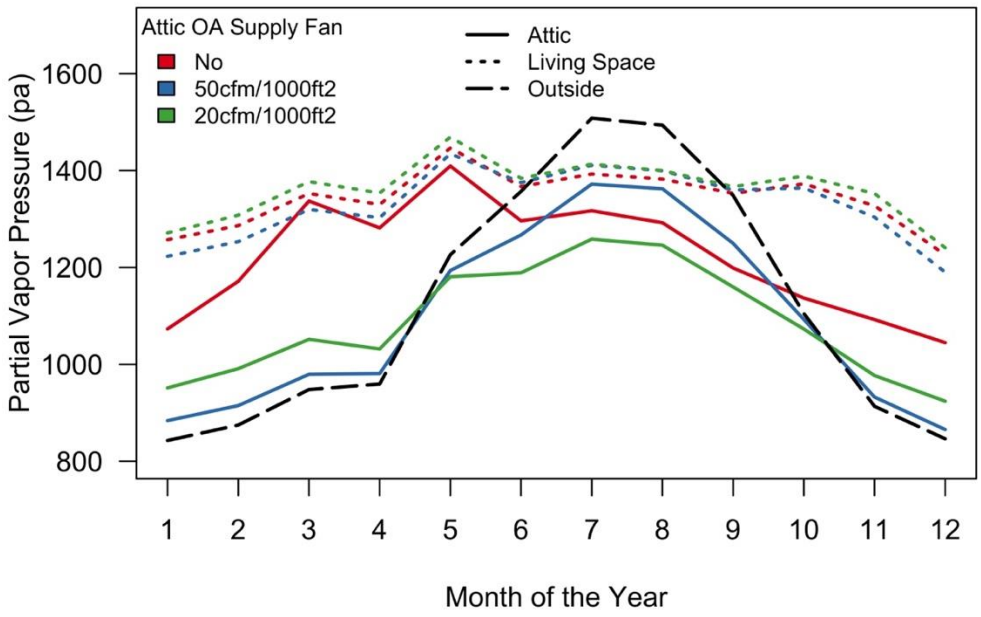

Figure 198 Monthly mean mass exchange rates for the living space and attic, with and without an outdoor air supply fan in the attic.

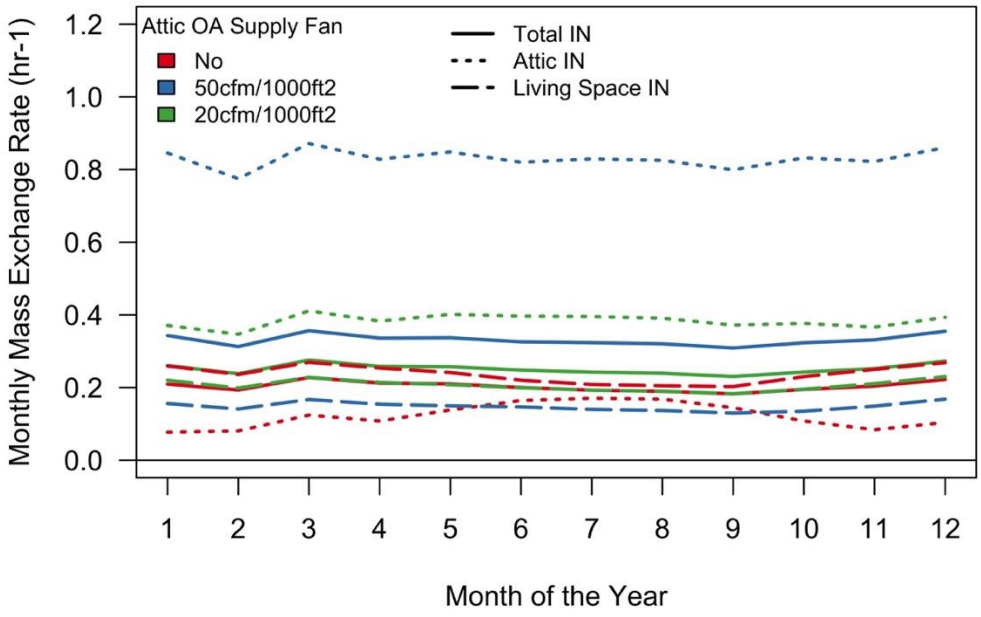

While clearly effective from a moisture control standpoint, outdoor air supply fans use mechanical energy and they increase the thermal loads on the attic. This substantially increased total energy consumption for sealed attics (see Figure 200 Total HVAC site energy use for each climate zone, with and without an outdoor air supply fan in the attic.) and reduced the energy savings. Site energy use increased an average of 428 kWh/year and 871 kWh/year for the 20

and 50 cfm per 1,000 ft^2 targets, respectively. In Figure 199, we show average savings for each climate zone with each attic supply fan option, compared with savings when no supply fan is used. Overall, median savings with no supply fan were 17.6%, which was reduced to 11.4% for a 20 cfm per 1,000 ft^2 target, and to only 4% for the 50 cfm target. This erosion of energy savings is substantial, especially for the 50 cfm target, which was required to eliminate all mold index failures in CZ 1, 2, 12 and 13. While not explored in this work, such supply fans may only be needed during certain times of the year, and they could potentially be controlled to strongly limit the current energy penalties.

Figure 199 Total HVAC site energy savings for each climate zone, with and without an outdoor air supply fan in the attic.

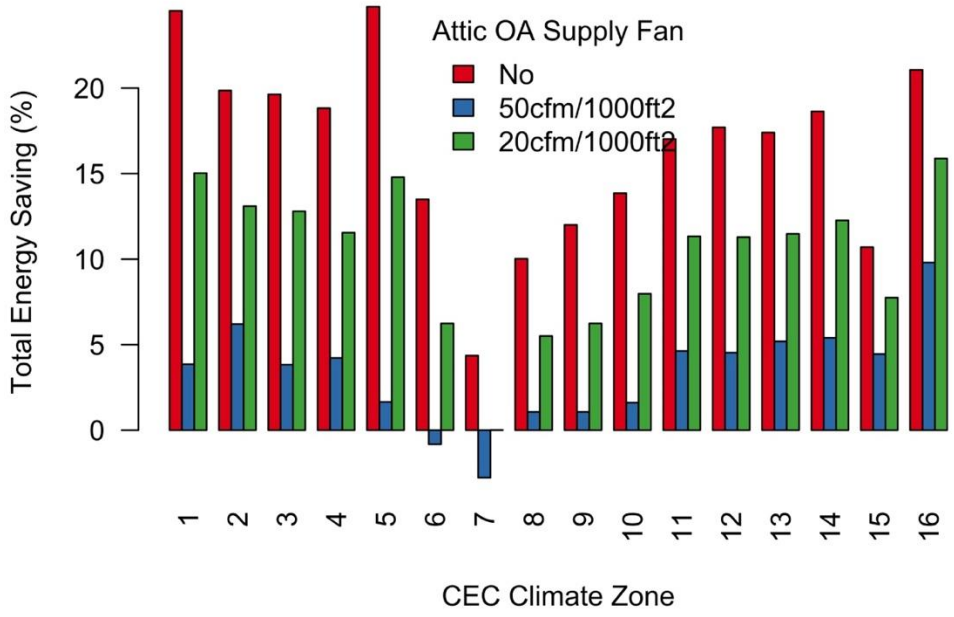

Figure 200 Total HVAC site energy use for each climate zone, with and without an outdoor air supply fan in the attic.

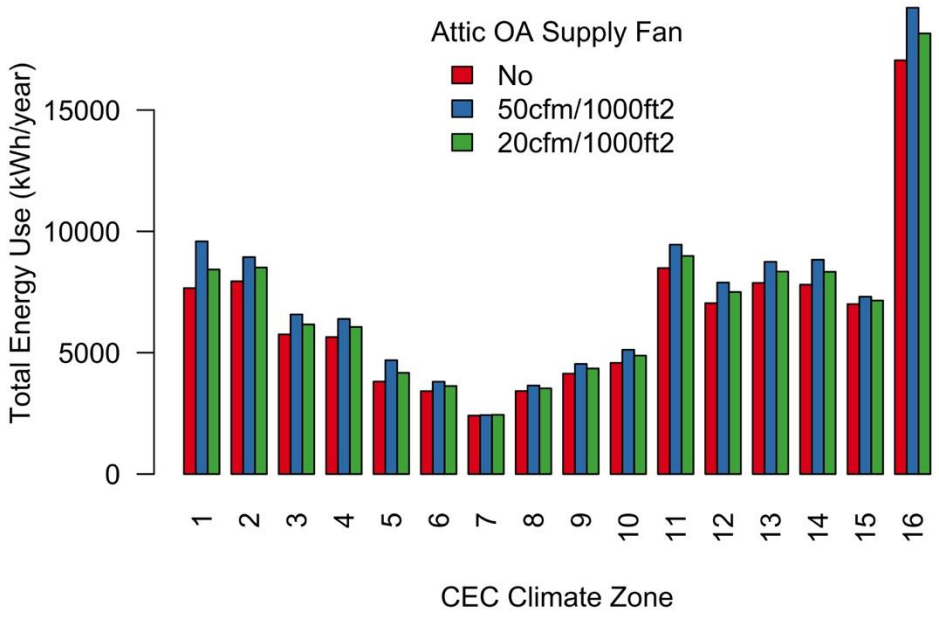

Table 40 North sheathing, mold index failures with and without an outdoor air supply fan in the attic.

Proto type	Moisture Gains	ACH_{50}	Duct Leakage	Attic Leakage	Ceiling Leakage	Vent Fan Sizing	CZ	Outdoor Air Supply Into Attic?		
								50 cfm per 1,000 ft^2	20 cfm per 1,000 ft^2	None
M	H	3	5d	50a	50c	None	1	1.87	5.29	5.30
L	H	3	5d	50a	50c	None	1	1.29	5.29	5.30
L	H	3	5d	50a	50c	None	2	0.58	3.7	5.30
L	H	3	5d	50a	50c	None	13	0.4	3.7	5.30
M	M	3	5d	50a	50c	None	1	1.04	3.55	5.30
M	H	3	5d	50a	50c	None	2	0.68	3.33	5.30
M	H	3	5d	50a	50c	2010	1	1.31	3.31	5.28
L	M	3	5d	50a	50c	None	1	0.73	3.17	5.29
L	H	3	5d	50a	50c	None	12	0.67	3.11	5.29
L	H	3	5d	50a	50c	None	3	0.16	2.65	5.30
M	H	3	5d	50a	50c	None	13	0.36	2.43	5.30
L	H	3	5d	50a	50c	2010	1	0.65	2.17	5.29
M	H	3	5d	50a	50c	None	12	0.71	2.14	5.30
M	H	3	5d	50a	50c	None	3	0.3	2.06	5.30
L	H	3	5d	50a	50c	Buil	1	0.59	1.26	4.81
M	M	3	5d	50a	50c	None	2	0.4	1.06	5.30

L	M	3	5d	50a	50c	None	2	0.33	1.05	3.05
M	H	3	5d	50a	50c	2010	2	0.49	1.01	3.22
L	M	3	5d	50a	50c	None	13	0.12	1	3.05
M	M	3	5d	50a	50c	None	12	0.44	0.98	5.29
L	H	3	5d	50a	50c	2010	2	0.28	0.85	3.47
M	H	3	5d	50a	50c	None	11	0.17	0.78	5.30
M	M	3	5d	50a	50c	None	13	0.12	0.78	5.30
L	H	3	5d	50a	50c	2010	13	0.05	0.74	3.99
L	H	3	5d	50a	50c	None	4	0.01	0.72	4.87
M	M	3	5d	50a	50c	None	3	0.12	0.66	5.30
M	H	3	5d	50a	50c	2010	13	0.2	0.64	5.08
L	H	3	5d	50a	50c	None	5	0	0.64	5.00
M	H	3	5d	50a	50c	None	5	0	0.38	5.30
M	H	3	5d	50a	50c	None	4	0.01	0.37	5.30
L	H	3	5d	50a	50c	None	6	0	0.05	4.27
M	M	3	5d	50a	50c	None	4	0	0.02	5.05
M	M	3	5d	50a	50c	None	5	0	0.02	5.30
M	H	3	5d	50a	50c	None	16	0	0.01	5.30
M	H	3	5d	50a	50c	None	10	0	0	4.89
M	H	3	5d	50a	50c	None	14	0	0	5.30
M	H	3	5d	50a	50c	None	6	0	0	5.30
M	H	3	5d	50a	50c	None	7	0	0	5.30
M	H	3	5d	50a	50c	None	8	0	0	5.30
M	H	3	5d	50a	50c	None	9	0	0	5.30
M	M	3	5d	50a	50c	None	6	0	0	5.30
M	M	3	5d	50a	50c	None	7	0	0	5.13
M	M	3	5d	50a	50c	None	8	0	0	5.05

Table 41 Bulk framing, mold index failures with and without an outdoor air supply fan in the attic.

Proto type	Moisture Gains	ACH_{50}	Duct Leakage	Attic Leakage	Ceiling Leakage	Vent Fan Sizing	CZ	Outdoor Air Supply Into Attic?		
								50 cfm per 1,000 ft^2	20 cfm per 1,000 ft^2	None
M	H	3	5d	50a	50c	None	2	0	0.03	6.00
M	H	3	5d	50a	50c	None	3	0	0.01	6.00
M	H	3	5d	50a	50c	2010	6	0.01	0	5.90
M	H	3	5d	50a	50c	None	6	0.01	0	5.99
M	H	3	5d	50a	50c	2010	13	0	0	5.97
M	H	3	5d	50a	50c	2010	16	0	0	5.85
M	H	3	5d	50a	50c	None	1	0	0	5.99

M	H	3	5d	50a	50c	None	10	0	0	5.99
M	H	3	5d	50a	50c	None	12	0	0	5.98
M	H	3	5d	50a	50c	None	13	0	0	5.99
M	H	3	5d	50a	50c	None	14	0	0	5.84
M	H	3	5d	50a	50c	None	16	0	0	5.99
M	H	3	5d	50a	50c	None	4	0	0	5.99
M	H	3	5d	50a	50c	None	5	0	0	5.99
M	H	3	5d	50a	50c	None	7	0	0	5.99
M	H	3	5d	50a	50c	None	8	0	0	5.99
M	H	3	5d	50a	50c	None	9	0	0	5.98
M	M	3	5d	50a	50c	None	1	0	0	5.96
M	M	3	5d	50a	50c	None	10	0	0	5.99
M	M	3	5d	50a	50c	None	13	0	0	5.97
M	M	3	5d	50a	50c	None	16	0	0	4.47
M	M	3	5d	50a	50c	None	2	0	0	5.99
M	M	3	5d	50a	50c	None	3	0	0	5.99
M	M	3	5d	50a	50c	None	5	0	0	5.99
M	M	3	5d	50a	50c	None	6	0	0	5.99
M	M	3	5d	50a	50c	None	7	0	0	5.98
M	M	3	5d	50a	50c	None	8	0	0	5.98

7.3 Energy Performance

While secondary to the moisture risk assessment presented in Section 7.2, the REGCAP simulations also provide estimates of HVAC energy consumption and savings estimates for sealed and insulated attics. In the sections above, we have, where relevant, already covered how the simulation factors and moisture mitigations affect energy consumption and savings estimates. Here we summarize the typical total HVAC energy consumption for each of the three attic types—vented, HPA and sealed (see Section 7.3.1). We then assess energy savings for the sealed and insulated attics relative only to the vented attics. Total HVAC and end-use energy savings are assessed in aggregate, along with peak cooling power savings (Section 7.3.2).

7.3.1 Total HVAC Consumption Across Attic Types

Total HVAC site energy consumption for sealed and insulated attics is compared with vented and HPA attics in Figure 201 for each CEC climate zone. The bars represent median values calculated across prototypes, airtightness and other parameters. The sealed attics use the least energy in all climate zones. The most common pattern is for vented attics to have the highest total consumption, followed by HPA and then sealed attics. Though in CZ 3 and 5-7, the HPA have the greatest total consumption, higher even than the vented attics.

Total HVAC TDV energy consumption is shown in Figure 202. We see that the climate zone patterns change for TDV consumption, with greater emphasis (and total TDV consumption) shifting towards cooling energy consumption. CZ16 remains the highest usage climate zone,

but CZ1, for example, which has no cooling consumption, falls to one of the lowest consuming zones. However, the trends across attic types remain the same, with the sealed and insulated attics always using the least energy, while vented attics are usually the highest consuming. We also note that the relative difference between TDV energy for vented and sealed attics is less than the difference when comparing on the basis of site energy.

Figure 201 Median total annual HVAC site energy consumption in vented, HPA and sealed attics, by climate zone.

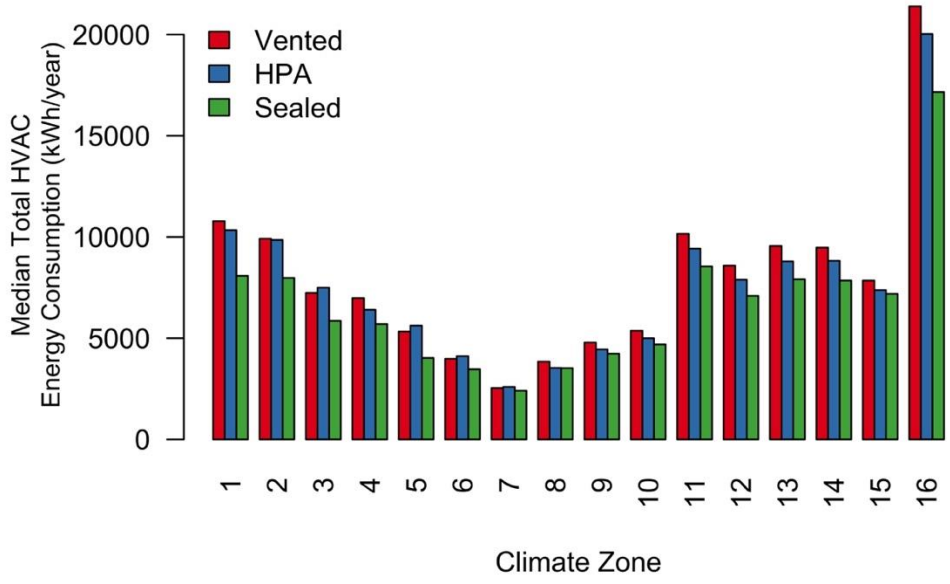

Figure 202 Median total annual HVAC TDV energy consumption in vented, HPA and sealed attics, by climate zone.

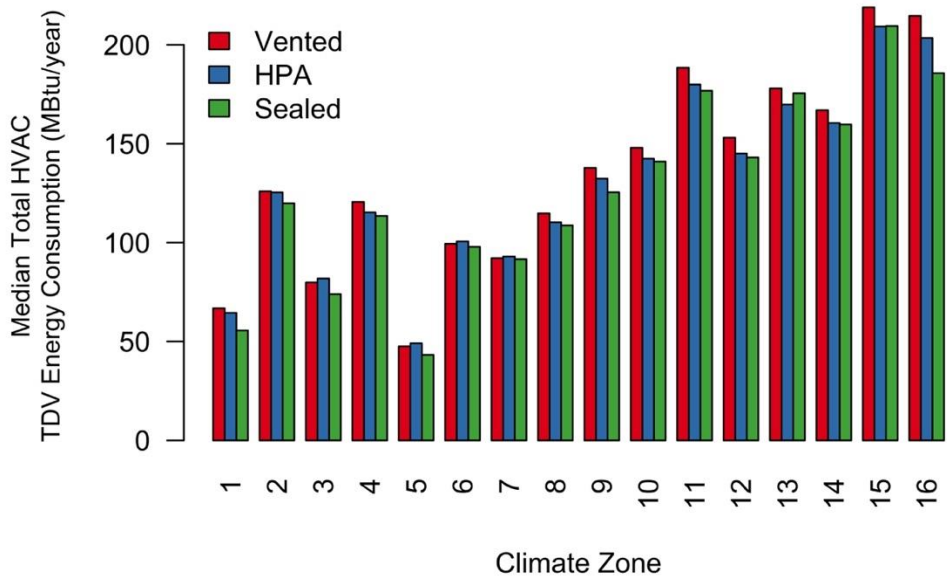

7.3.2 Energy Savings—Sealed and Insulated vs. Vented Attics

Percent energy savings for sealed and insulated attics are summarized by climate zone relative to traditional vented attics in Table 42 (site energy end-uses) and Table 43 (TDV energy end-uses). Within each climate zone, these values represent the median savings across varying levels of simulation parameters, including envelope airtightness, house prototype, duct leakage and attic and ceiling leakage. Median absolute site energy savings for each end-use are plotted for each climate zone in Figure 203. Savings distributions including all of these parameters are shown by boxplots in Figure 205 (site total %), Figure 206 (site total kWh), Figure 207 (TDV total %), Figure 208 (TDV total MBtu), Figure 209 (site heating %), Figure 210 (TDV heating %), Figure 211 (cooling site %) and Figure 212 (cooling TDV %).

Median total site energy savings were 18% across all cases (1,352 kWh/year savings), with climate zone variation between roughly 4 and 25% (392 to 4,489 kWh/year savings). Total TDV savings were roughly 50% lower, with median savings of only 8% (12.1 MBtu/year savings), varying between 2 and 23% (1.3 and 32.5 MMBtu/year). Heating energy savings were much higher than cooling energy savings, with median values of 27 and 5% site energy savings, respectively. In fact, in CZ3 and CZ5, cooling energy consumption increased. This is discussed in greater detail in Section 7.3.2.1. Similarly, heating energy savings strongly dominated the absolute savings in all locations except CZ15, which has nearly no heating consumption (see Figure 203). Median heating percent energy savings were quite high in some locations, namely CZ6-8 and 15, with median savings greater than 30%. All of these cases represent small numbers in an absolute sense, because these climates have very low overall heating demand. Small absolute changes in consumption translate to large percentage values. For example, in

CZ7 42% heating savings correspond to only 106 kWh in absolute savings. Accordingly, these same climates have relatively low overall savings.

Sealed and insulated attics were not very effective at reducing cooling energy consumption, and cooling energy use dominates TDV energy assessments due to overall higher TDV for electricity and greater peak period sensitivity. As such, TDV savings are less than half those in site energy units, with a median of only 8%. Heating TDV savings percentages remain high (median 27%), but heating made up only 18% of total TDV consumption annually across all cases. The locations with the highest overall TDV percent savings are those locations with the lowest cooling demand (i.e., CZ 1, 5 and 16).

Consistent with these low overall cooling savings estimates, we show the average peak cooling site power savings during the 10-hottest days of the year for the hours of 2-6pm in Figure 204. Peak power reductions were generally on the order of 10 to 70 watts, which accounts for 0.5% to 1.5% of total peak power.

Table 42 Median site energy savings sealed and insulated attic versus vented attic, aggregated by climate zone.

	Site Energy Savings (%)				
Climate Zone	**AHU**	**Heating**	**Cooling**	**IAQ Fan**	**Total**
1	25	25	NA	0	25
2	12	23	4	0	20
3	9	23	-7	0	20
4	9	26	3	0	19
5	13	29	-16	0	24
6	4	33	1	0	13
7	1	42	0	0	4
8	6	31	5	0	10
9	7	28	6	0	12
10	8	28	7	0	14
11	11	23	8	0	17
12	10	24	7	0	18
13	10	24	9	0	17
14	11	27	8	0	19
15	9	32	10	0	11
16	16	22	5	0	21
Overall	10	27	5	0	18

Table 43 Median TDV energy savings sealed and insulated attic versus vented attic, aggregated by climate zone.

	TDV Energy Savings (%)				
Climate Zone	**AHU**	**Heating**	**Cooling**	**IAQ Fan**	**Total**
1	24	24	NA	0	23
2	6	23	2	0	10
3	4	23	-5	0	9
4	4	26	1	0	7
5	7	29	-12	0	14
6	3	33	1	0	4
7	1	41	1	0	2
8	4	30	4	0	5
9	4	28	4	0	6
10	5	28	4	0	6
11	6	23	5	0	9
12	6	23	4	0	8
13	7	24	5	0	9
14	7	27	5	0	10
15	7	32	8	0	8
16	10	22	3	0	15
Overall	6	27	4	0	8

Figure 203 Median site energy end-use savings for sealed and insulated attic compared to a vented attic, by climate zone.

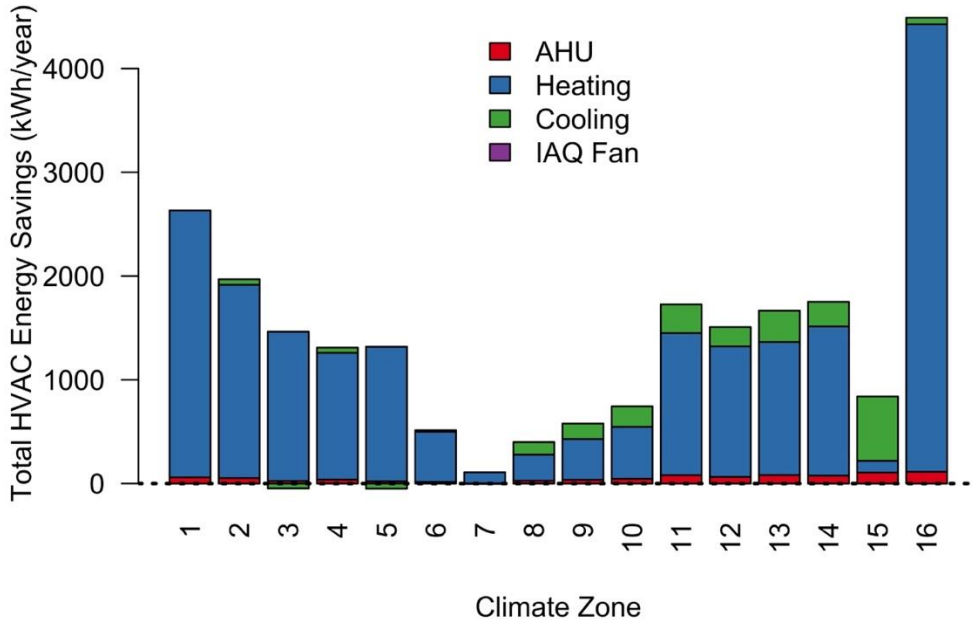

Figure 204 Peak cooling site power savings for each climate zone, by house prototype.

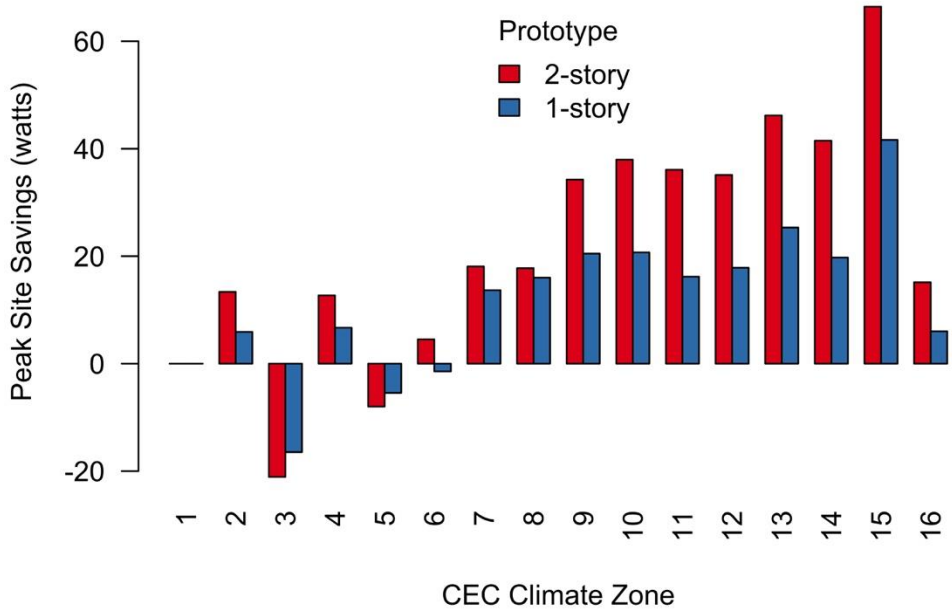

Figure 205 Total HVAC energy savings (%) by CEC climate zone for sealed attics compared to traditional vented attics.

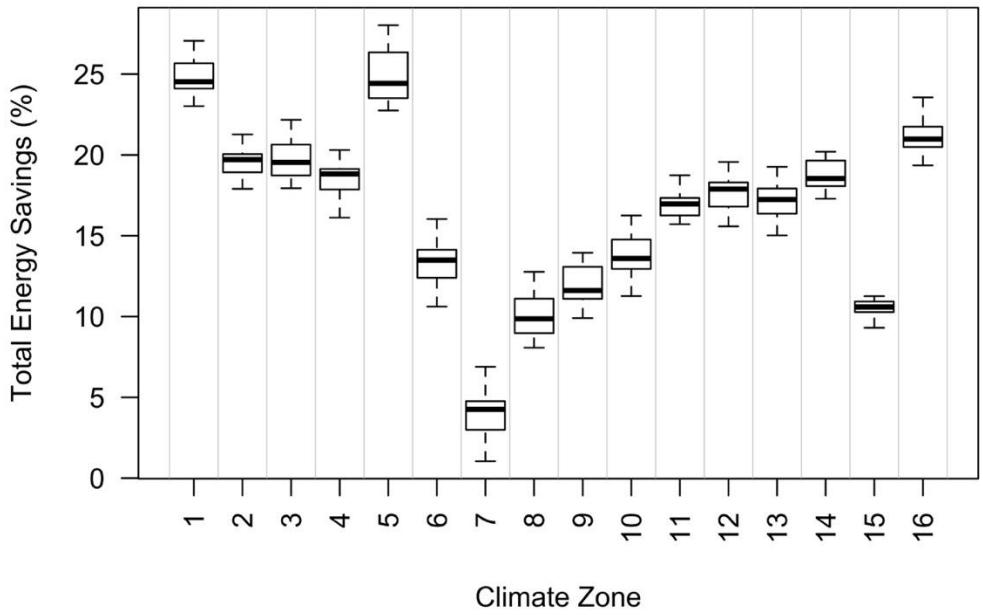

Figure 206 Total HVAC energy savings (kWh/year) by CEC climate zone for sealed attics compared to traditional vented attics.

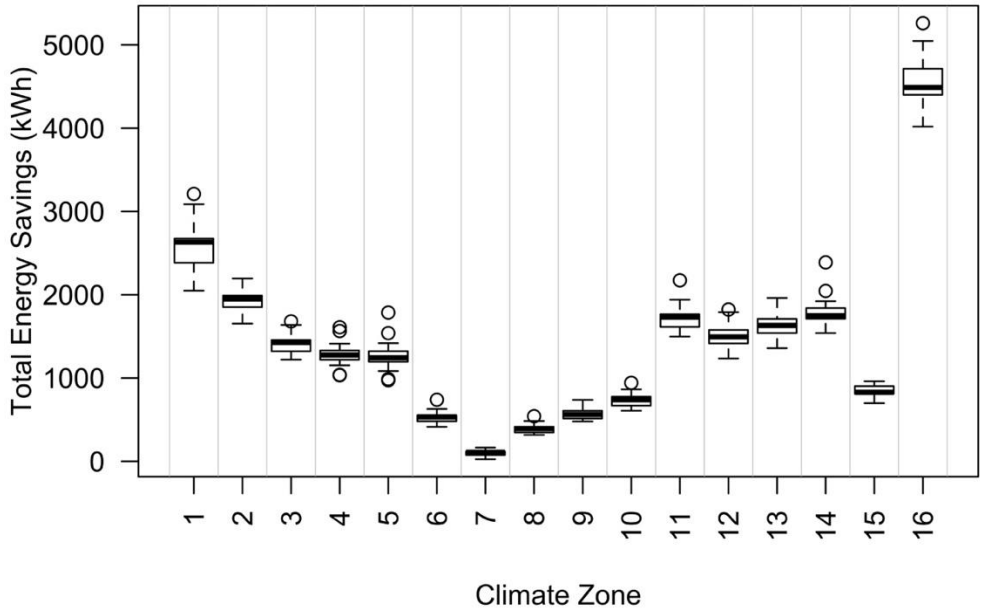

Figure 207 Total HVAC TDV energy savings (%) by CEC climate zone, sealed vs. traditional vented attics.

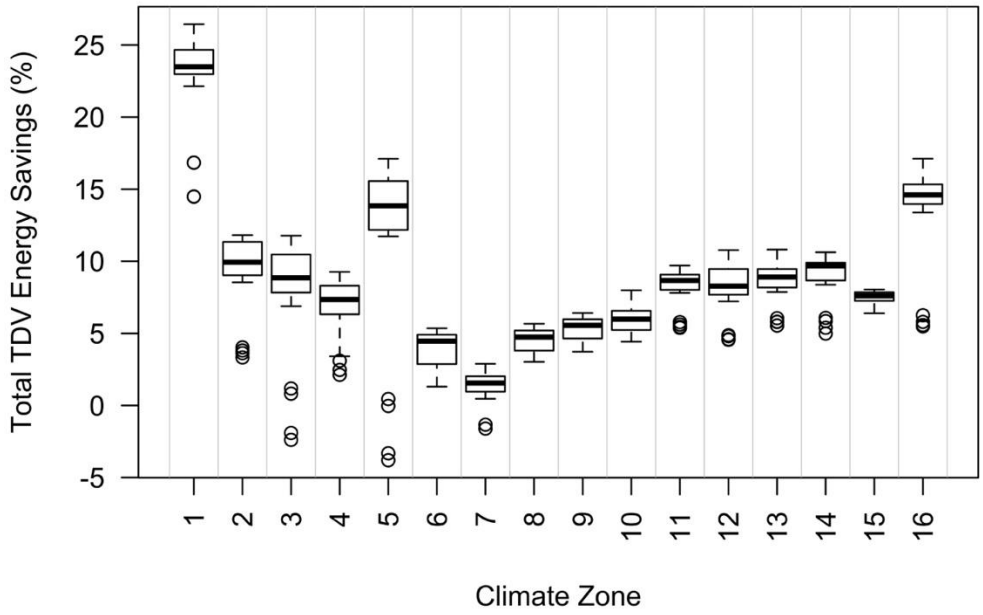

Figure 208 Total HVAC TDV energy savings (kWh/year) by CEC climate zone, sealed vs. traditional vented attics.

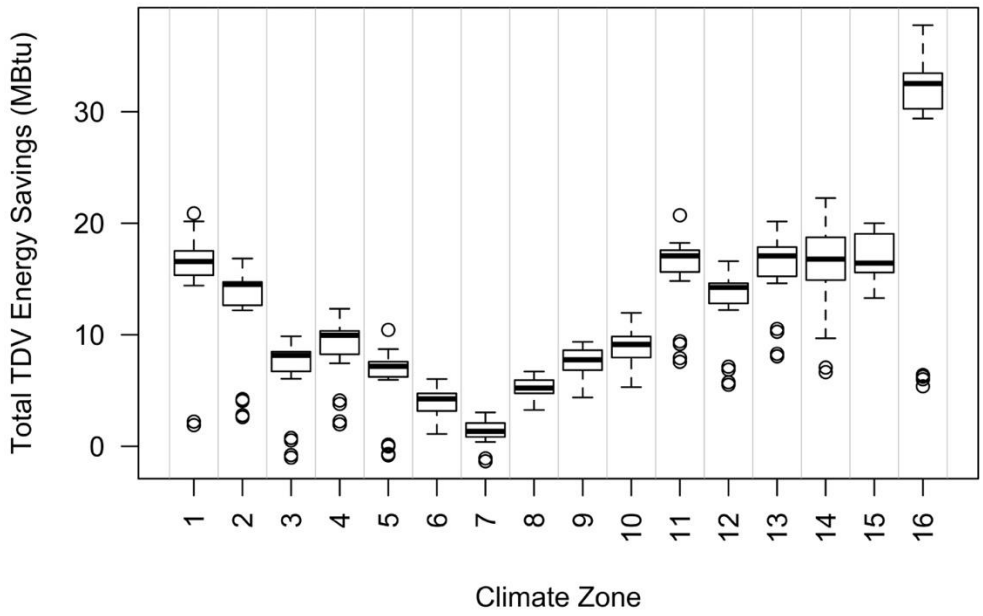

Figure 209 Heating energy savings (%) by CEC climate zone, sealed vs. traditional vented attics.

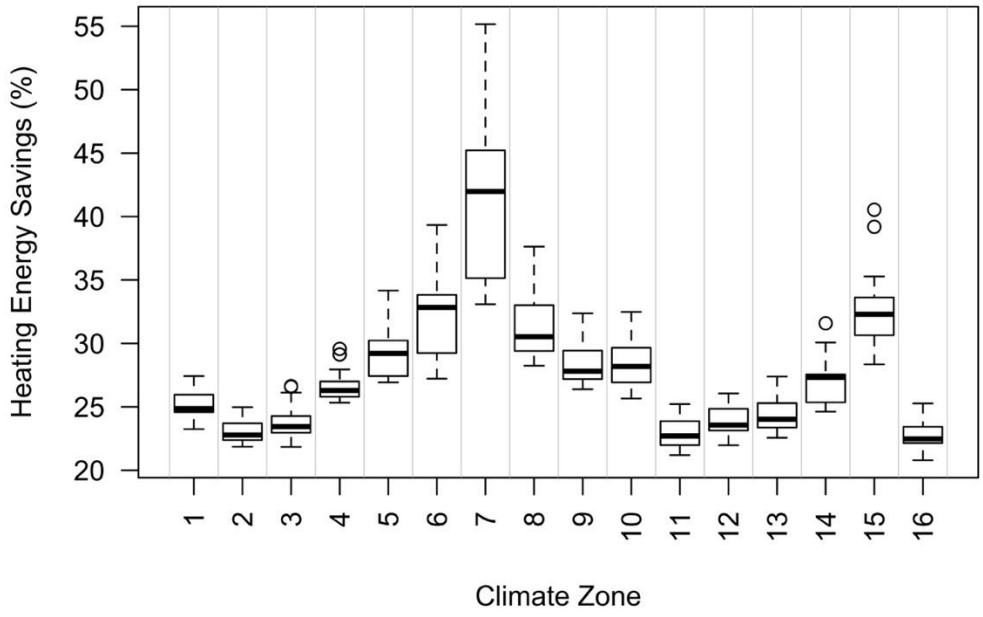

Figure 210 Heating TDV energy savings (%) by CEC climate zone, sealed vs. traditional vented attics.

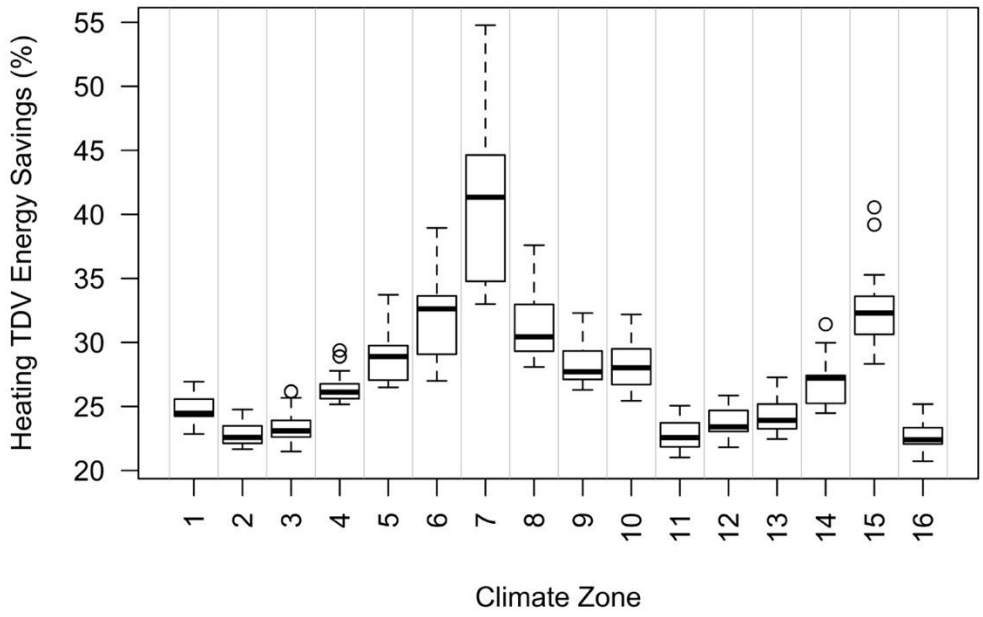

Figure 211 Cooling energy savings (%) by CEC climate zone, sealed vs. traditional vented attics.

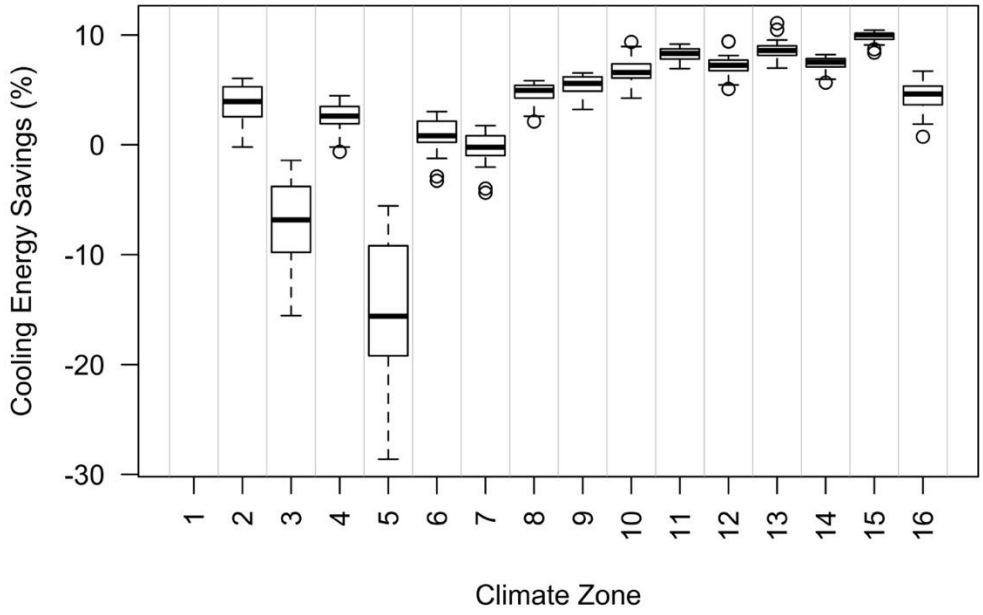

Figure 212 Cooling TDV energy savings (%) by CEC climate zone, sealed vs. traditional vented attics.

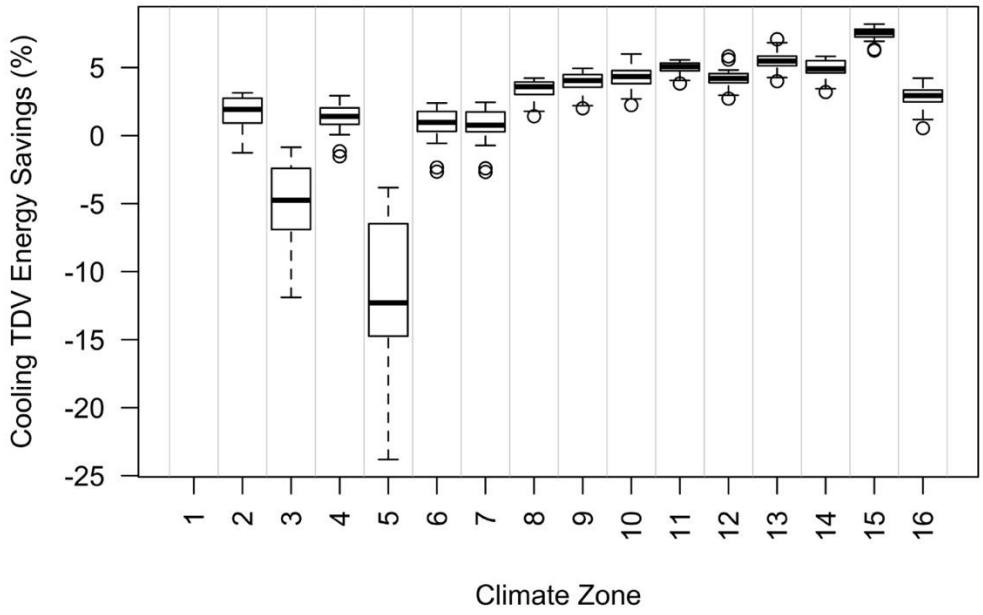

7.3.2.1 Assembly Temperature Differences and Cooling Performance

The lack of cooling energy savings in the simulations was initially surprising, because the ducts are located in the sealed and insulated attics, and the attic air temperatures were indeed nearly identical to those in the conditioned occupied zone air. This should (and does) largely eliminate

duct system losses for the sealed and insulated attics. Yet, duct system losses are only part of the thermal impact of moving insulation from the flat ceiling to the sloped roof deck. Two other factors also impact space-conditioning energy: (1) envelope surface area (which increases for the sloped roof approach) and (2) differing assembly temperature differences due to tighter-coupling of the sloped roof surface to the sky, both in terms of solar gains and night sky losses.

We hypothesized that the temperature differences across the sloped roof insulation assembly (from sheathing to attic air) would be greater in the cooling season than the difference across the insulated ceiling in a vented attic (from house to attic air). This results from the direct solar heating of the roof deck, whereas the attic air is only secondarily heated by insolation. Similarly, we expect that the temperature differences will also differ in the heating season.

To test this, we eliminated all duct losses from our model, so that we could isolate these thermal envelope effects. We show calculated assembly temperature differences for an example 1-story home in CZ13 during the cooling season in Figure 213. The green and orange lines represent the two sloped roof surfaces of the sealed and insulated attic, while the purple line represents the ceiling assembly in the vented attic. As hypothesized, the sloped roof assembly experiences much higher temperature differences during the daytime hours (increased heat gains), while having slightly lower differences at nightime (increased heat losses). The net-effects are the average temperature differences shown in the figure legend. Indeed, relative to the vented attic ceiling assembly, the sealed attic roof assemblies have average temperature differences that are 36% and 46% greater for North and South-faces, respectively (9.8 and 10.5°C compared with 7.2°C). The differences during the daytime cooling hours may be more relevant for cooling energy predictions. During these periods, the typical peak temperature difference across the ceiling assembly of a vented attic is roughly 20°C, while the sloped roof surfaces have temperature differences typically averaging around 35°C. This is a roughly 75% increase in the assembly temperature difference during peak cooling hours.

When we examine the total cooling energy consumption for these two cases with perfect ducts, we see that cooling consumption is 4.5% higher for the sealed attic (132 kWh/year). Again, this increased consumption is the result of more heat transfer area (sloped roof and gable walls vs. flat ceiling) along with increased assembly temperature differences during cooling periods. When the duct losses are put back into these models, this case still has net-cooling savings of 9%, because of the recovery of the duct losses in the sealed attic. But some locations have increase cooling energy use, because the duct savings are overwhelmed by the envelope penalties (e.g., CZ3 and 5 in Table 42 and Table 43).

The same plot is shown for a typical heating period in Figure 214. The sloped roof surfaces (South in particular) have more heat gain during the daytime hours (i.e., free heating), and slightly increased heat losses during the nighttime hours due to night sky coupling. The average temperature difference is 7% less for the sloped roof surfaces (less heating demand), with the South face 21% lower and the North face 6% higher. So, with no duct losses, annual heating savings of 6% still exist for the sealed and insulated attic relative to the vented attic. And when ducts are added back into the model, the heating savings increase from 6% to 24%.

As noted by Less et al. (2016) in their review of sealed and insulated attic hygrothermal and energy performance, no field studies have been able to document measured HVAC energy savings for a sealed attic relative to a vented attic with airtight and insulated ducts. This cooling energy penalty could be the explanation, as most tests of varying duct leakage were done in the cooling season, in hot-dry climates (e.g., Hendron et al. (2002)). Similarly, (Parker et al., 2002) compared the cooling energy and peak cooling demand of various cool roof materials over vented attics against a sealed and insulated attic, as well as a traditional dark shingle vented attic. They found the sealed attic had less than half the cooling energy savings of the cool roof cases, and they reported nearly no peak cooling demand savings for the sealed attic (0.3%) versus 34-40% peak savings for the cool roof cases. Despite their rapid adoption in hot-dry climates, sealed and insulated attics may not be ideal for cooling dominated locations.

Figure 213 Cooling period illustration of roof deck and ceiling assembly temperature differences in sealed and insulated vs. vented attics in CZ13 1-story prototype. These cases are for attics without HVAC systems.

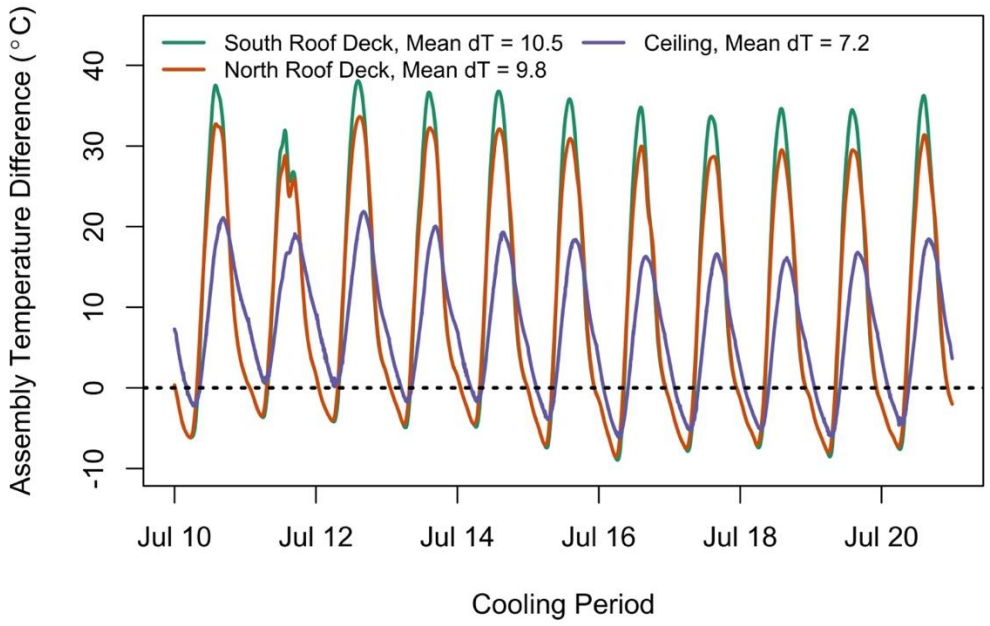

Figure 214 Heating period illustration of roof deck and ceiling assembly temperature differences in sealed and insulated vs. vented attics in CZ13 1-story prototype. These cases are for attics without HVAC systems.

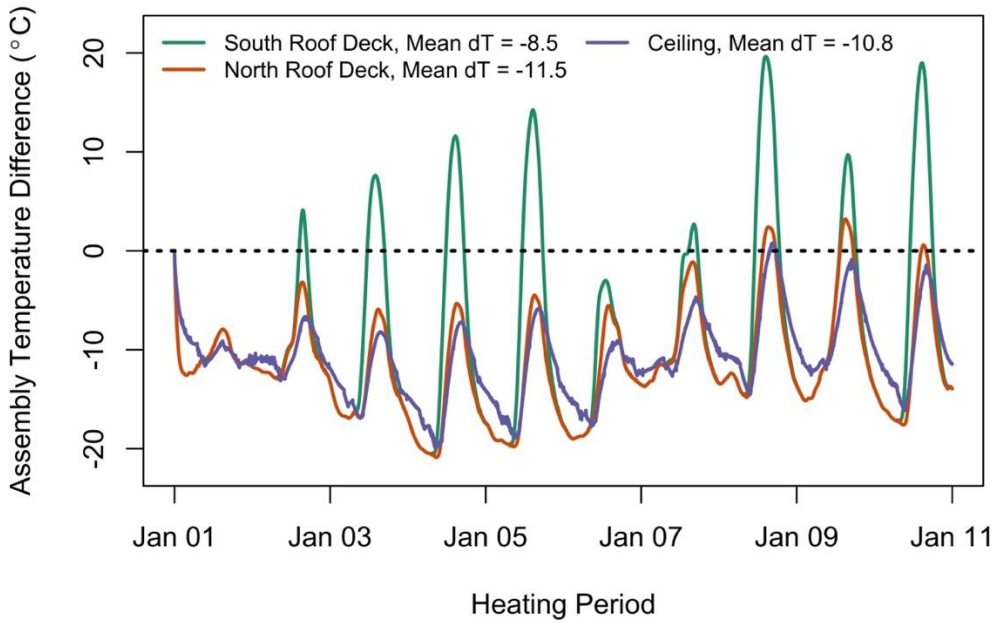

7.4 Simulation Study Summary

7.4.1 Overall

- Statewide, total HVAC energy savings are predicted be 18% in terms of site energy and 8% for TDV energy and are dominated by heating energy savings. Thermal penalties of insulated roof decks partly counteract the benefits of ducts inside the conditioned space, which reduces cooling energy savings, limits peak cooling demand reductions, and provides lower TDV than site energy savings.
- Across a wide variety of parameters, mold index failures occurred in roughly 15% of sealed attics at the North roof deck. Failure rates were lower for wood moisture content rot and decay thresholds. Failures were largely concentrated in homes with any of the following features: 1-story geometry, higher internal moisture generation rates, no IAQ fan operating, or very airtight envelopes. Any one of these elements represents a risk for a sealed attic home, though in combination they dramatically increased likelihood of moisture failure. Climate zone variability was the other primary driver of moisture risk, with the worst locations being Pacific coastal and select Central Valley locations. Attic air relative humidity was sometimes at unacceptable levels (>80%) leading to potential mold growth on attic framing, as moisture that accumulated in the roof deck during winter was driven into the attic air by solar radiation during sunny late-winter and spring days.
- Primary moisture interventions should be either: (1) a vapor retarder on the attic air side of the fibrous insulation[12], or (2) outside air supplied mechanically to the attic volume at

[12] "Smart" vapor retarders with permeability that varies with the surrounding relative humidity have been shown to be potentially even more effective than fixed 1-perm vapor retarders in this

either 20 or 50 cfm per 1,000 ft^2 of ceiling area, depending on climate region. The latter substantially increases energy use. If the air impermeable insulation requirements are to be kept in the CRC (Table R806.5), the insulation values should be increased to improve their effectiveness in controlling mold risk. This strategy may work better when air and vapor impermeable insulation is installed below the roof deck, rather than above the roof deck. Finally, while not modeled in this work, other research in this field has demonstrated that the installation of vapor diffusion vents at the ridge will also aid in controlling moisture levels in sealed and insulated attics, and should be considered amongst the best moisture mitigations for these assemblies.

7.4.2 HVAC Energy Savings

The simulations were used to estimate potential HVAC energy savings for new homes in California climate regions. We found median total HVAC energy savings of 18% (from 4 to 25% by climate region) across all homes and climate regions, comprised of 27% heating energy savings, 5% cooling savings and 10% air handler savings. Savings were strongly dominated by heating energy. We found that insulated roof decks are strongly coupled to the sky, including solar heat gains and nighttime heat losses. This increased the thermal gains across the insulated surface in cooling season (roof finish vs. attic air), relative to those across an insulated flat sheetrock ceiling in a vented attic (attic air vs. living space air). So, sealed attics benefit from eliminating duct system energy losses, but they face cooling penalties due to this sky-coupling. These effects reduced and sometimes eliminated cooling energy savings. Similarly, peak cooling power demand reductions were minimal (though positive), and time-dependent valuation energy savings were roughly half the site energy savings (median of 8%), because electricity is heavily weighted in TDV assessments and the simulated homes used electric cooling and gas heating. Energy performance of sealed attics was robust across the varied simulation parameters, such that savings were not substantially affected by varying envelope leakage, duct leakage, fan type, etc. Climate region was the primary driver of varying energy performance.

7.4.3 Moisture Risk

Many simulated sealed and insulated attic assemblies met moisture performance criteria, such that we classify them as safe. Yet, a substantial minority of the simulated cases had elevated risks for surface mold growth (mold index >3) and high wood surface moisture content (>28% for 7-days or more) sufficient to potentially lead to structural damage. Mold index failures were most common in the North sheathing location (18% failure rate) and general attic framing nodes (19% failure rate), and were less frequent at the South sheathing (4% failure rate). The 28% wood moisture content metric was exceeded in 10% of cases at the North sheathing, while failures at the attic framing and South sheathing were much lower, at 1% and 0%, respectively. As expected, the highest risk location was the North-oriented roof deck. The roof deck risks were associated with cold periods in the heating season particularly on clear nights when the roof

---

application in Cold climate regions (Ueno & Lstiburek, 2018). Examples include, DuPont Air Guard Smart, Intello, and CertainTeed MemBrain,

deck surface temperatures were substantially below the outside air temperature. The attic framing and attic air humidity were at their highest in the late-winter and spring seasons, which we hypothesize to be the result of moisture storage in the roof deck during winter, which is then emitted into the attic air with increasing outside temperatures and greater solar gains.

The most important house features in determining moisture risk at the North roof deck in sealed and insulated attics using solely fibrous, vapor permeable insulation were:

- **CEC climate region**, estimated highest to lowest risk were: 1, 13, 2, 5, 6, 3, 12, 7, 4, 8, 11, 16, 9, 14, 10, 15.
- **IAQ fan sizing** (larger fans reduced mold and WMC risk)
- **House prototype** (1-story 2,100 ft^2 prototype had substantially higher risk than the 2-story 2,700 ft^2 prototype)
- **Envelope leakage** (more leakage led to less risk)
- **Attic leakage** (more leakage led to less risk)
- **Internal moisture generation rate** (higher internal generation led to greater risk)
- **IAQ fan type** (exhaust IAQ fans had lower risk than supply fans)

Our observations about moisture risk in sealed attics lead us to the following more general principles or design guidance:

- Sealed attics have much higher moisture risks than vented or HPA attics throughout the state.
- Climate zone is one of the strongest drivers of moisture risk. The ordering of climate zones by risk is not intuitive, and it varies for North sheathing risk vs. bulk attic framing risk (attic framing risk was highest in CZ 2, 3, 5-8 and 13). The climate drivers of mold risk may be different at sheathing locations vs. the general attic framing. The coldest locations do not necessarily have the highest risk; instead coastal climates and select central valley locations seem most at risk.
- Increased outside air exchange reduced mold and wood moisture risks, whether through larger IAQ fans, greater envelope or attic leakage areas, greater natural infiltration in 2-story vs. 1-story homes, or mechanical supply of outside air into the attic.
- Increased mixing of the attic and living space air volumes tended to marginally increase mold risk, whether this resulted from increased duct leakage or ceiling leakage, or by intentional supply of HVAC air into the attic (as required by the 2018 IECC). This finding assumes that the living space has moisture content elevated above the attic, which may not be a consistent assumption. Overall, impacts of mixing are marginal. Mixing may help to avoid elevated attic air moisture during spring, when moisture that accumulates in the roof deck during winter is re-emitted.
- Roof deck moisture risk was driven by cold roof sheathing temperatures, so parameters that increased roof deck temperatures during cold nights reduced moisture risks. This included the placement of air impermeable insulation above the roof deck per the CRC (2018), and the use of tile roofing vs. asphalt shingles.
- The living space is the source of moisture for sealed and insulated attics, and outside air is generally a source of potential drying in California climates. This explains why supply IAQ fans worsened moisture performance, because they drove living space moist air into the attic and reduced the amount of air coming into the attic from outside.
- Most attics had low ventilation rates, even when the living spaces were adequately ventilated by mechanical IAQ fans. Ideally, attics should be ventilated with outside air, rather than through transfer of living space air.

7.4.4 Moisture Interventions

The moisture interventions had widely varying effects, most of which are predictable from the principles listed above. The most effective interventions were the use of a 1-perm vapor retarder on the surface of the fibrous insulation at the roof deck, and the provision of mechanically supplied outside air directly into the attic air volume. The use of the vapor retarder had nearly no impact on energy use, whereas the outside air ventilation increased energy consumption in all cases (and reduced savings), by an average of 428 or 871 kWh, depending on the outside airflow target. The use of insulation above the roof deck at levels required by the California Residential Code drastically reduced condensation at the roof deck, but it was much less effective at reducing the risk of mold growth. This strategy warmed the roof deck surface, which reduced the surface relative humidity. Condensation was nearly eliminated, but the surface RH at the roof deck remained high enough (>80%) to support mold growth in many instances. Finally, the addition of HVAC supply air into the attic volume, which is required by the IECC (2018) model code, actually marginally increased the mold risk, wood moisture content and condensation levels in our simulations. It also increased energy use on average by 161 kWh/year. This strategy did reduce springtime elevated attic air moisture and it supplied dehumidified air to the attic in the cooling season. This strategy was developed for use in humid climate regions, and we expect it may be effective in those locations, but it does not appear beneficial in California new homes.

8 Conclusions & Recommendations

Throughout the many mild and dry climates of California, a dramatically lower-cost insulated roof deck assembly consisting only of fiberglass or cellulose (batts or blown) may be possible without undue moisture risk, potentially eliminating the costly model code requirements and avoiding the potential chemical exposures and global warming impacts from SPF products. On behalf of the California Energy Commission's (CEC) Title 24 Building Energy Code (T24), we have investigated the thermal, moisture and energy performance of sealed and insulated attics in new homes, using only fibrous insulations, such as fiberglass or cellulose.

There are two key questions to be answered by this study:

Q1. Do fibrous insulation approaches result in an attic that can be considered thermally within conditioned space with consummate energy savings?

A1. Yes – temperature differences are small between the house and attic, and this insulation approach leads to statewide total HVAC energy savings of 18% in terms of site energy and 8% for TDV energy.

Q2. Does moisture and air permeable insulation used in new California homes lead to increased moisture risk or definite moisture problems in the state's climate regions?

A2. Yes – there are increased risks of moisture issues using vapor and air permeable insulation, particularly for north facing sheathing in homes with high occupant density. There is considerable climate variability with no uniform trend from warm to cool climates.

Based on the field measurements we conclude that:

- The sealed and insulated attics are the same temperature on average as the living space, such that they can be considered to be inside conditioned space from a modeling and Title 24 compliance perspective. But particularities of attic and house geometry, attic leakage, presence of HVAC equipment, and other factors can contribute to some sealed attics having widely varying thermal performance.
- Moisture risk at the North ridge sheathing is evident, and while mold index calculations predict safe assemblies, visual inspection revealed suspected mold growth in the Clovis home. The wood moisture content and surface condensation did not reach high levels, and measured wood moisture contents were in the safe range below fiber saturation at all measured locations. Current methods for predicting safe moisture performance in sealed attic assemblies may be inadequate to the complexities inherent in these assemblies, particularly when they are completely vapor and air permeable, as they were in this research.
- Design, implementation and inspection issues were observed in the sealed attics of field study homes, including large areas of missing insulation above an unconditioned garage and substantial disruption to the roof deck insulation by other subcontractors. Careful design review and planning are critical, as are experienced energy raters and building inspectors. Also, all sealed attics should be designed to be accessible for inspection or remedial work if ever needed. Finally, sealed attic eave locations should be treated with raised heal trusses or the like, similar to vented attics.

Based on the simulation study we conclude that:

- Statewide, total HVAC energy savings are predicted be 18% in terms of site energy and 8% for TDV energy. Thermal penalties of insulated roof decks partly counteract the benefits of ducts inside the conditioned space, which reduces cooling energy savings, limits peak cooling demand reductions, and provides lower TDV than site energy savings.
- Across a wide variety of parameters, mold index failures occurred in roughly 15% of sealed attics at the North roof deck. Failure rates were lower for wood moisture content rot and decay thresholds. Failures were largely concentrated in homes with any of the following features: 1-story geometry, higher internal moisture generation rates, no IAQ fan operating, or very airtight envelopes. Any one of these elements represents a risk for a sealed attic home, though in combination they dramatically increased likelihood of moisture failure. Climate zone variability was the other primary driver of moisture risk, with the worst locations being Pacific coastal and select Central Valley locations. Attic air relative humidity was sometimes at unacceptable levels (>80%) leading to potential mold growth on attic framing, as moisture that accumulated in the roof deck during winter was driven into the attic air by solar radiation during sunny late-winter and spring days.
- Primary moisture interventions should be either: (1) a vapor retarder on the attic air side of the fibrous insulation, or (2) outside air supplied mechanically to the attic volume at either 20 or 50 cfm per 1,000 ft^2 of ceiling area, depending on climate region. The latter substantially increases energy use. If the air impermeable insulation requirements are to be kept in the CRC (Table R806.5), the insulation values should be increased to improve their effectiveness in controlling mold risk. This strategy may work better when air and vapor impermeable insulation is installed below the roof deck, rather than above the roof deck. Finally, while not modeled in this work, other research in this field has demonstrated that the installation of vapor diffusion vents at the ridge will also aid in controlling moisture levels in sealed and insulated attics, and should be considered amongst the best moisture mitigations for these assemblies.

Based on this research we recommend:

- Do not have maximum airtightness requirements for attics or homes, because increasing airtightness leads to increased moisture problems for low energy savings (when in the presence of IAQ fan ventilation).
- All sealed and insulated attic homes should be mechanically ventilated, preferably with exhaust fans. Mold risk is particularly exacerbated when the IAQ fans are turned off in sealed attic homes. Tighter homes need more mechanical ventilation to control moisture levels. The energy cost for increasing ventilation is small (less than 1% of HVAC energy).
- Moisture mitigations should be preferred that are robust in many situations and do not have undue energy penalties associated with them. The use of an attic air side vapor retarder is the best option explored in this work. Future work should explore the operation of variable permeance, “smart” vapor retarders in this application.
- Requirements for ceiling leakage are not required, because thermal and moisture performance are not very sensitive to this parameter.
- Tile roofing has been shown to reduce moisture risk, because it elevates the roof deck temperatures through its insulating value. Extra moisture mitigation may be warranted on asphalt shingle roofs.
- External impermeable insulation requirements in the CRC should be revisited due to limited effectiveness for protection against mold risk, though they did control condensation effectively.

- Adding mixing between the attic and house should only be done in spring to be effective as this is when the attic is more moist than the home due to release of seasonally stored moisture.
- Duct leakage minimum requirements should be retained for sealed attics, because increased leakage led to more mixing with the living space, which tended to worsen moisture problems.

California Building Code and Building Energy Code Concerns and Possible Code Changes

Current Code Concerns:

- The proposed 2019 Residential Compliance Manual Section 3.6.1 describes requirements for unvented attics in energy code compliance. It references the requirements contained in the 2016 California Building code Section R806.5. The compliance manual then goes on to specify two conditions under which unvented attics are acceptable, and both conditions in part contradict Section R806.5 of the CBC.
    - Item 1 in Section 3.6.1 of the compliance manual states that unvented assemblies can use air permeable insulation below and in direct contact with the underside of the roof sheathing, if they also provide at least R5 insulation above the sheathing. This contradicts the referenced Section R806.5 in the CBC. The CBC explicitly allows use of assemblies composed entirely of air permeable insulation in homes with tile roofing in CZ 6-15 (Table R806.5). It also requires air impermeable insulation at R10 and R15 in select climates. Our work shows this may be inadequate to control mold risk in some situations.
    - Item 2 in Section 3.6.1 states that all assemblies using air impermeable insulation below the roof deck (e.g., spray foam or board foam) must also provide a layer of air permeable insulation (e.g., fiberglass or cellulose) below the air impermeable insulation. This essentially forbids the use of assemblies composed entirely of spray foam or board foam. In contrast, the CBC explicitly allows assemblies composed entirely of air impermeable insulation (R806.5.5.1.1).
- The California Building Code Section R806.5.4 requires that in CZ 14 and 16, any air impermeable insulation must be a class II vapor retarder (or be covered by one). Our simulation work has shown that these are not the most risk-prone climate regions in the state. In fact, CZ 14 and 16 were among the safest locations assessed. We recommend that this requirement be revised.
- The California Building Code Section R806.5.4.1 is unclear in what climate regions it applies to. It appears to apply only in CZ14 and 16. It requires that any air permeable insulation (e.g., fiberglass) in an unvented attic be covered with a class I or II vapor retarder on the indirectly conditioned space side. The following clarifications are required:
    - In what climate zones is this applicable?
    - Does this apply only to assemblies composed entirely of air permeable insulation? Or does it also apply to assemblies with other vapor/air control mechanisms, such as air impermeable insulation (e.g., closed cell SPF) installed below and in direct contact with the roof sheathing, which is then covered from below with air permeable insulation? Or when air permeable insulation is used below the roof sheathing, but additional insulation is placed above the roof sheathing?

Suggested Code Changes:

There is a need for improved guidance and requirements for the design, construction and inspection of unvented attic assemblies in the California building codes and reference compliance manuals. In order to protect the health and safety of California residents and durability of their homes, we suggest that all sealed and insulated roof deck assemblies should provide a vapor control layer between the attic air and the roof sheathing/attic framing. The following are examples of roof assemblies that would be acceptable:

- Roof insulation composed entirely of vapor impermeable insulation (class II vapor retarder or less) below the roof deck (e.g., closed cell SPF or foam board).
- Roof assembly composed entirely of vapor permeable insulation below the roof deck (e.g., fiberglass, cellulose, open cell SPF) with a class II vapor retarder installed on the inside surface of the insulation.
- Hybrid roof assemblies composed of a layer of vapor impermeable insulation (class II vapor retarder) below and in direct contact with the roof sheathing, with vapor permeable insulation on the inside of this impermeable layer. The vapor impermeable insulation must enclose the top chord of the roof framing.
- Hybrid roof assemblies composed of insulation above the roof sheathing, along with vapor permeable insulation below and in direct contact with the roof sheathing, with a class II vapor retarder on the inside surface of the vapor permeable insulation.
- Roof assembly with all insulation (either vapor permeable or impermeable, rock wool board, foam board, SPF, etc.) placed above the sheathing with no vapor retarder in the unvented attic.

9 References

Arundel, A. V., Sterling, E. M., Biggin, J. H., & Sterling, T. D. (1986). Indirect health effects of relative humidity in indoor environments. *Environmental Health Perspectives*, *65*, 351.

ASHRAE. (2016). *ASHRAE Standard 160-2016 - Design Criteria for Moisture Control in Buildings*. Atlanta, GA: ASHRAE. Retrieved from https://www.techstreet.com/standards/ashrae-160-2016?product_id=1939166

BASC. (2018). Controlling Moisture in Unvented Attics - Code Compliance Brief | Building America Solution Center. Retrieved March 22, 2018, from https://basc.pnnl.gov/code-compliance/controlling-moisture-unvented-attics-code-compliance-brief

Baughman, A., & Arens, E. A. (1996). Indoor Humidity and Human Health–Part I: Literature Review of Health Effects of Humidity-Influenced Indoor Pollutants. *ASHRAE Transactions*, *102*, 193.

Boardman, C. R., Glass, S. V., & Lebow, P. K. (2017). Simple and accurate temperature correction for moisture pin calibrations in oriented strand board. *Building and Environment*, *112*, 250–260. https://doi.org/10.1016/j.buildenv.2016.11.039

CalEPA DTSC. (2014). *REVISED PRIORITY PRODUCT PROFILE - SPRAY POLYURETHANE FOAM SYSTEMS CONTAINING UNREACTED METHYLENE DIPHENYL DIISOCYANATES* (Priority Product Profile). Sacramento, CA: California Environmental Protection Agency, Department of Toxic Substances Control. Retrieved from https://www.dtsc.ca.gov/SCP/upload/SPWP_RevisedSPF_9-14.pdf

California Energy Commission. (2015). *2016 Building Energy Efficiency Standards for Residential and Non-Residential Buildings - Title-24, Part-6 and Associated Administrative Regulations in Part 1* (No. CEC-400-2015-037-CMF). Sacramento, CA: California Energy Commission. Retrieved from http://www.energy.ca.gov/2015publications/CEC-400-2015-037/CEC-400-2015-037-CMF.pdf

Chan, W. R., Kim, Y.-S., Less, B. D., Singer, B. C., & Walker, I. S. (2018). *Ventilation and Indoor Air Quality in New California Homes with Gas Appliances and Mechanical Ventilation* (Final Project Report No. PIR-14-007). Sacramento, CA: California Energy Commission, Energy Research and Devleopment Division.

Emmerich, S. J., Howard-Reed, C., & Gupte, A. (2005). *Modeling the IAQ Impact of HHI Interventions in Inner-city Housing* (No. NISTIR 7212). Washington, D.C.: National Institute of Standards and Technology. Retrieved from http://fire.nist.gov/bfrlpubs/build05/PDF/b05054.pdf

Finch, G., LePage, R., Ricketts, L., Higgins, J., & Dell, M. (2015). The Problems With and Solutions for Ventilated Attics. In *30th RCI International Convention and Trade Show* (pp. 203–216). San Antonio, TX: RCI Inc. Retrieved from http://rdh.com/wp-content/uploads/2015/05/The-Problems-with-and-Solutions-or-Ventilated-Attics-GFINCH.pdf

Forest, T. W., & Walker, I. S. (1993). *Attic Ventilation and Moisture*. Edmonton, Alberta: Canada Mortgage and Housing Corporation. Retrieved from ftp://ftp.cmhc-schl.gc.ca/chic-

ccdh/Research_Reports-Rapports_de_recherche/Older11/Ca1%20MH%2093A78%20v.%201_w.pdf

Fraunhofer IBP. (2018, April 9). ASHRAE standard 160 mold criteria now available in WUFI® Mold Index VTT | WUFI (en). Retrieved July 31, 2018, from https://wufi.de/en/2018/04/09/ashrae-standard-160-mold-criteria-now-available-in-wufi-mold-index-vtt/

GARD Analytics, Inc. (2003a). *Cost & Savings for Houses Built With Ducts in Conditioned Space: Technical Information Report* (Technical Report No. 500- 03- 082- A-31). Sacramento, CA: California Energy Commission. Retrieved from http://www.energy.ca.gov/2003publications/CEC-500-2003-082/CEC-500-2003-082-A-31.PDF

GARD Analytics, Inc. (2003b). *Residential Duct Placement: Market Barriers* (CEC Report No. 500-03- 082- A-30). Sacramento, CA: California Energy Commission. Retrieved from http://www.energy.ca.gov/2003publications/CEC-500-2003-082/CEC-500-2003-082-A-30.PDF

Glass, S. V., Gatland, S. D., Ueno, K., & Schumacher, C. J. (2017). Analysis of Improved Criteria for Mold Growth in ASHRAE Standard 160 by Comparison with Field Observations. In P. Mukhopadhyaya & D. Fisler (Eds.), *Advances in Hygrothermal Performance of Building Envelopes: Materials, Systems and Simulations* (pp. 1–27). 100 Barr Harbor Drive, PO Box C700, West Conshohocken, PA 19428-2959: ASTM International. https://doi.org/10.1520/STP159920160106

Hendron, R., Anderson, R., Reeves, P., & Hancock, E. (2002). *Thermal Performance of Unvented Attics in Hot-Dry Climates* (No. NREL/TP-550-30839). Golden, CO: National Renewable Energy Laboratory. Retrieved from http://www.nrel.gov/docs/fy02osti/30839.pdf

Hoeschele, M., Weitzel, E., German, A., & Chitwood, R. (2015). *Evaluation of Ducts in Conditioned Space for New California Homes* (No. ET13PGE1062). Pacific Gas and Electric Co. Retrieved from https://www.etcc-ca.com/reports/evaluation-ducts-conditioned-space-new-california-homes?dl=1521753309

ICC. (2012). International Residential Code for One- and Two-Family Dwellings. International Code Council. Retrieved from http://publicecodes.cyberregs.com/icod/irc/2012/

Ineichen, Pi., Perez, R. R., Seal, R. D., Maxwell, E. L., & Zalenka, A. (1992). Dynamic global-to-direct irradiance conversion models. *ASHRAE Transactions*, *98*(1), 354–369.

Johnas, C., & Terrinoni, H. W. (2011). A Life Cycle Look at Spray Foam Expansion Agents: A Cradleto-Grave Analysis. DuPont. Retrieved from https://www.chemours.com/Formacel/en_US/assets/downloads/201109_Life_Cycle_Analysis_Spray_Foam.pdf

Less, B., Walker, I., & Levinson, R. (2016). *A Literature Review of Sealed and Insulated Attics—Thermal, Moisture and Energy Performance* (No. LBNL--1006493, 1340304). https://doi.org/10.2172/1340304

Maxwell, E. L. (1987). *A Quasi-Physical Model for Converting Hourly Global Horizontal to Direct Normal Insolation* (No. SERI/R-215-3087). Golden, CO: Solar Energy Research Institute. Retrieved from https://rredc.nrel.gov/solar/pubs/PDFs/TR-215-3087.pdf

Miller, W., Railkar, S., Shiao, M., & Desjarlais, A. O. (2016). Sealed Attics Exposed to Two Years of Weathering in a Hot and Humid Climate. Presented at the Thermal Performance of the Exterior Envelopes of Whole Buildings XIII, Clearwater Beach, FL: ASHRAE. Retrieved from https://www.osti.gov/servlets/purl/1344250

Morrison Hershfield. (2014). *Attic Ventilation and Moisture Research Study* (No. 5113295). Canada: BC Housing. Retrieved from https://www.bchousing.org/publications/Attic-Ventilation-Moisture.pdf

Nittler, K., & Wilcox, B. (2006). *Residential Housing Starts and Prototypes: 2008 California Building Energy Efficiency Standards*. Sacramento, CA: California Energy Commission. Retrieved from http://www.energy.ca.gov/title24/2008standards/prerulemaking/documents/2006-03-28_workshop/2006-03-27_RES_STARTS-PROTOTYPES.PDF

Ojanen, T., Viitanen, H., Peuhkuri, R., Lahdesmaki, K., Vinha, J., & Salminen, K. (2010). Mold Growth Modeling of Building Structures Using Sensitivity Classes of Materials. Presented at the Buildings XI: Thermal Performance of Exterior Envelopes of Whole Buildings, Atlanta, GA: ASHRAE.

Owens Corning. (2015). ProPink High Performance Conditioned Attic System. Owens Corning. Retrieved from http://www2.owenscorning.com/literature/pdfs/HPCA%20Installation%20Instructions.pdf

Parker, D., Sonne, J., & Sherwin, J. (2002). Comparative Evaluation of the Impact of Roofing Systems on Residential Cooling Energy Demand in Florida (pp. 219–234). Presented at the ACEEE Summer Study on Energy Efficiency in Buildings, Pacific Grove, CA: American Council for an Energy-Efficient Economy. Retrieved from http://www.fsec.ucf.edu/en/publications/html/FSEC-CR-1220-00-es/roofing.pdf

Poppendieck, D. G., Nabinger, S., Schlegel, M., & Persily, A. K. (2014). Long Term Emission from Spray Polyurethane Foam Insulation. In *Proceedings of 13th International Conference on Indoor Air Quality and Climate, Indoor Air 2014* (p. HP0126). Hong Kong. Retrieved from https://ws680.nist.gov/publication/get_pdf.cfm?pub_id=915781

Poppendieck, D. G., Persily, A. K., & Nabinger, S. (2014). *Characterization of Emissions from Spray Polyurethane Foam*. Washington, D.C.: NIST. Retrieved from https://ws680.nist.gov/publication/get_pdf.cfm?pub_id=916100

pvlib-python. (n.d.). pvlib.irradiance.dirint. Retrieved September 10, 2018, from https://wholmgren-pvlib-python-new.readthedocs.io/en/doc-reorg2/generated/irradiance/pvlib.irradiance.dirint.html#pvlib.irradiance.dirint

RESNET. (2006). 2006 Mortgage Industry National Home Energy Rating Systems Standards. Residential Energy Services Network. Retrieved from http://www.resnet.us/professional/standards/mortgage

Richard, B., Cai, Z., Carll, C. G., Clausen, C. A., Dietenberger, M. A., Falk, R. H., … Zelinka, S. L. (2010). *Wood Handbook - Wood As An Engineering Material* (General Technical Report No. FPL-GTR-190). Madison, WI: Forest Products Laboratory - United States Department of Agriculture Forest Service. Retrieved from http://www.fpl.fs.fed.us/documnts/fplgtr/fpl_gtr190.pdf

Roppel, P., Norris, N., & Lawton, M. (2013). Highly Insulated, Ventilated, Wood-Framed Attics in Cool Marine Climates. In *Thermal Performance of the Exterior Envelopes of Whole Buildings*. Clearwater Beach, FL: ASHRAE. Retrieved from https://web.ornl.gov/sci/buildings/conf-archive/2013%20B12%20papers/119_Roppeo.pdf

Rudd, A. (2005). Field Performance of Unvented Cathedralized (UC) Attics in the USA. *Journal of Building Physics*, *29*(2), 145–169. https://doi.org/10.1177/1744259105057695

Rudd, A., & Lstiburek, J. (1996). *Measurement of Attic Temperatures and Cooling Energy Use in Vented and Sealed Attics in Las Vegas, Nevada* (No. RR-9701). Building Science Corporation. Retrieved from http://buildingscience.com/documents/reports/rr-9701-measurement-of-attic-temperatures-and-cooling-energy-use-in-vented-and-sealed-attics-in-las-vegas-nevada/view

Rudd, A., & Lstiburek, J. (1998). Vented and Sealed Attics in Hot Climates. *ASHRAE Transactions*, *104*(2). Retrieved from https://buildingscience.com/documents/reports/rr-9801-vented-and-sealed-attics-in-hot-climates/view

Rudd, A., Ueno, K., & Lstiburek, J. (1999). *Unvented-cathedralized attics: Where we've been and where we're going* (No. RR-9904). Building Science Corporation. Retrieved from http://buildingscience.com/documents/reports/rr-9904-unvented-cathedralized-attics-where-we-ve-been-and-where-we-re-going/view

Stratton, C., Walker, I., & Wray, C. P. (2012). *Measuring Residential Ventilation System Airflows: Part 2 - Field Evaluation of Airflow Meter Devices and System Flow Verification* (No. LBNL-5982E). Berkeley, CA: Lawrence Berkeley National Lab. Retrieved from http://homes.lbl.gov/sites/all/files/lbnl-5982e.pdf

Straube, J., Smegal, J., & Smith, J. (2010). *Moisture-Safe Unvented Wood Roof Systems* (Building America Report No. 1001). Building Science Corporation. Retrieved from http://buildingscience.com/documents/bareports/ba-1001-moisture-safe-unvented-wood-roof-systems/view

TenWolde, A., & Rose, W. B. (1999). Issues Related to Venting of Attics and Cathedral Ceilings. *ASHRAE Transactions*, *105*(1). Retrieved from http://www.aivc.org/sites/default/files/airbase_11919.pdf

Ueno, K., & Lstiburek, J. (2015). *Field Testing Unvented Roofs with Asphalt Shingles in Cold and Hot-Humid Climates* (Building America Report No. BA-1409). Westford, MA: Building Science Corporation. Retrieved from http://buildingscience.com/documents/ba-1409-field-testing-unvented-roofs-asphalt-shingles-cold-and-hot-humid-climates

Ueno, K., & Lstiburek, J. (2016). Monitoring of Two Unvented Roofs with Air-Permable Insulation in Climate Zone 2A. Presented at the Thermal Performance of the Exterior Envelopes of Whole Buildings XIII International Conference, Clearwater Beach, FL: ASHRAE. Retrieved from https://buildingscience.com/documents/conference-papers/cp-1302-monitoring-two-unvented-roofs-air-permeable-insulation-climate

Ueno, K., & Lstiburek, J. (2018, September). *Unvented Roof Without Spray Foam: The Latest Building America Research*. Presented at the 13th Annual North American Passive House

Conference, Boston, MA. Retrieved from http://www.phius.org/NAPHC2018/2018-09-14%20Ueno%20NAPHC%20Unvented%20Roofs.pdf

Vereecken, E., Vanoirbeek, K., & Roels, S. (2015). Towards a more thoughtful use of mould prediction models: A critical view on experimental mould growth research. *Journal of Building Physics*, *39*(2), 102–123. https://doi.org/10.1177/1744259115588718

Vereecken, Evy, & Roels, S. (2012). Review of mould prediction models and their influence on mould risk evaluation. *Building and Environment*, *51*, 296–310. https://doi.org/10.1016/j.buildenv.2011.11.003

Viitanen, H., Vinha, J., Salminen, K., Ojanen, T., Peuhkuri, R., Paajanen, L., & Lahdesmaki, K. (2010). Moisture and Bio-deterioration Risk of Building Materials and Structures. *Journal of Building Physics*, *33*(3), 201–224. https://doi.org/10.1177/1744259109343511

Viitanen, Hannu, & Ojanen, T. (2007). Improved Model to Predict Mold Growth in Building Materials. Presented at the Thermal Performance of the Exterior Envelopes of Whole Buildings X, Atlanta, GA: ASHRAE. Retrieved from https://www.aecb.net/wp-content/plugins/aecb-carbonlite-knowledgebase/librarian.php?id=10364&file=10365

Walker, Iain S. (1993). *Attic Ventilation, Heat and Moisture Transfer* (Ph.D. Thesis). University of Alberta, Deptartment of Mechanical Engineering, Edmonton, Alberta.

Walker, Iain S., & Sherman, M. (2007). Humidity Implications for Meeting Residential Ventilation Requirements. In *Thermal Performance of the Exterior Envelopes of Whole Buildings*. Clearwater Beach, FL: ASHRAE. Retrieved from http://epb.lbl.gov/publications/pdf/lbnl-62182.pdf

Walker, Iain S., & Sherman, M. H. (2006). *Evaluation of Existing Technologies for Meeting Residential Ventilation Requirements* (No. LBNL-59998). Berkeley, CA: Lawrence Berkeley National Lab. Retrieved from https://buildings.lbl.gov/sites/all/files/lbnl-59998.pdf

Walker, I.S., Forest, T. W., & Wilson, D. J. (2005). An attic-interior infiltration and interzone transport model of a house. *Building and Environment*, *40*(5), 701–718. https://doi.org/10.1016/j.buildenv.2004.08.002

Wei, J., Pande, A., Chappell, C., Christie, M., & Dawe, M. (2014). *Residential Ducts in Conditioned Space / High Performance Attics* (Codes and Standards Enhancement Initiative (CASE) Report No. 2016- RES- ENVI- F). Sacramento, CA: California Public Utilities Commission. Retrieved from http://energy.ca.gov/title24/2016standards/prerulemaking/documents/2014-07-21_workshop/final_case_reports/2016_Title_24_Final_CASE_Report_HPA-DCS-Oct2014.pdf

Wilson, A. (2010, June 1). Avoiding the Global Warming Impact of Insulation. Environmental Building News. Retrieved from https://www.buildinggreen.com/feature/avoiding-global-warming-impact-insulation